LBL-11885

Lawrence Berkeley Laboratory

UNIVERSITY OF CALIFORNIA

Materials & Chemical Sciences Division

Selectivity in Multiple Quantum Nuclear Magnetic Resonance

W.S. Warren
(Ph.D. Thesis)

November 1980

Prepared for the U.S. Department of Energy under Contract Number DE-AC03-76SF00098

LBL-11885

Selectivity in Multiple Quantum Nuclear Magnetic Resonance

Warren Sloan Warren

Department of Chemistry
University of California

and

Materials and Molecular Research Division
Lawrence Berkeley Laboratory
University of California
Berkeley, CA 94720

November 1980

This work was supported by the Division of Materials Sciences, Office of Basic Energy Sciences, U.S. Department of Energy under Contract W-7405-ENG-48.

SELECTIVITY IN MULTIPLE QUANTUM NUCLEAR MAGNETIC RESONANCE

Warren Sloan Warren

Materials and Molecular Research Division

Lawrence Berkeley Laboratory

Abstract

The observation of multiple-quantum nuclear magnetic resonance transitions in isotropic or anisotropic liquids is shown to give readily interpretable information on molecular configurations, rates of motional processes, and intramolecular interactions. However, the observed intensity of high multiple-quantum transitions falls off dramatically as the number of coupled spins increases. The theory of multiple-quantum NMR is developed through the density matrix formalism, and exact intensities are derived for several cases (isotropic first-order systems and anisotropic systems with high symmetry) to show that this intensity decrease is expected if standard multiple-quantum pulse sequences are used.

New pulse sequences are developed which excite coherences and produce population inversions only between selected states, even though other transitions are simultaneously resonant. One type of selective excitation presented only allows molecules to absorb and emit photons in groups of n. Coherent averaging theory is extended to describe these selective sequences, and to design sequences which are selective to arbitrarily high order in the Magnus expansion. This theory and computer calculations both show that extremely good selectivity and large signal

enhancements are possible. For example, the 10-quantum transition in a 10-spin system can be enhanced by more than four orders of magnitude. Other types of selective excitation presented include selection of only transitions with A_1 symmetry, elimination of zero-quantum transitions, excitation with only a few pulses in isotropic and anisotropic systems, and excitation from nonequilibrium initial conditions. Experiments with four-quantum, six-quantum, and eight-quantum selection verify the coherent averaging and computer calculations. Noise reduction from two-dimensional spectroscopy, multiple-quantum NMR in exchanging systems, and statistical aspects of multiple-quantum coherence (including an information theory treatment) are also presented.

Acknowledgements

It has been my great pleasure to work with Professor Alexander Pines for the last several years. He has directed his research group towards projects which are challenging, interesting and important, yet he recognizes the importance of giving his students freedom to follow their interests and instincts. I have learned much from him through our conversations, and I consider him a friend.

Alex has attracted good graduate students, and has created a group which is intellectually stimulating and hardworking, yet is relaxed and friendly. I consider this to be an impressive accomplishment, unmatched in the other groups I have seen. I will miss the many times Dan Weitekamp and I have locked horns; our arguments have occasionally become heated, but that is only because our discussions have been challenging, and I think that we have both profited from them. Jim Murdoch has given me extensive help with computer calculations, and has kept the group's spirit lively by his indefatigable humor. Gary Drobny's experimental expertise has been very valuable, as have my conversations with him, Steve Sinton, Joel Garbow, Dr. Luciano Mueller, Jau-Huei Tang, Larry Sterna, Dick Eckman and Yu-Sze Yen on multiple-quantum NMR and general chemical physics. In addition Sid Wolfe's synthetic organic efforts have been very helpful.

I would also like to thank Professor Robert A. Harris, Professor Charles B. Harris, and Dr. Melvin Klein for their advice and help, and Professors Shaul Mukamel and R. D. Levine for initiating the information theory treatment in section 6.3 of this work. The National Science Foundation through its Graduate Fellowship Program, the Department of

Chemistry, and the Materials and Molecular Research Division of Lawrence Berkeley Laboratory have supported me financially, and the Laboratory of Chemical Biodynamics has generously provided access to its computer. Without this access many of the calculations in Chapter IV would not have been possible. Carol Hacker's excellent typing of the final draft of this thesis and Marshall Tuttle's work on the figures are also sincerely appreciated.

Finally, I would like to thank my wife Kathleen for putting up with all of the problems that come with marrying a graduate student, for typing several of my papers and the first draft of this work, and for putting off her dreams and ambitions so that I could achieve mine. This thesis would not have been completed now without her, so it is to her and to my family that I dedicate it.

This research was supported in part by the Division of Materials Sciences, Office of Basic Energy Sciences, U. S. Department of Energy under contract W-7405-ENG-48.

I. Introduction and Overview

1.1 The Basic Magnetic Resonance Experiment 1

1.2 The Spin Hamiltonian. 2

1.2.1 Zeeman Hamiltonian 2

1.2.2 Radio Frequency Hamiltonian. 4

1.2.3 Quadrupolar Hamiltonian. 4

1.2.4 Direct and Indirect Dipole-Dipole Hamiltonian. . 5

1.2.5 Chemical Shift Hamiltonian 6

1.2.6 Simplifications of the Hamiltonian 7

1.3 Selection Rules and Spectral Complexity 9

1.4 The Information Content of Spectra. 13

1.4.1 General Spin System. 13

1.4.2 Symmetry Considerations for Anisotropic Systems and Analogy to Isotopic Spin Labeling. 17

1.4.3 Examples of Multiple-Quantum Spectra and the Isotopic Labeling Analogy. 20

1.5 Conclusions 31

II. Theory of Multiple-Quantum NMR

2.1 Operator Formalisms 32

2.1.1 The Density Matrix 32

2.1.2 Fictitious Spin Operators. 36

2.2 Simple NMR Experiments. 39

2.2.1 Continuous Irradiation 39

2.2.2 Pulse Methods: Single-Quantum Experiments . . . 43

2.2.3 Pulse Methods: Multiple-Quantum Experiments . . 46

2.3 Preparation of Multiple-Quantum Coherences. 51

2.3.1 Small Values of τ. 52

2.3.2 Long Values of τ 55

2.4 Signal Intensities; Ensemble Averaging. 66

2.5 Conclusions 76

III. Theory of Selective Excitation of Multiple-Quantum Transitions

3.1 Review of Average Hamiltonian Theory. 78

3.1.1 Expansions for the Propagator. 78

3.1.2 Examples of Multiple-Pulse Sequences 80

3.1.3 Estimation of Correction Terms 83

3.2 Extension of Average Hamiltonian Theory to Selective Sequences 85

3.2.1 Definitions. 85

3.2.2 Theorems for Selective Sequences 86

3.3 Design of Selective Sequences 90

3.3.1 Zero-Order Selective Sequences 90

3.3.2 Sequences Selective to Arbitrary Order 93

3.4 Application of Selective Sequences to Multiple-Quantum NMR 96

3.4.1 Design of Effective Subcycles. 96

3.4.2 The Use of Time Reversal in Subcycles. 97

3.4.3 Effects of Imperfect Time Reversal 103

3.4.4 Other Subcycle Sequences 103

3.5 Selective Sequences in the Multiple-Quantum NMR Experiment. 104

3.5.1 Optimum Relation between Preparation and Mixing Propagators 104

3.5.2 Phases of Selected Transitions; Time Reversal Mixing. 105

3.5.3 Potential Signal Gains; Selective Population Inversion. 106

3.5.4 Coherent Initial Conditions. 113

3.5.5 Symmetry Selection 114

3.5.6 Heteronuclear Selective Excitation 114

3.6 Extent of Selectivity in Non-ideal Selective Sequences. 116

3.6.1 General Systems. 116

3.6.2 Application to Multiple-Quantum NMR. 123

3.6.3 Removal of Zero-Quantum Operators from Selective Sequences. 127

3.7 Conclusions 131

IV. Computer Calculations of Selectivity

4.1 Motivation. 132

4.2 Programming Details 136

4.3 Zero-Order Selective Sequences. 137

4.3.1 Nk-quantum Selection 137

4.3.2 Lower-quantum Selection. 146

4.4 Higher-Order Selective Sequences. 149

4.4.1 Nk-quantum Selection 149

4.4.2 Lower-quantum Selection. 157

4.5 Suppression of Zero-quantum Operators 158

4.6 The Importance of Time Reversal 159

4.6.1 Simple Selective Sequences 160

4.6.2 Use of Line Narrowing Sequences. 161

4.6.3 Selectivity in Isotropic Systems 168

4.7 Conclusions 172

V. Selective Experiments

5.1 The Spectrometer. 174

5.1.1 Magnet 174

5.1.2 Frequency Generation 174

5.1.3 Detectors. 175

5.1.4 Digitization 175

5.1.5 Pulse Programmer 175

5.1.6 Probes 175

5.1.7 Phase Shifting 176

5.2 Experimental Results: Oriented Benzene 177

5.2.1 Four-quantum Selection with Time Reversal. . . . 177

5.2.2 Four-quantum Selection with Simplified Sequences. 188

5.2.3 Six-quantum Selection; Coherent Initial Conditions 188

5.2.4 Symmetry Selection 190

5.3 Experimental Results: Oriented 1-Bromobutane 193

5.3.1 Four-quantum Selection 193

5.3.2 Eight-quantum Selection. 200

5.4 Experimental Results: Cyclopentane 203

5.5 Conclusions 203

VI. Other Topics in Multiple-Quantum NMR

6.1 Two-dimensional Techniques. 205

6.1.1 Nonselective Experiments 207

6.1.2 The Second Fourier Transformation; Optimal Filtering. 209

6.1.3 Selective Experiments 211

6.1.4 Conclusions 212

6.2 Multiple-Quantum NMR in Exchanging Systems 212

6.2.1 Density Matrix Equations of Motion. 212

6.2.2 Signal Size and Enhancement Techniques for General Exchanging Systems. 215

6.2.3 One Example - Cyclooctatetraene 215

6.2.4 Multiple Pulse Techniques to Measure Exchange . . 225

6.3 An Information Theory Treatment of Multiple-Quantum Coherence. 228

6.3.1 Introduction. 228

6.3.2 Statistical Calculations. 229

6.3.3 Forms for the Pumping Operator. 234

6.3.4 Density Matrix Reduction Schemes: Coherent verses Incoherent Pumping 243

6.3.5 Conclusions 246

Appendix A. Counting Schemes for (N-2)-quantum and Lower-quantum Transitions. 248

Appendix B. Listings of Computer Programs. 250

Appendix C. Tables of Computer Data for Selective Sequences. . . . 285

Appendix D. Residual Nonselective Terms for Selective Sequences. . 319

Appendix E. Some Matrix Relations. 325

References 329

I. Introduction and Overview

1.1 The Basic Magnetic Resonance Experiment

The observation of energy level differences between spin states in a magnetic field dates back to the experiments of Stern and Gerlach in 1922.[1] However, measurement of these differences for nuclear spins in bulk material, with the possibility of observing the effects of interatomic interactions, did not occur until more than twenty years later.[2,3] The development of nuclear magnetic resonance since that time has been phenomenal. This development has been summarized elsewhere.[4-8] It is important, however, to point out the reasons why NMR has become so useful, and the information which can be extracted from spectra.

Every nucleus has a characteristic total spin angular momentum $\hbar^2 I(I+1)$, where 2I must be a nonnegative integer; for protons I=1/2. When the nucleus is placed in a static magnetic field $B_o\hat{z}$, the z-component of this spin angular momentum is quantized. It is restricted to $I_z = m\hbar$, where m can take on any of the (2I+1) values -I, -I+1, ..., I. This angular momentum generates a magnetic dipole moment μ, whose interaction with the applied field (the Zeeman interaction) has the classical form $E = -\vec{\mu}\cdot\vec{B}_o = -\hbar\gamma m B_o$. The energy levels are therefore bounded and discrete, and if no other interactions are present the spectrum can only give the value of γ, which has been measured for virtually every known nucleus (or B_o if γ is known).

Thus, the interactions are what makes nuclear magnetic resonance interesting. It is useful to think of the interacting group of N spins as a composite system. For example, if I = 1/2, the total z-component of the angular momentum $M = \sum_i m_i$ can have any of 2N values from

$M = -N/2$ to $M = N/2$. If interactions are ignored, all of the $(N!/((N/2)+M)!((N/2)-M)!)$ energy levels with a fixed value of M are degenerate. The interactions break this degeneracy. The energy splittings that are produced are much smaller than the Zeeman energy splittings for all the cases to be considered in this work, so the energy levels end up as in Figure I.1. There are 2^N distinct energy levels in a system with N spins - 1/2, and if transitions between any two levels are allowed there can be $2^N(2^{N-1})$ different transitions.

1.2 The Spin Hamiltonian

A macroscopic sample might contain 10^{18} nuclei, and if $N = 10^{18}$ the number of energy levels is astronomically large. If all of these are nondegenerate, the individual transitions will certainly not be resolvable. Fortunately the degeneracy is often not completely lifted; the amount of degeneracy which remains (and hence the number of distinct transitions) is determined by the form of the spin Hamiltonian.

The terms in the spin Hamiltonian which will be considered in this work (in rough order of decreasing strength) are:[9]

1.2.1 Zeeman Hamiltonian

$H_Z = -\sum_i \hbar\gamma_i B_o I_{zi} = -\sum_i \omega_o^i I_{zi}$ (in units of $\hbar = 1$), where I_{zi} is the operator for the z-component of the spin angular momentum of the ith spin. If all the spins are identical, this is written as $H_Z = -\omega_o I_z$. This term will be present in all of the systems to be considered in this work. Typically $B_o \sim 50$ kG, which makes $\omega_o \sim 10^9$ rad/sec for protons.

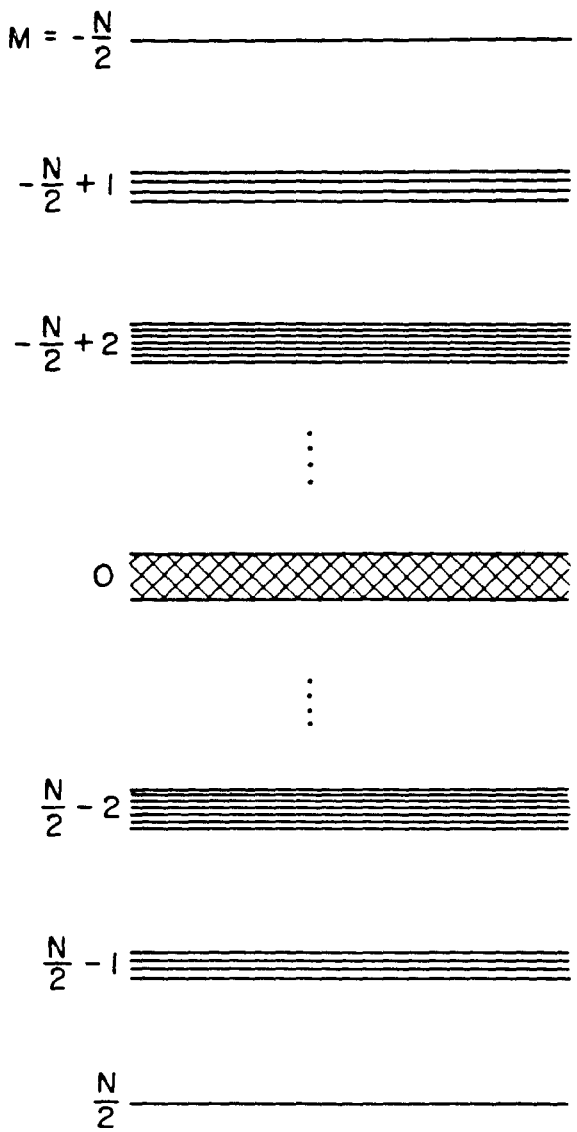

XBL 7710-10022

Figure I.1 Schematic energy level diagram for a system of N spins-1/2 without symmetry. All the eigenstates can be nondegenerate. The manifolds correspond to different values of M, and have degeneracy N!/((N/2)+M)!((N/2)-M)!.

1.2.2 Radio Frequency Hamiltonian

If an oscillating radio frequency (rf) magnetic field $B_1(t)\cos(\omega t+\phi(t))\hat{x}$ is applied to the sample it will cause an interaction of the form $H_{rf} = -\sum_i \gamma_i B_1(t)\cos(\omega t+\phi(t))I_{xi} = -\Sigma 2\omega_1 \cos(\omega t+\phi(t))I_{xi}$. If all the spins are identical, this is written as $H_{rf} = -2\omega_1(t)\cos(\omega t+\phi(t))I_x$. The interesting case is $\omega \sim \omega_o$, and in this case one normally goes to an interaction representation (the "rotating frame")[10] defined by $\mathcal{H} = \exp(-i\omega I_z t)\, H \exp(i\omega I_z t)$. The mathematical details will be postponed until Chapter II, but the effect is to make the system appear to evolve under a Zeeman Hamiltonian

$$\mathcal{H}_Z = -(\omega_o-\omega)I_z = \Delta\omega I_z \tag{I.1}$$

and an rf Hamiltonian

$$\mathcal{H}_{rf} = -\omega_1(t)\{I_x\cos\phi(t)+I_y\sin\phi(t)\} \quad . \tag{I.2}$$

Other terms also appear, but they oscillate at high frequencies and are neglected (the "rotating wave approximation").[10] The magnitude of ω_1 is controlled by the experimenter.

1.2.3 Quadrupolar Hamiltonian

A nucleus with spin $I \geq 1$ has an interaction with electric field gradients of the form

$$H_Q \sim \sum_i \vec{I}_i \cdot \underset{\approx}{V}^i \cdot \vec{I}_i \tag{I.3}$$

where $V^i_{\alpha\beta} = \frac{\delta^2 V}{\delta\alpha\delta\beta}$ (α,β = x,y, or z), the second derivatives of the potential. $\underset{\approx}{V}^i$ must be traceless and symmetric (i.e., an irreducible second-rank tensor[11,12]) and this implies that $H_Q = \sum_i \sum_{m=-2}^{2} C_{mi}(T^2_m)_i$. In the rotating wave approximation only $(T^2_o)_i$ (the secular term, which

commutes with I_z) survives. For example, if the gradients are axially symmetric this term can be explicitly written as

$$\mathcal{H}_Q = \sum_i \frac{eQ_i V^i_{zz}}{4I(2I-1)} \left(3I^2_{zi} - I(I+1)\right) \tag{I.4}$$

where Q_i is the quadrupole moment of the ith nucleus.

1.2.4 Direct and Indirect Dipole-Dipole Hamiltonian

Any two magnetic moments μ_1 and μ_2 have an interaction energy, which can be written as

$$H_D \sim \sum_{i>j} \vec{I}_i \cdot \underset{\approx}{D}^{ij} \cdot \vec{I}_j \quad , \quad H_J \sim \sum_{i>j} \vec{I}_i \cdot \underset{\approx}{J}^{ij} \cdot \vec{I}_j \tag{I.5}$$

$\underset{\approx}{D}^{ij}$ represents the direct interaction (the energy of one dipole in the magnetic field of the other), and is traceless and symmetric. $\underset{\approx}{J}^{ij}$ represents the indirect interaction (for example, one dipole induces a magnetic moment in surrounding electrons, which then interacts with the other dipole).[4,5,13] $\underset{\approx}{J}^{ij}$ is not necessarily traceless or symmetric, but the antisymmetric part is unobservable.[14] If all the nuclei are identical, the secular terms can be written explicitly as

$$\mathcal{H}_D = \sum_{i>j} D_{ij}(3I_{zi}I_{zj} - \vec{I}_i \cdot \vec{I}_j) \quad , \quad D_{ij} = \frac{\gamma_i \gamma_j (3\cos^2\theta_{ij} - 1)}{r_{ij}^3} \tag{I.6}$$

where θ_{ij} is the angle between the z-axis and the internuclear vector $\vec{r}_{ij}$, and $r_{ij} = |\vec{r}_{ij}|$;

$$\mathcal{H}_J = \sum_{i>j} J_{ij}(\vec{I}_i \cdot \vec{I}_j) + J^{aniso}_{ij}(3I_{zi}I_{zj} - \vec{I}_i \cdot \vec{I}_j) \quad . \tag{I.7}$$

Most of the systems to be discussed in this work have $\mathcal{H}_D$ as the dominant term in the Hamiltonian. Since the terms D_{ij} depend on θ_{ij} and r_{ij}, they supply a wealth of structural information. The terms J_{ij} are sensitive to the electronic configuration.

The secular part of the couplings between two unlike spins I and S has a somewhat different form. In this case, only those terms which commute with both I_z and S_z are retained, which gives

$$\mathcal{H}_D = \sum_{i>j} 2D_{ij}(I_{zi}S_{zj})$$

$$\mathcal{H}_J = \sum_{i>j} J_{ij}(I_{zi}S_{zj}) \quad .$$

Frequently the homonuclear and heteronuclear cases are distinguished by writing a_{ij} instead of D_{ij} for homonuclear pairs, and b_{ij} for heteronuclear pairs. A similar distinction can be made for $\mathcal{H}_J$, but it will not be needed in this work.

1.2.5 Chemical Shift Hamiltonian

Electrons induce a magnetic field $-\underset{\approx}{\sigma}^i \cdot B_o \hat{z}$ at the site of the ith nucleus. This magnetic field interacts with the nuclear magnetic moment to produce the chemical shift Hamiltonian

$$\mathcal{H}_{cs} \sim \sum_i \vec{I}_i \cdot \underset{\approx}{\sigma}^i \cdot B_o \hat{z} \quad . \tag{I.8}$$

The secular term can be written as

$$\mathcal{H}_{cs} = -\Sigma \sigma_i I_{zi} \quad . \tag{I.9}$$

1.2.6 Simplifications of the Hamiltonian

In the most general case, all of the terms in the Hamiltonian of the last subsection must be retained. However, in many systems some of these terms can be eliminated. Three special cases will be considered.

1.2.6.1 Solid Samples

$\mathcal{H}_Q$ is usually the dominant term in the Hamiltonian if $I > 1/2$. For protons, however, $\mathcal{H}_Q = 0$, and $\mathcal{H}_D$ dominates. The summations over nuclei must theoretically run over the entire sample, but crystal symmetries may simplify this calculation somewhat.[15] The spectrum generally does not contain resolvable lines. A typical spectral width for proton transitions with $\Delta M = 1$ is 50 KHz.

The small terms in the Hamiltonian, such as $\mathcal{H}_{cs}$, do not produce observable effects in the presence of $\mathcal{H}_D$ or $\mathcal{H}_Q$. However, different terms have different symmetry properties under manipulations in spin or coordinate space. For example, both the spatial parts and the spin parts of $\mathcal{H}_Q$ and $\mathcal{H}_D$ are irreducible second-rank tensors; the spatial part of $\mathcal{H}_{cs}$ is the sum of an irreducible zero-rank tensor and an irreducible second-rank tensor, and the spin part is a first-rank tensor. Techniques for discriminating between tensors of different rank are detailed in reference (9), and one of these techniques (line-narrowing rf pulse sequences) will be discussed in Chapter III.

1.2.6.2 Isotropic Liquid Samples

All the molecules in isotropic samples undergo rapid diffusion and reorientation. As a result, the spatial terms in the operators $\underset{\approx}{V}$, $\underset{\approx}{\sigma}$, $\underset{\approx}{D}$ and $\underset{\approx}{J}$ must be averaged over all orientations, and only the

isotropic (zero-rank tensor) portions survive. This implies that $\mathcal{H}_D$, $\mathcal{H}_Q$, and J_{ij}^{aniso} vanish. The total homonuclear Hamiltonian is then

$$\mathcal{H}_z = \Delta\omega I_z - \sum_i \sigma_i I_{zi} + \sum_{i>j} J_{ij}(\vec{I}_i \cdot \vec{I}_j) \qquad (I.10)$$

in the absence of rf irradiation. In addition, all intermolecular couplings vanish, so the summations only involve the spins of a single molecule. This simple Hamiltonian produces relatively few distinct transitions.

Isotropic spectra are of course useful for compound identification,[8] because the chemical shifts of different electronic environments are well known. The spectral width is proportional to the static field. For protons at 50 kG, the maximum width for transitions with $\Delta M = 1$ is about 2 kHz, and individual transitions are often less than 1 Hz wide.

1.2.6.3 Anisotropic Liquid Samples

A liquid crystal becomes partially oriented when placed in a large magnetic field, as will most molecules dissolved in a liquid crystal.[13,16] Rapid diffusion still occurs, but the molecules have a preferred direction so reorientation is not isotropic. The diffusion causes all intermolecular couplings to vanish, as in the case of isotropic liquids. However, intramolecular couplings are only partially averaged.

The most important case to be considered in this work is the case where the only spins are protons. The Hamiltonian is then

$$\mathcal{H}_z = \sum_{i>j} D_{ij} \left(3I_{zi}I_{zj} - \vec{I}_i \cdot \vec{I}_j\right) + \sum_{i>j} J_{ij}\left(\vec{I}_i \cdot \vec{I}_j\right) - \sum_i \sigma_i I_{zi} + \Delta\omega I_z \tag{I.11}$$

where

$$D_{ij} = \frac{\gamma_i \gamma_j}{4\langle r_{ij}^3 \rangle} \langle 3\cos^2\theta_{ij} - 1 \rangle \quad . \tag{I.12}$$

J_{ij}^{aniso} is usually negligible for protons, and $\mathcal{H}_Q = 0$.

The averaging in equation (I.11) is over all allowed orientations (averaged values must also be used for J_{ij} and σ_i). D_{ij} can also be expressed in terms of the molecular ordering matrix $S_{\alpha\beta}$.

$$S_{\alpha\beta} = 1/2 \langle 3 \cos\theta_{\alpha a} \cos\theta_{\beta a} - \delta_{\alpha\beta} \rangle$$

where $\theta_{\alpha a}$ is the angle made by the α axis (molecular coordinate system) with the a axis (the laboratory coordinate system direction of the static field B_o). $\underset{\approx}{S}$ is traceless and symmetric, and the number of independent components depends on the symmetry of the molecule.[18,19] The important point is that the terms D_{ij} depend on $\langle r_{ij}^{-3} \rangle$, θ_{ij}, and at most five ordering parameters, so they convey structural information.

The only term added in going from isotropic to anisotropic liquids is $\mathcal{H}_D$, but anisotropic spectra generally have more transitions. A typical spectral width for transitions with $\Delta M = 1$ is 10 kHz for molecules dissolved in a liquid crystal, and 40 kHz for the liquid crystal itself. If the individual transitions are resolvable, they will typically be no more than a few Hz wide.

1.3 Selection Rules and Spectral Complexity

The different systems of section 1.2.6 were compared in terms

of the spectral width for transitions with $\Delta M = 1$. Historically these were the first transitions to be observed. In fact it can be shown (and will be shown in section 2.2) that in the limit of weak irradiation $\Delta M = 1$ transitions are the only ones allowed.[20] This selection rule also holds for the transitions induced by a single strong pulse.[6,21] Spectra produced by one of these two techniques will be termed single-quantum or conventional. If the single-quantum spectrum is resolvable, it is in principle possible to determine the coefficients D_{ij}, J_{ij} or σ_i. Sometimes this analysis can be done by hand, as with first-order isotropic spectra[8] or small, highly symmetric molecules.[8,22] More often the analysis requires a computer calculation.[23] If the spectrum is not resolvable, however, this analysis becomes impossible. Thus, for example, individual couplings are not observed in solids.

The situation is somewhat better with liquid samples. However, the number of allowed single-quantum transitions grows very rapidly as the number of spins increases. This is illustrated for the proton spectra of anisotropic systems by Figure I.2. If only a few protons are present, all of the transitions are easily resolvable, but the spectra become extremely complex if more than five or six spins are present. As an example of this spectral complexity, consider the proton spectrum of oriented cyclooctatetraene, which is a fairly small molecule. The symmetry dictates that there are only six unique D_{ij} values and one value for σ_i, yet there are 2070 distinct transitions.[24] Clearly most of the lines give redundant information and these additional lines can make analysis impossible.

One approach to simplifying spectra is isotopic substitution (for example, replacing protons with deuterons). This NMR version of a spin

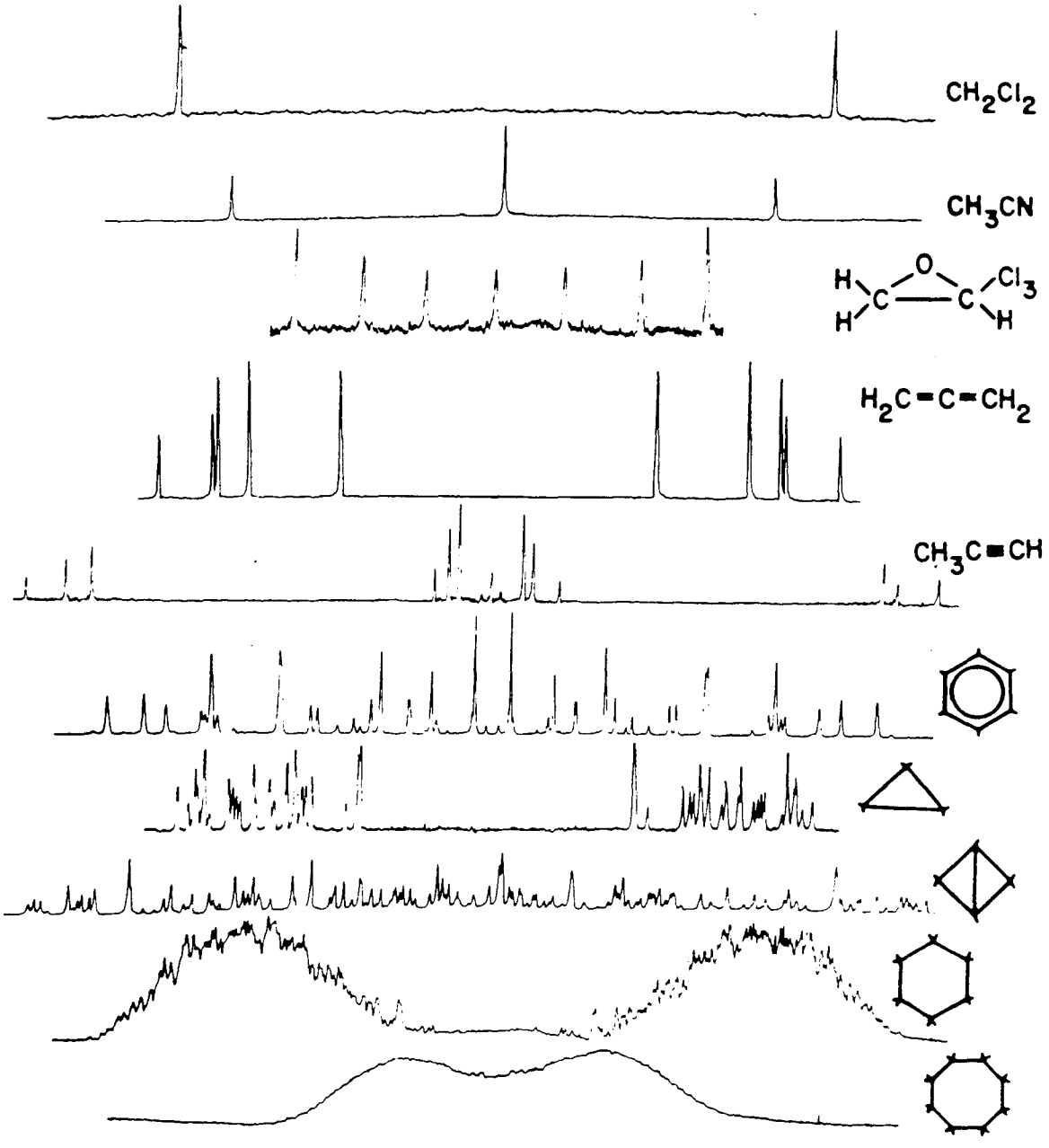

XBL 7910-12344

Figure I.2 The single-quantum spectra of several oriented molecules. The number of transitions increases dramatically as the number of spins is increased. (Figure courtesy of Dr. Zeev Luz.)

labeling experiment[25,26] is useful, since replacing most of the protons reduces the number of possible transitions. Thus, one way to find the six coupling constants of oriented cyclooctatetraene would be to synthesize the six different species which have only two protons. Each of these species would have a simple spectrum. This approach has been extensively used to study large molecules,[13,24,27] but it has two important disadvantages: isotopic substitution may change the molecular configuration, the order parameters,[27] or the rate of internal processes, and synthesis of selectively labeled molecules is often difficult.

Pulse sequences (to be discussed in Chapter II) have been designed which overcome the selection rule $\Delta M = 1$ of conventional NMR spectroscopy, thus permitting the observation of transitions between states with arbitrary ΔM.[28-34] These multiple-quantum transitions can also be used to determine the dipole-dipole coupling constants. In addition, because the number of possibly distinct transitions falls off rapidly as ΔM increases, multiple-quantum spectra do not require isotopic labeling to make them resolvable. In fact, the observation of multiple-quantum transitions is a practical alternative to isotopic labeling, and there is a great deal of similarity between these two techniques. Roughly speaking, the coherent flipping of n out of N spins inherently labels the (N-n) spins left behind. These ideas will be made more quantitative in the next section.

1.4 The Information Content of Spectra[35]

1.4.1 General Spin Systems

Consider the energy level diagram for a system of N spins - 1/2, illustrated in Figure I.1. The energy levels are broken up into manifolds of states with equal M, and the degeneracies of the manifolds are $N!/((N/2)-M)!((N/2)+M)!$ If the overall Hamiltonian has absolutely no symmetry elements, all of the levels can be nondegenerate and the number of distinct n-quantum transitions is $(2N)!/(N+n)!(N-n)!$[34]

For example, there is only one transition with $\Delta M = N$, because there is only one state with $M = N/2$ (all spins α) and only one state with $M = -N/2$ (all spins β). Even if the overall Hamiltonian has no symmetry, some parts of it have allowed symmetry operations. For example, $\mathcal{H}_D$ and $\mathcal{H}_J$ contain only bilinear operators, and are unaffected by flipping all the spins. This means that the energy of the N-quantum transitions have no direct or indirect dipole coupling term. On the other hand, all the terms in $\mathcal{H}_{cs}$ and $\mathcal{H}_z$ are linear, so they are multiplied by -1 when all the spins are flipped. It is then easy to see that

$$\langle \prod_i \alpha_i | \mathcal{H}_z | \prod_i \alpha_i \rangle = \langle \prod_i \alpha_i | \mathcal{H}_D + \mathcal{H}_J | \prod_i \alpha_i \rangle - \frac{1}{2} \Sigma \sigma_i + \frac{1}{2} N\Delta\omega \qquad (I.13)$$

$$\langle \prod_i \beta_i | \mathcal{H}_z | \prod_i \beta_i \rangle = \langle \prod_i \alpha_i | \mathcal{H}_D + \mathcal{H}_J | \prod_i \alpha_i \rangle + \frac{1}{2} \Sigma \sigma_i - \frac{1}{2} N\Delta\omega \qquad (I.14)$$

$$\Delta E = N\Delta\omega - \Sigma \sigma_i \quad . \qquad (I.15)$$

Therefore, the N-quantum transition gives the resonance offset (or, if chemical shifts are present, the sum of the shifts) directly.

The result is the same, no matter what the sample is; of course, if the sample is a solid, this formula applies strictly only to the 10^{18}-quantum transition (or however many spins are present) unless the spins of interest are sufficiently dilute to make long-range couplings negligible.

The frequency of a single transition contains very little information about complicated molecules. The (N-1)-quantum and (N-2)-quantum spectra are still far simpler than the single-quantum spectrum, but contain enough transitions to be useful. There are N states with $M = \pm ((N/2)-1)$, and $(N^2-N)/2$ states with $M = \pm ((N/2)-2)$. The number of allowed transitions involving these states depends on the symmetry of the Hamiltonian. If absolutely no symmetry elements are present (as is possible in an isotropic system), there are 2N (N-1)-quantum transitions and N(2N-1) (N-2)-quantum transitions. In such an isotropic system there are N chemical shifts and N(N-1)/2 spin-spin couplings, so the (N-1)-quantum and (N-2)-quantum spectra generally contain enough transitions for a complete assignment. As mentioned earlier, a typical transition is less than 1 Hz wide in a homogeneous magnet, and the spectral width might typically be 1 KHz, so these transitions are usually resolvable.

A totally unsymmetrical anisotropic system would have N(N-1)/2 direct dipolar couplings, the same number of indirect couplings, and N chemical shifts. $\mathcal{H}_D$ is usually a few orders of magnitude larger than $\mathcal{H}_{cs}$, and the chemical shifts can be suppressed without affecting $\mathcal{H}_D$[36,37] (see section III.1) so for the rest of the section $\mathcal{H}_{cs}$ in anisotropic systems will be ignored. In this case the (N-1)-quantum spectrum has N pairs of lines ($M = (N/2)-1 \rightarrow M = N/2$, or $M = N/2 \rightarrow$

$M = -((N/2)-1)$, and is symmetric about $(N-1)\Delta\omega$. This spectrum is similar to the single-quantum spectrum which could be produced if all of the molecules were cooled down into the ground state $M = -N/2$;[38] the only allowed transitions in that case would be to $M = -((N/2)-1)$ states, so N lines would be produced, and the frequencies are the same as those of half the lines in the (N-1)-quantum spectrum if $\Delta\omega = 0$. The (N-2)-quantum spectrum is also symmetric, and has N(N-1) pairs of lines ($M = N/2 \rightarrow M = -((N/2)-2)$, $M = (N/2)-1 \rightarrow M = -((N/2)-1)$, or $M = (N/2)-2 \rightarrow M = -N/2$) plus a highly degenerate peak at $(N-2)\Delta\omega$, arising from transitions between any $M=(N/2)-1$ eigenstate and the $M = -((N/2)-1)$ eigenstate generated by flipping all the spins. There are N(N-1) possibly different direct and indirect couplings, so roughly this many pairs of lines are needed for complete characterization. Typically, each transition would be a few Hz wide, out of a total spectral width of many KHz. Therefore, the (N-1)-quantum and (N-2)-quantum transitions for anisotropic systems are also usually resolvable, and assignment of these two spectra is sufficient to determine all dipolar couplings.

If the Hamiltonian has additional symmetry operations on an NMR time scale, the number of transitions decreases, because the eigenstates can be assigned to several irreducible representations (Figure I.3). Since the multiple-quantum spectra contain few lines to begin with, symmetry effects are easily noticed. The number of transitions can be determined by generating symmetry adapted states and this has been done for general isotropic systems.[34] However, for anisotropic systems this process can be quite involved. If only the number of transitions is required, simpler symmetry arguments will suffice.

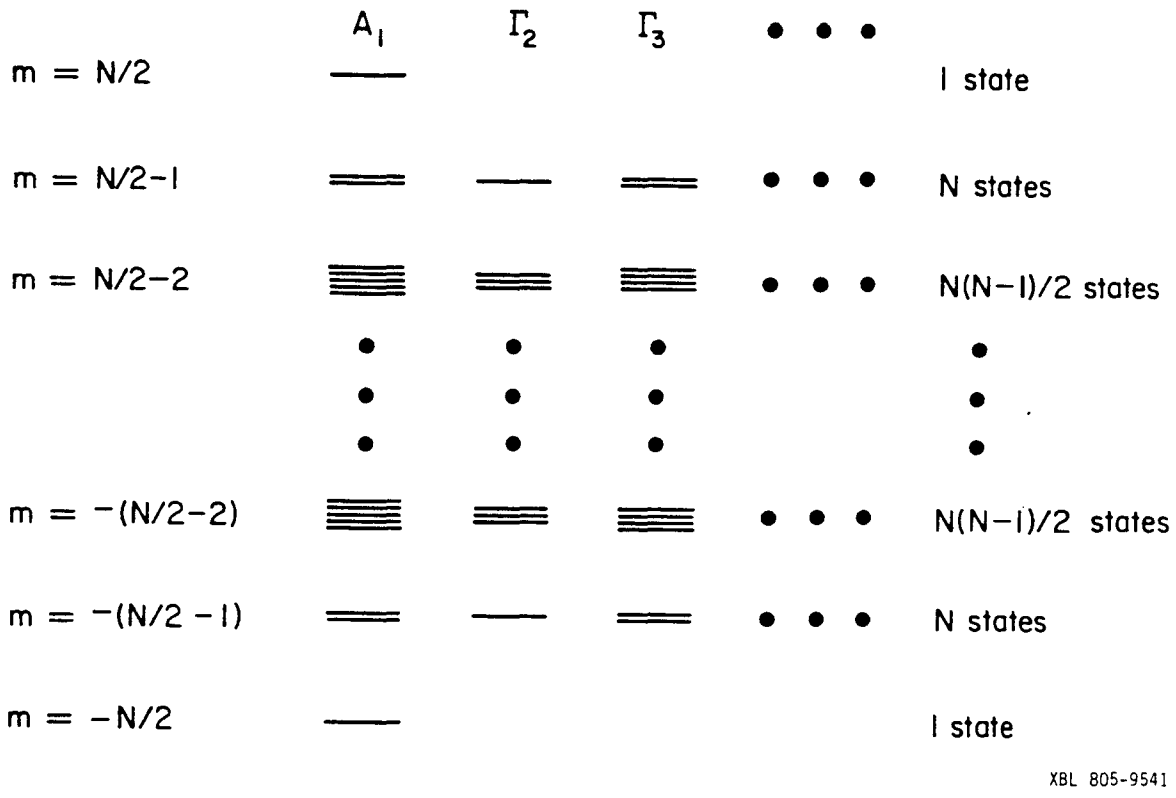

Figure I.3 Schematic energy level diagram for a system of N spins-1/2 with symmetry. The states with M = ±N/2 belong to the totally symmetric representation A_1, so all N-quantum or (N-1)-quantum transitions are in that representation. (N-2)-quantum transitions can come from other representations as well.

1.4.2 Symmetry Considerations for Anisotropic Systems and Analogy to Isotopic Spin Labeling

Consider first the (N-1)-quantum spectrum. The states with M=N/2 (all spins α) and M=-N/2 (all spins β) are invariant to all molecular symmetry operations, hence they belong to the totally symmetric representation A_1. Therefore, the (N-1)-quantum transitions all have A_1 symmetry, and each A_1 eigenstate for M=(N/2)-1 will generate one transition, as will each A_1 eigenstate for M=-((N/2)-1). There is no symmetry reason for any of these transitions to be degenerate. In the spin product (SP) basis set, the states with M=((N/2)-1) are the N states with (N-1) spins α, and the remaining spin β; the opposite is true for M=-((N/2)-1). A_1 symmetry adapted states can be generated from this basis set by taking one SP state and applying all the symmetry operations of the spin system to it.[39] If this process is repeated for all the SP states, all the A_1 states are generated.

The symmetry operations of the spin system can be described from two different perspectives. Symmetry operations such as planes or axes of rotation can be defined, and eigenstates can be classified according to their behavior under these symmetry operations.[39] A more versatile approach, which we will use here, is to describe symmetry operations by allowed permutations of the nuclei.[40,41] Two nuclei a and b are magnetically equivalent if there is a symmetry operation which turns a into b; this same symmetry operation need not convert b into a. If no such operation exists, the nuclei are inequivalent. Since each state in the SP basis for M = ±((N/2)-1)

can be described by its single different spin, this definition implies that the number of A_1 symmetry adapted states will be equal to the number of inequivalent spins. Thus, each inequivalent spin produces one pair of (N-1)-quantum lines.

Spin product states are more easily visualized than are symmetry adapted eigenstates, and therefore it is convenient to work in this basis. It can be shown readily that the number of distinct n-quantum transitions can be determined from any convenient basis set (not necessarily the eigenbasis) by counting the number of n-quantum matrix elements which can evolve independently. Therefore, the number of transitions (but not the transition frequencies) can be determined in the spin product basis. In this basis, an (N-1)-quantum matrix element corresponds to flipping (N-1) spins in the local field of one spin; it is still a proton, but it is distinguishable from all the other spins. The spin can be either α or β, so we expect one pair of lines for each inequivalent spin; if two spins are equivalent, there is a symmetry element which forces the two corresponding (N-1)-quantum matrix elements to be equal at all times. The number of inequivalent spins is equal to the number of possible monosubstituted species, so we assign one pair of lines to each of those species.

The number of (N-2)-quantum transitions can also be easily determined in the SP basis set, and symmetry arguments (given in Appendix A) show that the following counting scheme is correct. There are two fundamentally different ways to generate an (N-2)-quantum transition in the SP basis set. One way to generate an (N-2)-quantum transition is to flip all N spins, starting from a state with one spin β and the rest α; therefore, these transitions correspond to

$M = (N/2)-1 \rightarrow M = -((N/2)-1)$. Since all the spins flip, these N transitions have no dipolar energy, so they all occur at $(N-2)\Delta\omega$. An (N-2)-quantum transition can also be generated by flipping (N-2) spins in the local field of the remaining two, which we label x and y. The number of distinguishable ways in which two spins can be chosen out of N is determined by the symmetry of the molecule. It is equal to the number of different species with (N-2) isotopic labels. The two remaining spins may be $\alpha\alpha$, $\alpha\beta$, $\beta\alpha$, or $\beta\beta$, which gives a quartet if there is no symmetry element $x \rightarrow y$, $y \rightarrow x$, and a triplet if there is such a symmetry element (because then $\alpha\beta$ and $\beta\alpha$ are equivalent). Therefore, each unique <u>ordered</u> pair (xy) of spins in the molecule gives one pair of lines; in addition, there is always a highly degenerate peak at $(N-2)\Delta\omega$.

(N-3)-quantum transitions and lower orders can also be counted by similar schemes. However, the arguments above show that there is always at least one pair of lines in the (N-2)-quantum spectrum for each unique direct coupling constant, so the (N-3)-quantum spectrum mainly provides redundant structural information. In addition, the effects of intramolecular motion, if they can be detected at all by NMR, can be detected in the (N-1)- or (N-2)-quantum spectra. Any process which causes exchange or pseudoexchange (rotation about a bond, for example) between inequivalent sites would decrease the number of possible monosubstituted species, and therefore would affect the (N-1)-quantum spectrum. If only magnetically equivalent sites are involved, the motion operator commutes with the Hamiltonian in equation (I.11) unless the ordered pair of spins (ij) is transformed

into an inequivalent ordered pair (kl). Since this process would decrease the number of possible disubstituted species, it affects the (N-2)-quantum spectrum. The main advantage of assigning transitions in the (N-3)-quantum spectra or lower-quantum spectra is that the additional line assignments give coupling constants with better accuracy.

1.4.3 Examples of Multiple-Quantum Spectra and the Isotopic Labeling Analogy

This subsection shows how multiple-quantum NMR can be applied to specific molecules, and illustrates the use of the isotopic labeling analogy. The number of (N-1)-quantum pairs will always be equal to the number of different species with all but one of the protons removed. Each possible species with all but two protons removed contributes either a triplet or a quartet to the (N-2)-quantum spectrum. If we label the two remaining protons x and y, and if there is a symmetry element which exchanges x and y, a triplet results; if there is no such element, a quartet (two pairs) results, as mentioned earlier. Thus, one pair of lines can be assigned to each different way that one proton can be labeled x, and another proton y. This scheme is used in the examples that follow. These molecules have all been studied by members of the Pines research group.

1.4.3.1 Acetonitrile (A_3, with C_{3v} symmetry)

The acetonitrile molecule (CH_3CN) contains only three protons, so its single-quantum spectrum is easily resolvable. However, the multiple-quantum spectra are useful in studying the relaxation of an oriented methyl group.[42] An unsymmetrical three-spin system would

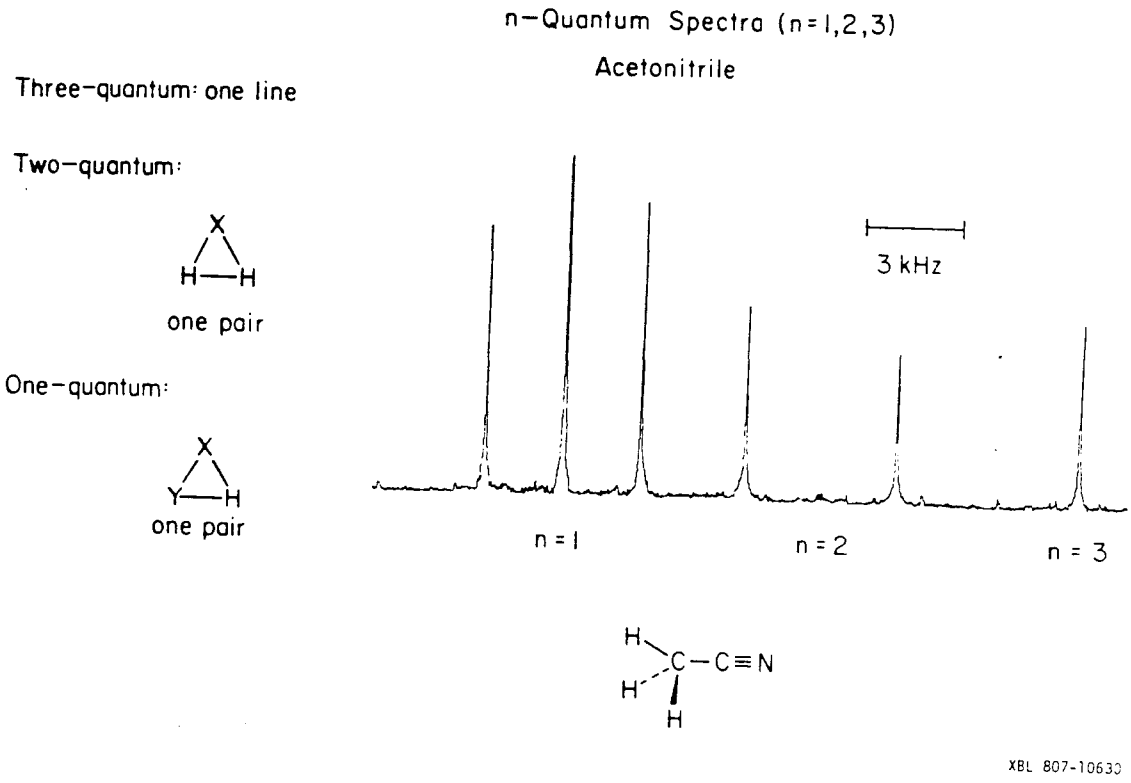

Figure I.4 The multiple-quantum spectra of the methyl group of acetonitrile. The high symmetry allows for only one monoprotonated and one diprotonated species, so the two-quantum spectrum has one doublet, and the three-quantum spectrum has one triplet.

have one three-quantum transitions, six two-quantum transitions, and fifteen one-quantum transitions (three of these are degenerate and six others are weak if chemical shift differences are small) because there are three eigenstates each for $M = \pm 1/2$ and one eigenstate each for $M = \pm 3/2$. The high symmetry of a methyl group reduces the number of transitions considerably, as shown in Figure I.4. There is only one pair of two-quantum transitions, since there is only one monoprotonated species CD_2HCN; the position of the proton is labeled x in the figure. Similarly, there is only one diprotonated species CDH_2CN, and this gives a triplet in the one-quantum spectrum, because there is a symmetry operation which exchanges the two protons. This can be seen by labeling the two protons x and y, as in the figure, and noting that the two ways to do this are related by a mirror plane. The three protons are magnetically fully equivalent (each spin is coupled identically to every other spin), so the indirect intramethyl spin-spin coupling is unobservable unless the full equivalence is broken (for example, by heteronuclear interactions). The singlet direct spin-spin coupling can be extracted from the one-quantum or the two-quantum spectrum.

1.4.3.2 Benzene (AA'A''A'''A''''A'''''', with C_{6v} symmetry)

The single-quantum spectrum of a six-spin system without symmetry would have 792 transitions, but only 15 different coupling constants. The C_{6v} symmetry of benzene reduces the number of single-quantum transitions to 76 and the number of different couplings to three.[43] All the spins are magnetically equivalent, but they are not magnetically fully equivalent because there is more than one coupling; this makes

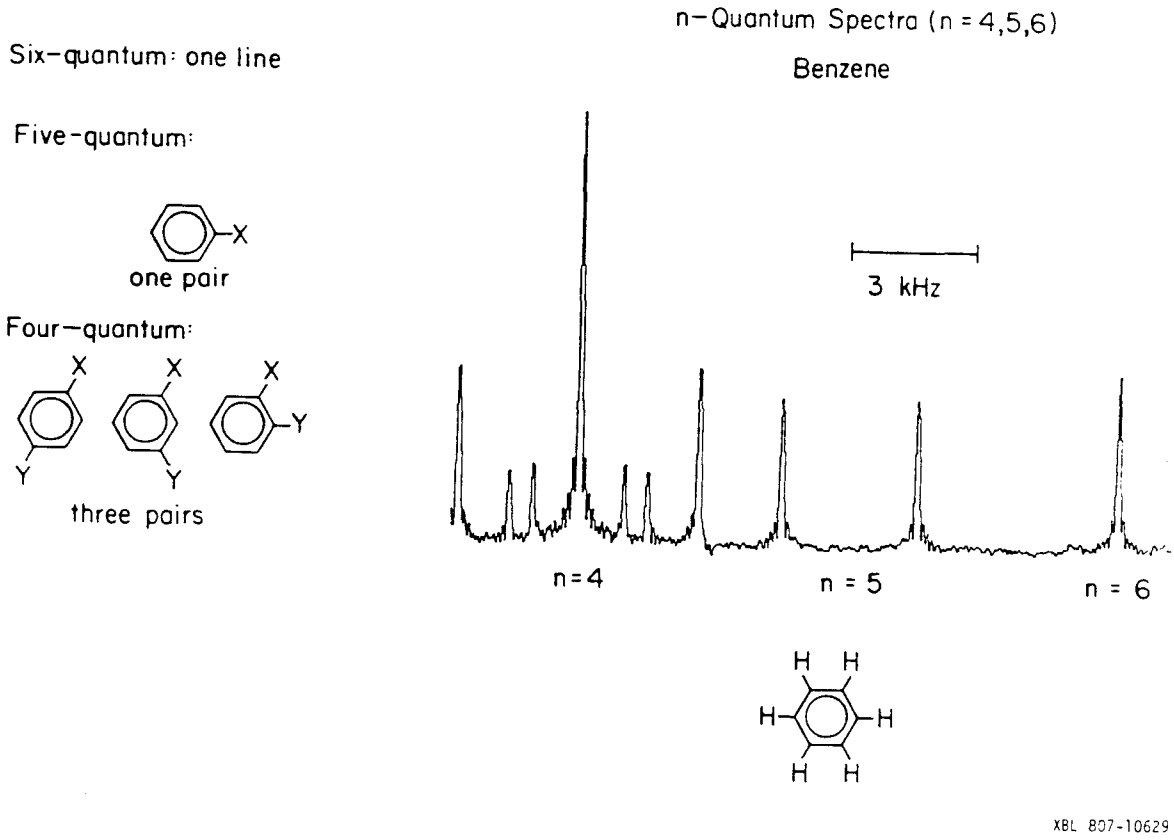

Figure I.5 The multiple-quantum spectra of benzene. There is only one possible monoprotonated species, so there is one pair of five-quantum lines. The three diprotonated species imply three triplets (seven lines) in the four-quantum spectrum.

the spectroscopic notation AA'A''A'''A''''A''''' in anisotropic solvents, as opposed to A_6 in isotropic solvents.

The high symmetry also reduces the number of allowed multiple-quantum transitions,[28,29] as shown in Figure I.5. There is only one species of monoprotonated benzene ($C_6D_5H_1$) so the five-quantum spectrum has one pair of lines, instead of the six pairs expected for an unsymmetrical molecule. There are only three possible diprotonated benzenes ($C_6D_4H_2$), corresponding to the ortho, meta, and para configurations, so the four-quantum spectrum consists of three triplets, for a total of seven lines, instead of the 61 four-quantum lines found for an unsymmetrical six-spin molecule. The experimental spectra verify these predictions, and therefore are consistent with the assumed geometry.

It is useful to consider how the spectra would change if distortions were present on an NMR time scale. Most distortions, such as an elongation along an axis perpendicular to the C_6 axis, would make the spins inequivalent and therefore would create more five-quantum and more four-quantum transitions. However, if the bonds alternated between two different lengths, as in the classical nonresonant structure with three double bonds, all the spins would remain equivalent, and the five-quantum spectrum would still have only one pair of lines. In this case more lines would be added to the four-quantum spectrum. However, the extra lines might be expected to be weak if distortions are small, and would not be produced at all if the distortions were rapid (which they certainly are in this system.)[44]

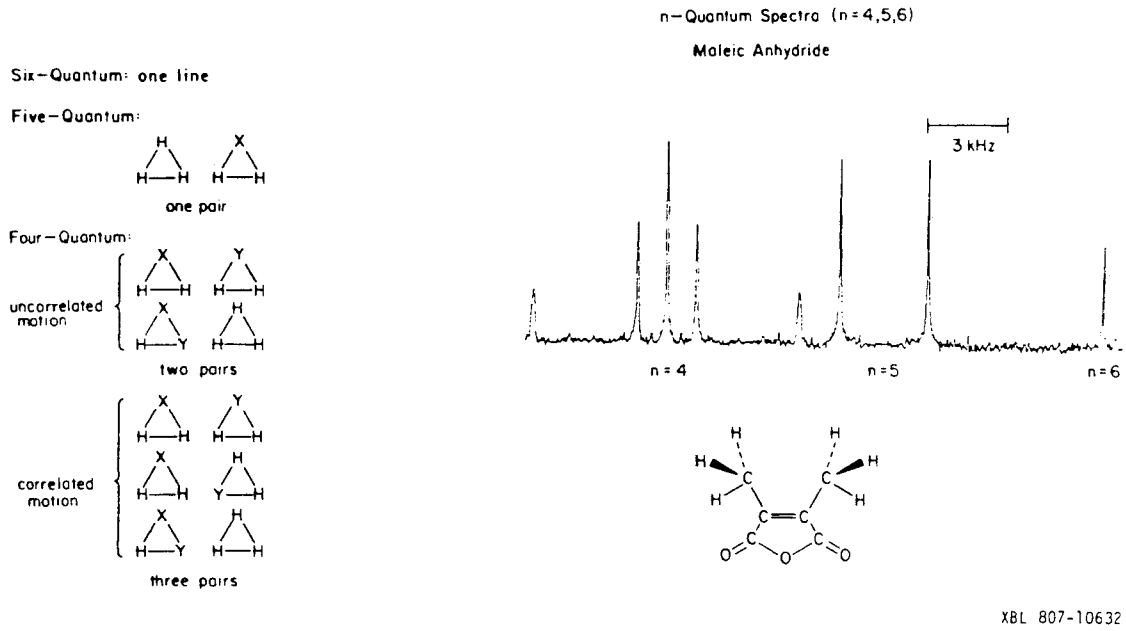

Figure I.6 The multiple-quantum spectra of maleic anhydride. The two methyl groups would give three diprotonated species if their motions were correlated, but only two if not, so the number of four-quantum lines depends on the motional model. There is only one monoprotonated species, so the five-quantum spectrum does not reflect correlations.

1.4.3.3 Maleic Anhydride (A_3A_3' with uncorrelated methyl group motion)

At room temperature the two methyl groups of this molecule are expected to rotate rapidly. As a result, all six spins are equivalent. There is only one possible monoprotonated species, so there is only one pair of five-quantum lines, as shown in Figure I.6. However, the equivalence of the spins reveals nothing about possible correlated motion between the two groups. Multiple-quantum spectroscopy provides a particularly elegant test of correlation, because the number of lines in the four-quantum spectrum is affected. If the methyl group undergoes uncorrelated motion, there are only two possible diprotonated species, giving five lines; if the motions are correlated like two gears, there are three possible disubstituted species and seven lines. Recent studies by Jau-Huei Tang[45] have shown that only five lines are present at room temperature, and that their positions are consistent with uncorrelated motion.

1.4.3.4 Cyclooctatetraene (COT)($AA'A''A^{(3')}A^{(4')}A^{(5')}A^{(6')}A^{(7')}$; symmetry depends on temperature)

Cyclooctatetraene, C_8H_8, has been shown to have D_{2d} symmetry at low temperatures by electron diffraction studies.[46] With this tub-shaped symmetry, the single-quantum spectrum has 2070 transitions,[24] as mentioned earlier. At room temperature, almost all of these transitions are broadened by a bond shift process, as shown in Figure I.7. This process can be viewed as a pseudorotation; spin 1 becomes spin 2, spin 2 becomes spin 3, and so forth. The transitions are not resolvable, so the bond shift process has been analyzed by isotopic substitution;[24] the spectra of a random mixture of all possible

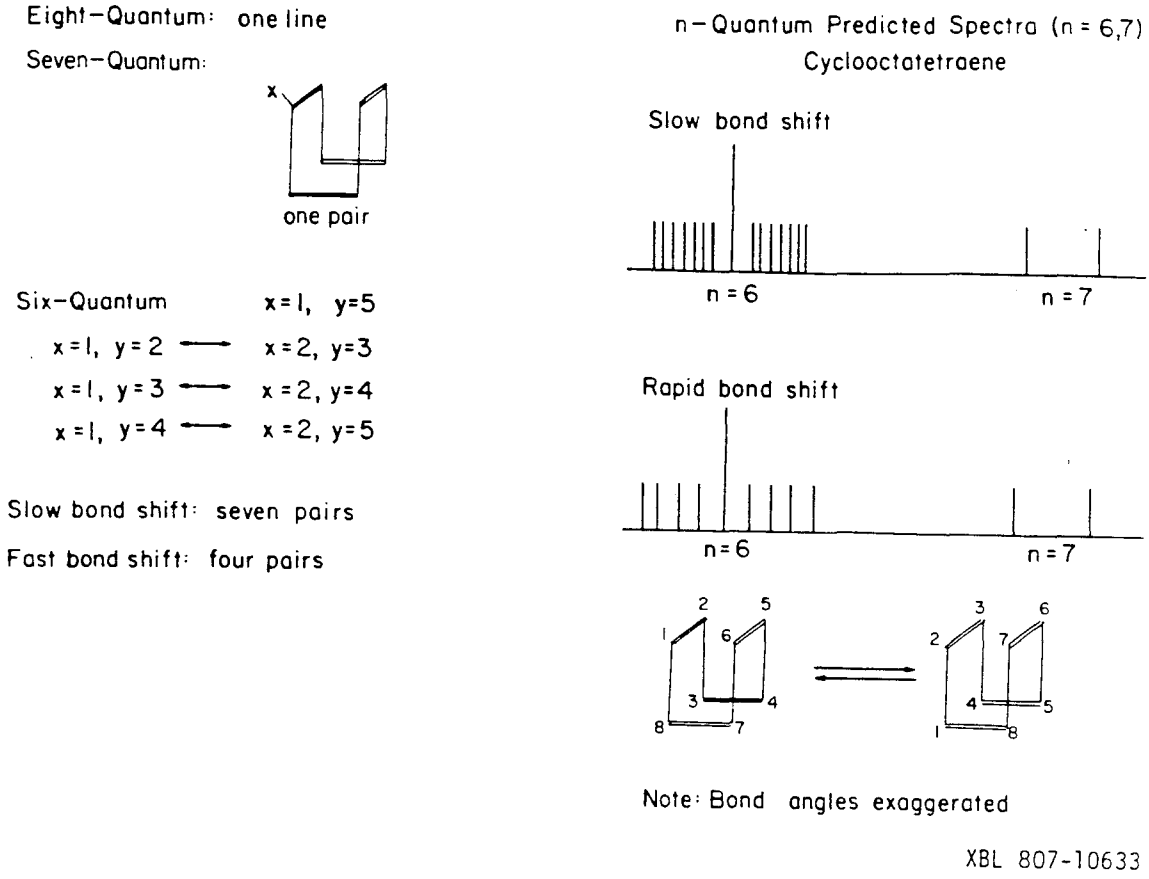

Figure I.7 The multiple-quantum spectra of cyclooctatetraene. The single-quantum spectrum has 2070 lines, and is totally unresolvable when the bond shift rate is comparable to dipolar couplings. The six-quantum transitions also broaden, but they are still resolvable. In the high temperature limit, six lines have disappeared since the number of diprotonated species is reduced. There is only one mono-protonated species at any temperature, so the seven-quantum spectrum is unaffected by the bond shifts. This molecule will be discussed further in section 6.2.

diprotonated species were analyzed.

Multiple-quantum spectroscopy allows the fully protonated species to be directly studied. Since all the spins are equivalent, there is only one monoprotonated species, independent of the bond shift rate; therefore there would be only one pair of seven-quantum lines, and these lines give no kinetic information. However, the six-quantum spectrum is affected by the bond shift. At low temperatures the D_{2d} symmetry should give six independent dipolar coupling constants (D_{12}, D_{13}, D_{14}, D_{15}, D_{16} and D_{18}; $D_{17} = D_{13}$ by symmetry), so there are six diprotonated species. The species (1,3) gives a quartet, since there are no symmetry operations $1 \rightarrow 3$, $3 \rightarrow 1$; all the other species give triplets. Labeling the two protons x and y as before, we find x=1, y=2; x=1, y=3; x=3, y=1 ($\equiv$ x=2, y=4 by symmetry); x=1, y=4; x=1, y=5; x=1, y=6 ($\equiv$ x=2, y=5 by symmetry); and x=1, y=8 ($\equiv$ x=2, y=3 by symmetry), so there should be seven pairs of lines. At high temperature, the rapid bond shift makes x=1, y=2 equivalent to x=2, y=3; x=1, y=3 equivalent to x=2, y=4; and x=1, y=4 equivalent to x=2, y=5. The number of six-quantum pairs should therefore be reduced to four.

The effective permutation group is the same as that of a regular octagon; however, since $D_{ij} \sim \langle r_{ij}^{-3} \rangle$, the coupling constants will not have the ratios that octagonal symmetry would dictate. This molecule will be discussed again in section 6.2

1.4.3.5 Substituted Biphenyls (AA'A''A'''BB'B''B'''; symmetry depends on model)

The relative motion of the two phenyl groups of biphenyl and its derivatives can be studied by measuring the direct coupling constants.

However, the single-quantum spectrum of biphenyl is extremely complex. Some simplification can be achieved by removing the two protons on the ends of the molecule, since their distance is independent of the ring motion, but even with this substitution the single-quantum lines cannot be completely resolved. Diehl and co-workers[47a] analyzed the spectrum of 4,4'-dichlorobiphenyl by picking out a number of the transitions and iterating on their frequencies. The spectrum of 4,4'-bipyridyl has also been analyzed.[47b]

By contrast, the multiple-quantum spectra of substituted biphenyls are easily resolvable. The seven-quantum spectrum will always contain two pairs of lines if the substituents are identical, since there are two monoprotonated species, as shown in Figure I.8. Even if the substituents are not identical, the biphenyl structure is not likely to be substantially distorted, so two pairs are still expected (although the lines may be split).[48] The number of six-quantum lines depends on the motional model. Either free rotation or jumps between four equivalent sites (corresponding to inter-ring angles θ, $-\theta$, $\pi + \theta$, and $\pi - \theta$) will give seven diprotonated species; labeling the spins x and y shows that there are ten pairs of lines. However, jumps between only two sites (corresponding to inter-ring angles θ and $-\theta$) will give fourteen pairs of lines, as will a small amplitude rocking motion around a single site. Steve Sinton has shown that eight pairs of lines are visible above the noise level in the six-quantum spectrum of 4-cyano-4'-pentyl-d_{11}-biphenyl,[48] and their positions coincide with those of eight of the ten pairs which a four-site model would generate. Computer simulations have shown

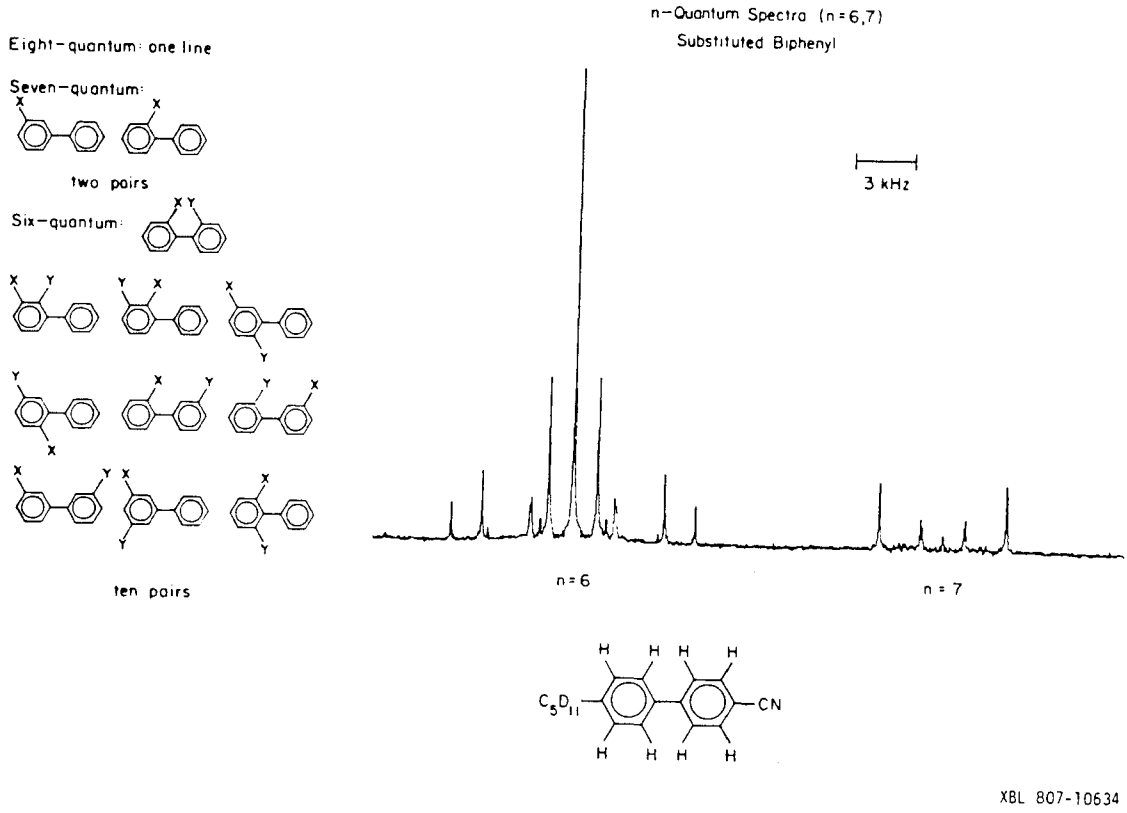

Figure I.8 The multiple-quantum spectra of a typical para-disubstituted biphenyl. The two substituents are different, but the rings should not be strongly distorted, and the dipolar Hamiltonian is assumed to have a symmetry operation which exchanges them. There are then two mono-protonated species, so there are two pairs of seven-quantum lines. Jumps between four equivalent values for the inter-ring angle would give seven diprotonated species (four triplets and three quartets) and ten pairs of lines.

that the remaining two pairs are expected to be weak, and extensive signal averaging would probably be required to observe them. It is interesting to note that isotopic labeling of the substituents was combined with multiple-quantum NMR to study this molecule. Synthesizing the molecule with a perdeuterated chain is straightforward[49] but selective substitution on the rings is more difficult.

1.5 Conclusions

The conventionally observed $\Delta M = 1$ transitions do not have any special information content that cannot be found in other transitions. In fact, the dramatic spectral simplification which occurs as ΔM increases makes the observation of multiple-quantum transitions advantageous. The multiple-quantum transitions are readily interpretable and generally resolvable, and this makes their observation an important and practical alternative to spin labeling.

II. Theory of Multiple-Quantum NMR

It was shown in Chapter I that the observation of multiple-quantum transitions provides dramatic spectral simplifications compared to the observation of single-quantum transitions, without any real loss of information content. Nevertheless, until recently multiple-quantum NMR has not been extensively used, and single-quantum NMR is still much more common. One important reason is that, while it is possible to produce multiple-quantum transitions by cw techniques,[50-54] the technique has serious limitations which will be discussed in section 2.2. Even if a spectrometer is designed to give rf pulses, it may not be versatile enough for multiple-quantum experiments. It should also be noted that single-quantum spectra are not always as complicated as the worst cases discussed in section 1.4 would imply. In an isotropic system, for example, many transitions will be nearly degenerate or will have vanishingly small intensities if the chemical shift differences are much larger than the J couplings.[8]

The most important reason, however, is the difficulty of producing multiple-quantum spectra with good signal-to-noise ratios. It is not coincidental that all of the molecules listed in section 1.4.3 are fairly small (eight spins or less with some symmetry). The problem is best understood through the density matrix formalism, which will be developed in the next several sections.

2.1 Operator Formalisms

2.2.1 The Density Matrix

The density matrix is a standard quantum mechanical tool for dealing with coherent processes and mixed states.[5,55] Any pure state

can be written as a linear combination of the basis functions of any complete orthonormal set

$$|\Psi\rangle = \sum_i c_i |i\rangle \quad . \tag{II.1}$$

The expectation value of any observable operator A is then

$$\langle\Psi|A|\Psi\rangle = \sum_{i,j} c_i c_j^* \langle j|A|i\rangle \quad . \tag{II.2}$$

The operator A can be represented by a set of numbers A_{ij} such that $A_{ij} = \langle i|A|j\rangle$; these numbers are usually written in matrix form. If the system is not known to be in a pure state (for example, if only ensemble averages of observables over a macroscopic sample can be measured) then equation (II.2) is replaced by

$$\overline{\langle\Psi|A|\Psi\rangle} \equiv \langle A\rangle = \sum_{i,j} \overline{c_i c_j^*} \langle j|A|i\rangle \quad . \tag{II.3}$$

The density matrix element ρ_{ij} is defined to be equal to $\overline{c_i c_j^*}$; the density operator $\rho = \sum_{i,j} \rho_{ij} |i\rangle\langle j|$. It can be seen from equation (II.1) that ρ_{ii} is the population of state i, and that ρ_{ij} $(i \neq j)$ is only nonzero if there is a definite phase relationship between the coefficients c_i and c_j that survives the ensemble averaging. This phase relationship is called coherence.

Equation (II.3) can be further rewritten as

$$\langle A\rangle = \sum_{i,j} \rho_{ij} A_{jk} = \sum_i (\rho A)_{ii} = \mathrm{Tr}(\rho A) \quad . \tag{II.4}$$

Thus the expectation values of all observables can be predicted if all the elements of ρ are known, and therefore ρ contains all the

available information about the system.

The equation of motion under a Hamiltonian $\mathcal{H}(t)$ is

$$\dot{\rho}(t) = i[\rho(t),\mathcal{H}(t)] \quad . \tag{II.5}$$

If the Hamiltonian is time independent ($\mathcal{H}(t) = \mathcal{H}$), equation (II.5) can be simplified considerably. In this case

$$\dot{\rho}(t) = i[\rho(t), \mathcal{H}] \tag{II.6a}$$

$$\ddot{\rho}(t) = i[\dot{\rho}(t), \mathcal{H}] \tag{II.6b}$$

$$\rho^{(n)}(t) = i[\rho^{(n-1)}(t),\mathcal{H}] \tag{II.6c}$$

$$\rho(t) = \exp(-i\mathcal{H}t)\rho(o)\ \exp(i\mathcal{H}t) \quad . \tag{II.7}$$

Thus, in the absence of relaxation, $\rho(t)$ is related to $\rho(o)$ by a unitary transformation, called the propagator. This relation holds even if $\mathcal{H}$ is not time independent; in that case the propagator is T exp $(-i\int\mathcal{H}(t)dt)$, where T is the Dyson time-ordering operator. All properties which are invariant under unitary transformation are therefore constants of the motion; these include $Tr(\rho) = \sum_i \rho_{ii} = 1$, $Tr(\rho^2) = \sum_{ij} |\rho_{ij}|^2$, and the entropy $S = -kTr(\rho \ln \rho)$.[56]

From statistical mechanics it is known that at equilibrium the density matrix for a canonical ensemble will be $\rho_o = \exp(-\mathcal{H}/kT)/Tr(\exp(-\mathcal{H}/kT))$. The Zeeman Hamiltonian $\mathcal{H}_z$ is usually the largest term by far in $\mathcal{H}$, so that

$$\rho_o = 1 - \beta I_z + \ldots$$

$$\beta = (\gamma B_o/kT)/Tr(\exp(-\mathcal{H}_z/kT)) \tag{II.8}$$

and at normal magnetic field strengths $\beta << 1$ unless $T << 1$ K, so only the first two terms in the expansion in equation (II.8) are retained. In fact, the identity operator is frequently omitted, since it commutes with all other operators and does not affect the evolution. This produces a reduced density matrix $\rho_o = -\beta I_z$. The same symbol will be used for the full density matrix and the reduced density matrix, with the meaning clear from context (the reduced density matrix will be used exclusively for the rest of this work, except for section 6.3). All the properties of the density matrix also hold for the reduced density matrix, except that the reduced density matrix is traceless.

It is frequently convenient to separate the system Hamiltonian into two parts $H_0 + H_1$, and then go to an interaction representation defined by[10]

$$\tilde{A} = \exp(iH_0t)A\exp(-iH_0t) \tag{II.9}$$

A is any operator, including the density operator. It can be readily shown that

$$\dot{\tilde{\rho}} = i[\tilde{\rho},\tilde{H}_1] \tag{II.10}$$

$$\langle\tilde{A}\rangle = \mathrm{Tr}(\tilde{\rho}A) \quad . \tag{II.11}$$

For a system which is irradiated at frequency ω the choice $H_0 = \omega I_z$ is particularly convenient. This generates the rotating frame Hamiltonians of section 1.2, in which continuous irradiation gives a time independent $\mathcal{H}_{rf}$. Equation (II.11) implies that all observables must be referenced to the radiofrequency field. For example, $\tilde{I}_x$

is not parallel to the laboratory x-axis at all times, but it does have a definite phase relation with the rf. The tildes will be dropped for the rest of this work, but the rotating frame is assumed.

Equations (II.5-7) are only valid for nonexchanging systems in the absence of relaxation. The theory of exchanging systems will be discussed in section 6.2. The simplest treatment of relaxation[57,58] introduces relaxation times T_1 and T_2 for the off-diagonal and diagonal matrix elements respectively:

$$\dot{\rho}_{ii} = i[\rho,\mathcal{H}]_{ii} - \frac{\rho_{ii}-(-\beta I_z)_{ii}}{T_1} \qquad \text{(II.12)}$$

$$\dot{\rho}_{ij} = i[\rho,\mathcal{H}]_{ij} - \frac{\rho_{ij}}{(T_2)_{ij}} \qquad \text{(II.13)}$$

where $(-\beta\ I_z)_{ii}$ is the equilibrium population of the ith state. In the most general case $(T_2)_{ij}$ is different for every transition.[58]

2.1.2 Fictitious Spin Operators

The evolution of a system in the density operator formalism can be viewed from two different perspectives. One possibility is to examine matrices, i.e., focus on an individual element ρ_{ij} of the density matrix, and observe how this element changes with time. The element is calculated through matrix manipulations. This perspective is useful for computer calculations. ρ_{ij} depends on the choice of the basis set, and the obvious choice is the Hamiltonian eigenbasis, but frequently the values of chemical shifts and coupling constants are not known in advance, so this basis cannot be determined.

The other possibility is to examine operators. For example,

the equilibrium density operator is $-\beta I_z = -\beta \sum_i I_{zi}$, where I_{zi} acts only on the ith spin. An operator which acts on n spins (for example, $I_{x1}I_{y2}I_{z3}$) may connect states with $\Delta M = 0, \pm 1, \ldots, \pm n$. However, not all n-spin operators give $\Delta M = n$. The expectation values of all operators can be calculated as a function of time to describe the evolution of the system.

Clearly, the choice of a basis set is as important for an operator perspective as it is for a matrix perspective. A system of N spins-1/2 has 2^N eigenstates, and 4^N linearly independent operators are required to describe it completely (there is one constraint, Tr $\rho = 1$). Several useful basis sets are:

2.1.2.1 Single Spin-1/2 Operators

Each spin has two states α and β, so it has four linearly independent operators. These four can be chosen as I_{xi}, I_{yi}, I_{zi}, and I_i.[59] This gives 4^N operators for the entire system, and the constraint Tr $\rho = 1$ simply specifies the expectation value of the operator $1_1 1_2 1_3 \ldots 1_n$. The identity matrices are generally omitted from all other operators.

One disadvantage of this basis is that it can be difficult to tell what values of ΔM are produced by certain linear combinations. For example, the operator $I_{x1}I_{x2}$ connects states with $\Delta M = 0, \pm 2$, as does the operator $I_{y1}I_{y2}$. However, $I_{x1}I_{x2} + I_{y1}I_{y2} = \vec{I}_1 \cdot \vec{I}_2 - I_{z1}I_{z2}$ commutes with I_z, and hence only connects states with $\Delta M = 0$. This problem can be avoided by the use of raising or lowering operators $I^{\pm} = I_x \pm iI_y$, and either I_z and 1 or $I^{0\pm} = 1/2 \pm I_z$.[59,60] Commutator relations and matrix representations

for these operators are listed in Appendix E.

A single operator in the basis I^+, I^-, I^{0+}, I^{0-} (for example, $I_1^+I_2^-I_3^+$) corresponds to a single density matrix element in the spin product (SP) basis, and this basis is useful for that reason. Every operator in the I_x, I_y, I_z, 1 basis set has 2^N elements in the SP basis. Operators in the I^+, I^-, I_z, 1 basis set have 2^g elements, where g is the number of times I_z or 1 occurs.

2.1.2.2 Generalized Spin Operators

Fictitious spin-1/2 operators were defined by Vega and Pines for spin-1 systems.[61] These are:

$$
\begin{array}{lll}
I_{x,1}=1/2\ I_x & I_{y,1}=1/2\ I_y & I_{z,1}=1/2\ I_z \\
I_{x,2}=1/2(I_yI_z+I_zI_y) & I_{y,2}=1/2(I_zI_x+I_xI_z) & I_{z,2}=1/2(I_xI_y+I_yI_x) \\
I_{x,3}=1/2(I_z^2-I_y^2) & I_{y,3}=1/2(I_x^2-I_z^2) & I_{z,3}=1/2(I_y^2-I_x^2)
\end{array}
\qquad \text{(II.14)}
$$

A spin-1 has three states and nine linearly independent operators. All nine of the operators in equation (II.14) are traceless, so they cannot all be linearly independent, and in fact $I_{x,3} + I_{y,3} + I_{z,3} = 0$. Double-quantum transitions in the presence of quadrupolar interactions are readily described in this basis. These operators are easily generalized to the case of N coupled spins-1.

A set of fictitious spin-1/2 operators for general multiple-quantum transitions can also be defined.[62] Every pair of eigenstates $|r\rangle$ and $|s\rangle$ becomes an effective two-level system, with three operators

$$\langle i|I^x_{rs}|j\rangle = \frac{1}{2}\,(\delta_{ir}\delta_{js} + \delta_{is}\delta_{jr})$$

$$\langle i|I^y_{rs}|j\rangle = (-i/2)(\delta_{ir}\delta_{js} - \delta_{is}\delta_{jr})$$

$$\langle i|I^z_{rs}|j\rangle = \frac{1}{2}\,(\delta_{ir}\delta_{jr} - \delta_{is}\delta_{js}) \qquad \text{(II.15)}$$

These operators can be used for spin-1 systems, and in these systems are related to the operators defined by Vega and Pines. In a system with N spins-1/2 there are $2^N(2^N-1)$ possible pairs of spins, so there are far more operators than can be linearly independent (for example, if N = 6 there are 12096 operators, all of which are traceless, but only 4095 traceless linearly independent operators). This makes these operators inconvenient for large systems.

2.2 Simple NMR Experiments

2.2.1 Continuous Irradiation

The simplest method of inducing transitions between two states $|i\rangle$ and $|j\rangle$ is to irradiate the system with photons which have an energy equal to the transition energy and monitor the absorption. In the presence of continuous rf irradiation at the frequency ω, the rotating frame Hamiltonian can be written as

$$\begin{aligned}\mathcal{H} &= \Delta\omega I_z + (\mathcal{H}_{cs}+\mathcal{H}_J+\mathcal{H}_D+\mathcal{H}_Q) - \omega_1 I_x \\ &= \mathcal{H}_z - \omega_1 I_x \qquad . \qquad \text{(II.16)}\end{aligned}$$

All of these symbols were defined in section 1.2. The density matrix equation of motion (II.12-13) is most conveniently expressed in the $\mathcal{H}_z$ eigenbasis:

$$\dot{\rho}_{ii} = i\omega_1[I_x,\rho]_{ii} - \frac{\rho_{ii}+\beta I_z}{T_1} \tag{II.17}$$

$$\rho_{ij} = i\omega_1[I_x,\rho]_{ij} + i\omega_{ij}\rho_{ij} - \frac{\rho_{ij}}{(T_2)_{ij}} \tag{II.18}$$

$$\omega_{ij} = \langle i|\mathcal{H}_z|i\rangle - \langle j|\mathcal{H}_z|j\rangle \tag{II.19}$$

The observable operator is the transverse magnetization in the rotating frame

$$\langle M_y\rangle = C\ \mathrm{Tr}(\rho I_y) = C \sum_{i,j} \rho_{ij}\ (I_y)_{ji} \tag{II.20}$$

The spectrum is obtained by sweeping ω_o or ω over the region of interest. If this sweep is done slowly, it may be assumed that $\dot{\rho} = 0$. This gives:

$$\rho_{ii} = (-\beta I_z)_{ii} - i\omega_1 T_1[I_x,\rho]_{ii} \tag{II.21}$$

$$\rho_{ij} = \left(\frac{i\omega_1(T_2)_{ij}}{1-i\omega_{ij}(T_2)_{ij}}\right)\ [I_x,\rho]_{ij} \tag{II.22}$$

The steady-state solution for the signal S is easily expanded in powers of ω_1:

$$\rho = \rho^{(0)} + \omega_1\rho^{(1)} + \omega_1{}^2\rho^{(2)} + \ldots \tag{II.23}$$

$$\rho^{(0)} = -\beta I_z = \rho^{eq};\ S^{(0)} = \mathrm{Tr}(I_y\rho^{(0)}) = 0 \tag{II.24}$$

$$\omega_1\rho_{ii}^{(1)} = 0\ ;\ \omega_1\rho_{ij}^{(1)} = \left(\frac{\beta\omega_1(T_2)_{ij}}{1-i\omega_{ij}(T_2)_{ij}}\right)\ (I_y)_{ij}\ ;$$

$$S^{(1)} = C\,\mathrm{Tr}(I_y\rho^{(1)}) = C\,\beta \sum_{ij} |I_y|^2_{ij} \left\{\frac{\omega_1(T_2)_{ij}}{1-i\omega_{ij}(T_2)_{ij}}\right\} \qquad \text{(II.25)}$$

Equation (II.24) merely shows that there is no transverse magnetization if $\omega_1 = 0$, since the system is then at equilibrium with the static field. Equation (II.25) gives the conventional high-resolution NMR spectrum, and several important features should be noted. $\rho^{(1)}_{ij} = 0$ if $(I_y)_{ij} = 0$, and since I_y is a single-quantum operator only matrix elements with $\Delta M = 1$ can be excited. In addition, $\rho^{(1)}_{ij}$ is small if $\omega_{ij}(T_2)_{ij} << 1$, so ω must be within a few linewidths of the frequency difference between states $|i\rangle$ and $|j\rangle$ for $\rho^{(1)}_{ij}$ to be substantial. Thus only transitions which are nearly resonant contribute to the signal. Finally, the lineshapes are Lorentzian, and the intensity of the transition between states $|i\rangle$ and $|j\rangle$ is proportional to $|I_y|^2_{ij}$.

Multiple-quantum coherences will only appear to higher powers in ω_1. For example, $\omega_1{}^2\rho^{(2)}$ is:

$$\omega_1{}^2\rho_{ii}{}^{(2)} = -2i\omega_1\, T_1\beta \left(\sum_k \left(\frac{\omega_1(T_2)_{ik}}{1+\omega^2_{ik}(T_2)^2_{ik}}\right)(I_x)_{ik}(I_y)_{ki}\right)$$

$$\omega_1{}^2\rho_{ij}{}^{(2)} = \frac{i\omega_1(T_2)_{ij}\beta}{1-i\omega_{ij}(T_2)_{ij}} \left(\sum_k \frac{\omega_1(T_2)_{kj}}{1-i\omega_{kj}(T_2)_{ikj}}(I_x)_{ik}(I_y)_{kj} - \right.$$

$$\left. \frac{\omega_1(T_2)_{ik}}{1-i\omega_{ik}(T_2)_{ik}}(I_y)_{ik}(I_x)_{kj}\right) \qquad \text{(II.26)}$$

$\rho^{(2)}_{ij}$ can have nonvanishing matrix elements only between states with $\Delta M = 0, \pm 2$. For these matrix elements to be substantial the following

conditions must be fulfilled.

1. $\omega_{ij}(T_2)_{ij} \lesssim 1$. If $\Delta M = 2$ this implies that 2ω is nearly equal to the frequency difference between states i and j; if $\Delta M = 0$ this condition cannot be matched by changing ω. Thus $\rho^{(2)}$ does not have substantial zero-quantum operators.

2. ω_1 must be at least comparable to $\langle\omega_{ik} - \omega_{kj}\rangle$, the frequency spread of the single-quantum transitions.

3. However, the energy levels which are connected by I_x or I_y must have some anharmonicity. If the levels are perfectly harmonic and $\Delta M = 2$, then $\omega_{ik} = \omega_{kj}$ and $\rho_{ij}^{(2)} = 0$. Similar results hold for other values of ΔM.

Even if all of these conditions are met, so that $\rho^{(2)}$ has two-quantum operators, $S^{(2)} = \mathrm{Tr}(I_y\rho^{(2)}) = 0$. Only single-quantum operators are observable. However, a large two-quantum operator generates single-quantum operators in $\rho^{(3)}$, and therefore $S^{(3)}$ (which is proportional to ω_1^3) gives signal for two-quantum transitions.

Transitions with $\Delta M > 2$ require higher-order perturbation theory, which will not be done here. A complete solution can be found in reference (52). However, the form of equations (II.21-22) allows some qualitative comments. The first term which has n-quantum operators is $\rho^{(n)}$; if n is even, $\rho^{(n)}$ has only even-quantum operators, and if n is odd it has only odd-quantum operators. The n-quantum operators must generate even higher-order terms with single-quantum operators in order to be observable, and the first such term is $\rho^{(2n-1)}$, so the signal is proportional to $\omega_1^{(2n-1)}$. The n-quantum transition can only give substantial signal if $n\omega$ is nearly equal to

its frequency difference, and this implies that zero-quantum transitions do not appear because they cannot be put on resonance. However, if $S^{(2n+1)}$ is large the signal for the n-quantum transition will tend to decrease. For example if the single-quantum transition $|i\rangle \rightarrow |k\rangle$ $(M_k=M_i+1)$ is the only resonant transition, then $\rho_{ii}^{(2)} < 0$, $\rho_{kk}^{(2)} > 0$, the population differences are depleted, and $S^{(3)}$ reduces the signal. This effect is called saturation. Lower-quantum transitions saturate at lower powers, but the high-quantum transitions have only a narrow range for ω_1 between the value which starts to produce them and the value which causes them to disappear through saturation.

The net result is that continuous wave multiple-quantum NMR is sometimes useful for two-quantum or even three-quantum transitions,[51] but is not really useful for higher quanta. In a small spin system the two-quantum transitions can help in line assignments,[53] but in larger systems the two-quantum spectra are hardly simpler than the single-quantum spectra, and the additional experimental difficulties are rarely justified.

2.2.2 Pulse Methods: Single-quantum Experiments

An alternative method of observing NMR transitions involves applying one or more intense rf pulses and then observing the transverse magnetization as it evolves under $\mathcal{H}_z$. The simplest experiment is to apply one pulse as in Figure (II.1a). During the pulse the Hamiltonian is that of equation (II.16). If the pulse has a length t_p, the density matrix at the end of it is, from equation (II.7),

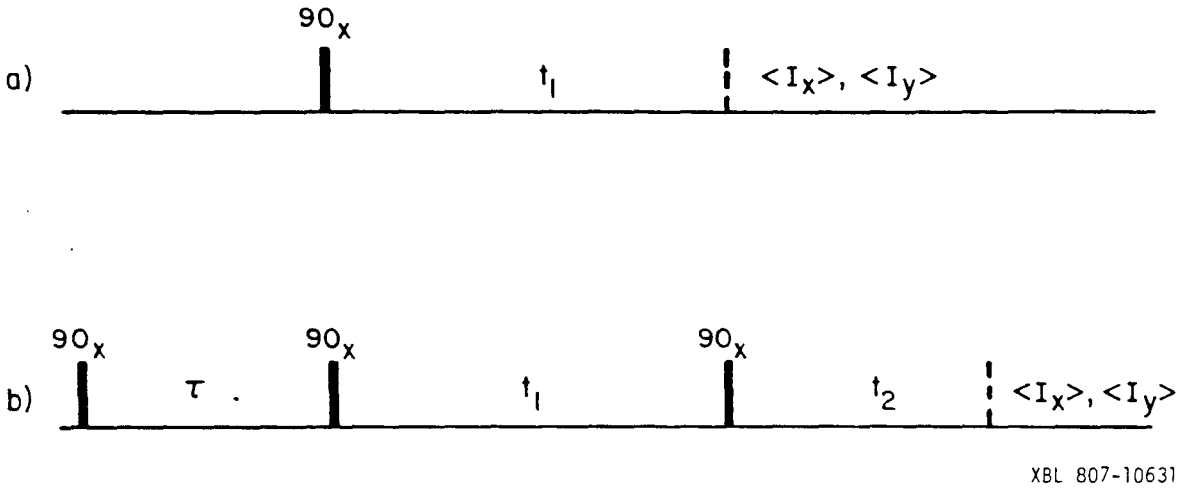

Figure II.1. Simple pulse sequences for NMR experiments. In this notation 90 is the flip angle of the pulses in degrees ($\theta = 180\ \omega_1 t_p/\pi$, where ω_1 is the rf field strength and t_p is the pulse width) and the subscript indicates the phase of the rf relative to some reference wave. The sequence in part a prepares and detects only single-quantum transitions. The sequence in part b prepares and detects multiple-quantum transitions.

$$\rho(t_p) = \exp(-i(\mathcal{H}_z-\omega_1 I_x)t_p)(-\beta I_z)\exp(i(\mathcal{H}_z-\omega_1 I_x)t_p) \qquad \text{(II.27)}$$

ω_1 and t_p are controlled by the experimenter. If ω_1 is large enough, it is possible to pick t_p such that $\omega_1 t_p \sim 1$ but all matrix elements of $\mathcal{H}_z$ are much less than 1. Using the concept of the norm of a matrix defined in Appendix E, and the expansions for exponential operators given there, one finds that

$$\rho(t_p) \sim \exp(i\omega_1 t_p I_x)(-\beta I_z)\ \exp(-i\omega_1 t_p I_x)$$

$$= -\beta(I_z\cos(\omega_1 t_p) - I_y\sin(\omega_1 t_p)) \qquad \text{(II.28)}$$

since the contribution of $\mathcal{H}_z$ is negligible. The dipole moment $\vec{\mu} = \gamma\vec{I}$ is rotated by an angle $\theta = \omega_1 t_p$ away from the z-axis.[6] If $\theta = \pi/2$ all of the population differences are simultaneously depleted, and these differences are transferred into single-quantum coherence. The signal after a time t_1 of free evolution is:

$$\langle M_y(t_1)\rangle = C\ \mathrm{Tr}(\rho(t_1)I_y) = C \sum_{ij} \rho_{ij}(t_1)(I_y)_{ji}$$

$$= C \sum_{ij} \rho_{ij}(t_p)\ \exp(i\omega_{ij}t_1)\ \exp(-t_1/(T_2)_{ij})(I_y)_{ji}$$

$$= -C\beta \sum_{ij} |I_y|^2_{ij}\ \exp(i\omega_{ij}t_1)\ \exp(-t_1/(T_2)_{ij})\ \sin(\omega_1 t_p)$$

$$\text{(II.29)}$$

Fourier transformation with respect to t_1 gives:

$$S(\omega) = -C\beta \sin(\omega_1 t_p) \sum_{ij} |I_y|^2_{ij} (T_2)_{ij}/(1-i(\omega-\omega_{ij})(T_2)_{ij}) \tag{II.30}$$

Comparison of equations (II.30) and (II.25) show that the spectrum obtained from weak cw irradiation is exactly proportional to the spectrum obtained from Fourier transforming the free induction decay (FID) after one pulse.[21]

2.2.3 Pulse Methods: Multiple-Quantum Experiments

2.2.3.1 Simplest Multiple-Quantum Sequence

The simplest pulse sequence for producing nonselective wideband multiple-quantum spectra is shown in Figure (II.1(b)).[28,32,63] The first two pulses are separated by a delay τ. At the end of the second pulse, the reduced density matrix is:

$$\rho_{MQ}(t) = -\beta \exp(-i\pi I_y/2) \exp(-i\mathcal{H}_z\tau) \exp(i\pi I_y/2) I_z \exp(-i\pi I_y/2)$$

$$\exp(i\mathcal{H}_z\tau) \exp(i\pi I_y/2) \equiv -\beta \exp(-i\mathcal{H}_x\tau) I_z \exp(i\mathcal{H}_x\tau) \tag{II.31}$$

$$\mathcal{H}_x = \sum_{i\,j} D_{ij}(3I_{xi}I_{xj} - \vec{I}_i\cdot\vec{I}_j) + \sum_{i\,j} J_{ij}(\vec{I}_i\cdot\vec{I}_j) - \Sigma\sigma_i I_{xi} + \Delta\omega I_x \quad . \tag{II.32}$$

In general $\mathcal{H}_x$ will contain zero-quantum, one-quantum and two-quantum operators, so the complex exponential can give ρ matrix elements corresponding to all multiple-quantum orders. After these pulses, the system evolves under $\mathcal{H}_z$ for a time t_1. Multiple-quantum coherences do not correspond to oscillating magnetization, so they cannot be directly detected, and a third pulse plus a delay t_2 are

needed to partially transfer them back into the observables $\langle I_x \rangle$ and $\langle I_y \rangle$. The sequence is repeated with different values of t_1. The signal as a function of t_1 is

$$\langle M_x(t_1)\rangle = C\ \mathrm{Tr}(\rho I_x) = C\ \mathrm{Tr}(\rho\ \exp(-i\pi I_y/2)\ I_z\ \exp(i\pi I_y/2)$$

$$= -C\beta\ \mathrm{Tr}(\exp(i\mathcal{H}_x t_2) I_z\ \exp(-i\mathcal{H}_x t_2)\ \exp(-i\mathcal{H}_z t_1)$$

$$\times \exp\ (-i\mathcal{H}_x \tau) I_z\ \exp(i\mathcal{H}_x \tau)\ \exp(i\mathcal{H}_z t_1)) \qquad \text{(II.33)}$$

$$= -C\beta^{-1} \sum_{ij} (\rho_{MQ}(\tau))_{ji} (\rho_{MQ}(-t_2))_{ij}\ \exp(i\omega_{ij} t_1) \qquad \text{(II.34)}$$

where $\rho_{MQ}(-t_2)$ is defined by analogy with equation (II.31). The signal is Fourier transformed with respect to t_1 to produce a multiple-quantum spectrum. For simplicity of notation relaxation terms have been neglected; if t_1, $t_2 \ll T_2$ they can be included in Equation (II.34) by replacing $\exp(\ i\omega_{ij} t_1)$ with $\exp(i\omega_{ij} t_1)$ $\exp(-t_1/(T_2)_{ij})$.

Equation (II.34) reveals several differences between pulse and cw multiple-quantum experiments. The linewidth of each transition is $(T_2)_{ij}$ for the pulses, but this is true only for the single-quantum transitions in the cw experiment. The apparent frequency of a n-quantum transition is the frequency difference (in the rotating frame) between the two states with the pulse sequence, but is a factor of n smaller than this in the cw case. The most important difference, however, is that the rf field strength ω_1 does not appear in the pulse expression, as long as ω_1 is large enough so that $\mathcal{H}_z$ can be

neglected during t_p. As a result, there are no saturation effects.

2.2.3.2 Separation of Orders; Removal of Static Inhomogeneity

Several simple multiple-quantum pulse sequences are illustrated in Figure (II.2). Inspection of $\mathcal{H}_z$ shows that the n-quantum spectrum is centered at $n\Delta\omega$ with the sequence in Figure (II.2(a)), so different values of n will be completely separated if $\Delta\omega$ is greater than the spectral width $||\mathcal{H}_z||$. However, if the field is inhomogeneous, the resonance offset term must be replaced with $\Delta\omega(\vec{r})I_z$, and the n-quantum transitions are n times wider than the single-quantum transitions.

The simplest method of removing this inhomogeneous broadening is to put echo pulses[36,37,63] in t_1. For example, if $\mathcal{H}_z = \mathcal{H}_D + \Delta\omega(\vec{r})I_z$, a single 180° pulse at $t_1/2$ is sufficient (Figure (II.2(b)), with $\phi = y$ and $\phi + \pi = \bar{y}$). In this case the evolution propagator $\exp(-i\mathcal{H}_z t_1)$ in equation (II.34) is replaced with

$$\exp(-i(\mathcal{H}_D+\Delta\omega(\vec{r})I_z)t_1/2)\ \exp(-i(\mathcal{H}_D-\Delta\omega(\vec{r})I_z)t_1/2)$$

$$= \exp(-i\mathcal{H}_D t_1) \qquad \text{(II.35)}$$

since $[\mathcal{H}_D,\Delta\omega(\vec{r})I_z] = 0$. The broadening is completely eliminated, but all of the multiple-quantum spectra are centered at $\omega = 0$. This overlap also occurs in continuous wave multiple-quantum, but there the number of quanta can be identified by the ω_1 power dependence of the transition.

Several different techniques exist for determining the number of quanta associated with a particular transition. For example, a static field gradient can be applied for a short interval δ in t_1; the n-quantum coherences will dephase n times faster than the single-

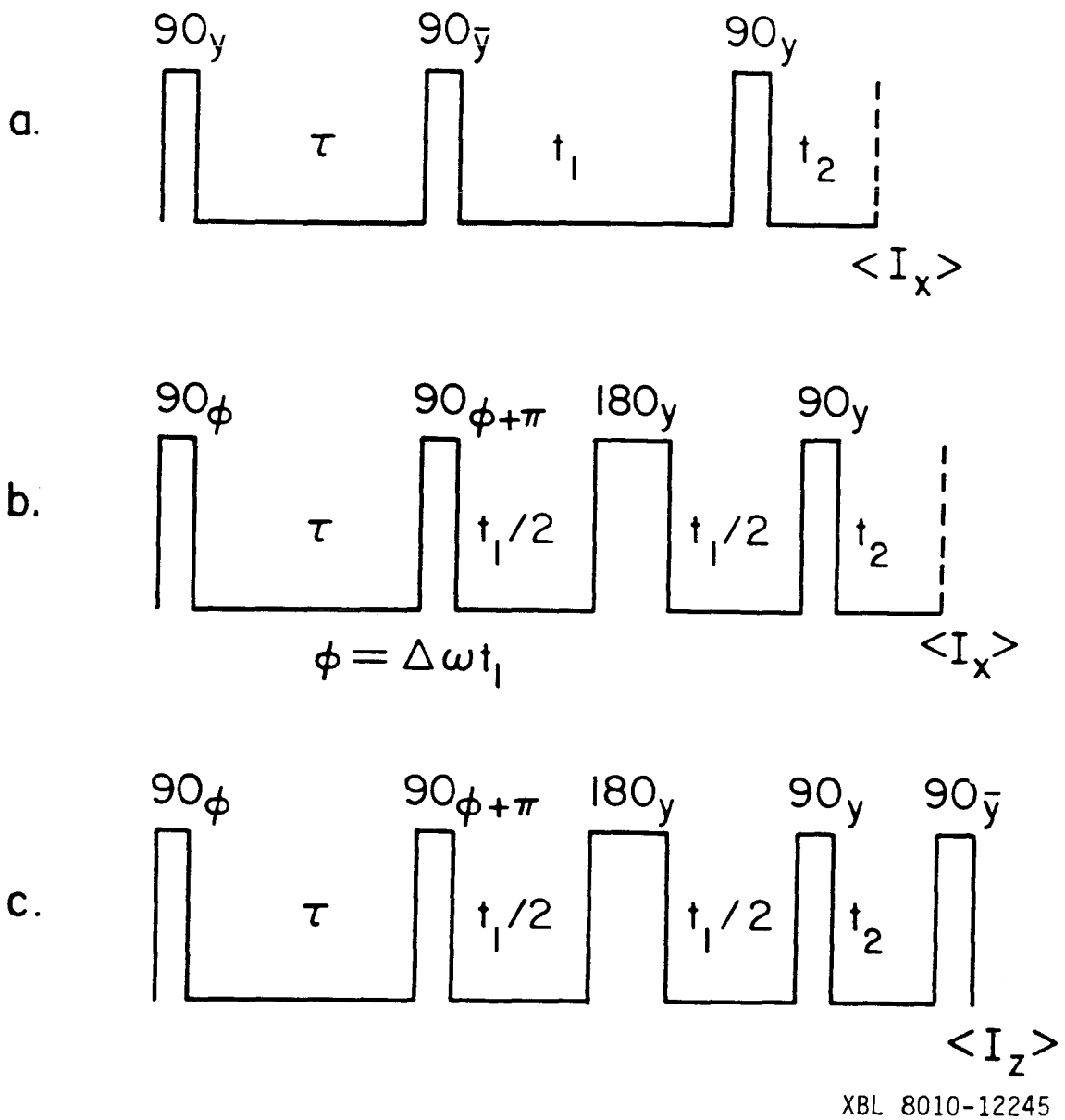

XBL 8010-12245

Figure II.2. Several common pulse sequences for multiple-quantum NMR experiments. The sequence in part b) removes static inhomogeneity terms. Part c) illustrates a useful concept for understanding multiple-quantum NMR: the pulse sequences are more symmetric if I_z is imagined to be observable.

quantum coherences. If the same gradient is applied during t_2, any magnetization arising from single-quantum coherences in t_1 will refocus after the same interval δ, but signal from n-quantum coherences will refocus at $n\delta$.[33,64]

Other approaches rely on the behavior of n-quantum coherences under phase shifts of the irradiating field. A phase shift of ϕ in the first two pulses of any of the multiple-quantum sequences discussed so far will change $\rho_{MQ}(\tau)$ in equations (II.31) and (II.34) to $\rho'_{MQ}(\tau)$:

$$\rho'_{MQ}(\tau) = \exp(-i\phi I_z)\ \rho_{MQ}(t)\ \exp(i\phi I_z) \qquad \text{(II.36)}$$

$$(\rho'_{MQ}(\tau))_{ij} = (\rho_{MQ}(\tau))_{ij}\ \exp(-i\phi(m_i - m_j)) \qquad \text{(II.37)}$$

For example, if $\phi = \pi$ all of the (2n+1)-quantum coherences are multiplied by -1, but all the (2n)-quantum coherences are unaffected. Adding spectra with $\phi = 0$ to spectra with $\phi = \pi$ will eliminate all odd-quantum coherences.[28,34,63] This method is readily generalized; for example, adding n spectra, each shifted by $\phi = 2\pi/n$, retains only transitions with $\Delta M = nk$ ($k = 0, \pm 1, \pm 2, \ldots$).

A third method, which permits the simultaneous observation of all multiple-quantum transitions, is known as time proportional phase incrementation (TPPI).[29,30] In this experiment, whenever t_1 is incremented by Δt_1, the phases of the first two pulses are incremented by $\Delta\phi = (\Delta\omega')\Delta t_1$. Then $\phi = \Delta\omega' t_1$ in equations (II.36-37). Substitution into equation (II.33) shows that the n-quantum coherences appear to evolve at $n\Delta\omega' + \omega_{ij}$, so if $\Delta\omega' > ||\mathcal{H}_z||$ all of the transitions are

separated, and the spectrum is the same as would be produced by a perfectly homogeneous field without echoes.

2.2.3.3 The Choice of Observable Operators

There is actually a great deal of similarity between the roles of τ and t_2 in equation (II.34). This symmetry is partly hidden in the pulse sequence by the experimental need to measure $\langle I_x \rangle$ or $\langle I_y \rangle$ even though the initial density matrix is proportional to I_z. If instead it is assumed that $\langle I_z \rangle$ can be measured, as in Figure (II.2(c)), an additional pulse is needed at the end of t_2. The sequences in parts (b) and (c) would always give the same spectra, but in part (c) the symmetry between τ and t_2 is apparent. For this reason the theory will be developed (here and in later chapters) as if $\langle I_z \rangle$ were detected. The experimental pulse sequences will always include one additional pulse immediately before detection, to sample $\langle I_x \rangle$ or $\langle I_y \rangle$.

2.3 Preparation of Multiple-Quantum Coherences

It is clear from equation (II.34) that multiple-quantum coherences will only be observed if they appear in $\rho_{MQ}(\tau)$ and $\rho_{MQ}(-t_2)$. However, not all values of τ or t_2 are useful. For example, if $\tau = 0$, equation (II.31) reduces to $\rho_{MQ}(0) = -\beta I_z$, and no coherences can be observed. The same problem obviously occurs if $t_2 = 0$. On the other hand, there is clearly an upper limit to desirable values of τ and t_2 because of relaxation effects. Thus, a very important problem is to determine the optimum values of τ and t_2 for observing a particular transition.

If $\mathcal{H}_z$ is known, this problem may not seem difficult; in principle $\rho_{MQ}(\tau)$ can be calculated exactly. In fact this can be done by hand for

very small systems (for example, a single isolated spin-1)[61-63] but since the number of states for a system with N spins-1/2 as 2^N explicit calculations rapidly become difficult. Some computer calculations with systems as large as six spins without symmetry or eight spins with symmetry have been completed[66] (see also sections 3.2 and 4.2). However, in most actual experiments $\mathcal{H}_z$ is unknown (the purpose of the experiment is to measure it). In this case, explicit calculations are not possible. Nonetheless, even in this case several important conclusions can be drawn from the form of equation (II.31).

2.3.1 Small Values of τ

One useful approach is to differentiate with respect to τ:

$$\dot{\rho}_{MQ}(\tau) = i[\rho_{MQ}(\tau),\mathcal{H}_x] \tag{II.38}$$

$$\rho_{MQ}^{(n)}(\tau) = i[\rho_{MQ}^{(n-1)}(\tau),\mathcal{H}_x] \tag{II.39}$$

Equation (II.39) can be used to generate a power series expansion around $\tau = 0$:

$$\rho_{MQ}(\tau) = -\beta(I_z+i\tau[I_z,\mathcal{H}_x] - \frac{\tau^2}{2}[[I_z,\mathcal{H}_x],\mathcal{H}_x] + \ldots) \tag{II.40}$$

As expected, $\rho_{MQ}(0) = -\beta I_z$. All other terms involve commutators, and their form depends very much on the nature of the system being studied.

2.3.1.1 Isotropic Systems

In this case $\mathcal{H}_x$ is, from equation (I.10),

$$\mathcal{H}_x = \Delta\omega I_x - \sum_i \sigma_i I_{xi} + \sum_{i>j} J_{ij}(\vec{I}_i\cdot\vec{I}_j) \tag{II.41}$$

$I_z = \sum_i I_{zi}$ is the sum of operators which act on only a single spin; so are $\Delta\omega I_x$ and $\Sigma\sigma_i I_{xi}$. The commutator between any two single spin operators is also a single spin operator (in fact it is the sum of operators I_{xi}, I_{yi} and I_{zi}). However, a n-quantum operator must involve n spins. Therefore, if $\mathcal{H}_J = 0$ multiple-quantum coherences never develop. In addition, $[\mathcal{H}_J, I_z] = [\mathcal{H}_J, I_y] = [\mathcal{H}_J, I_z] = 0$. This implies that if all the chemical shifts are equal (in which case they can all be made zero by redefining $\Delta\omega$) then equation (II.31) becomes

$$\rho_{MQ}(\tau) = -\beta \exp(-i\Delta\omega I_x\tau) \exp(-i\mathcal{H}_J\tau) I_z \exp(i\mathcal{H}_J\tau) \exp(i\Delta\omega I_x\tau)$$

$$= -\beta(I_z\cos(\Delta\omega\tau) - I_y\sin(\Delta\omega\tau)) \qquad \text{(II.42)}$$

and again no multiple-quantum coherences are produced.

Even if neither of these conditions holds, the term proportional to τ is:

$$-i\tau\beta[I_z, \mathcal{H}_x] = (-\Delta\omega I_y + \Sigma\sigma_i I_{yi})\tau\beta \qquad \text{(II.43)}$$

which has only single-spin single-quantum operators. The term proportional to τ^2 is

$$\beta \frac{\tau^2}{2} [[I_z, \mathcal{H}_x], \mathcal{H}_x] = \frac{1}{2} \beta\tau^2(\Delta\omega^2 I_z - 2\Delta\omega \sum_i \sigma_i I_{zi} + \sum_i \sigma_i^2 I_{zi}$$

$$+ \sum_{i>j} J_{ij}(\sigma_i - \sigma_j)(I_{zi}I_{xj} - I_{xi}I_{zj})) \qquad \text{(II.44)}$$

The second and third terms are secular, but they do not commute with $\mathcal{H}_z$, so they can generate coherences between states with $\Delta M = 0$. The

fourth term has two-spin operators, but they are only single-quantum. The term proportional to τ^3 has three-spin operators which come from the commutator of the fourth term in equation (II.44) with $\mathcal{H}_J$. However, all these operators are still single-quantum since $\mathcal{H}_J$ is secular. It also has two-spin two-quantum operators which come from the commutator of the fourth term in equation (II.44) with $\sum_i \sigma_i I_{xi}$. These are:

$$\frac{i}{12}\beta\tau^3\left(\sum_{i>j} J_{ij}(\sigma_i-\sigma_j)^2\ (I_i^+I_j^+-I_i^-I_j^-)\right) \qquad \text{(II.45)}$$

Thus the first two-quantum operators are proportional to τ^3. Roughly speaking, the two-quantum operators will not be significantly large until $\langle J_{ij}(\sigma_i-\sigma_j)^2\tau^3\rangle \sim 1$. Frequently this implies values for τ (and t_2) of tens or hundred of milliseconds.

This line of reasoning is easily extended. In general, the first n-spin operators are proportional to τ^n, but these operators are only single-quantum; the first n-quantum operators only occur after (n-1) more commutators, so they are proportional to $\tau^{(2n-1)}$.

2.3.1.2 Anisotropic Systems

The additional term here is $\mathcal{H}_{xx} = \Sigma\ D_{ij}(3I_{xi}I_{xj}-\vec{I}_i\cdot\vec{I}_j)$, which has zero-quantum and two-quantum operators:

$$\mathcal{H}_{xx} = -\frac{1}{2}\mathcal{H}_{zz} + \sum_{i>j}\frac{3}{4}D_{ij}\ (I_i^+I_j^+ + I_i^-I_j^-) \qquad \text{(II.46)}$$

Equation (II.46) is readily verified by examining the rotational properties of second-rank tensors. The term proportional to τ is:

$$-i\tau\beta[I_z,\mathcal{H}_x] = \tau\beta(\Delta\omega I_y - \Sigma\ \sigma_i I_{yi} + \Sigma\ \frac{3}{4}D_{ij}(iI_i^+I_j^+ - iI_i^-I_j^-)) \quad . \qquad \text{(II.47)}$$

Single-quantum and double-quantum operators first appear proportional to τ. Unlike the isotropic case, multiple-quantum coherences are produced even if $\mathcal{H}_{cs} = 0$. In fact if $\mathcal{H}_{cs} = 0$ and $\Delta\omega = 0$ $\mathcal{H}_x$ has only zero-quantum and two-quantum operators, so $\rho_{MQ}(\tau)$ has only even-quantum coherences.[63] This term will be substantial when $<|D_{ij}\tau|^2>^{1/2} \sim 1$, and typically this is a fraction of a millisecond.

The τ^2 term is proportional to the commutator of equation (II.47) with $\mathcal{H}_x$. It can immediately be seen that no operators involving more than three spins are present; in addition, the three-spin operators arise from the commutators of $\mathcal{H}_J$ or $\mathcal{H}_{xx}$ with the last term of equation (II.47) so they are even-quantum. In general, the term proportional to τ^2 then has operators with $\Delta M = 0, \pm 1, \pm 2$. As with isotropic systems, this reasoning is readily extended. The first n-spin ($n > 1$) operator is proportional to $\tau^{(n-1)}$. If n is even, this term has n-quantum operators; if n is odd the next term does. The dependence on τ for different values of ΔM is listed in Table II.1.

2.3.2 Long values of τ

2.3.2.1 Isotropic Systems

The results of section 2.3.1.1 show that a reasonable intensity for multiple-quantum transitions can only be expected if terms proportional to high powers of τ cannot be neglected, in which case a power series expansion does not converge. A more profitable approach in this case is to expand the propagator in powers of J_{ij}, since typically $||\mathcal{H}_{cs}|| >> ||\mathcal{H}_J||$ (see Appendix E for the definition of this norm and for the expansion). $\rho_{MQ}(\tau)$ can be written as:

Table II.1

Dependence on τ of multiple-quantum coherences produced by the sequence $(90_y - \tau - 90_{\bar{y}})$

	Initial τ power dependence	
ΔM	Isotropic	Anisotropic
0	2	2
1	1	1
2	3	1
3	5	3
4	7	3
n(even)	(2n-1)	n-1
n(odd)	(2n-1)	n

$$\rho_{MQ}(\tau) = \beta R\{\exp(-i(\mathcal{H}_{cs}+\mathcal{H}_J+\Delta\omega I_z)\tau)I_x \exp(i(\mathcal{H}_{cs}+\mathcal{H}_J+\Delta\omega I_z)\tau)\}R^{\dagger}$$

(II.48)

where $R = \exp(-i\pi I_y/2)$. The effect of R and $R^{\dagger}$ can be calculated by replacing $I_{zi} \to I_{xi}$, $I_{xi} \to -I_{zi}$, $I_{yi} \to I_{yi}$ in any explicit operator expression found for the quantity in brackets. In the spin product basis set, $\mathcal{H}_{cs} + \Delta\omega I_z + \Sigma\, J_{ij}I_{zi}I_{zj}$ is diagonal. Choosing this as A in the expansion for exp(A+B) given in equation (E.10) one finds:

$$\exp(-i(\mathcal{H}_{cs}+\mathcal{H}_J+\Delta\omega I_z)\tau) = \exp(-i\mathcal{H}^{o}\tau)$$

$$+ \frac{1}{2}\Sigma\, J_{ij}(I_i^+I_j^- + I_i^-I_j^+)\left(\frac{\exp(-i\mathcal{H}^{o}\tau)_{ii} - \exp(-i\mathcal{H}^{o}\tau)_{jj}}{\mathcal{H}^{o}_{ii} - \mathcal{H}^{o}_{jj}}\right) \qquad \text{(II.49)}$$

$$\mathcal{H}^{o} = \Delta\omega I_z - \sum_i \sigma_i I_{zi} + \sum_{i>j} J_{ij}I_{zi}I_{zj} \qquad \text{(II.50)}$$

For simplicity assume that $|\mathcal{H}^{o}_{ii} - \mathcal{H}^{o}_{jj}| >> J_{ij}$ (this is equivalent to the condition that the spectra be first order) and $|\mathcal{H}^{o}_{ii} - \mathcal{H}^{o}_{jj}|\ \tau \gtrsim 1$. Then the second term in equation (II.49), and all higher-order terms in equation (E.10), are much smaller than the first. The three parts of $\mathcal{H}^{o}$ all commute with each other so equation (II.48) reduces to:

$$\rho_{MQ}(\tau) = \beta U(\sum_i I_{zi}\cos(\Delta\omega-\sigma_i)\tau - \sum_i I_{yi}\sin(\Delta\omega-\sigma_i)\tau)U^{\dagger} \qquad \text{(II.51)}$$

$$U = \exp(-i \sum_{i>j} J_{ij}I_{xi}I_{xj}\tau)$$

$$= \prod_{i>j} \exp(-i\, J_{ij}I_{xi}I_{xj}\tau) \qquad \text{(II.52)}$$

To simplify this further, pick a particular value of i (say $i = 1$). Then all terms $J_{jk}I_{xk}I_{xj}$ $(j,k \neq i)$ in (II.52) can be neglected, since they commute with I_{z1} and I_{y1}, and only (n-1) products appear in (II.52). It is readily shown that

$$\exp(-iJ_{ij}I_{xi}I_{xj}\tau)I_{zi}\exp(iJ_{ij}I_{xi}I_{xj}\tau)$$

$$= I_{zi}\cos(J_{ij}\tau/2) - 2I_{yi}I_{xj}\sin(J_{ij}\tau/2) \qquad \text{(II.53)}$$

$$\exp(-iJ_{ij}I_{xi}I_{xj}\tau)I_{yi}\exp(iJ_{ij}I_{xi}I_{xj}\tau)$$

$$= I_{yi}\cos(J_{ij}\tau/2) + 2I_{zi}I_{xj}\sin(J_{ij}\tau/2) \qquad \text{(II.54)}$$

This permits the coefficients for any operator in $\rho_{MQ}(\tau)$ to be explicitly written. As an example, consider the N-quantum transition in a system with N spins-1/2. For any given i, the only operator in (II.51) which induces N-quantum transitions is $(I_{yi})(\prod_{i\neq j} I_{xj})$. Its coefficient is:

$$\beta(\cos((\Delta\omega-\sigma_i)\tau)\prod_{j\neq i} 2\sin(J_{ij}\tau/2)) \qquad \text{(N even)}$$

$$\beta(\sin((\Delta\omega-\sigma_i)\tau)\prod_{j\neq i} 2\sin(J_{ij}\tau/2)) \qquad \text{(N odd)}$$

$(I_{yi})(\sum_{i\neq j} I_{xj})$ has the N-quantum operator $(i)(2^{-N})(\prod_i I_i^+)$, plus other operators. Finally, the magnitude of the coefficient of the N-quantum coherence in the density matrix is

$$\frac{1}{2}\beta\left(\sum_i \cos((\Delta\omega-\sigma_i)\tau)\prod_{j\neq i}\sin(J_{ij}\tau/2)\right) \qquad \text{(N even)}$$

$$\frac{1}{2}\beta\left(\sum_i \sin((\Delta\omega-\sigma_i)\tau)\prod_{j\neq i}\sin(J_{ij}\tau/2)\right) \qquad \text{(N odd)}$$

(II.55)

The actual value is imaginary if the phases of the first two pulses are chosen as y and $\bar{y}$. These expressions have several important features.

1. The maximum value for the N-quantum coherence is β N/2, for a value of τ which makes all of these sine and cosine terms equal to 1. This is only possible if all the J_{ij} and σ_i values have rational ratios, but even if this is not the case the signal can come arbitrarily close to β N/2. This is equal to the value of βI_z for the extreme states. It will be shown in section 3.5.1 that this is the maximum value any coherence can have.

This maximum can only be achieved if the predicted value of $\tau \ll T_2$. In general, some of the spins will be weakly coupled ($J_{ij} \ll 1$ Hz) and in this case $\sin(J_{ij}\tau/2) \sim 1$ implies an unacceptably large value of τ. Relaxation effects are easily included if it is assumed that all coherences dephase with the same value of T_2; the expressions in (II.55) must then be multiplied by $\exp(-\tau/T_2)$.

2. Neglecting relaxation, it is possible to formally integrate over τ to get an estimate of the average N-quantum coherence magnitude. The result is:

$$\langle|\rho_{MQ}(\tau)|^2\rangle_{N/2,-N/2} = \frac{1}{4}\beta^2 N\, 2^{-N} \qquad \text{(II.55)}$$

This can be compared to an average coherence magnitude since $\rho_{MQ}(\tau)$ is related to βI_z by a unitary transformation. Then

$$\mathrm{Tr}(\rho_{MQ}(\tau)^2) = \sum_{ij} |\rho_{MQ}(\tau)|^2_{ij} = \mathrm{Tr}((\beta I_z)^2)$$

$$= \beta^2 \; N \; 2^N/4$$

$$<|\rho_{MQ}(\tau)|^2>_{ij} = \frac{1}{4} \beta^2 \; N \; 2^{-N} \qquad \text{(II.56)}$$

The average N-quantum coherence magnitude is exactly the same as the overall average coherence magnitude. However, if one spin is coupled very weakly to all the rest ($J_{ij}T_2 << 1$ for all j with one specific i) the magnitude of the N-quantum coherence for acceptable values of τ is much smaller. Lower-quantum coherences are not as seriously affected, since those operators do not involve couplings from one spin to all others.

3. Assume that the coupling J_{ij} is weak. Then the terms involving σ_i or σ_j in (II.55) are very small. The dominant terms in the sum over i will be from spins which are relatively strongly coupled to all others. The form of (II.55) implies that the N-quantum coherence depends on the product of the couplings of all spins to one (Figure (II.3a)) rather than a chain of couplings (Figure (II.3b)).

4. The N-quantum coherence oscillates rapidly as τ changes because of the $(\Delta\omega-\sigma_i)$ terms. Slower oscillations come from the J_{ij} terms. The most probable value of the magnitude is not 0, as would be expected if the distribution were Gaussian about the origin. Instead, as the number of strongly coupled spins increases, the

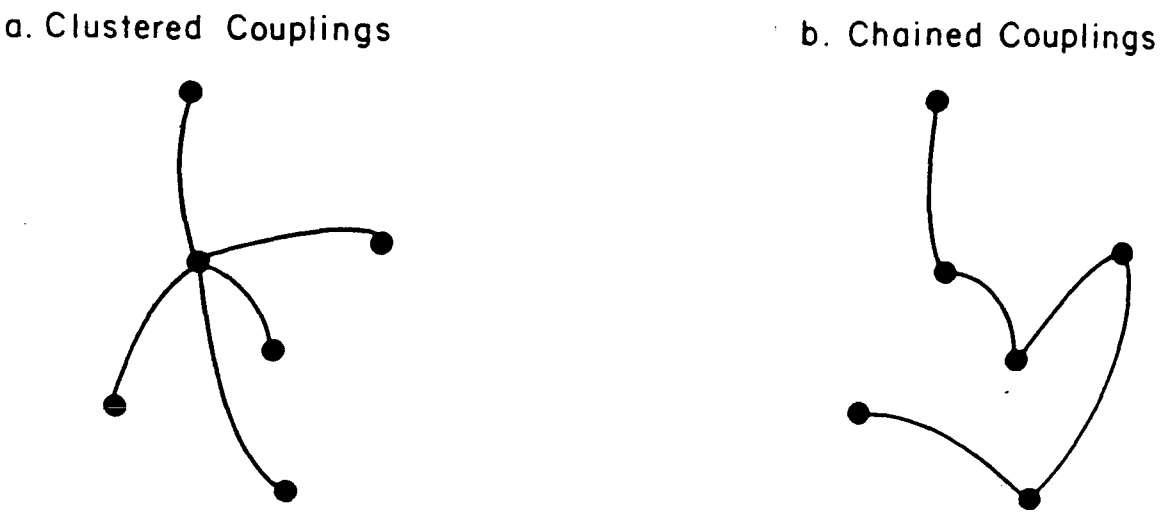

XBL 8010-12248

Figure II.3. Two general schemes for development of multiple-quantum coherence. In isotropic first-order systems only the product of the couplings from one spin to all others matter, as in part a). In anisotropic systems the chained product of couplings also contributes, as in part b).

oscillations will tend to die away and deviations from the average will become less frequent.

2.3.2.2 Anisotropic Systems

In most isotropic systems the largest terms in the Hamiltonian are mutually commuting, which considerably simplifies the analysis. This is not the case for general anisotropic systems unless $||\mathcal{H}_{cs}|| >> ||\mathcal{H}_D||$ and for most systems this implies static magnetic fields orders of magnitude larger than are currently available. One special case that can be solved exactly occurs if all the spins are magnetically fully equivalent, which implies that all the D_{ij}s are equal. One example is bullvalene,[65] which has 10 spins. In this case

$$\mathcal{H} = \Delta\omega I_z + D\,\Sigma(3I_{zi}I_{zj} - \vec{I}_i\cdot\vec{I}_j) + J\,\Sigma\,\vec{I}_i\cdot\vec{I}_j$$

All the terms involving $I_i\cdot I_j$ commute with the rest of the Hamiltonian, so they can be deleted.[13] The remaining terms are mathematically identical to equation (II.50) with the substitutions $J_{ij} = 3\,D, \sigma_i = 0$. The N-quantum coherence in an N-spin system is then

$$\frac{N\beta}{2}\cos(\Delta\omega\tau)\,\sin^{N-1}(3D\tau/2) \qquad \text{(N even)}$$

$$\frac{N\beta}{2}\sin(\Delta\omega\tau)\,\sin^{N-1}(3D\tau/2) \qquad \text{(N odd)} \qquad \text{(II.57)}$$

Again the maximum possible value is $\beta N/2$ but unlike the isotropic case this value is easily attained (for example, in an even-spin system set $\Delta\omega = 0$ and $\tau = \pi/3D$). When N is large the $\sin^{N-1}$ term produces very sharp peaks and broad valleys as τ is

changed and this has important implications for two-dimensional spectroscopy (to be discussed in section 6.1). The average N-quantum signal is

$$<|\rho_{MQ}(\tau)|^2>_{N/2,-N/2} = \beta^2 N^2\ 2^{-(2N+1)}(2N-2)!/(N-1)!^2 \qquad \text{(II.58)}$$

This is generally much larger than (II.55). Here, however, the magnitude of an average coherence should be calculated using the known symmetry. Total spin I is a good quantum number[40] so the N-quantum coherence belongs to an irreducible representation which has only N+1 states, one for each value of M. The available portion of $Tr(I_z^2)$ is $N(N+1)(N+2)/12$ so that

$$<|\rho_{MQ}(\tau)|^2>_{I=N} = \beta^2\ N(N+2)/12(N+1) \qquad \text{(II.59)}$$

These values are compared in Table II.2. It is clear that the symmetry greatly strengthens the allowed transitions, and that the N-quantum transition is somewhat stronger than average even when symmetry affects are included.

If the system has lower symmetry, analysis is much more complicated. Only $\mathcal{H}_D$ and $\Delta\omega I_z$ will be retained in what follows.

$$\rho_{MQ}(\tau) = -\beta\ \exp(-i(\mathcal{H}_{xx}+\Delta\omega I_x))I_z\ \exp(i(\mathcal{H}_{xx}+\Delta\omega I_x))$$

$$= -\ \exp(-i\mathcal{H}_{xx}\tau)(I_z\ \cos(\Delta\omega\tau)-I_y\sin(\Delta\omega\tau))\exp(i\mathcal{H}_{xx}\tau) \qquad \text{(II.60)}$$

Thus $\Delta\omega\tau = (2k+1)(\pi/2)$ gives odd-quantum coherences only, and $\Delta\omega\tau = k\pi$ gives even-quantum only.[63] The terms in $\mathcal{H}_{xx}$ are not

mutually commuting, so about all that can easily be said is that if $||\mathcal{H}_{xx}\tau|| >> 1$, the propagator has matrix elements corresponding to all values of ΔM, and if one spin is coupled weakly to all other spins the N-quantum coherence will be weaker.

Computer calculations have been done for small systems.[66] The results are quite similar to what would be predicted for isotropic systems, with a few exceptions. If all the D_{ij} constants are approximately equal and have random signs, the average coherence magnitude is roughly independent of ΔM. If all the D_{ij} constants have the same sign, the N-quantum coherences will be stronger than the average. This can be interpreted as a symmetry effect. If all the couplings are equal, the N-quantum transition is much stronger than the overall average without symmetry (Table II.2). When all the D_{ij} couplings have the same sign this highly symmetric operator is a significant part of $\mathcal{H}_{zz}$, so even though the true eigenstates have no symmetry this operator pumps N-quantum transitions more strongly.

Computer calculations also show that in anisotropic systems multiple-quantum coherences can be produced by either of the pathways of Figure II.3. Recall that the form of coupling in Figure II.3(b) (i.e., $J_{ij}J_{jk}J_{kl}$ ...) is precluded in the isotropic case, because the operators in the propagator are mutually commuting. This means that the operator I_{zi} in the initial density matrix is unaffected by propagator terms proportional to J_{jk}, $(j,k\neq i)$. In the anisotropic case this simplification is not possible. One important consequence of this difference is that anisotropic multiple-quantum NMR is useful

Table II.2

Average N-quantum transition intensity for A_n systems, versus the overall average transition intensity with and without symmetry.

N	N-quantum	Overall (with symmetry)	Overall (without symmetry)
6	1.107β	$.571\beta$	0.023β
8	1.676β	$.741\beta$	0.0078β
10	2.32β	$.889\beta$	0.00244β
12	3.03β	1.077β	0.00073β

$(\beta = (\gamma B_o/kT)(2^{-N}))$

in systems such as chains, where each nucleus is strongly coupled to nearby spins, but no spin is strongly coupled to all others.

2.4 Signal Intensities; Ensemble Averaging

Fourier transformation of equation (II.34) shows that the multiple-quantum spectrum is:

$$S(\omega) = -C\,\beta \sum_{ij} (\rho_{MQ}(\tau))_{ji} (\rho_{MQ}(-t_2))_{ij}\ \delta(\omega - \omega_{ij})$$

For arbitrary values of t_2 and τ the intensities and phases of the different transitions can vary widely. For example, Figure II.4(a) shows the spectrum of oriented benzene (14 wt % in Eastman liquid crystal #15320) at 24.0°C with $\Delta\omega$ = 500 Hz and $\tau = t_2$ = 10 msec. There is no simple way to put all the transitions in phase, and therefore the spectra are usually presented in magnitude form, as in Figure II.4(b). If the linewidths are important, well-resolved transitions can be individually phase corrected. If $\tau = -t_2$ all of the transitions have the same phase, and magnitude spectra are not needed. Time reversal of the dipolar Hamiltonian is possible, as will be discussed in section 3.4, but it is complicated.

Any specific value of t_2 or τ will pump some transitions more strongly than others. For example, one of the three allowed pairs of four-quantum transitions is not visible above the noise level in Figure II.4 and the five-quantum and six-quantum transitions are not visible either. For this reason one generally averages together magnitude spectra corresponding to many different values of t_2 and τ. This process is termed ensemble averaging, and was used to produce all of the spectra shown in section 1.4.

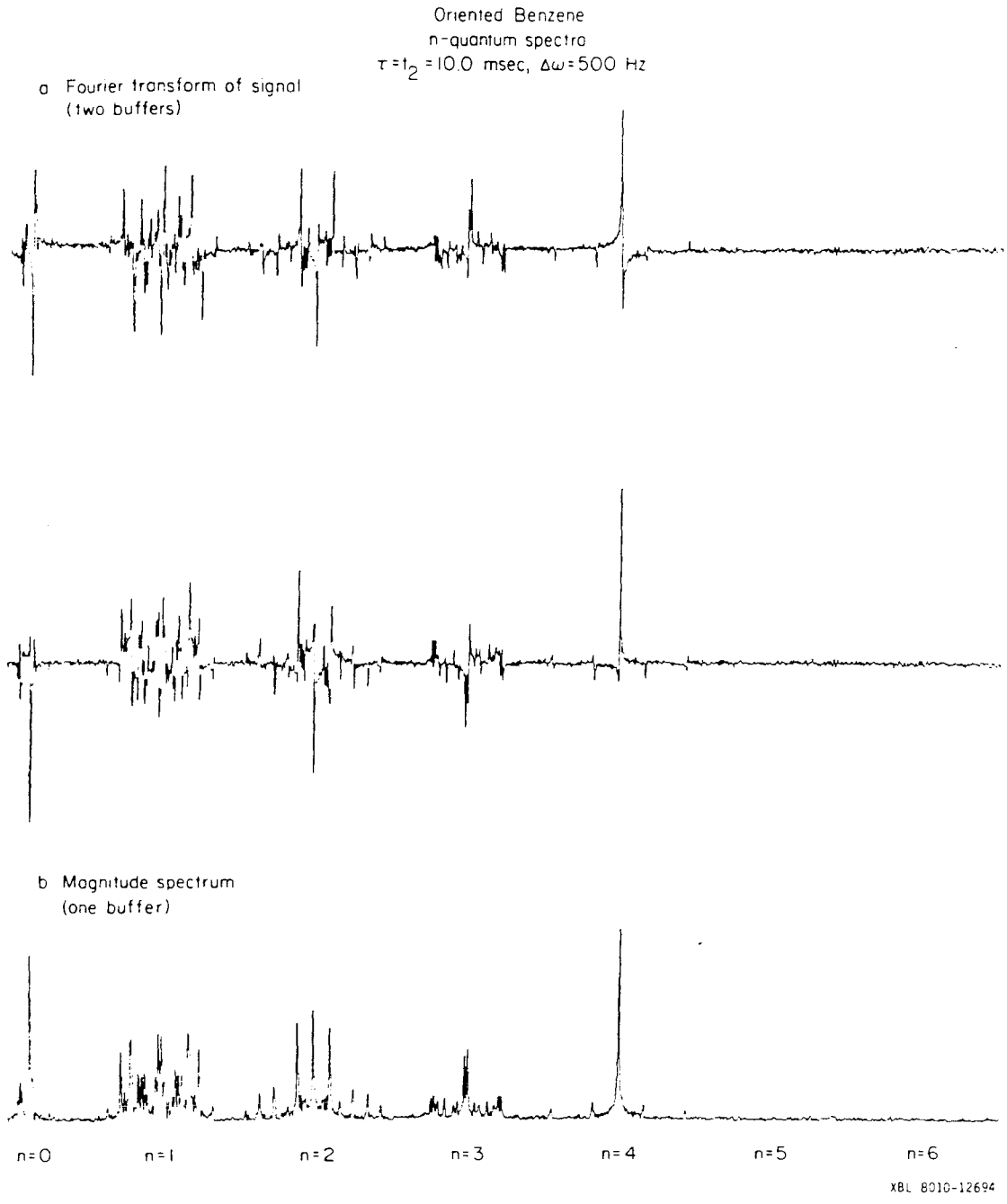

Figure II.4. The multiple-quantum spectra of oriented benzene (14 wt % in Eastman liquid crystal #15320) at 24.0° with $\tau = t_2 = 10$ msec and $\Delta\omega = 500$ Hz.

An ensemble averaged spectrum for benzene is shown in Figure II.5. Transitions corresponding to all values of ΔM are present in this spectrum. The simplest statistical assumption (to be discussed further in section 6.3) would be to assume that, on the average, each symmetry allowed transition is pumped about equally well. A computer simulation for this case is shown in Figure II.6(a). This gives a good qualitative description of the intensity distribution. The integrated intensity of each order should then approach a binomial distribution if there is no symmetry, because the number of transitions has that distribution. This is also qualitatively correct, as shown in Figure II.7.

However, the intensities do vary somewhat, and this variation cannot be completely eliminated even by extensive averaging, as shown in Figure II.6(b). Some transitions are inherently stronger than others. For example, the arguments presented in section 2.3.2.2 suggest that the average intensity should increase as ΔM increases, since $D_{12} \sim 3\sqrt{3}\, D_{13} \sim 8\, D_{14}$ for the hexagonal symmetry, and therefore all the coupling constants have the same sign. This increase actually does occur experimentally as shown in Figure II.8.

The total intensity of the spectrum for any specific τ and t_2 is:

$$S = -C\,\beta \sum_{i,j} \left|(\rho_{MQ}(\tau))_{ij}(\rho_{MQ}(-t_2))_{ji}\right| \qquad \text{(II.61)}$$

if all the transitions are nondegenerate. It is easily seen that this sum is maximized when $|\rho_{MQ}(\tau)|_{ij} = |\rho_{MQ}(-t_2)|_{ji}$, and in this case the sum is equal to $-C\,\beta\, \mathrm{Tr}(\rho_{MQ}(\tau)^2)$. Invariance to unitary

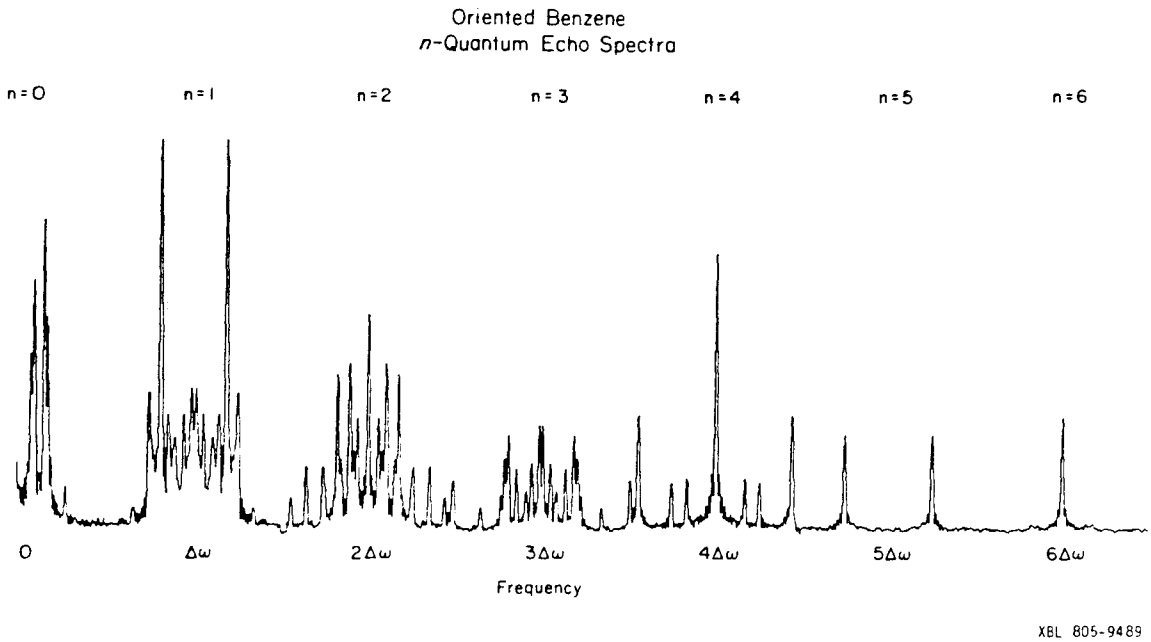

Figure II.5. Nonselective multiple-quantum spectra of oriented benzene averaged over four values of $\tau = t_2$. The integrated intensity falls off as ΔM increases.

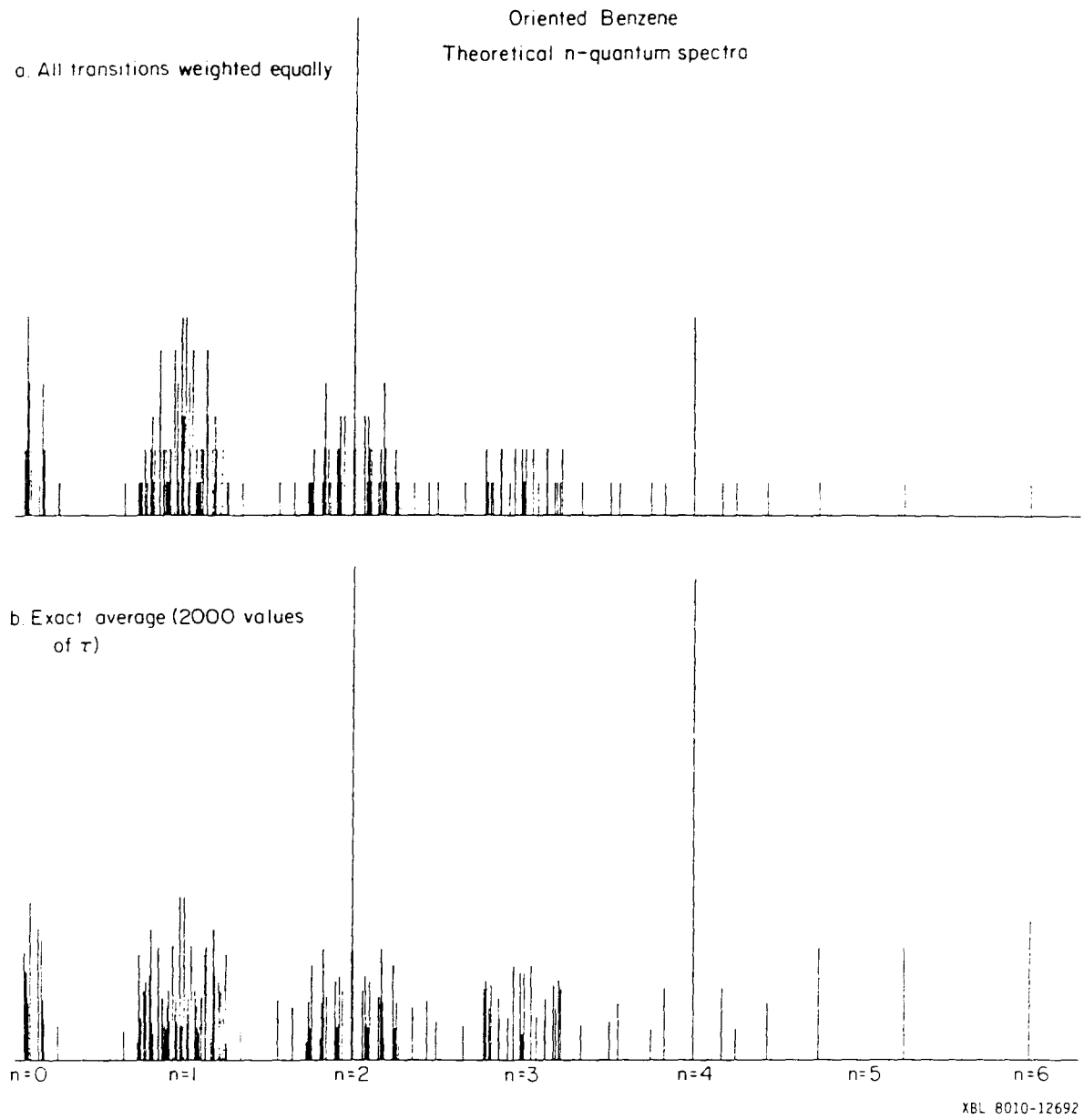

Figure II.6. Computer simulations of benzene multiple-quantum spectra. In part a) all allowed transitions are weighted equally. Part b) corresponds to averaging over 2000 values of $\tau = t_2$.

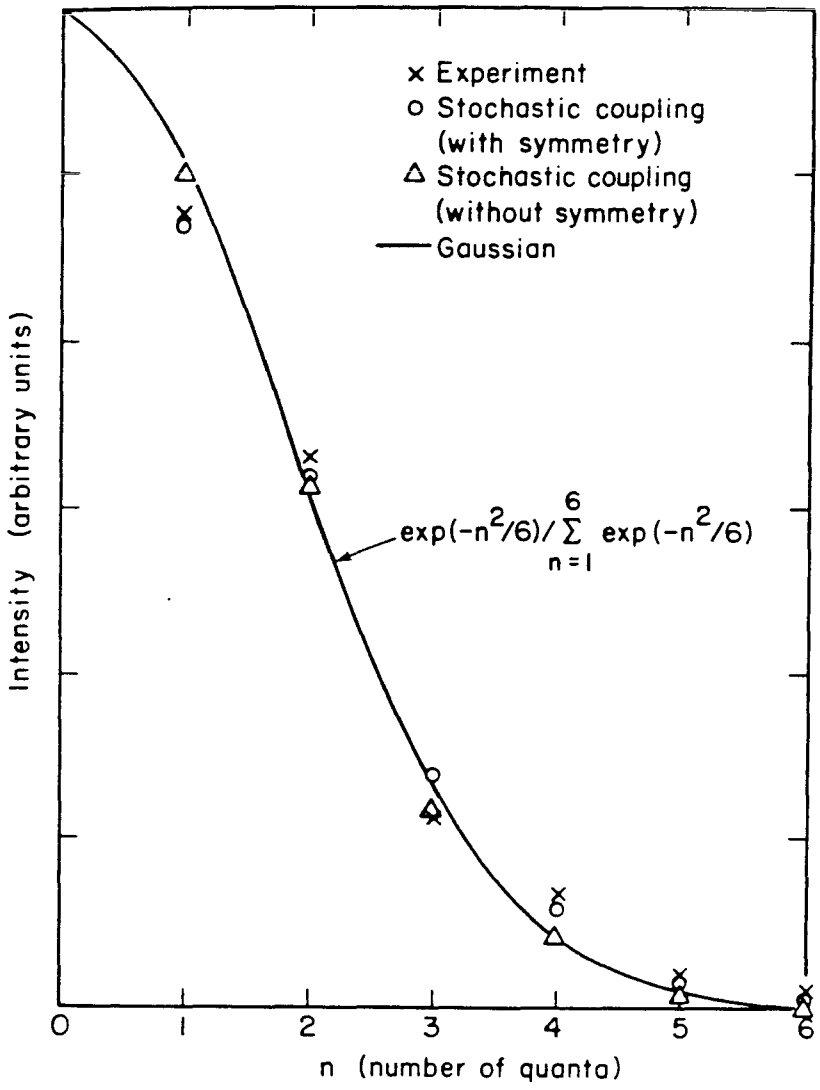

XBL 788-10117

Figure II.7. The integrated intensity pattern for benzene, compared to the predicted pattern if all transitions are pumped equally. Symmetry effects are not important in this integrated pattern. The prediction without symmetry is a binomial distribution, which approaches a Gaussian as the number of spins is increased.

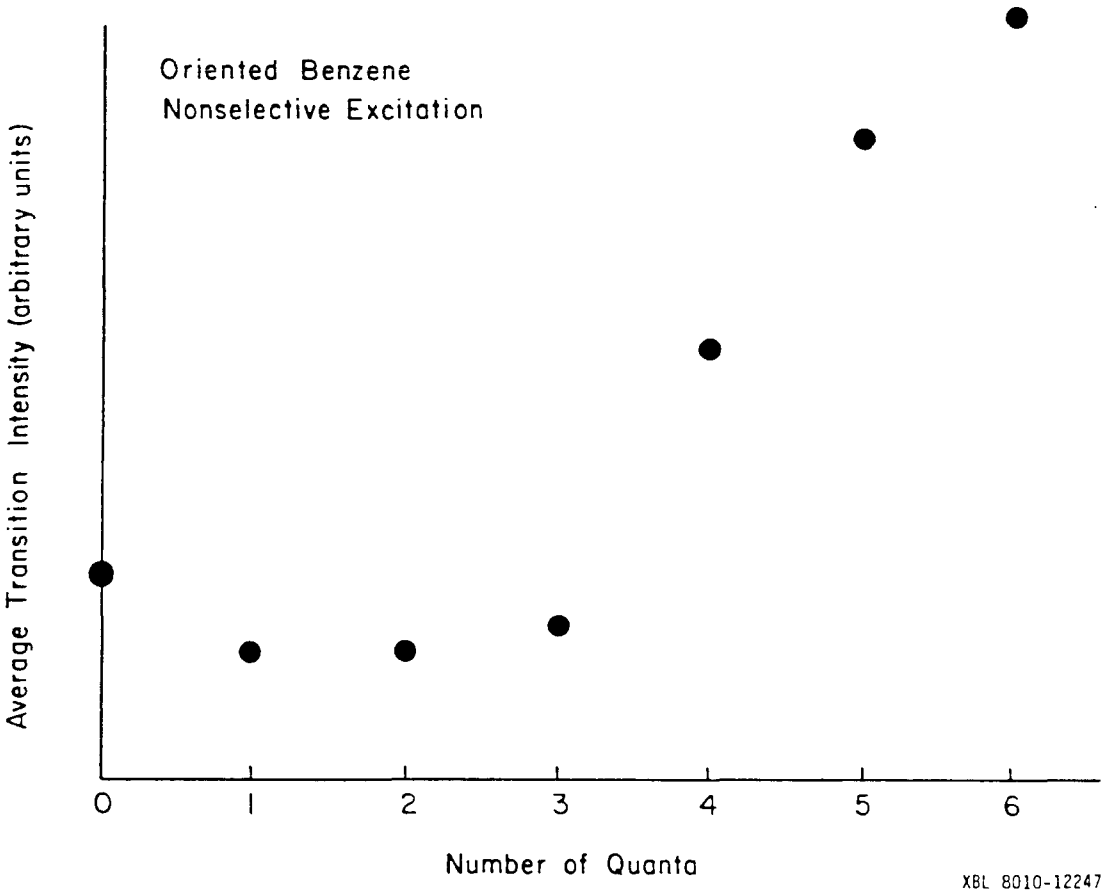

Figure II.8. The intensity of an average allowed transition taken from Figure II.5. All the dipolar couplings have the same sign, so the high multiple-quantum transitions are expected to be strongest.

transformation implies that this equals $-C\ \beta\ \mathrm{Tr}(I_z^{\ 2})$, which is also the integrated intensity of the single-quantum spectrum in a conventional one-pulse experiment.

Actually, this result holds for all pulse multiple-quantum experiments. In the general case (Figure II.9) a pulse sequence (which need not be cyclic) is applied to produce multiple-quantum coherences. This is called the preparation sequence, and its propagator will be called U. The spins then evolve under $\mathcal{H}_z$ for a time t_1. In the simplest experiments no pulses are applied during t_1; however, decoupling, spin echoes, or more complicated sequences are possible if suppression of part of $\mathcal{H}_z$ is desired. Another pulse sequence (called the mixing sequence, with propagator V) is used to transfer the multiple-quantum coherences that evolved during t_1 into observables $\langle I_x \rangle$ and $\langle I_y \rangle$. These are detected after a time t_2 (note that this definition of t_2 is not equivalent to the one used in Figures II.1-2). In this subsection $t_2=0$ is assumed (the general case is treated in section 6.1). If $\langle I_z \rangle$ is again assumed to be observable the signal is

$$
\begin{aligned}
-C\ \beta\ \langle I_z \rangle &= -C\ \beta\ \mathrm{Tr}(\rho I_z) \\
&= -C\ \beta\ \mathrm{Tr}(V\ \exp(-i\mathcal{H}_z t_1) U I_z U^{\dagger}\ \exp(i\mathcal{H}_z t_1) V^{\dagger} I_z) \\
&= -C\ \beta\ \mathrm{Tr}(U I_z U^{\dagger})\ \exp(I\mathcal{H}_z t_1)(V^{\dagger} I_z V)\ \exp(-i\mathcal{H}_z t_1)) \\
&= -C\ \beta\ \sum_{mn} (U I_z U^{\dagger})_{mn} (V^{\dagger} I_z V)_{nm}\ e^{i\omega_{mn} t_1} \qquad \text{(II.62)}
\end{aligned}
$$

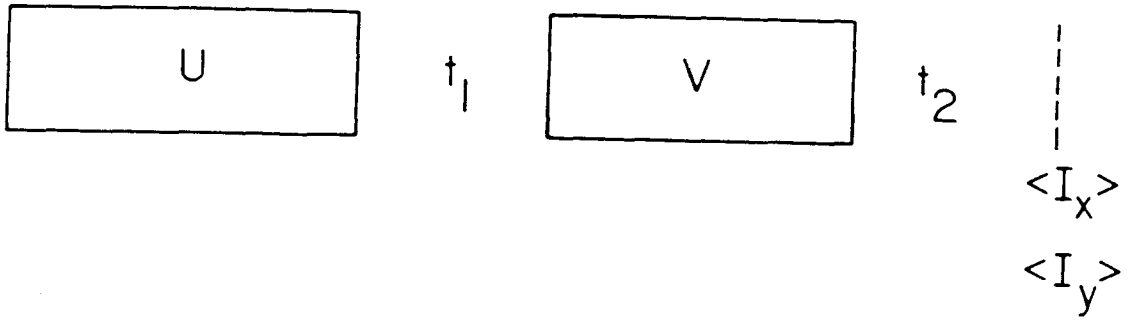

XBL 8010-12486

Figure II.9. Generalized pulse sequence for multiple-quantum experiments. A sequence with propagator U (the preparation sequence) creates multiple-quantum coherences. These coherences evolve during t_1, and are partially transferred into observable single-quantum operators by a sequence with propagator V (the mixing sequence). The observables are detected after a delay t_2.

The maximum signal is obtained when $|(UI_zU^\dagger)_{mn}| = |(V^\dagger I_z V)_{mn}|$ for every matrix element and again is $-C\,\beta\,\mathrm{Tr}(I_z^2)$.

This condition for maximum signal is obviously satisfied if $U = V^\dagger$; this case corresponds to $\tau = -t_2$ for the simplest pulse sequence. Fortunately, $\tau = t_2$ is just as good. $\mathcal{H}_x$ is a real operator (i.e., all of the matrix elements of $\mathcal{H}_x$ can be made real by an intelligent choice of basis set). This implies that

$$(\exp(-i\mathcal{H}_x\tau)I_z\ \exp(i\mathcal{H}_x\tau))_{ij} = (\exp(i\mathcal{H}_x\tau)I_z\ \exp(-i\mathcal{H}_x\tau))_{ji} \qquad \text{(II.63)}$$

so inspection of equation (II.34) shows that the only difference between $\tau = t_2$ and $\tau = -t_2$ is that all the lines are in phase with each other in the time reversal case. If some of the lines are degenerate this may matter, but the important transitions are usually nondegenerate (see section 1.4). The general case ($\tau \neq \pm\, t_2$) will be discussed in section 6.1, and general conditions for $|(UI_zU^\dagger)|_{ij} = |(V^\dagger I_z V)|_{ji}$ will be discussed in section 3.5.1.

If the multiple-quantum matrix elements are inefficiently excited (for example if $||\mathcal{H}_z\tau|| << 1$), $\rho_{MQ}(\tau)$ has large matrix elements along its diagonal. These matrix elements are populations, so they do not evolve, and most of the intensity of the multiple-quantum spectrum is found at $\omega = 0$. An efficient two-pulse excitation has little intensity at $\omega = 0$, and is expected to make all coherences roughly equal as explained in the last section. This means that the total magnetization ($-C\,\beta\,\mathrm{Tr}(I_z^2)$) is divided up among 4^N matrix elements in a system with N spins-1/2. In going from a N-spin system

to a (N+1)-spin system the magnetization increases by a factor of (1+(1/N)), but the number of matrix elements increases by a factor of 4. Thus the accumulation time for the same signal-to-noise ratio is almost a factor of 16 larger.

As a result, multiple-quantum spectra for large spin systems are weak. All of the spectra in section 1.4 were taken with the sequences of Figure (II.2(b)). With the experimental apparatus currently available to our research group (to be described in section 6.1) accumulation times of several weeks for an eight-spin system are not uncommon. Larger systems therefore cannot be readily studied by the techniques examined in this chapter.

2.5 Conclusions

The density matrix formalism has been developed to describe both continuous wave and pulsed NMR experiments. In particular, pulse sequences to produce and detect multiple-quantum coherences have been analysed. The simplest sequences can pump all symmetry allowed coherences about equally, independent of ΔM. Nonetheless the intensity of any individual transition falls off rapidly as the number of spins increases. Techniques to increase signal/noise ratios will be discussed in the next several chapters.

III. Theory of Selective Excitation of Multiple-Quantum Transitions

The signal-to-noise ratio in the standard multiple-quantum experiment falls off rapidly as the number of spins increases, as noted in the last section, because the number of observed transitions grows very rapidly. One way to solve this problem would be to distribute the total spectral intensity between only a few transitions, instead of driving all transitions equally. In a small system with a known Hamiltonian this can be done. For example, in a two-level system the population difference can be completely transferred into coherence by a 90° pulse. In a three-level system the propagator is a 3 x 3 matrix, and pulse sequences can readily be designed which produce only two-quantum coherence, if all of the couplings are given.[61,62] But this approach is not readily generalized to larger systems, except in such simple cases as isotropic first-order systems (section 2.3.2.1) or anisotropic systems with A_N symmetry (section 2.3.2.2). In addition, the couplings are generally not known in advance (if they are known, most of the justification for taking the multiple-quantum spectra disappears). Thus, aside from even-odd selection due to the bilinear form of spin coupling operators (see section 2.3.2.2) no general method of selective excitation has been proposed.

In this chapter, and the papers which preceded it,[67-70] general methods of selective excitation of multiple-quantum coherences are proposed. The theory of selective excitation is derived here as an extension of coherent averaging theory. In chapter IV computer simulations of selective experiments are presented and discussed.

In chapter V selective spectra are presented, and practical considerations for producing good selective sequences are detailed. The results of these chapters will show that selective excitation of multiple-quantum transitions in NMR is theoretically and experimentally possible, that this technique can provide enormous signal enhancement, and that general selective sequences are applicable to a wide range of spectroscopic systems.

3.1 Review of Average Hamiltonian Theory

3.1.1 Expansions for the Propagator

The effect of any sequence of irradiating pulses and delays on a general system in the absence of relaxation can be represented by a single unitary transformation U (the propagator). Calculating U directly by multiplying together the propagators for each part of the sequence is extremely tedious if many eigenstates are involved. However, this calculation can be avoided for certain pulse sequences by a technique known as average Hamiltonian theory. This technique is thoroughly documented,[9,71,72] so only a brief summary of important results will be reproduced in this subsection. In the next subsection the results will be generalized to describe sequences which are inherently selective.

The total Hamiltonian of a system is written as $\mathcal{H}(t)=\mathcal{H}_{int}+\mathcal{H}_1(t)$, where $\mathcal{H}_{int}$ is the internal Hamiltonian of the system (for example, the interactions between pairs of magnetic dipoles) and $\mathcal{H}_1(t)$ is the explicitly time-dependent interaction controlled by the experimenter (for example, the interaction with radiation). $\mathcal{H}_1(t)$ is termed cyclic with cycle time t_c if $\mathcal{H}_1(t)$ and the propagator

$U_1(t) = T\exp(-i\int_0^t \mathcal{H}_1(t')dt')$ are periodic, and if t_c is the shortest interval that constitutes a period for both $U_1(t)$ and $\mathcal{H}_1(t)$. If $\mathcal{H}_1(t)$ is a pulse sequence made up of an integral number N of cycles, the propagator for the entire sequence is the Nth power of the propagator corresponding to one cycle, and therefore only a single cycle need be considered.

The propagator for a single cycle can be shown to be:

$$U = \exp(-i\mathcal{H}t_c) = \exp(-i(\bar{\mathcal{H}}^{(0)} + \bar{\mathcal{H}}^{(1)} + \ldots + \bar{\mathcal{H}}^{(n)})t_c) \qquad \text{(III.1)}$$

where:

$$\bar{\mathcal{H}}^{(0)} = \frac{1}{t_c}\int_0^{t_c} \tilde{\mathcal{H}}_{int}(t)dt \qquad \text{(III.2)}$$

$$\bar{\mathcal{H}}^{(1)} = \frac{-i}{2t_c}\int_0^{t_c} dt_2 \int_0^{t_2} dt_1 \quad [\tilde{\mathcal{H}}_{int}(t_2), \tilde{\mathcal{H}}_{int}(t_1)] \qquad \text{(III.3)}$$

$$\bar{\mathcal{H}}^{(2)} = -\frac{1}{6t_c}\int_0^{t_c} dt_3 \int_0^{t_3} dt_2 \int_0^{t_2} dt_1 \; \{[(\tilde{\mathcal{H}}_{int}(t_3),$$

$$[\tilde{\mathcal{H}}_{int}(t_2),\tilde{\mathcal{H}}_{int}(t_1)]] + [\tilde{\mathcal{H}}_{int}(t_1),[\tilde{\mathcal{H}}_{int}(t_2),\tilde{\mathcal{H}}_{int}(t_3)]]\} \qquad \text{(III.4)}$$

and

$$\tilde{\mathcal{H}}_{int}(t) = U_1^{-1}(t)\,\mathcal{H}_{int}U_1(t) \quad .$$

This is a Magnus expansion[73] of the propagator in powers of the cycle time. The average Hamiltonian expansion is a perturbation expansion in powers of a smallness parameter t_c that has a physical meaning; t_c and $\tilde{\mathcal{H}}_{int}(t)$ are simultaneously varied by lengthening the

sequence. For this reason, $\bar{\mathcal{H}}^{(i)}$ is termed a correction term of order i and is proportional to $t_c^{\,i}$. $\bar{\mathcal{H}}^{(0)}$ is the zero-order or average Hamiltonian, and $\mathcal{H}$ is the effective Hamiltonian. The advantage of this expansion is that a complex time dependent process has been expressed by a time independent Hamiltonian.

3.1.2 Examples of Multiple-Pulse Sequences

Pulse sequences are usually designed so that $\bar{\mathcal{H}}^{(0)}$ has some particular desired property, and then higher-order terms are minimized. Two simple examples are shown in Figure (III.1). Figure (III.1(a)) is called a Carr-Purcell sequence.[37] The sequence is cyclic because $U_1(2T) = 1$. If the pulses are assumed to have negligible width, $\tilde{\mathcal{H}}_{int}(t)$ is:

$$\tilde{\mathcal{H}}_{int}(t) = \mathcal{H}_D + \mathcal{H}_Q + \mathcal{H}_J + \mathcal{H}_{cs} + \mathcal{H}_Z \qquad (0 \leq t < T/2)$$

$$= \mathcal{H}_D + \mathcal{H}_Q + \mathcal{H}_J - \mathcal{H}_{cs} - \mathcal{H}_Z \qquad (T/2 \leq t < 3T/2)$$

$$= \mathcal{H}_D + \mathcal{H}_Q + \mathcal{H}_J + \mathcal{H}_{cs} + \mathcal{H}_Z \qquad (3T/2 \leq t \leq 2T) \qquad \text{(III.5)}$$

because the first-rank spin tensors $\mathcal{H}_{cs}$ and $\mathcal{H}_Z$ are inverted by a 180° rotation. Then

$$\bar{\mathcal{H}}^{(0)} = \mathcal{H}_D + \mathcal{H}_Q + \mathcal{H}_J$$

and the chemical shifts have been suppressed. If a pulse sequence is symmetric, such that $\tilde{\mathcal{H}}_{int}(t) = \tilde{\mathcal{H}}_{int}(t_c - t)$, $\bar{\mathcal{H}}^{(1)}$ and all other odd-order correction terms vanish. This sequence is symmetric, so the major corrections come from $\bar{\mathcal{H}}^{(2)}$ and from pulse sequence

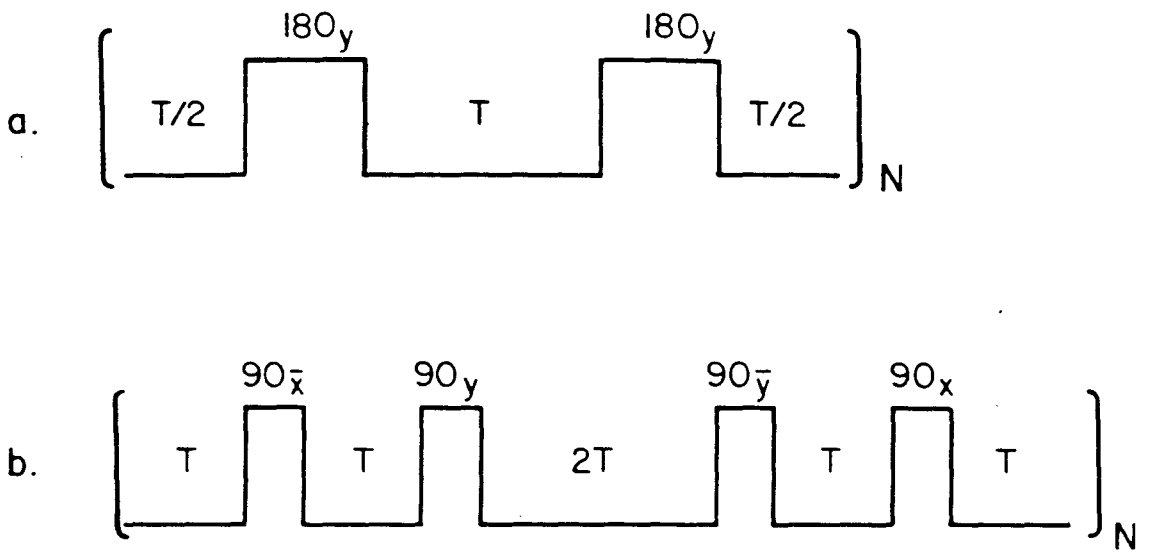

XBL 8010-12249

Figure III.1 Two multiple-pulse sequences for suppressing some parts of the Hamiltonian. Part a) shows a Carr-Purcell sequence, which suppresses first-rank tensor interactions. Part b) shows a WAHUHA sequence, which suppresses second-rank tensor interactions.

imperfections (inhomogeneity, timing errors, and the like).

Figure (III.1(b)) is called a WAHUHA sequence.[74] $\mathcal{H}_z$ can be decomposed into three parts: zero-rank tensors ($\Sigma\ J_{ij}\vec{I}_i\cdot\vec{I}_j$), first-rank tensors ($-\Sigma\ \sigma_i I_{zi} + \Delta\omega I_z$), and second-rank tensors ($\mathcal{H}_D$, $\mathcal{H}_Q$ and terms with J_{ij}^{aniso}). Zero-rank tensors are not affected by rotations. Second-rank tensors are proportional to $3I_{zi}I_{zj} - \vec{I}_i\cdot\vec{I}_j$ (for $\mathcal{H}_Q$ i=j), and first-rank tensors are proportional to I_{zi}. $\tilde{\mathcal{H}}_{int}$ is then:

$$\tilde{\mathcal{H}}_{int}(t) \sim (3I_{zi}I_{zj} - \vec{I}_i\cdot\vec{I}_j) + I_{zi} + (\vec{I}_i\cdot\vec{I}_j) \quad (0 \le t < T)$$

$$\sim (3I_{yi}I_{yj} - \vec{I}_i\cdot\vec{I}_j) + I_{yi} + (\vec{I}_i\cdot\vec{I}_j) \quad (T \le t < 2T)$$

$$\sim (3I_{xi}I_{xj} - \vec{I}_i\cdot\vec{I}_j) + I_{xi} + (\vec{I}_i\cdot\vec{I}_j) \quad (2T \le t < 3T)$$

$$\tilde{\mathcal{H}}_{int}(6T-t) = \tilde{\mathcal{H}}_{int}(t) \tag{III.6}$$

This gives

$$\bar{\mathcal{H}}^{(0)} = \frac{1}{3}\left(\Delta\omega(I_x+I_y+I_z) - \Sigma\sigma_i(I_{xi}+I_{yi}+I_{zi})\right) + \Sigma\ J_{ij}(\vec{I}_i\cdot\vec{I}_j)$$

$$\bar{\mathcal{H}}^{(1)} = 0 \tag{III.7}$$

This sequence eliminates dipolar and quadrupolar terms, thus permitting the observation of chemical shifts in solids. More sophisticated sequences are designed to have smaller error terms. For example, one very powerful method of reducing these terms

involves alternating between two or more different cycles (called subcycles) to form a new, larger cycle. Under certain conditions, some of the higher-order terms for the entire cycle are simply equal to the sum of the corresponding terms for the subcycles; such terms are said to decouple.[75] Decoupled pulse cycles for line narrowing have been produced that have $\bar{\mathcal{H}}^{(2)} = 0$ for the dipolar Hamiltonian, and have small error terms.[75]

3.1.3 Estimation of Correction Terms

Higher-order terms are usually difficult to calculate, but their size (and therefore their contribution to residual line widths) can sometimes be estimated. If $\bar{\mathcal{H}}^{(0)} = \bar{\mathcal{H}}^{(1)} = \bar{\mathcal{H}}^{(2)} \ldots = \bar{\mathcal{H}}^{(n-1)} = 0$, then $\bar{\mathcal{H}}^{(k)} = \bar{\bar{\mathcal{H}}}^{(k)}$, where $\bar{\bar{\mathcal{H}}}^{(k)}$ is defined as

$$\bar{\bar{\mathcal{H}}}^{(k)} = \frac{(-i)^k}{t_c} \int_0^{t_c} dt_{k+1} \int_0^{t_{k+1}} dt_k \ldots \int_0^{t_2} dt_1 \, \tilde{\mathcal{H}}_{int}(t_{k+1}) \, \tilde{\mathcal{H}}_{int}(t_k) \ldots$$

$$k=n,\ n+1 \ldots 2n \qquad \text{(III.8)}$$

Reference (9) contains a weaker version of this theorem, which requires $\bar{\mathcal{H}}^{(j)} = 0$ for all $j<n$ for $\bar{\mathcal{H}}^{(n)} = \bar{\bar{\mathcal{H}}}^{(n)}$, but inspection of their proof[76] leads to the immediate conclusion that $\bar{\mathcal{H}}^{(j)} = 0$ for all $j < (n-1)/2$ is sufficient for $\bar{\mathcal{H}}^{(n)} = \bar{\bar{\mathcal{H}}}^{(n)}$.

The volume of integration is $(t_c)^{n+1}$, so $\bar{\bar{\mathcal{H}}}^{(n)}$ can be easily estimated in terms of $\mathcal{H}_{int}$. This estimation requires the concept of the norm of a matrix. The norm of an arbitrary $N_T \times N_T$ matrix A can be defined as:

$$||A|| = \left(\frac{1}{N_T} \mathrm{Tr}(AA^{\dagger})\right)^{1/2} \quad . \qquad \text{(III.9)}$$

$\|A\|$ is invariant under unitary transformations, so if A is Hermitian, $\|A\|$ is the root-mean square eigenvalue of A, called $M_2^{1/2}(A)$. Other convenient properties that are proven in Appendix E are:

1. If A and B are Hermitian, $\|AB\| = \|BA\| \leq N_T^{1/2}\|A\|\ \|B\|$.

2. $\|I\| = 1$, where I is the identity matrix.

3. If A is Hermitian, $\|A^n\|$ is the square root of the (2n)-th moment of the distribution of the eigenvalues, called $M_{2n}^{1/2}(A)$. Since $M_{2n}^{1/2}(A) \geq (M_2^{1/2}(A))^n$ for any distribution, $\|A^n\| \geq (\|A\|)^n$.

4. If A and B are similar Hermitian matrices, such that $A = UBU^\dagger$, $\|AB\| \leq \|A^2\| = \|B^2\|$.

5. However, if A and B are two different matrices, with nothing else known about either matrix, then $(AB)_{mn} = \sum_i A_{mi}B_{in}$ is the sum of N_T numbers, which are expected to add randomly. This implies $\|AB\| \sim \|A\|\ \|B\|$.

Properties (3) and (4) imply that $\|\tilde{\mathcal{H}}_{int}(t_{n+1})\ \tilde{\mathcal{H}}_{int}(t_n)\ \ldots\ \tilde{\mathcal{H}}_{int}(t_1)\| \leq \|(\tilde{\mathcal{H}}_{int}(t_1))^{n+1}\|$. For many systems the eigenvalues of $\mathcal{H}_{int}$ have roughly a Gaussian distribution, and in this case

$$M_{2n}^{1/2} = (1\cdot 3\cdot 5\ \ldots\ (2n-1))^{1/2}\ (M_2^{1/2})^n = ((2n)!/(2^n)n!)^{1/2}(M_2^{1/2})^n \quad . \tag{III.10}$$

Thus

$$\|\bar{\mathcal{H}}^{(n)}{}_{t_c}\| \leq (\|\mathcal{H}_{int}{}_{t_c}\|^{n+1})((2n)!/2^n n!((n+1)!)^2)^{1/2} \quad . \tag{III.11}$$

In fact, if the cycle contains many pulses so that $\tilde{\mathcal{H}}_{int}(t)$ varies rapidly, $\|\tilde{\mathcal{H}}_{int}(t_{n+1})\ \tilde{\mathcal{H}}_{int}(t_n)\ \ldots\ \tilde{\mathcal{H}}_{int}(t_1)\| \sim \|\mathcal{H}_{int}\|^{n+1}$.

Thus $\|\bar{\mathcal{H}}^{(n)} t_c\| \sim \|\mathcal{H}_{int} t_c\|^{n+1}/(n+1)!$, and for those terms for which $\bar{\mathcal{H}}^{(m+1)} = \bar{\mathcal{H}}^{(m+1)}$, $\|\bar{\mathcal{H}}^{(n+1)}\|/\|\bar{\mathcal{H}}^{(n)}\| \sim \|\mathcal{H}_{int} t_c\|/(m+1)$. For higher-order terms expressions involving commutators, such as equations (III.3-4) are required.

All of the results presented so far are applicable to any cyclic pulse sequence. It is now necessary to extend average Hamiltonian theory, in order to create pulse sequences which selectively excite only a few transitions.

3.2 Extension of Average Hamiltonian Theory to Selective Sequences

3.2.1 Definitions

An operator is nk-quantum selective if it can be completely decomposed into irreducible tensors T^j_{nk}, with k allowed to have any integral value including 0. If only $k = \pm 1$ is required, the operator is n-quantum selective. If tensor components that are not integral multiples of n are required, the operator is nonselective. Any nonselective operator can be decomposed into an nk-quantum selective operator and a remainder which we call non-nk-quantum selective (abbreviated nns). From the definition of tensor operators, the product or sum of two nk-quantum operators is also an nk-quantum operator. In addition, an operator is nk-quantum selective if and only if it is invariant to a rotation of $2\pi/n$ about the z-axis.

A cyclic pulse sequence is j-order nk-quantum selective if all the operators $\bar{\mathcal{H}}^{(i)}$ $(i \leq j)$ in the average Hamiltonian expansion of the propagator are nk-quantum selective operators. (For example, if $\bar{\mathcal{H}}^{(0)}$ is 4k-quantum selective but $\bar{\mathcal{H}}^{(1)}$ is not, the sequence is zero-order 4k-quantum selective). An equivalent definition is that

all terms in the propagator proportional to $(t_c)^{i+1}$ $(i \leq j)$ are nk-quantum selective. If the initial density matrix has no coherences, the final density matrix will contain only nk-quantum selective operators, up to terms proportional to $(t_c)^{j+1}$.

The physical meaning of nk-quantum operators depends on the system being considered. If the axis of propagation of the radiation is chosen as the z-axis, an nk-quantum operator causes a net absorption or emission of a multiple of n photons, and changes the z-component of the angular momentum of the applied field by some multiple of $n\hbar$. If the z-component of angular momentum is a good quantum number for the system (as it is, for example, in NMR at normal magnetic field strengths), conservation of angular momentum implies that the system can develop coherences only between states for which this quantum number differs by a multiple of n. If this is not a good quantum number, the selection rules for n-quantum transitions are more complicated.

3.2.2 Theorems for Selective Sequences

Many of the theorems of average Hamiltonian theory are directly applicable to selective sequences. In addition, two new theorems which can be viewed as generalizations of known theorems for line narrowing sequences are useful.

Theorem I. Suppose a cycle (cycle time t_c) consists of m subcycles (cycle times t_{c1}, t_{c2}, ... t_{cm}), each of which is j-order nk-quantum selective. Then the cycle is also j-order nk-quantum selective. Furthermore, the non-nk-quantum selective (nns) part of $\bar{\mathcal{H}}^{(j+1)}$ for the cycle decouples, i.e.,

$$(\bar{\mathcal{H}}^{(j+1)} t_c)_{nns} = \sum_{i=1}^{m} (\bar{\mathcal{H}}_i^{(j+1)} t_{ci})_{nns} \tag{III.12}$$

Proof: For simplicity of notation only the case m=2 will be explicitly proven, since repeated application of this theorem with m=2 proves the theorem for arbitrary m.

The propagator for the cycle is equal to the product of the propagators for the two subcycles:

$$\exp(-i(\bar{\mathcal{H}}^{(0)} + \bar{\mathcal{H}}^{(1)} + \ldots)t_c) = \exp(-i(\bar{\mathcal{H}}_2^{(0)} + \bar{\mathcal{H}}_2^{(1)} + \ldots)t_{c2})$$

$$\times \quad \exp(-i(\bar{\mathcal{H}}_1^{(0)} + \bar{\mathcal{H}}_1^{(1)} + \ldots)t_{c1}) \quad . \tag{III.13}$$

Expansion in powers of t_c, t_{c1} and t_{c2} (recalling that $\bar{\mathcal{H}}^{(k)} \sim t_c^k$ and $\bar{\mathcal{H}}_j^{(k)} \sim t_{cj}^k$) shows that the term proportional to $(t_c)^{k+1}$ is:

$$-i\bar{\mathcal{H}}^{(k)} t_c + \frac{1}{2} \sum_{k',k''} \bar{\mathcal{H}}^{(k')} \bar{\mathcal{H}}^{(k'')} t_c^{\,2} + \ldots$$

$$= \sum_{k_1+k_2=k-1} (-i\bar{\mathcal{H}}_2^{(k_2)} t_{c2} + \frac{1}{2} \sum_{k_2',k_2''}{}' \bar{\mathcal{H}}_2^{(k_2')} \bar{\mathcal{H}}_2^{(k_2'')} t_{c2}^2 + \ldots)$$

$$\times (-i\bar{\mathcal{H}}_1^{(k_1)} t_{c1} + \frac{1}{2} \sum_{k_1',k_1''}{}' \bar{\mathcal{H}}_1^{(k_1')} \bar{\mathcal{H}}_1^{(k_1'')} t_{c1}^2 + \ldots)$$

$$k'+k'' = k-1$$

$$k_1'+k_1'' = k_1-1$$

$$k_2'+k_2'' = k_2-1 \tag{III.14}$$

In this expression $k_1, k_2 \geq -1$; if $k_i = -1$ the terms involving t_{ci} are

ignored. The terms represented by (...) are products of three or more operators, multiplied by $(t_c)^3$ or higher powers of t_c. $\bar{\mathcal{H}}^{(k)}$ can only appear in the first term on the l.h.s., and all other terms must have smaller superscripts. By assumption, $\bar{\mathcal{H}}^{(k_i)}$ is nk-quantum selective for all $k_i \leq j$. When k=0, equation (III.14) simplifies to

$$i\bar{\mathcal{H}}^{(0)} t_c = i(\bar{\mathcal{H}}_1^{(0)} t_{c1} + \bar{\mathcal{H}}_2^{(0)} t_{c2}) \qquad \text{(III.15)}$$

so $\bar{\mathcal{H}}^{(0)}$ is nk-quantum selective if $j \geq 0$. It follows by induction that all the operators $\bar{\mathcal{H}}^{(k)}$ $(k \leq j)$ are nk-quantum selective by considering progressively higher powers of t_c, through $(t_c)^{j+1}$.

The only possible nns term proportional to $(t_c)^{j+2}$ on the l.h.s. is then $(-i\bar{\mathcal{H}}^{(j+1)} tc)_{nns}$ since all other terms involve only lower-order operators which are nk-quantum selective. Similarly, the only possible nns term on the r.h.s. is $-i(\bar{\mathcal{H}}_1^{(j+1)} t_{c1} + \bar{\mathcal{H}}_2^{(j+1)} t_{c2})_{nns}$. By equating these two expressions, Theorem I is proven.

The only property of nk-quantum selective operators that was needed to prove Theorem I was closure of this set of operators under addition and multiplication, and similar theorems can be proven for any other set of operators with these two closure properties. In particular, the null set is closed under addition and multiplication. A decoupling theorem for that case (i.e., $\bar{\mathcal{H}}^{(0)} = \bar{\mathcal{H}}^{(1)} \ldots = \bar{\mathcal{H}}^{(j)} = 0$) was proven by Burum and Rhim.[75] Their version of the decoupling theorem was used to cancel residual error terms by combining cycles. A similar approach will be taken in section 3.3 to create selective sequences. Incidentally, another

set which satisfies the required closure properties is the set of N-quantum operators in a N spin-$\frac{1}{2}$ NMR system, plus the populations of the two extreme states; this case will be discussed later.

The size of the <u>first</u> nns term for a j-order nk-quantum selective sequence can be readily estimated.

Theorem II. If a sequence is j-order nk-quantum selective, the non-nk-quantum selective (nns) part of $\bar{\mathcal{H}}^{(j+1)}$ can be written as:

$$(\bar{\mathcal{H}}^{(j+1)})_{nns} = ((-i)^{j+1}/t_c) \int_0^{t_c} dt_{j+2} \ldots \int_0^{t_2} dt_1 \, \tilde{\mathcal{H}}_{int}(t_{j+2}) \ldots$$

$$\tilde{\mathcal{H}}_{int}(t_1))_{nns} \quad . \qquad \text{(III.16)}$$

Proof: The proof of this theorem is identical to the proof that $\bar{\mathcal{H}}^{(j+1)}$ has this form if $\bar{\mathcal{H}}^{(j)} = 0$ for all $i \leq j$, contained in reference (9), so it will merely be outlined. The most general expression for the term proportional to $(t_c)^{j+2}$ in the propagator is

$$(-i)^{j+2} \int_0^{t_c} dt_{j+2} \int_0^{t_{j+2}} dt_{j+1} \ldots \int_0^{t_2} dt_1 \, \tilde{\mathcal{H}}_{int}(t_{n+1}) \, \tilde{\mathcal{H}}_{int}(t_n) \ldots$$

$$\tilde{\mathcal{H}}_{int}(t_1) \quad . \qquad \text{(III.17)}$$

Expanding $U = \exp(-i\bar{\mathcal{H}}^{(0)} + \bar{\mathcal{H}}^{(1)} + \ldots \bar{\mathcal{H}}^{(n)} \ldots)t_c)$ as in the l.h.s. of equation (III.14), the only possible non-nk-quantum selective term proportional to $(t_c)^{j+2}$ is $(-i\bar{\mathcal{H}}^{(j+1)} t_c)_{nns}$, which proves the theorem.

It should be noted that equation (III.16) is only valid for the <u>first</u> nns term, while if $\bar{\mathcal{H}}^{(n)} = 0$ for all $n < j$ a similar expression holds for all terms up to $\bar{\mathcal{H}}^{(2n)}$. The difference is that the l.h.s.

of equation (III.14) contains operators such as $\bar{\mathcal{H}}^{(k_1)}\bar{\mathcal{H}}^{(k_2)}$, which vanish if either $\bar{\mathcal{H}}^{(k_1)}$ or $\bar{\mathcal{H}}^{(k_2)}$ vanishes, but which are generally nk-quantum selective only if <u>both</u> $\bar{\mathcal{H}}^{(k_1)}$ and $\bar{\mathcal{H}}^{(k_2)}$ are nk-quantum selective.

3.3 Design of Selective Sequences

3.3.1 Zero-Order Selective Sequences

A sequence which is zero-order nk-quantum selective can be produced from any cyclic sequence of pulses and delays, using a technique called phase cycling, illustrated in Figure III.2(a). Assume that the cyclic sequence has a duration $\Delta\tau_p$ (called a sub-cycle), an effective Hamiltonian $\mathcal{H}_o = \bar{\mathcal{H}}_o^{(0)} + \bar{\mathcal{H}}_o^{(1)} + \ldots \bar{\mathcal{H}}_o^{(n)} \ldots$, and a propagator $U_o = \exp(-i\mathcal{H}_o\Delta\tau_p)$. At the end of the interval $\Delta\tau_p$, the sequence is repeated with all radiation phase shifted by $\phi = 2\pi/n$ about the z-axis, giving a new effective Hamiltonian $\mathcal{H}_\phi$ and propagator U_ϕ. $\mathcal{H}_\phi$ is related to $\mathcal{H}_o$ by a rotation of $-\phi$ about the z-axis:

$$\mathcal{H}_\phi = \exp(i\phi I_z)\, \mathcal{H}_o \exp(-i\phi I_z) \tag{III.18}$$

$$(\mathcal{H}_\phi)_{ij} = (\mathcal{H}_o)_{ij} \exp(i\phi(M_i - M_j)) \tag{III.19}$$

and U_ϕ is related to U_o in exactly the same manner. This phase shift is repeated n times, creating a cycle with cycle time $t_c = n\Delta\tau_p$. To calculate $\bar{\mathcal{H}}^{(j)}$ for the cycle, note that t_c is proportional to $\Delta\tau_p$. Therefore $\bar{\mathcal{H}}_o^{(j)}$ and $\bar{\mathcal{H}}^{(j)}$ scale in exactly the same manner when t_c is changed, and equating terms proportional to t_c with those proportional to $\Delta\tau_p$ shows that:

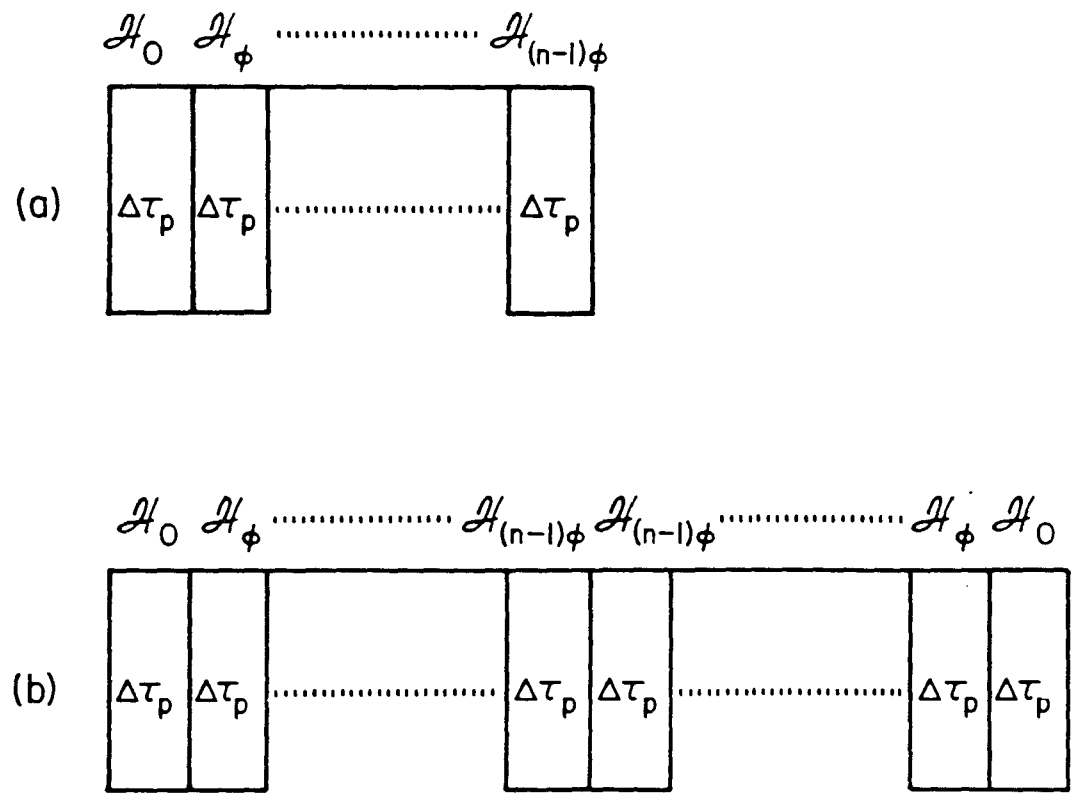

XBL 803-8899

Figure III.2a Phase cycling can be used to create nk-quantum selective sequences, using phase shifts of $\phi = 2\pi/n$. The cycle of n subcycles is more selective by one order in the average Hamiltonian theory expansion.

Figure III.2b The cycle of 2n subcycles formed by phase cycling and symmetrization is more selective by two orders.

$$\bar{\mathcal{H}}^{(0)} = \frac{1}{n} \sum_{\ell=0}^{n-1} \bar{\mathcal{H}}^{(0)}_{\ell\phi} = \frac{1}{n} \sum_{\ell=0}^{n} \exp(i\ell\phi I_z)\, \bar{\mathcal{H}}^{(0)}_{o} \exp(-i\ell\phi I_z) \quad . \tag{III.20}$$

This sum scales the matrix element $(\bar{\mathcal{H}}^{(0)}_{o})_{ij}$ by $(1/n) \sum_{m=0}^{n-1} e^{i2\pi p\ell/n}$, where $p = m_i - m_j$; this scaling factor is zero unless $p = nk$. Therefore, $\bar{\mathcal{H}}^{(0)}$ is a pure nk-quantum selective operator. Since $\bar{\mathcal{H}}^{(0)}$ decouples, any other permutation of the subcycles is also acceptable. Higher order terms have some nk-quantum selective parts (for example, there is a contribution $\sum_{\ell=0}^{n-1} \bar{\mathcal{H}}^{(1)}_{\ell\phi}$ to $\bar{\mathcal{H}}^{(1)}$) but no higher order terms are completely selective. Thus, the sequence obtained by phase cycling is zero-order nk-quantum selective. Equivalently, the propagator after n subcycles can be written as:

$$\begin{aligned} U &= \prod_{p=0}^{n-1} \exp(-i\mathcal{H}_{\phi=2\pi p/n}\Delta\tau_p) \\ &= 1 - i\Delta\tau_p\Big(\sum_{p=0}^{n-1} \mathcal{H}_{\phi=2\pi p/n}\Big) + O\{\|\mathcal{H}_\phi \Delta\tau_p\|^2\} \end{aligned} \tag{III.21}$$

If $\|\mathcal{H}_\phi \Delta\tau_p\| \ll 1$, the last term can be neglected. Combining equations (III.4) and (III.5) to first order in $\Delta\tau_p$ we can write

$$\begin{aligned} U_{ij} &\simeq \delta_{ij} - i\Delta\tau_p\Big(\sum_{p=0}^{n-1} \exp(i2\pi p(M_i - M_j)/n)\Big)(\mathcal{H}_o)_{ij} \\ &= \delta_{ij} - in\Delta\tau_p(\mathcal{H}_o)_{ij}\, \delta((M_i - M_j) - nk) \quad . \end{aligned} \tag{III.22}$$

Thus U will only induce transitions between states with $\Delta M = nk$, to first order in $\Delta\tau_p$. If t_c can be made arbitrarily small, all the higher-order terms in the average Hamiltonian expansion become

unimportant, and this zero-order selective sequence becomes completely selective; of course, the selective term $\|\bar{\mathcal{H}}^{(0)} t_c\| \to 0$ as $t_c \to 0$, but this can be remedied by repeating the zero-order sequences many times. An operator which only induces transitions between states with $\Delta M = nk$ will also only transfer populations between states with $\Delta M = nk$. Thus selective sequences can create selective population inversions.

This application of average Hamiltonian theory is somewhat unusual, in the sense that $\tilde{\mathcal{H}}_{int}(t)$ (i.e., $\mathcal{H}_o$, $\mathcal{H}_\phi$, ...) is given instead of generated from a time independent $\mathcal{H}_{int}$. Figure (III.3) shows schematically how this difference can be eliminated. The phase shifts are equivalent to a series of z pulses on a system with an otherwise time independent $\mathcal{H}_o$. Since the pulses have strange flip angles, phase shifting can probably be done more accurately.

3.3.2 Sequences Selective to Arbitrary Order

In general, the cycle time cannot be made vanishingly small, so higher-order selectivity is desirable. One simple way to get a first-order selective sequence is to symmetrize the cycle, as illustrated in Figure (III.2(b)). $\bar{\mathcal{H}}^{(0)}$ is still nk-quantum selective, and the symmetrization causes $\bar{\mathcal{H}}^{(j)}$ to vanish for all odd j, so the first nonselective term is $\bar{\mathcal{H}}^{(2)}$.

In fact, sequences which are selective to arbitrarily high order can be designed. Suppose that the sequence for $\mathcal{H}_o$ in Figure III.2(a) is already j-order nk-quantum selective, instead of being nonselective as was assumed earlier. Theorem I proves that the sequence obtained by phase cycling is (j+1)-order nk-quantum selective, because

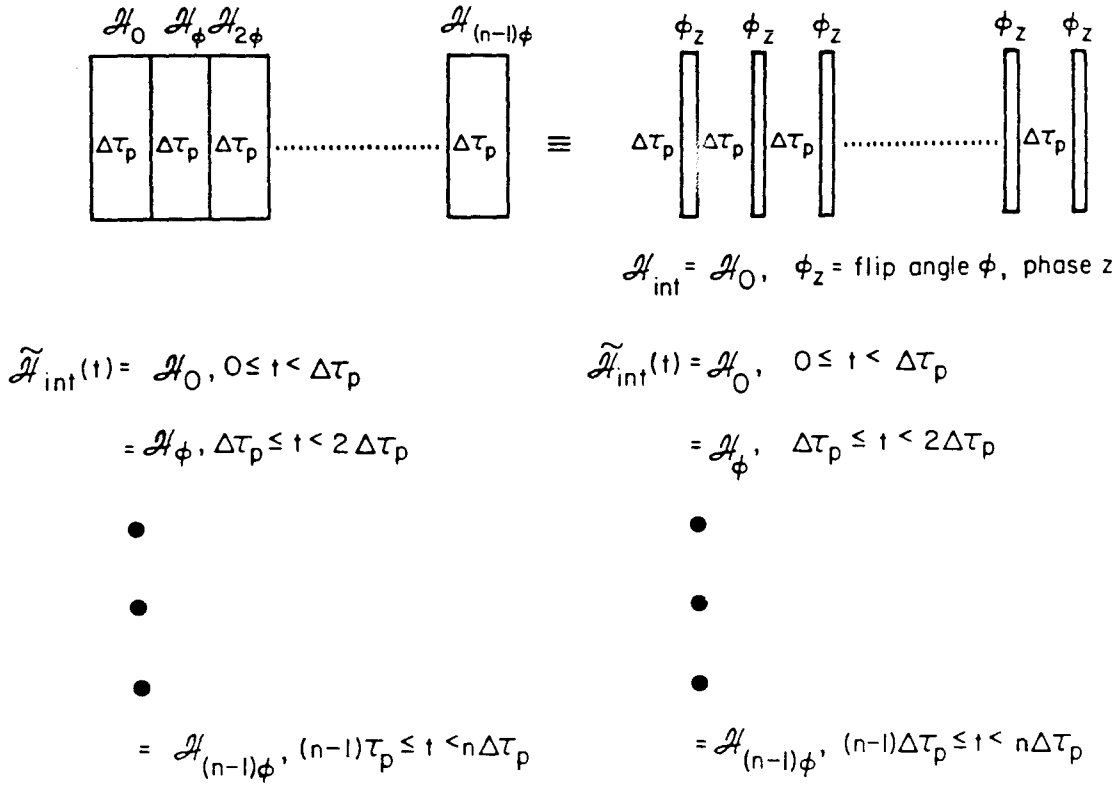

Figure III.3. The analogy between a phase cycled sequence consisting of subcycles with effective Hamiltonians $\mathcal{H}_\phi$ and a pulse sequence on a hypothetical system with $\mathcal{H}_{int} = \mathcal{H}_o$. Average Hamiltonian theory can be applied to the pulse sequence.

$(\bar{\mathcal{H}}^{(j+1)})_{nns}$ decouples:

$$(\bar{\mathcal{H}}^{(j+1)})_{nns} = \sum_{\ell=0}^{n-1} (\bar{\mathcal{H}}^{(j+1)}_{\ell\phi})_{nns} = \sum_{\ell=0}^{n-1} (\exp(i\ell\phi I_z)\ \bar{\mathcal{H}}^{(j+1)}_{o}$$

$$\exp(-i\ell\phi I_z))_{nns} = 0 \quad . \qquad \text{(III.24)}$$

Therefore, starting from a nonselective $\mathcal{H}_o$, (j+1) phase cyclings produce a sequence that is j-order nk-quantum selective, requiring $n^{(j+1)}$ subcycles; each block of n subcycles is zero-order nk-quantum selective, each block of n^2 subcycles is first-order nk-quantum selective, and so forth. For example, a first-order 4k-quantum selective sequence may be constructed from $4^2 = 16$ subcycles, and the phases of the subcycles can be written schematically ($0:\phi=0$, $1:\phi=\pi/2$, $2:\phi=\pi$, $3:\phi=3\pi/2$) as (0123) (1230) (2301) (3012). Each group in parentheses is a zero-order nk-quantum selective sequence, and is phase shifted by $\pi/2$ to produce the next group.

In the absence of relaxation, there is no limit to the number of times phase cycling can be applied, and therefore sequences which are selective to arbitrarily high order can be designed. In any real system, only a limited number of subcycles could be completed before relaxation effects make the average Hamiltonian calculation invalid. One way to reduce the number of subcycles required to achieve a given order of selectivity is to combine phase cycling and symmetrization, as in Figure III.2(b). The sequence is first-order nk-quantum selective even if $\mathcal{H}_o$ is nonselective. If $\mathcal{H}_o$ is already j-order nk-quantum selective (j odd), the phase cycling and symmetrization requires 2n subcycles to make a (j+2)-order nk-quantum

selective sequence, instead of the n^2 subcycles required for two phase cyclings. Thus, a (2j+1)-order nk-quantum selective sequence requires $(2n)^{j+1}$ subcycles ((j+1) phase cyclings and (j+1) symmetrizations) and a (2j)-order nk-quantum selective sequence requires $n(2n)^j$ subcycles ((j+1) phase cyclings and j symmetrizations) For example, a third-order 4k-quantum selective sequence requires $(2n)^2 = 64$ subcycles, and the relative phase can be written schematically as (0123)(3210)(1230)(0321)(2301)(1032)(3012)(2103)(3012)(2103)(2301)(1032)(1230)(0321)(0123)(3210).

3.4 Application of Selective Sequences to Multiple-Quantum NMR

3.4.1 Design of Effective Subcycles

In this subsection the general principles of selective excitation are applied to the particular case of a system of directly dipole coupled nuclear spins. The high resolution and simplicity of the high multiple-quantum spectra of these systems was discussed in section 1.4. It will be shown how the use of selective sequences can overcome the problem of small signal intensity, thus making these spectra observable in large spin systems.

The Hamiltonian for the N spins-1/2 of an oriented molecule in a large magnetic field can be written in the rotating frame (in units of $\hbar = 1$) as

$$\mathcal{H}_z = \sum_{i>j} D_{ij}(3I_{zi}I_{zj} - \vec{I}_i \cdot \vec{I}_j) + \sum_{i>j} J_{ij}(\vec{I}_i \cdot \vec{I}_j) + (-\sum_i \sigma_i I_{zi} + \Delta\omega I_z)$$

$$\equiv \mathcal{H}_{zz} + \mathcal{H}_J + (\mathcal{H}_{cs} + \Delta\omega I_z) \qquad \text{(III.24)}$$

where typically $\|\mathcal{H}_{zz}\| >> \|\mathcal{H}_{cs}\|, \|\mathcal{H}_J\|$. All of these terms were

defined in Chapter I. The evolution under this Hamiltonian must be converted, by some as yet unspecified sequence of pulses and delays, into the propagator U_o (and effective Hamiltonian $\mathcal{H}_o$) of the last subsection. If the sequence can be designed to have high quantum operators in the leading terms of its effective Hamiltonian, then the cycle need only be selective to a low order since high-quantum operators will appear in its leading terms. Since $\mathcal{H}_z$ contains only first and second-rank operators, no simple rotation of $\mathcal{H}_z$ can contain high-quantum operators. In fact, it can be shown that no matter what the actual pulse sequence is for $\mathcal{H}_o$, it cannot contain multiple-quantum operators unless $\|\mathcal{H}_z \Delta\tau_p\| > 1$. If the cycle consists of many subcycles then $\|\mathcal{H}_z t_c\| >> 1$, but convergence of the effective Hamiltonian expansion generally requires $\|\mathcal{H}_o t_c\| < 1$. For this reason the pulse sequence for $\mathcal{H}_o$ must be constructed such that $\|\mathcal{H}_o\| << \|\mathcal{H}_z\|$. Several approaches will be discussed.

3.4.2 The Use of Time Reversal in Subcycles

3.4.2.1 General Principles

One general approach to subcycle design uses the method of time reversal and is illustrated in Figure (III.4(a)). Pulse sequences can be designed with $\bar{\mathcal{H}}_D^{(o)} = 1/2(\mathcal{H}_{D,xx} + \mathcal{H}_{D,yy}) = -1/2\ \mathcal{H}_{D,zz}$; the effect of such sequences is to make the spin system appear to evolve backwards in time.[77] If such a pulse sequence is applied for a time 2T and then turned off, the initial condition will return after a time T. If $\|\mathcal{H}_{D,zz}T\| \geq 1$, both the forward time and reversed time propagators can contain irreducible tensor operators of arbitrarily high rank, but will commute with I_z. Similarly, pulse sequences can

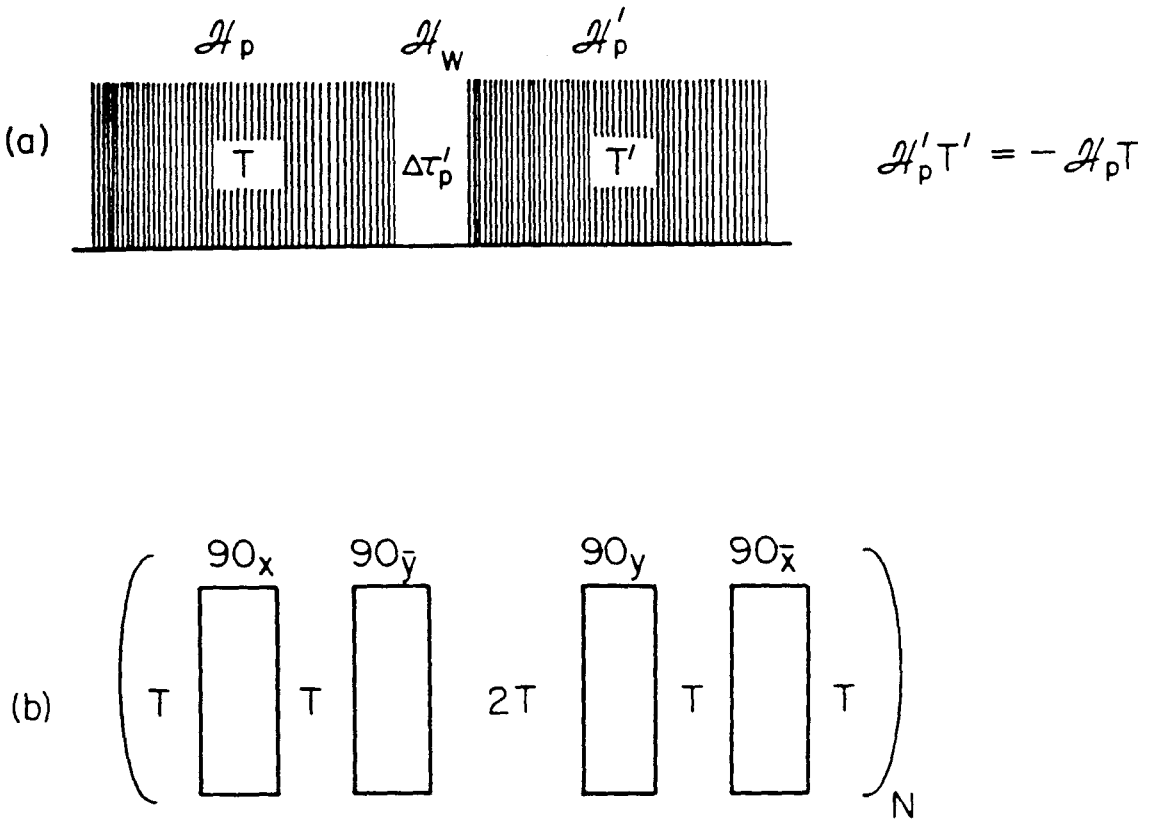

Figure III.4. Possible pulse sequences for the subcycles in Figure III.2. In part (a) time reversal sequences generate $\mathcal{H}_p'T' = -\mathcal{H}_pT$, so that $\|\mathcal{H}_o\| << \|\mathcal{H}_{D,zz}\|$, but $\mathcal{H}_o$ contains multiple-quantum coherences. In part (b) a WAHUHA sequence with a long cycle time has the same effect.

be designed with $\bar{\mathcal{H}}_D^{(o)} = 1/2\ (\mathcal{H}_{D,yy} + \mathcal{H}_{D,zz}) = -1/2\ \mathcal{H}_{D,xx}$. In this case, the propagator obtained from a sequence with $\|\mathcal{H}_{D,xx}T\| \gtrsim 1$ will contain irreducible tensor operators of arbitrarily high rank, but will <u>not</u> commute with I_z. Such a propagator can generate multiple-quantum coherences and can be viewed as a multiple-quantum rotation (as opposed to the rotation produced by a single strong pulse, which will only generate single-quantum coherences from a density matrix proportional to I_z).

The propagator for the subcycle of Figure (III.4(a)) is $U(\Delta\tau_p) = \exp(-i\mathcal{H}_p'T')\ \exp(-i\mathcal{H}_w\Delta\tau_p')\ \exp(-i\mathcal{H}_pT)$. Time reversal techniques are used to make $\mathcal{H}_p'T' = -\mathcal{H}_pT$. When this condition holds, the periods T and T' may be viewed as a complementary pair of multiple-quantum rotations which sandwich the period $\Delta\tau_p'$. Together they form a cycle, and the propagator is:

$$U(\Delta\tau_p) = \exp(-i\Delta\tau_p'(\exp(-i\mathcal{H}_pT)\mathcal{H}_w\ \exp(-i\mathcal{H}_pT))) \qquad \text{(III.25)}$$

Therefore

$$\mathcal{H}_o = (\Delta\tau_p'/\Delta\tau_p)(\exp(i\mathcal{H}_pT)\mathcal{H}_w\ \exp(-i\mathcal{H}_pT)) \qquad \text{(III.26)}$$

If $\mathcal{H}_p$ is nonsecular, bilinear and does not commute with $\mathcal{H}_w$ then $\mathcal{H}_o$ will contain high multiple-quantum operators when $\|\mathcal{H}_pT\| \gtrsim 1$. Since the exponential operators constitute a unitary transformation $\|\mathcal{H}_o\| = \frac{\Delta\tau_p'}{\Delta\tau_p}\|\mathcal{H}_w\|$. The desired effect of reducing the norm of the subcycle Hamiltonian is achieved when $\Delta\tau_p' << \Delta\tau_p$.

Since $\|\mathcal{H}_o\Delta\tau_p\| = \|\mathcal{H}_w\Delta\tau_p'\|$ the small interval $\Delta\tau_p'$ may be thought of as an effective cycle time for the subcycle. This concept is very

useful in understanding the application of average Hamiltonian theory to selective sequences. $\bar{\mathcal{H}}^{(i)}$ is defined to be the term which scales as $(t_c)^i$ when the cycle time is changed, but implicit in this definition is the assumption that $\tilde{\mathcal{H}}_{int}(t)$ is also scaled proportionately. Thus, if every delay in a specific pulse sequence is doubled and the length of each pulse is doubled while keeping the flip angle constant, the term $\bar{\mathcal{H}}^{(i)}$ is multiplied by 2^i. In a selective sequence $\tilde{\mathcal{H}}_{int}(t)$ is replaced with $\mathcal{H}_o$, $\mathcal{H}_\phi$, and so forth. In fact, $\Delta\tau_p = 2T + \Delta\tau_p'$ for the sequence in Figure (III.4(a)), but if T is changed at all $\mathcal{H}_o$ will change. The only way to double each matrix element of $\mathcal{H}_o\Delta\tau_p$ (which is analogous to scaling $\tilde{\mathcal{H}}_{int}(t)$) is to double $\Delta\tau_p'$ but leave T alone. Thus T should be viewed as a fixed parameter, and $\Delta\tau_p'$ is effectively the length of the subcycle.

3.4.2.2 Specific Subcycle Sequences

Several choices are possible for $\mathcal{H}_p$, $\mathcal{H}_p'$, and $\mathcal{H}_w$. One choice is to let $\mathcal{H}_p = \mathcal{H}_{xx} = \sum_{i>j} \alpha_{ij}(3I_{xi}I_{xj}-I_i\cdot I_j)$, produced by the sequence $90_y - T - 90_{\bar{y}}$. $\mathcal{H}_{cs}$ has been neglected; if this is a bad approximation, an echo sequence can be used. $\mathcal{H}_p' = -\frac{1}{2}\mathcal{H}_{xx}$, produced by a time reversing sequence, such as $(\frac{1}{2}\tau - 90_x - \tau - 90_x - \tau - 90_{\bar{x}} - \tau - 90_{\bar{x}} - \tau - 90_{\bar{x}} - \tau - 90_{\bar{x}} - \tau - 90_x - \tau - 90_x - \frac{1}{2}\tau)$, repeated enough times to fill a period $T' = 2T$, and $\mathcal{H}_w = \mathcal{H}_{zz}$ using no pulses at all ($\mathcal{H}_w$ is a "window" in the sequence). The particular time reversing sequence chosen for $\mathcal{H}_p'$ has $\bar{\mathcal{H}}_D^{(0)} = -\frac{1}{2}\mathcal{H}_{D,xx}$; it is symmetric, so $\bar{\mathcal{H}}_D^{(1)} = 0$. Using the notation of reference (75) for various error terms from pulse imperfections, one finds $\bar{\mathcal{H}}_0^{(0)}$ (resonance offset and chemical shift terms) = 0; $\bar{\mathcal{H}}_{\varepsilon D}^{(0)}$(rf inhomogeneity effects) = 0

(to order ε); and $\bar{\mathcal{H}}^{(0)}_{\delta D}$ (nonzero pulse width) = 0. Neglecting all correction terms, we have

$$\mathcal{H}_{\phi=0}\Delta\tau_p = \exp(i\mathcal{H}_{xx}T)(\mathcal{H}_z\Delta\tau'_p)\ \exp(-i\mathcal{H}_{xx}T) \quad , \qquad \text{(II.27)}$$

which is purely even-quantum. This is sometimes convenient; for example, a third order 10k-quantum selective sequence requires $4n^2 = 400$ subcycles, but a third order 5k-quantum selective sequence only requires 100 subcycles, and if no odd-quantum coherences are present in $\mathcal{H}_\phi$ the two sequences have the same effect.

3.4.2.3 Pure Double-Quantum Sequences

The sequence $90_y - T - 90_{\bar{y}}$ only gives $\mathcal{H}_p = \mathcal{H}_{xx}$ if there are no chemical shifts, if $\Delta\omega = 0$, if the rf homogeneity and the static homogeneity are perfect, and if the pulse widths are negligible. Thus even if τ is kept short in the sequence for T', usually $\|\mathcal{H}_\phi\Delta\tau_p\| >> \|\mathcal{H}_w\Delta\tau'_p\|$ because neglected error terms would enter. One very convenient way to lessen the severity of error terms is to design a sequence with an effective Hamiltonian having only double-quantum terms; then time reversal can be achieved by a phase shift. For example, the sequence $(\frac{\tau}{2} - 90_x - \tau' - 90_x - \tau - 90_{\bar{x}} - \tau' - 90_{\bar{x}} - \tau - 90_{\bar{x}} - \tau' - 90_{\bar{x}} - \tau - 90_x - \tau' - 90_x - \frac{\tau}{2})$ has an average Hamiltonian $\bar{\mathcal{H}}^{(0)}_D = (\tau'/\tau+\tau')\mathcal{H}_{yy} + (\tau/\tau+\tau')\mathcal{H}_{zz}$ in the limit of δ-function pulses, and if $\tau' = 2\tau$,

$$\bar{\mathcal{H}}^{(0)}_D = \frac{1}{3}\,(2\mathcal{H}_{D,yy} + \mathcal{H}_{D,zz}) = \frac{1}{3}\,(\mathcal{H}_{D,yy} - \mathcal{H}_{D,xx}) \quad . \qquad \text{(III.28)}$$

This is a pure double-quantum operator. If the pulses are assumed to have a square envelope but a finite width t_p, $\bar{\mathcal{H}}^{(0)}_D$ is a pure

double-quantum operator for $\tau' = 2\tau + t_p$; other pulse errors may change this relation slightly.

Since $\bar{\mathcal{H}}_D^{(0)}$ is purely a two-quantum operator, a phase shift of 90° multiplies it by -1; this can also be seen by substituting $I_x \to I_y$, $I_y \to -I_x$, $I_z \to I_z$ in equation (III.28). Therefore, if the pulse sequence is run with y and $\bar{y}$ pulses instead of x and $\bar{x}$ pulses, the zero-order average of the dipolar Hamiltonian is inverted. $(\mathcal{H}_{cs} + \Delta\omega I_z)$ is cancelled to lowest order by this sequence, and $\mathcal{H}_J$ is unaffected. In most anisotropic systems, $\|\mathcal{H}_{zz}\|$ is several orders of magnitude larger than $\|\mathcal{H}_J\|$, so $\bar{\mathcal{H}}_D^{(0)}$ dominates when $\|\mathcal{H}_z\tau\| << 1$ and very good time reversal is possible.

This sequence compensates for several common pulse errors. Static inhomogeneity would force $\Delta\omega$ to be written as $\Delta\omega(\vec{r})$, but the zero-order average vanishes. Similarly, rf inhomogeneity, which can be represented by a pulse flip angle of $90-\varepsilon$, does not appear in $\bar{\mathcal{H}}_D^{(0)}$ to order ε. The largest nonvanishing error term in $\bar{\mathcal{H}}^{(0)}$ should be the cross term between static and rf inhomogeneity, which is minimized by making $\Delta\omega \sim 0$. The sequence looks symmetric to the dipolar Hamiltonian, so $\bar{\mathcal{H}}_D^{(1)} = 0$, and under ideal experimental conditions the ultimate limitations to time reversal come from $\bar{\mathcal{H}}_D^{(2)}$ and $\mathcal{H}_J$. These terms will make $\|\mathcal{H}_o\Delta\tau_p\| > \|\mathcal{H}_w\Delta\tau_p'\|$. Fortunately, one feature of the selective experiment is that perfect time reversal is unnecessary since imperfections merely cause $\|\mathcal{H}_o\|$ to be larger than in the ideal case.

Potential sequences for $\mathcal{H}_w$ include:

1. No pulses, giving $\mathcal{H}_w = \mathcal{H}_z$ and even-quantum selection for initial condition βI_z.

2. $45_x - \Delta\tau'_p - 45_{\bar{x}}$, giving all orders in $\mathcal{H}_\phi$.

3. The same sequence as $\mathcal{H}_p$, except phase shifted by 45°.

Clearly $\mathcal{H}_w$ is also a pure two-quantum operator, but $[\mathcal{H}_p, \mathcal{H}_w] \neq 0$, so multiple-quantum coherences still develop. After a brief interval $\Delta\tau'_p$, another phase shift of 45° gives $\mathcal{H}'_p$.

Most of the experimental work to date (to be discussed in chapter V) has used $\mathcal{H}_w = \mathcal{H}_z$ and $\mathcal{H}_p = \frac{1}{3}(\mathcal{H}_{D,yy} - \mathcal{H}_{D,xx})$. Previous attempts with $\mathcal{H}_p = \mathcal{H}_{D,xx}$ and $\mathcal{H}'_p = -\frac{1}{2}\mathcal{H}_{D,xx}$, as discussed above, were less successful.

3.4.3 The Effects of Imperfect Time Reversal

As mentioned earlier, errors in the sequence for $\mathcal{H}_p$ and $\mathcal{H}'_p$ cause $\|\mathcal{H}_o\|$ to be larger than expected. If these effects are small they can be compensated for by decreasing $\Delta\tau'_p$. In some systems, however, perfect time reversal is impossible. One example is NMR is isotropic solvents; $\mathcal{H}_{cs}$ can easily be reversed, but $\mathcal{H}_J$ is a zero-rank tensor and cannot be affected by wideband pulses. Average Hamiltonian theory is not well suited to this calculation, since $\|\mathcal{H}_J T\| \gtrsim 1$ to generate multiple-quantum operators, so discussion of this case will be postponed to section 4.6.2.

3.4.4 Other Subcycle Sequences

The standard WAHUHA sequence, illustrated in Figure III.4(b) is another possible pulse sequence for $\mathcal{H}_o$. If $\mathcal{H}_{int} = \mathcal{H}_{zz}$, this sequence gives $\bar{\mathcal{H}}^{(0)} = \bar{\mathcal{H}}^{(1)} = 0$ (neglecting pulse errors). However, if $\|\mathcal{H}_{zz}T\| \gg 1$, $\mathcal{H}_o$ will have strong contributions from $\bar{\mathcal{H}}^{(2)}$, $\bar{\mathcal{H}}^{(4)}$ and higher-order terms which contain multiple-quantum coherences. For some values of T such that $\|\mathcal{H}_{zz}T\| \sim 1$, $\|\mathcal{H}_o\| \ll \|\mathcal{H}_{zz}\|$, but $\mathcal{H}_o$ contains

a substantial fraction of multiple-quantum coherences. The sequence is repeated N times, so $\Delta\tau_p = 6$ NT. When such a subcycle is incorporated into a selective excitation sequence, it will prove useful to think of T as a fixed parameter while N is varied in order to vary the cycle time; again this approach allows $\mathcal{H}_o$ to remain fixed.

Clearly, any other line narrowing sequence is also a candidate for producing $\mathcal{H}_o$, but this sequence would probably be the easiest to use for low-quantum selection because of its relatively large correction terms. A possible advantage over the use of time-reversing sequences is the very low duty cycle, which results because T is much longer than in a normal WAHUHA experiment. Simple sequences for $\mathcal{H}_o$ will be discussed further in section 4.6.1.

3.5 Selective Sequences in the Multiple-Quantum NMR Experiment

3.5.1 Optimum Relation between Preparation and Mixing Propagators

Any selective sequence can be incorporated into the general framework of a multiple-quantum experiment described in section 2.4. It was shown in that section that the total integrated intensity of the multiple-quantum spectrum is at most proportional to the equilibrium magnetization, $-C\ \beta\ \mathrm{Tr}(I_z^2)$. This can only be achieved if the preparation propagator U and mixing propagator V are matched such that $|UI_zU^\dagger|_{ij} = |V^\dagger I_z V|_{ji}$, and for nonselective experiments this implies $\tau = \pm t_2$.

For the selective experiment this constraint is more difficult to satisfy. The simplest experimental arrangement is to use the same sequence for preparation and detection, so U = V. If the effective Hamiltonian $\bar{\mathcal{H}}$ ($U = \exp(-i\bar{\mathcal{H}}t_c)$) is real then U is complex symmetric,

and this implies that $(UI_zU^\dagger)_{ij} = (U^\dagger I_z U)_{ji}$. An equally desirable arrangement is to have $\bar{\mathcal{H}}$ related to a real operator by a phase shift. (For example, all the four-quantum elements might be imaginary and all the zero-quantum elements real). This will always be true for N-quantum selection in an N spin-$\frac{1}{2}$ system because there are only two N-quantum elements and a phase shift which makes one real makes the other real. In addition, if the two-quantum sequence is used for $\mathcal{H}_p$ (in Figure III.4(a)), and if either the two-quantum sequence or $\mathcal{H}_z$ is used for $\mathcal{H}_w$, then $\mathcal{H}_o$ will be related to a real operator by a phase shift. In this case the constraint is satisfied for any zero-order or symmetrized first-order sequence. In other cases the signal may be somewhat reduced; this will be discussed in section 6.1.

3.5.2 Phases of Selected Transitions; Time Reversal Mixing

If the preparation and mixing sequences are designed such that $U = V^\dagger$ then equation (II.62) shows that all transitions will appear in phase. The condition $U = V^\dagger$ will be called time reversal mixing, since it can generally be accomplished by a mixing sequence which reverses the order of the pulses in the preparation sequence, phase shifts each pulse by 180°, and time reverses each delay. In addition, some pulse sequences allow simpler approaches. For example, if the two-quantum sequence is used for $\mathcal{H}_p$, $\mathcal{H}_w$, and $\mathcal{H}_p'$ (with phases 0, $\pi/4$, and $\pi/2$ respectively, as explained in section 3.4.2) and the sequence is symmetrized then $U = V^\dagger$ can be achieved by changing the phases to $\pi/2$, $\pi/4$ and 0 respectively. Pulse sequences which do not include time reversal mixing usually produce transitions with arbitrary phases, and magnitude spectra are then calculated.

3.5.3 Potential Signal Gains; Selective Population Inversion

An efficient wideband excitation drives all of the possible transitions about equally. Therefore, the average intensity of a single line in a multiple-quantum spectrum is smaller than the average intensity of a single line in an ordinary single pulse experiment, by a ratio (number of single-quantum transitions)/(number of excited multiple-quantum transitions). When there are many spins, the intensity of a single transition becomes extremely small. For example, a system with N spins-$\frac{1}{2}$ and no symmetry has 2^{2N} possible distinct matrix elements, so totally nonselective excitation gives a signal for each transition of $2^{-2N}(C\ \beta\ \mathrm{Tr}(I_z^{\ 2}))$.

If only certain orders of multiple-quantum transitions are excited, but the excitation is still efficient (in the sense that the population differences are substantially depleted) the intensity of a single transition grows. For example, if the resonance offset and chemical shifts are removed from the excitation and mixing periods of the standard nonselective experiment, only even-quantum coherences are excited, and since roughly half the coherences are even-quantum this increases the intensity of an average even-quantum transition by a factor of two. If only a few transitions are excited (by an extremely selective sequence) and the sequence is efficient, the intensity of each transition can be enormous. Suppose that selective excitation is used for both preparation and mixing, and that $UI_zU^\dagger$ and $V^\dagger I_z V$ in equation (II.59) could be prepared with all the matrix elements zero except for the single coherence with $\Delta M = +N$ and the single coherence with $\Delta M = -N$. In that case, the signal gain

relative to the nonselective experiment would be 2^{2N-1}. However, the density matrix that results is not related to the initial condition I_z by a unitary transformation, and therefore it cannot be produced by any sequence that does not include relaxation.

A more reasonable estimate of the maximum possible gain is obtained by finding the maximum possible value of $(UI_zU^\dagger)_{ab}$, where $|a\rangle$ is the single state with $M = +N/2$ and $|b\rangle$ is the single state with $M = -N/2$:

$$(UI_zU^\dagger)_{ab} = \sum_i U_{ai}(I_z)_{ii}U^\dagger_{ib} \tag{III.29}$$

$$= \sum_i U_{ai}(U_{bi})^*(I_z)_{ii} \tag{III.30}$$

$$\sum_i U_{ai}(U_{bi})^* = \delta_{ab} \quad . \tag{III.31}$$

The maximum can be readily seen to be $U_{aa} = 1/\sqrt{2}$, $U_{ab} = 1/\sqrt{2}$, $U_{ai} = 0$, $U_{ba} = -1/\sqrt{2}$, $U_{bb} = 1/\sqrt{2}$, $U_{bi} = 0$. The phases are not unique. Such a propagator concentrates the matrix elements of U in the states with the largest values of $|M|$. It couples states $|a\rangle$ and $|b\rangle$ only to each other, effectively creating a two-level system. The two-level system has

$$U = \begin{pmatrix} 1/\sqrt{2} & 1/\sqrt{2} \\ -1/\sqrt{2} & 1/\sqrt{2} \end{pmatrix} = \exp(i(\pi/2)I_y^{ab}) \ , \quad I_y^{ab} = \begin{pmatrix} 0 & -i/2 \\ i/2 & 0 \end{pmatrix} \tag{III.32}$$

where I_y^{ab} is a fictitious spin-$\frac{1}{2}$ operator for multiple-quantum

coherence.[62]

Thus, the maximum possible signal is obtained by a selective 90° pulse, shown schematically in Figure III.5. The signal from this transition is $-C\ \beta\ (UI_zU^\dagger)^2_{ab} = -C\ \beta\ (I_z^2)_{aa}$. The gain when compared to totally nonselective excitation is then

$$G_N = (\beta(I_z^2)_{aa})/(\beta 2^{-2N} tr(I_z^2))$$

$$= \beta(N/2)^2/\beta 2^{-2N}(N2^N/4) = N2^N \quad . \qquad \text{(III.33)}$$

To achieve this gain a sequence that couples the state $M = N/2$ only to the state $M = -N/2$ is needed. The effective Hamiltonian for this sequence should be some linear combination of I_y^{ab} and I_x^{ab}. This sequence would be used to create $UI_zU^\dagger$ and $V^\dagger I_z V$. If the effective Hamiltonian has this form for $M = \pm N/2$ it can have any form whatsoever for the other levels, and the signal in the N-quantum transition will be unaffected. A selective 180° pulse is also possible (for example, a sequence which produces a selective 90° pulse could be applied twice.) Such a pulse would not produce any signal, but would invert the population difference between the two extreme levels. This approach to population inversion has applications to other spectroscopic systems.

Often the (N-1)-quantum or (N-2)-quantum transitions in an N-spin system are more interesting than the N-quantum transition, since the N-quantum transition contains no dipolar information. If (N-1)-quantum selection is used, the number of transitions increases to 2N for a system without symmetry. In addition, while it is possible to

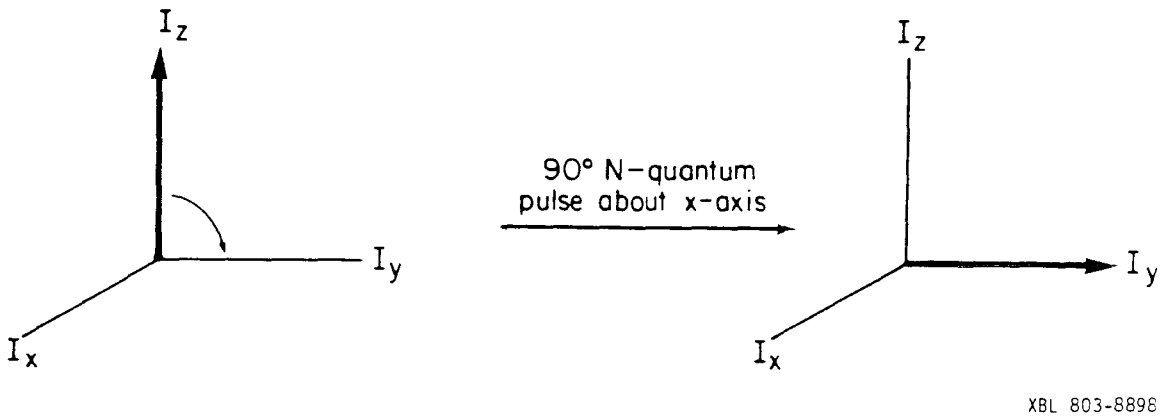

Figure III.5. Schematic illustration of the effect of N-quantum selective sequences, in terms of an effective two-level system involving only M = ± N/2. A selective 90° pulse transfers the entire population difference between those two states into N-quantum coherence, giving a gain relative to nonselective excitation of $N2^N$.

envision a $\pi/2$ pulse on a two-level system completely depleting the population difference, in a multilevel system it is very unlikely that all population differences can be eliminated simultaneously. Thus one also produces zero-quantum transitions and populations in the $M = \pm N/2$ and $M = \pm (N/2-1)$ manifolds, effectively increasing the total number of pumped matrix elements by $2N^2+2$. Now, however, the available fraction of I_z^2 is larger. The result of all of these effects is:

$$G_{N-1} = (\beta(2(I_z^2)_{M=N/2} + 2N(I_z^2)_{M=N/2-1})/(2N^2 + 2N + 2)(\beta 2^{-2N}\mathrm{Tr}(I_z^2))$$

$$= 2^N(N^2 - 3N + 4)/(N^2 + N + 1) \approx 2^N \text{ for } (N >> 1) \quad . \tag{III.34}$$

Values of G_N and G_{N-1} for systems without symmetry are listed in Table III.1. If symmetry is included, all gains are reduced, because fewer transitions are allowed and therefore the system is effectively a collection of smaller systems. All of the methods used here are still valid, except that the number of density matrix elements excited and the available fraction of I_z^2 should be recalculated using the known symmetry. In general, N-quantum and (N-1)-quantum transitions must have A_1 symmetry, since the states with $M = \pm N/2$ have that symmetry as noted in section 1.4. The relevant energy level diagram is not a binomial distribution but instead is the group of A_1 states. The calculations are straightforward, and benzene has been included in Table III.1 to illustrate symmetry effects.

These gains become extremely large for large N. However, the

Table III.1 Enhancement of N or (N-1)-Quantum Transitions in an N-Spin System by Selective Excitation

N	Symmetry	G_N	G_{N-1}
2	None	8	1.14
4	None	64	6.10
6	Benzene	47.5	17.2
6	None	384	32.7
8	None	2048	154
10	None	10240	683
12	None	49152	2922
14	None	229376	12269
16	None	1048576	50892
18	None	4718592	209409

Table III.1. Enhancement of high multiple-quantum transitions, using selective sequences. Sequences which select only N-quantum (or only (N-1)-quantum) are illustrated in Figure III.2.

Table III.2 Intensity of High Multiple-Quantum Transitions, With and Without Selectivity, Relative to Total Magnetization of the Sample

		Intensity (In Percent)		
N	Symmetry	Nonselective	xG_N	xG_{N-1}
6	Benzene A_1	0.197	9.38	3.69
6	None	0.024	9.38	0.80
8	None	1.5×10^{-3}	3.13	0.24
10	None	9.5×10^{-5}	0.98	0.065
12	None	5.9×10^{-6}	0.29	0.017
14	None	3.7×10^{-7}	0.085	4.5×10^{-3}
16	None	2.3×10^{-8}	0.024	1.2×10^{-3}
18	None	1.4×10^{-9}	0.0069	3.0×10^{-4}

single N-quantum transition contains only a tiny fraction of the total intensity in the nonselective experiment, and therefore the total signal available in the N-quantum and (N-1)-quantum transitions with and without selectivity should be calculated. This calculation is done in Table III.2 and assumes that the total number of protons in the sample is kept constant as N is changed. The signal size is calculated as a fraction of the total magnetization of the sample. The signal size still decreases as N increases, but the decrease is much slower than in the nonselective experiment, and Table III.2 indicates that selective excitation should dramatically increase the number of molecules which could be studied by multiple-quantum spectroscopy.

3.5.4 Coherent Initial Conditions

In all of the calculations so far, the initial density matrix has been assumed to be the equilibrium matrix $-\beta I_z$. However, other initial conditions are possible. If an nk-quantum selective operator is applied to an initial density matrix $-\beta I_x$ (produced by a single 90° pulse), only coherences with $\Delta M = nk \pm 1$ are produced. One important advantage of this technique is it is no longer necessary to pretend that the observable operator is $\langle I_z \rangle$; $\langle I_x \rangle$ is the operator which has signal. In the standard multiple-quantum experiment and in this experiment, the signal can be sampled long after the last pulse; in the selective experiment which starts from I_z, the signal should be sampled as close as possible to the last pulse, and this causes filtering problems.

Unfortunately, selective excitation from I_x is much less efficient than selective excitation from I_z, since all the single-quantum transitions are always excited. The number of single-quantum transitions in an unsymmetrical system with N spins-1/2 is $((2N)!/(N+1)!(N-1)!)$. Using Sterling's approximation one finds

$$(2N)!/(N+1)!(N-1)! \approx 2^{2N}/\sqrt{\pi N} \qquad \text{(III.35)}$$

so the fraction of pumped coherences is at least $2/(\pi N)^{1/2}$, and the expected gain is $\sqrt{N}\ (\sqrt{\pi}/2) = .89\sqrt{N}$. This small enhancement often will not justify the additional difficulties of a multiple-pulse experiment.

3.5.5 Symmetry Selection

One physically interesting application of selective sequences is the production of multiple-quantum transitions corresponding to a limited number of irreducible representations. The N-quantum and (N-1)-quantum transitions all have A_1 symmetry, so if a Nk-quantum or (N-1)k-quantum selective sequence is applied to a system at equilibrium only A_1 energy levels are perturbed. If one more pulse is applied after the selective sequence, the density matrix can have all orders of multiple-quantum A_1 coherences, but in the other irreducible representations can only have single-quantum coherences. Depending on the nature of the energy level diagram, it may be possible to select other representations as well. This symmetry selection will be discussed further in Chapter V.

3.5.6 Heteronuclear Selective Excitation

The differences between heteronuclear and homonuclear selective excitation are quite minor if the I-spin pulses and S-spin pulses

are always shifted by the same amount. The Hamiltonian has several additional terms not found in equation (III.24). The most important additional term in the heteronuclear dipolar coupling, $\Sigma\, b_{ij} I_{zi} S_{zi}$, which generates operators such as $I^+_1 S^+_2$ if an appropriate sequence is used. The sequence for $\mathcal{H}_o$ in Figure (III.4(a)) is still valid, but $\mathcal{H}_p$, $\mathcal{H}'_p$ and $\mathcal{H}_w$ should be changed. Many choices are possible. One simple option would be to make $\mathcal{H}_p$ and $\mathcal{H}'_p$ into two-quantum operators for both sets of nuclei, (i.e., apply the same pulses to both), but in addition supperss the heteronuclear couplings with echoes on one set of nuclei. As long as the heteronuclear couplings are not suppressed in $\mathcal{H}_w$, all multiple-quantum operators can be produced, with the S operators the same in $\mathcal{H}_o$ as they are in $\mathcal{H}_w$.

One interesting difference between homonuclear and heteronuclear selective excitation is the possibility of using different phase shifts for the different nuclei. For example, a sequence which is 4k-quantum selective for I spins and 3k-quantum selective for S spins can be generated by shifting I pulses by $\pi/2$, and S pulses by $2\,\pi/3$; such a sequence requires 12 subcycles. If there are 4 I spins and 3 S spins, all of which are spins-1/2, this sequence produces only $\Delta M_I = 0, \pm 4$; $\Delta M_s = 0, \pm 3$. However, shifting both sets of pulses together produces more high-quantum operators; in this example, if all the pulses are shifted by $2\,\pi/7$, only $\Delta M_I = 0$, $\Delta M_S = 0$; $\Delta M_I = +4$, $\Delta M_S = +3$; and $\Delta M_I = -4$; $\Delta M_S = -3$ operators are produced. Generalizations to spins with total angular momentum $> 1/2$ are straightforward.

3.6 Extent of Selectivity in Non-Ideal Selective Sequences

3.6.1 General Systems

As mentioned earlier, for any multiple-pulse sequence one expects $\|\mathcal{H}^{(n)}\| \lesssim \|\mathcal{H}_{int}\|^{n+1} t_c^{\,n}$. In a selective sequence, $\mathcal{H}_\phi$ is formally equivalent to $\tilde{\mathcal{H}}_{int}(t)$, as illustrated in Figure III.3. Therefore, as $\|\mathcal{H}_\phi t_c\| \to 0$, $\bar{\mathcal{H}}^{(0)}$ becomes the dominant term of $\mathcal{H}$. The nonselective terms of $U = \exp(i\mathcal{H}(Nt_c))$ can be made arbitrarily small in principle by making t_c very short, while if Nt_c is kept constant the selective contribution from $\bar{\mathcal{H}}^{(0)}$ is unaffected. In practice, the attainable selectivity is limited by several factors.

1. For technical reasons, t_c cannot be made arbitrarily short. For example, if each subcycle requires pulses with specified flip angles, each pulse has a finite width which depends on the strength of the exciting field.

2. The time required to pump multiphoton coherences is generally dependent on the "anharmonicity" of the energy level spacing. The excitation sequence needs to extend for a period comparable to the inverse of the anharmonic frequencies, which in the last section were the dipolar frequencies. This problem was investigated in depth in the last section; one solution is to construct a subcycle with an effective Hamiltonian $\|\mathcal{H}_o\| \ll \|\mathcal{H}_{int}\|$, so that $\|\mathcal{H}_o t_c\|$ can be small even though $\|\mathcal{H}_{int} t_c\|$ is not. If this is not possible, the general considerations of the preceding section still hold, but to retain selectivity the subcycles would need to be shorter, and cycles selective to higher order would be needed to obtain high quantum operators.

3. Because there is a lower limit to the length of a subcycle, the minimum time needed for a j-order nk-quantum selective sequence

increases rapidly as j increases. However, relaxation mechanisms make the average Hamiltonian calculation invalid if the total length of a sequence is comparable to T_2, the coherence dephasing time. Thus, for any system only a finite order of selectivity is possible. Inhomogeneous systems are a special case; excitation designed to compensate for such broadening may allow homogeneous selective excitation.

4. Timing errors, inaccurate phase shifts or other failures in control over coherence will reduce the selectivity of any sequence.

This subsection analyses these limitations for general spectroscopic systems. In order to estimate the importance of the first three problems listed above the size of the first non-nk-quantum selective operator from a j-order nk-quantum selective sequence (which is $(-i\bar{\mathcal{H}}^{(j+1)}t_c)_{nns}$) and plausible conditions for convergence of the average Hamiltonian expansion are calculated in Appendix D. Phase cycling and symmetrization are combined into one operation, which turns a (j-2)-order nk-quantum selective subcycle into a j-order nk-quantum selective cycle requiring 2n subcycles (Figure III.2(b)), assuming perfect phase shifts and no timing errors. The norm of the first nns term for the cycle, which is $(\bar{\mathcal{H}}^{(j+1)})_{nns}$, is shown in Appendix D to be related to that of the first nns term of the ith subcycle, which is $(\bar{\mathcal{H}}_i^{(j-1)})_{nns}$:

$$\|(\bar{\mathcal{H}}^{(j+1)}t_c)_{nns}\| \sim F(n)\|(\bar{\mathcal{H}}^{(0)}t_c)^2\| \; \|(\bar{\mathcal{H}}_i^{(j-1)}t_c)_{nns}\| \qquad \text{(III.36)}$$

$$F(n) = \left(\frac{8}{15}n^5 - \frac{2}{3}n^3 + \frac{2}{15}n\right)^{1/2}/8\,n^3 \sim .09\,n^{-1/2} \quad . \qquad \text{(III.37)}$$

If a (j-2)-order selective subcycle were repeated 2n times without phase shifting in between, the first nonselective term would be

$\mathcal{H}^{(j-1)}_{i,nns}\, t_c$; the first nonselective term in the j-order selective sequence is smaller than this only if $\| (\bar{\mathcal{H}}^{(0)} t_c)^2 \|\ F(n) < 1$. This result suggests that the average Hamiltonian expansion fails to converge when $\| (\bar{\mathcal{H}}^{(0)} t_c)^2 \| \gtrsim F(n)^{-1}$. Thus convergence requires

$$\| (\bar{\mathcal{H}}^{(0)} t_c)^2 \| < F(n)^{-1} \quad . \tag{III.38}$$

Values of F(n) are listed in Table III.3.

Equation (III.37) can be used (j-1)/2 times, to express $(\bar{\mathcal{H}}^{(j+1)})_{nns}$ in terms of $(\bar{\mathcal{H}}^{(2)})_{nns}$ for a first-order selective sequence. $(\bar{\mathcal{H}}^{(2)})_{nns}$ can then be calculated, using equation (III.16). The selectivity S of a j-order nk-quantum selective sequence is defined as the ratio between a typical matrix element of $\bar{\mathcal{H}}^{(0)}$ and a typical matrix element of $(\bar{\mathcal{H}}^{(j+1)})_{nns}$. At the limit of convergence ($\|(\bar{\mathcal{H}}^{(0)} t_c)^2\| \sim F(n)^{-1}$),

$$S = K^{-1} F(n)^{1/2} (2n)^{(j^2/4+7/4)} \left(\frac{n^2\alpha^2}{8K} + \frac{n\alpha^3}{12} \left(F(n) \| (\bar{\mathcal{H}}^{(0)} t_c)^3 \| / \| \bar{\mathcal{H}}^{(0)} t_c \|\right)^2\right)^{-1/2} \tag{III.39}$$

where K is defined as the total number of allowed transitions divided by the total number of nk-quantum transitions, and α is defined by the relation $\|\mathcal{H}_o\|^2 = \alpha K \|\bar{\mathcal{H}}^{(0)}\|^2$ (see equation (III.20)); the reason for the definition is that if all the matrix elements of $\mathcal{H}_\phi$ have roughly equal magnitude, $\alpha \sim 1$.

To go further the relative sizes of $\|\bar{\mathcal{H}}^{(0)}\|$, $\| (\bar{\mathcal{H}}^{(0)})^2 \|$ and $\| (\bar{\mathcal{H}}^{(0)})^3 \|$ are needed. If the eigenvalues of $\bar{\mathcal{H}}^{(0)}$ have a Gaussian distribution, equation (III.7) implies that $\| (\bar{\mathcal{H}}^{(0)})^2 \| = \sqrt{3}\ \|\bar{\mathcal{H}}^{(0)}\|^2$ and $\| (\bar{\mathcal{H}}^{(0)})^3 \| = \sqrt{15}\ \|\bar{\mathcal{H}}^{(0)}\|^3$. Another possibility is that the energy levels might be

Table III.3 Values of $F(n) = ((8/15)n^5-(2/3)n^3 + (2/15)n)^{1/2}/8n^3$ and $(F(n))^{-1}$. As long as $\|(\bar{\mathcal{H}}^{(0)}t_c)^2\| < (F(n))^{-1}$ the average Hamiltonian expansion is expected to converge rapidly.

n	F(n)	$F(n)^{-1}$
3	.090	11
4	.044	23
5	.036	27
6	.032	31
10	.029	35
12	.026	38
14	.024	41
16	.023	44
18	.022	46

spaced so that $\mathcal{H}_o$ has only two transitions which are nearly resonant, forming an effective three-level system, and $\bar{\mathcal{H}}^{(0)}$ contains a nonzero matrix element for only one of these transitions; in this case $N_T = 3$, and if $\bar{\mathcal{H}}^{(0)}$ is traceless one expects $\|(\bar{\mathcal{H}}^{(0)})^n\| = (3/2)^{(n-1)/2} \|\bar{\mathcal{H}}^{(0)}\|^n$. In both cases $\|(\bar{\mathcal{H}}^{(0)})^n\|$ does not grow greater than $\|\mathcal{H}^{(0)}\|^n$ very rapidly. However, if $K >> 1$, so that only a very small fraction of the matrix elements of $\mathcal{H}_o$ are selected by $\bar{\mathcal{H}}^{(0)}$, then $\|(\bar{\mathcal{H}}^{(0)})^n\| \sim (N_T)^{(n-1)/2}$ $\|\bar{\mathcal{H}}^{(0)}\|^n$ is possible. This case and the case of a Gaussian distribution will be discussed in the next section in connection with multiple-quantum NMR.

The factor $(2n)^{j^2/4+7/4}$ makes S grow very rapidly as j is increased, and fairly small values of j still give very selective sequences. For example, if a Gaussian distribution of eigenvalues is assumed for $\bar{\mathcal{H}}^{(0)}$, the selectivity of a third-order 10k-quantum selective sequence with $\alpha \sim 1$, $K \sim n$, and $F(n) = 0.028$ (from Table III.3) is $S = 1170$; a typical selected matrix element is more than three orders of magnitude larger than a typical nonselected matrix element, even near the limit of convergence. When $\|(\bar{\mathcal{H}}^{(0)} t_c)^2\| << F(n)^{-1}$, S will be much larger; in general, if $\|(\bar{\mathcal{H}}^{(0)} t_c)\|$ is scaled down by a factor of A, $\|\bar{\mathcal{H}}^{(n+1)} t_c\|_{nns}$ is scaled down by a factor of A^{j+2}, and S increases by a factor of A^{j+1}. It can be concluded that for many systems the use of cycles with only a finite order of selectivity is entirely satisfactory.

The effects of timing errors and imperfect phase shifts are more serious. Suppose that the length of subcycle i is $\Delta\tau_p + \delta_i$, and that the phase is $\phi_i + \varepsilon_i$, where $\sum_i \delta_i = \sum_i \varepsilon_i = 0$ (Figure III.6). Then

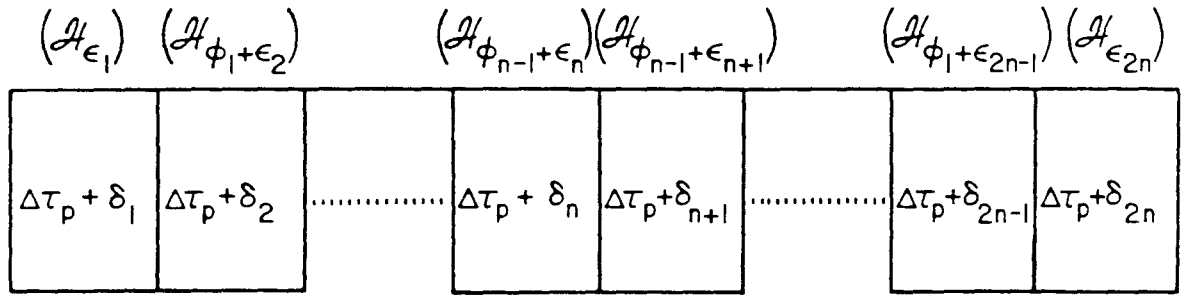

XBL 803-8943

Figure III.6 Modification of the symmetrized sequence of Figure III.2(b) to include phase errors δ_i and timing errors ε_i. We assume, without loss of generality, that $\langle\varepsilon_i\rangle = \langle\delta_i\rangle = 0$.

$$\bar{\mathcal{H}}^{(0)} = \frac{1}{2n\Delta\tau_p} \sum_i (\Delta\tau_p+\delta_i)(\exp(iI_z(\phi_i+\varepsilon_i))\mathcal{H}_o\exp(-iI_z(\phi_i+\varepsilon_i)) \quad \text{(III.40)}$$

which is no longer purely nk-quantum selective; the matrix element for an M-quantum transition is multiplied by

$$\frac{1}{2n\Delta\tau_p} \sum_i (\Delta\tau_p+\delta_i) \exp(im(\phi_i+\varepsilon_i)) \quad \text{(III.41)}$$

instead of 0. Assuming $\delta_j << \Delta\tau_p$ and $\varepsilon_j << 1$, this can be expanded out:

$$\frac{1}{2n\Delta\tau_p} \sum_i (\Delta\tau_p+\delta_i) \exp(im(\phi_i+\varepsilon_i)) =$$

$$\frac{1}{2n\Delta\tau_p} (\Sigma\Delta\tau_p \exp(im\phi_i) + \Sigma\, \delta_i \exp(im\phi_i) + \Sigma(\Delta\tau_p)(im\varepsilon_i)\exp(im\phi_i) + \ldots). \quad \text{(III.42)}$$

The first term on the r.h.s. corresponds to an ideal sequence and vanishes if m is not a multiple of n. If ε_i and δ_i are uncorrelated with ϕ_i, the last two terms reduce to $(2n)^{-1/2}((<\delta_j^2>/\Delta\tau_p^2) + m^2<\varepsilon_j^2>)^{1/2}$. If the number of subcycles increases (for example, by going to a higher-order selective sequence) this term decreases, so that the ratio $\|\bar{\mathcal{H}}^{(0)}\|_{\text{selective}}/\|\bar{\mathcal{H}}^{(0)}\|_{\text{nns}}$ can be made arbitrarily large. However, if ε_j or δ_j are completely correlated with ϕ_i (so that, for example, every time the phase should be $\phi = 0$ it is actually $\phi = \varepsilon_o$), $\|\bar{\mathcal{H}}^{(0)}\|_{\text{selective}}/\|\bar{\mathcal{H}}^{(0)}\|_{\text{nns}}$ is not reduced by increasing the order of the sequence. Such a situation arises with a miscalibrated phase shifting device or for one in which a digital approximation is made to the exact setting. One way to reduce this error is to use two (or more) phase shifting devices, so that the total error is not well correlated with the total phase. A specific example with a 2k-quantum selective sequence is

given in Figure III.7.

3.6.2 Application to Multiple-Quantum NMR

As mentioned earlier, an ideal N-quantum sequence that had no zero-quantum matrix elements could enhance the single N-quantum transition of an N-spin system by a factor of $N2^N$. A non-ideal Nk-quantum selective sequence (which has zero-quantum matrix elements) will not work as well, for two reasons. First, there may be nonzero matrix elements for the populations of the states $m = \pm N/2$ (populations may be thought of as a special type of zero-quantum coherence, with the initial state identical to the final state). In this case, the effective Hamiltonian for the two levels will be $a_x I_x^{ab} + a_y I_y^{ab} + a_z I_z^{ab}$ (Figure III.8) instead of containing only I_x^{ab} and I_y^{ab}. Depending on the relative size of the coefficient a_z it may be impossible to transfer population completely into coherence. Statistically the coefficients are expected to be of comparable size and in that case much of the population can be transferred into coherence. As mentioned earlier, the form of this effective Hamiltonian guarantees that U = V gives the maximum signal.

A much more serious effect comes from the requirement that the average Hamiltonian expansion converge. In general this would imply $\|(\bar{\mathcal{H}}^{(0)} t_c)^2\| < F(n)^{-1}$. For the sequences described, the distribution of eigenvalues of $\mathcal{H}_o$ is expected to resemble that of the eigenvalues of $\mathcal{H}_z$ which will be Gaussian if N is large. It is reasonable to assume that the eigenvalues of $\bar{\mathcal{H}}^{(0)}$ have a Gaussian distribution, since $\bar{\mathcal{H}}^{(0)}$ has many allowed 0-quantum transitions, and since the limit of $\bar{\mathcal{H}}^{(0)}$ as $T \to 0$ for Figure III4 is $\mathcal{H}_z$. The convergence criterion of equation (III.38) can then be written as $\|\bar{\mathcal{H}}^{(0)} t_c\| < 3^{-1/4} F(n)^{-1/2} \sim 2.1\ (n^{1/4})$.

(a)

$\phi = 0$	$\phi = \pi$	$\phi = \pi$	$\phi = 0$	$\phi = \pi$	$\phi = 0$	$\phi = 0$	$\phi = \pi$

$$\bar{\mathcal{H}}^{(0)} = \mathcal{H}_0 + \mathcal{H}_\pi = 0 \quad (m \text{ odd})$$

(b) One phase shifter: $\phi = \epsilon_0$ or $\phi = \pi + \epsilon_1$, $\epsilon_0 + \epsilon_1 = 0$

$\phi = \epsilon_0$	$\phi = \pi + \epsilon_1$	$\phi = \pi + \epsilon_1$	$\phi = \epsilon_0$	$\phi = \pi + \epsilon_1$	$\phi = \epsilon_0$	$\phi = \epsilon_0$	$\phi = \pi + \epsilon_1$

$$\bar{\mathcal{H}}^{(0)} = \frac{1}{2}\left(\mathcal{H}_{\epsilon_0} + \mathcal{H}_{\pi+\epsilon_1}\right) = 2\epsilon_0 m \mathcal{H}_0 \quad (m \text{ odd})$$

(c) Two phase shifters: $\phi = \epsilon_0$ or $\phi = \pi + \epsilon_1$ $\quad \epsilon_0 + \epsilon_1 = 0$

$\phi' = \epsilon'_0$ or $\phi' = \pi + \epsilon'_1$ $\quad \epsilon'_0 + \epsilon'_1 = 0$

$\phi = \epsilon_0$	$\phi = \pi + \epsilon_1$	$\phi = \pi + \epsilon_1$	$\phi = \epsilon_0$	$\phi = \epsilon_0$	$\phi = \pi + \epsilon_1$	$\phi = \pi + \epsilon_1$	$\phi = \epsilon_0$
$\phi' = \epsilon'_0$	$\phi' = \epsilon'_0$	$\phi' = \epsilon'_0$	$\phi' = \epsilon'_0$	$\phi' = \pi + \epsilon'_1$	$\phi' = \pi + \epsilon'_1$	$\phi' = \pi + \epsilon'_1$	$\phi' = \pi + \epsilon'_1$

$$\bar{\mathcal{H}}^{(0)} = \frac{1}{4}\left(\mathcal{H}_{\epsilon_0+\epsilon'_0} + \mathcal{H}_{\pi+\epsilon_1+\epsilon'_0} + \mathcal{H}_{\pi+\epsilon'_1+\epsilon_0} + \mathcal{H}_{\epsilon_1+\epsilon'_1}\right) = \mathcal{O}(\epsilon^2)$$

(m odd)

XBL 803-8900

Figure III.7 Reduction of phase shifting errors can be accomplished by using two (or more) uncorrelated shifters.

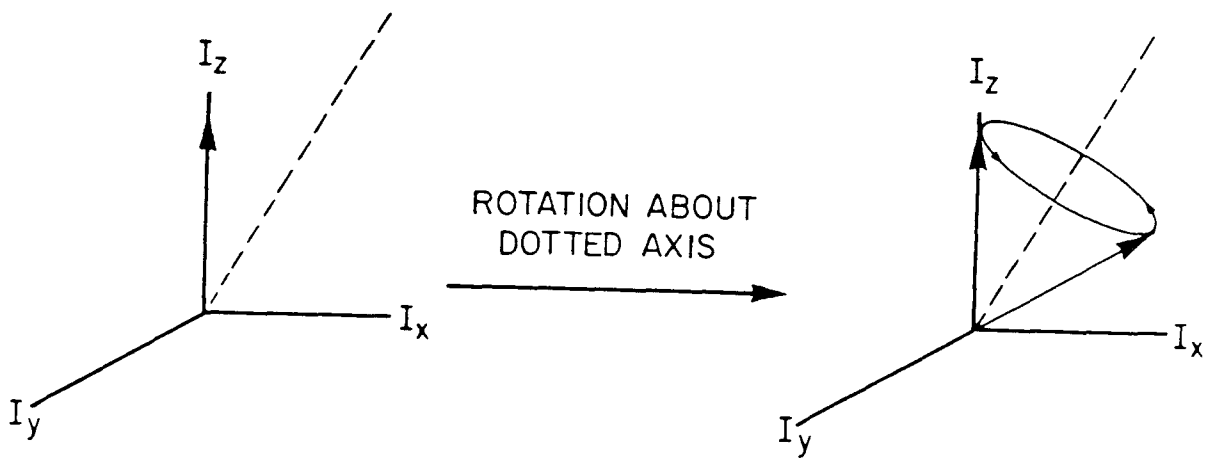

XBL 803-8941

Figure III.8 Schematic illustration of one effect of zero-quantum coherences on an N-quantum selective sequence. The sequence causes the population difference between the states $M = \pm N/2$ to be rotated about an arbitrary axis, and complete transfer of population difference into coherence may be impossible. Compare this to Figure III.5.

The definition of the norm by a 2^N by 2^N matrix gives:

$$\|\bar{\mathcal{H}}^{(0)}t_c\| = (2^{-N}\ \mathrm{tr}((\bar{\mathcal{H}}^{(0)}t_c)^2))^{1/2}$$

$$= (2^{-N} \sum_{mn} |\bar{\mathcal{H}}^{(0)}t_c|_{mn}^{\ 2})^{1/2}$$

$$= \sqrt{N_s}\ 2^{-N/2} \langle |\bar{\mathcal{H}}^{(0)}t_c|^2 \rangle_{mn}^{\ 1/2} \qquad \text{(III.43)}$$

where N_s is the number of possibly nonzero matrix elements, and the rms average only includes those elements. Therefore, to make an average excited matrix element comparable to 1 (which is needed if we want the effect of $\bar{\mathcal{H}}^{(0)}$ to approximate a selective 90° pulse between the levels $M = \pm N/2$) while keeping $\|\bar{\mathcal{H}}^{(0)}t_c\| \sim 1$ requires

$$N_s \lesssim 2^N \quad . \qquad \text{(III.44)}$$

There are 2^{2N} possibly nonvanishing matrix elements for a non-selective sequence, and if only zero-quantum and N-quantum elements are excited, $N_S \sim 2^{2N}\ N^{-1/2}/\pi^{1/2}$. Assuming that $\|\bar{\mathcal{H}}^{(0)}t_c\| \sim 1$ for a conservative estimate, one finds

$$\langle(\bar{\mathcal{H}}^{(0)}t_c)^2\rangle_{ab}^{\ 1/2} \sim N^{1/4}/(2^{N/2}) \ll 1 \qquad \text{(III.45)}$$

This scales down the possible gain because the selective sequence effectively produces only a small rotation instead of a 90° pulse. In fact,

$$|(UI_zU^\dagger)_{ab}(V^\dagger I_z V)_{ba}| \sim N^{5/2}2^{-N} \qquad \text{(III.46)}$$

so the gain is

$$G' = (\beta\sqrt{N}2^{-N}4(I_z^{\,2})_{M=N/2})/\beta 2^{-2N}\ \mathrm{tr}(I_z^{\,2}) = 4\ N^{3/2} \quad . \qquad \text{(III.47)}$$

This value of G' is only approximate, since it depends on the exact maximum permissible value of $\|\bar{\mathcal{H}}^{(0)}t_c\|$. The gain can be roughly assigned to two effects. Only $\sim 1/\sqrt{N}$ as many transitions are being pumped so each one is $\sqrt{N}$ times stronger; in addition, the N-quantum transition receives intensity from the equilibrium population difference of the extreme states for which the expectation value of $I_z^{\,2}$ is $N^2/4$, a factor of N greater than the expectation value averaged over all states. A more liberal estimate which allows $\|\bar{\mathcal{H}}^{(0)}t_c\| \sim 2.1\ n^{1/4}$ would give $G' \sim 16\ N^2$. While this gain is large, a much larger gain is possible if N_S can be reduced.

3.6.3 Removal of Zero-Quantum Operators from Selective Sequences

The gain can be increased if the zero-quantum coherences are removed from $\bar{\mathcal{H}}^{(0)}$. One way to do this is with the sequence shown in Figure III.9(a). The phase shift of π/N inverts the N-quantum coherence but leaves the zero-quantum coherence invariant, and the time reversal inverts every order of coherence, so the net result is that zero-quantum coherences are inverted every subcycle but N-quantum coherences are unaffected. The lowest-order average $\bar{\mathcal{H}}^{(0)}$ for the sequence in Figure III.9(a) contains only N-quantum, 3N-quantum ... (2k+1) N-quantum coherences after 2N subcycles. In an N-spin system, this makes $N_s << 2^N$, condition (III.44) is satisfied, and the ideal gain $G_N = N2^N$ of Table III.1 becomes possible.

The easiest way to design such a sequence for $\mathcal{H}_\phi$ is shown in

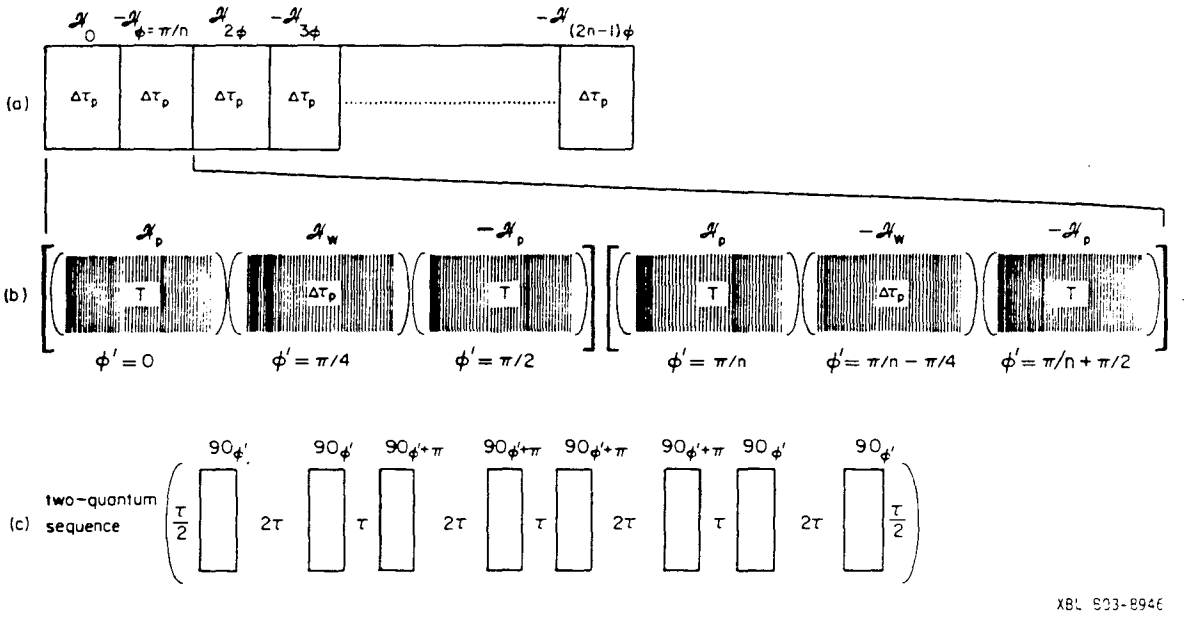

Figure III.9 Sequences to select only N-quantum, 3N-quantum ... (2k+1)N-quantum coherences. a) General sequence. Note that $\mathcal{H}_0$ is inverted after every subcycle, and that the phase shift is $\phi = \pi/N$, instead of $\phi = 2\pi/N$ in Figure III.2. b) $\mathcal{H}_0$ can be formed with the pure double-quantum sequence (part (c)), which is inverted by a $\pi/2$ phase shift.

Figure III.9(b). $\mathcal{H}_p$, $-\mathcal{H}_p$, $\mathcal{H}_w$ and $-\mathcal{H}_w$ are all generated from the double-quantum sequence, mentioned earlier and illustrated in Figure III.9(c) with relative phases 0, $\pi/2$, $\pi/4$, and $3\pi/4$ respectively. If $\|\mathcal{H}_w \Delta\tau_p\| << 1$, only the N-quantum transition appears. However, the value of $K = \|\mathcal{H}_\phi\|/\|\bar{\mathcal{H}}^{(0)}\|$ is now very large ($K \sim 2^N$) so the selectivity S from equation (III.39) will be somewhat weaker, and should be reconsidered. High-order selective sequences with no zero-quantum contributions can be generated from Figure III.9(a) in exactly the same way that high-order selective sequences with zero-quantum contributions were generated from Figure III.2(a). A third-order 10-quantum selective sequence requires $(4N)^2 = 1600$ subcycles (instead of $(2N)^2 = 400$ subcycles without suppression of zero-quantum). Equation (III.39) applies if $(2N)^{j^2/4+7/4}$ is replaced with $(4N)^{j^2/4+7/4}$ and N is replaced with 2N, since each symmetrized phase cycling now requires 4N subcycles.

The assumption of a Gaussian distribution of eigenvalues is no longer valid, since $\bar{\mathcal{H}}^{(0)}$ has only two nonzero matrix elements. Since $\bar{\mathcal{H}}^{(0)}$ is Hermitian, the two elements have the same magnitude $\frac{1}{2}$ R. The eigenvalues are $\pm \frac{1}{2}$ R, and 0 for all other states, because $\bar{\mathcal{H}}^{(0)}$ is traceless. Therefore

$$\|\bar{\mathcal{H}}^{(0)}{}_{t_c}\| = ((2^{-N})(2)(R^2/4))^{1/2} = R\ 2^{-(N+1)/2} \tag{III.48}$$

$$\|(\bar{\mathcal{H}}^{(0)}{}_{t_c})^2\| = ((2^{-N})(2)(R^4/16))^{1/2} = R^2 2^{-(N+3)/2} = 2^{(N-1)/2}\|\bar{\mathcal{H}}^{(0)}{}_{t_c}\|^2 \tag{III.49}$$

$$\|(\bar{\mathcal{H}}^{(0)}{}_{t_c})^3\| = ((2^{-N})(2)(R^6/64))^{1/2} = R^3 2^{-(N+5)/2} = 2^{(N-1)}\|\bar{\mathcal{H}}^{(0)}{}_{t_c}\|^3 \tag{III.50}$$

In the limit of convergence ($\|\bar{\mathcal{H}}^{(0)} t_c)^2\| \sim F(n)^{-1}$), the calculated selectivity of a third-order 10-quantum sequence with $\alpha = 1$, $K = 2^{2N-1}$ and $F(n) = 0.029$ (see equation (III.39)) is $S = 0.025$. However, $\|(\bar{\mathcal{H}}^{(0)} t_c)^2\|$ need not really be this large; all that is required in $Rt_c = \pi/2$, so $\|(\bar{\mathcal{H}}^{(0)} t_c)^2\| = .034$, a factor of 1400 smaller. When $\|(\bar{\mathcal{H}}^{(0)} t_c)^2\|$ has this value, then $S = 5.0 \times 10^4$.

The maximum gain G can be attained if the $4(2^N-2)$ non-N-quantum selective matrix elements that involve the $m = \pm N/2$ states transfer only a small fraction of $(I_z^2)_{M=\pm N/2}$ relative to the fraction transferred by the two N-quantum selective matrix elements. Since each selective matrix element is larger by a factor S, the intensity of the selected transition is larger by a factor S^2, and therefore

$$2\ S^2 \gg 4(2^N-2)$$

$$S^2 \gg 2^{N+1} \qquad \text{(III.51)}$$

is required which is satisfied in this example. It can be concluded that almost all the theoretical gain from an infinite-order selective sequence is attainable with a third-order selective sequence, and the potential gains in Table 1 should be approximately realizable.

Note that the theoretical maximum gain becomes more difficult to achieve as N increases, for several reasons. Equation (III.51) implies that the required selectivity for maximum gain is proportional to $(\sqrt{2})^N$, and therefore high-order selective sequences may be needed. However, the number of subcycles cannot be increased indefinitely, because each subcycle must have a minimum duration, and relaxation effects limit the maximum duration of the cycle to less than T_2.

Typically, $\|\mathcal{H}_{zz}\| \sim 10$ kHz and $T_2 \sim 100$ msec for liquid crystal systems, so no more than a few thousand subcycles would be possible; a third-order 18-quantum selective sequence that eliminates zero-quantum requires $(4n)^2 = 5184$ subcycles, and therefore, is impossible for many molecules. In addition, sample heating becomes a serious problem when many pulses are applied.

3.7 Conclusions

Average Hamiltonian theory has been extended to describe pulse sequences which produce coherences and population inversions between states with selected values of ΔM. Sequences have been constructed which are selective to arbitrarily high order in the Magnus expansion. These sequences theoretically provide large signal enhancements relative to nonselective techniques (for example, N-quantum selection in an N-spin system gives an enhancement of $N2^N$). Residual nonselective terms have been calculated, and convergence criteria for the expansions established. Thus, selective excitation should be a useful technique for increasing the number and size of molecules which can be studied by multiple-quantum NMR.

IV. Computer Calculations of Selectivity

4.1 Motivation

The theory of selective excitation, as derived in the last section, extends the formalisms of coherent averaging theory to describe pulse sequences which are inherently selective. The most important strength of this theory is its generality. For example, the pulse sequence represented schematically by Figure (III.2(a)) is zero-order nk-quantum selective, no matter what the Hamiltonian is, and no matter what the exact pulse sequence is for each subcycle. In addition, residual nonselective terms can be estimated for nonideal sequences, and this estimation only requires knowledge of $\|\mathcal{H}_D\|$ and the fraction of nk-quantum operators in the subcycle effective Hamiltonian. In practice this generality is extremely useful, because the most interesting applications of selective excitation are to molecules with unknown dipolar couplings and chemical shifts. Even if the individual couplings are unknown, $\|\mathcal{H}_D\|$ can be readily estimated from the width of the single-quantum spectrum; and if $\|\mathcal{H}_D \Delta\tau_p\| \gtrsim 1$, the fraction of nk-quantum operators can be approximately calculated (see sections 2.4 and 6.3).

However, this generality implies several important disadvantages. It was recognized in section 3.4 that even an infinite-order nk-quantum selective sequence (which would require an infinite number of pulses!) need not produce any nk-quantum coherences and that a lower limit must be imposed on the cycle time if high-quantum operators are desired. Even if this requirement is met, an unfortunate choice of pulse sequence parameters might produce a subcycle effective Hamiltonian $\mathcal{H}_o$ with a vanishingly small fraction of nk-quantum operators. $\mathcal{H}_o$ cannot be

calculated without prior knowledge of the coupling constants, no matter what the exact sequence is, because bilinear couplings are required to generate multiple-quantum coherences. Therefore, appropriate lengths for delays [such as $\Delta\tau_p'$ in Figure (III.4(a))] can only be estimated, not calculated exactly.

In addition, any calculation involving coherent averaging theory must be treated with caution unless convergence of the Magnus expansion can be shown. When convergence is questionable, the results can be completely wrong. As an example, consider the two sequences illustrated schematically in Figure (IV.1). Figure (IV.1(a)) is a zero-order 2k-quantum selective sequence repeated twice; the second sequence is first-order 2k-quantum selective, and consists of two phase cycles (or one phase cycle and symmetrization). The effective Hamiltonian for the first two subcycles can be written as $\mathcal{H}_e + \varepsilon\mathcal{H}_\sigma$, where $\mathcal{H}_e$ is 2k-quantum selective and $\mathcal{H}_\sigma$ is non-2k-quantum selective (i.e., contains only odd-quantum operators) and $\varepsilon << 1$ is assumed. The exact propagator for the first sequence is then $(\exp(-i(\mathcal{H}_e + \varepsilon\mathcal{H}_\sigma)(2\Delta\tau_p)))^2$. The effective Hamiltonian for the third and fourth subcycles of the second sequence is $\mathcal{H}_e - \varepsilon\mathcal{H}_\sigma$, since this half of the sequence is related to the first half by a phase shift of π; therefore the exact propagator for the second sequence is

$$\exp(-i(\mathcal{H}_e + \varepsilon\mathcal{H}_\sigma)2\Delta\tau_p)\ \exp(-i(\mathcal{H}_e - \varepsilon\mathcal{H}_\sigma)2\Delta\tau_p) \qquad \text{(IV.1)}$$

Intuitively, one might expect the second sequence to always be superior to the first, since it is selective to higher order in the average Hamiltonian expansion. Equivalently, expansion of the

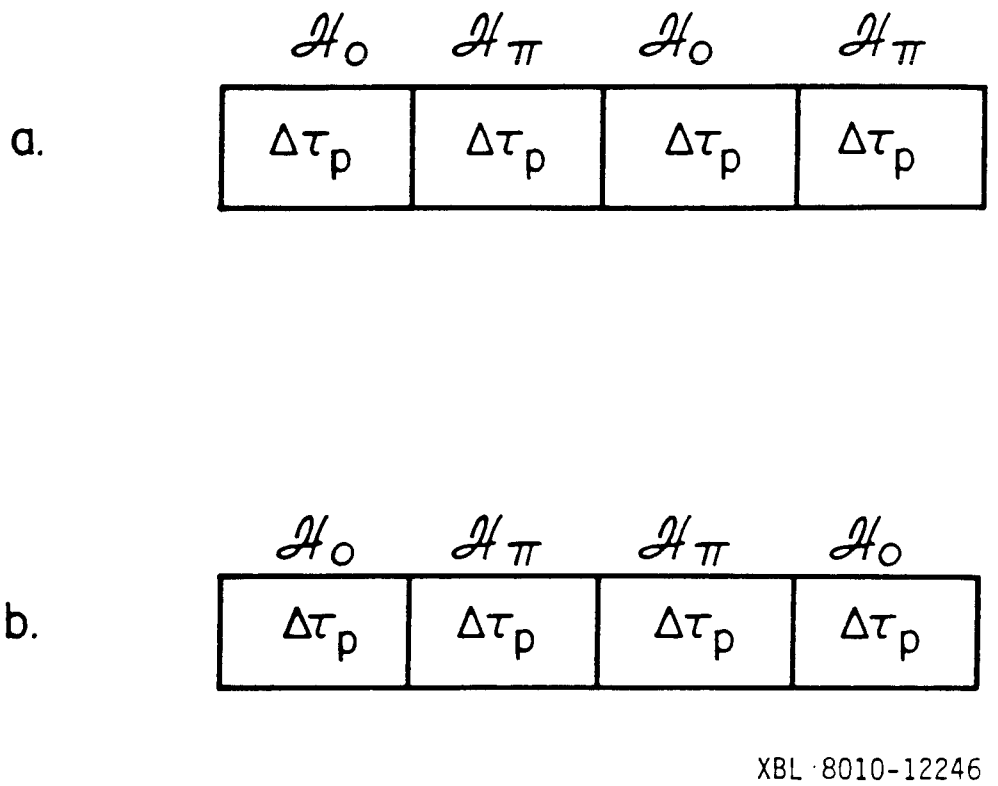

XBL 8010-12246

Figure IV.1 Two pulse sequences which illustrate that average Hamiltonian theory must be used with caution. Part b) is first-order 2k-quantum selective, and part a) is zero-order 2k-quantum selective. The sequence in part b) is more selective if $\Delta\tau_p$ is small. The sequence in part a) is more selective if $\Delta\tau_p$ is large (see text).

exponentials in powers of $\Delta\tau_p$ gives $U = 1-i(4\Delta\tau_p)(\mathcal{H}_e+\varepsilon\mathcal{H}_\sigma) + O(\Delta\tau_p^2)$ for the first sequence, and $U = 1-i(4\Delta\tau_p)(\mathcal{H}_e) + O(\Delta\tau_p^2)$ for the second sequence. However, when $\|\mathcal{H}_e\Delta\tau_p\|$ is large, expansion in powers of $\Delta\tau_p$ is invalid. As long as $\varepsilon << 1$, a different expansion can be used (see Appendix E):

$$\exp(A+\varepsilon B)_{jk} = (\exp(A))_{jj}\ \delta_{jk} + \varepsilon B_{jk}\left(\frac{\exp(A)_{jj}-\exp(A)_{kk}}{A_{jj}-A_{kk}}\right) + O(\varepsilon^2)$$

A and B are both written in a basis where A is diagonal. Using this expansion one finds

$$(\exp(-i(\mathcal{H}_e+\varepsilon\mathcal{H}_\sigma)(2\Delta\tau_p))^2)_{jk} \sim \exp(-i\mathcal{H}_e 4\Delta\tau_p)_{jj}\ \delta_{jk}$$

$$+ \varepsilon(\mathcal{H}_\sigma)_{jk}\left(\frac{\{\exp(-i\mathcal{H}_e(4\Delta\tau_p))_{jj} - \exp(-i\mathcal{H}_e(4\Delta\tau_p))_{kk}\}}{(\mathcal{H}_e)_{jj} - (\mathcal{H}_e)_{kk}}\right) \qquad \text{(IV.2)}$$

$$\exp(-i(\mathcal{H}_e+\varepsilon\mathcal{H}_\sigma)(2\Delta\tau_p))\ \exp(-i(\mathcal{H}_e-\varepsilon\mathcal{H}_\sigma)(2\Delta\tau_p)) \sim \exp(-i\mathcal{H}_e 4\Delta\tau_p)_{jj}\ \delta_{jk}$$

$$-\varepsilon(\mathcal{H}_\sigma)_{jk}\left(\frac{\{\exp(-i\mathcal{H}_e(2\Delta\tau_p))_{jj} - \exp(-i\mathcal{H}_e(2\Delta\tau_p))_{kk})^2\}}{(\mathcal{H}_e)_{jj} - (\mathcal{H}_e)_{kk}}\right) \qquad \text{(IV.3)}$$

As expected, the first nonselective term in equation (IV.2) is proportional to $\Delta\tau_p$ and the first nonselective term in equation (IV.3) is proportional to $(\Delta\tau_p)^2$, so when $\Delta\tau_p$ is small the first-order sequence is superior. When $\Delta\tau_p$ is large, however, $\exp(-i\mathcal{H}_e(2\Delta\tau_p))_{jj}$ and $\exp(-i\mathcal{H}_e(4\Delta\tau_p))_{jj}$ are essentially random numbers of magnitude 1; thus, the root-mean-squared value of the term in brackets is $\sqrt{2}$ in equation (IV.2) and 2 in equation (IV.3). Therefore the first-order

sequence is expected to actually be worse than the zero-order sequence for large $\Delta\tau_p$, where the average Hamiltonian calculation does not converge.

Convergence criteria were discussed at length in section 3.6, and reasonable guidelines were proposed. Nevertheless, it is useful to confirm the selectivity calculations by a totally independent technique, because the convergence problem is so important. For a small enough spin system with a given Hamiltonian, the exact effect of any pulse sequence can be calculated by solving the density matrix equation of motion on a computer. Since no approximations are required, such a calculation allows rigorous testing of the important concepts of the theory of selectivity, and in addition can show where convergence actually begins to be questionable. For this reason, computer studies were initiated. The results, to be described in the next several sections, verify the calculations of chapter III but give additional insight into the design of practical experimental sequences.

4.2 Programming Details

A general program for testing selective sequences is given in Appendix B. The propagator for any pulse sequence can be calculated by multiplying together the propagators for each individual pulse or delay. In a system with N spins-1/2, each propagator can be written as a $2^N \times 2^N$ matrix. Multiplying together two matrices of this size requires 2^{3N} individual multiplications, so the number of matrix multiplications should be kept to a minimum. One way to do this is to use the simple relationship (III.19) between the propagators for different subcycles. Thus, once the propagator U_0 for the first

subcycle has been calculated, the propagator for any other subcycle can be calculated with 2^{2N} multiplications, no matter how many pulses the subcycle contains. Similarly, calculations for high-order sequences involving several phase cycles can be simplified by calculating the propagator after the first phase cycle, and using (III.19) on it.

U_0 can only be calculated exactly if $\mathcal{H}_z$ is given. For some of the calculations, particularly those given in section 4.5, coupling constants are generated. In other calculations the generality of the theory of chapter III is retained by assuming a form for $\mathcal{H}_o$, usually one that has random matrix elements of roughly equal magnitude everywhere, subject only to the constraint that the matrix be Hermitian.

All computing was done on a VAX 11/70 system with 2.5 M byte memory and floating point accelerator hardware. On this system, for example, calculations for a third-order 4k-quantum selective sequence on an unsymmetrical four-spin system with 125 different values for the cycle time required roughly 30 minutes of processor time; thus an unsymmetrical five-spin system would require roughly four hours, and few tests with systems of this size were done. Benzene was extensively studied, because its A_1 manifold has only 13 states, and several different random four-spin and five-spin systems were also used. Many of the subroutines used were originally developed by Jim Murdoch for calculations with nonselective sequences.[66]

4.3 Zero-Order Selective Sequences.

4.3.1 Nk-Quantum Selection

4.3.1.1 Propagator Selectivity and Coherence Selectivity

As discussed in section 3.5.1, a Nk-quantum selective sequence

in a N-spin system creates an effective two-level system, since it will only connect the states with $|M| = N/2$. The average Hamiltonian (and, by implication, the propagator) can also have zero-quantum operators connecting other eigenstates, but these operators commute with I_z, so if that is the initial condition no zero-quantum coherences can develop.

Figure (IV.2-3) show the effects of a zero-order 4k-quantum selective sequence (Figure (III.2a)) on a four-spin system, starting with a random $\mathcal{H}_o$ and U_o. The results from five random $\mathcal{H}_o$ operators were averaged together. Figure (IV.2) shows the ratio of a typical 4k-quantum selective to a typical non-4k-quantum selective matrix element of the propagator. This will be called the propagator selectivity, to distinguish it from the selectivity defined in section 3.6, which is not identical because that definition is a ratio of matrix elements of the effective Hamiltonian. As expected, the propagator selectivity is proportional to $(t_c)^{-1}$ for small t_c, which implies that the sequence does in fact have a nonzero $(\bar{\mathcal{H}}^{(1)})_{nns}$. When t_c is large, the propagator selectivity is essentially unity. The criterion in equation (III.51) for acceptable selectivity ($S^2 >> 2^{N+1} - 1$) is violated when $S \sim 5.6$. This occurs when $\|\mathcal{H}_o t_c\| \sim 1.5$. Of the 256 matrix elements, 72 are 4k-quantum selective (16 populations, 2 four-quantum operators and 54 zero-quantum operators), so the relation $\|\bar{\mathcal{H}}^{(0)} t_c\|^2 = k\|\bar{\mathcal{H}}^{(0)}\|^2$ (see section 3.4.1) gives $\|\bar{\mathcal{H}}^{(0)} t_c\| \sim 0.8$ ($\alpha \sim 1$ by construction of $\mathcal{H}_o$).

The general convergence criterion $\|(\bar{\mathcal{H}}^{(0)} t_c)^2\| << F(n)^{-1}$ of equation (III.38) applies directly only to high-order symmetrized sequences.

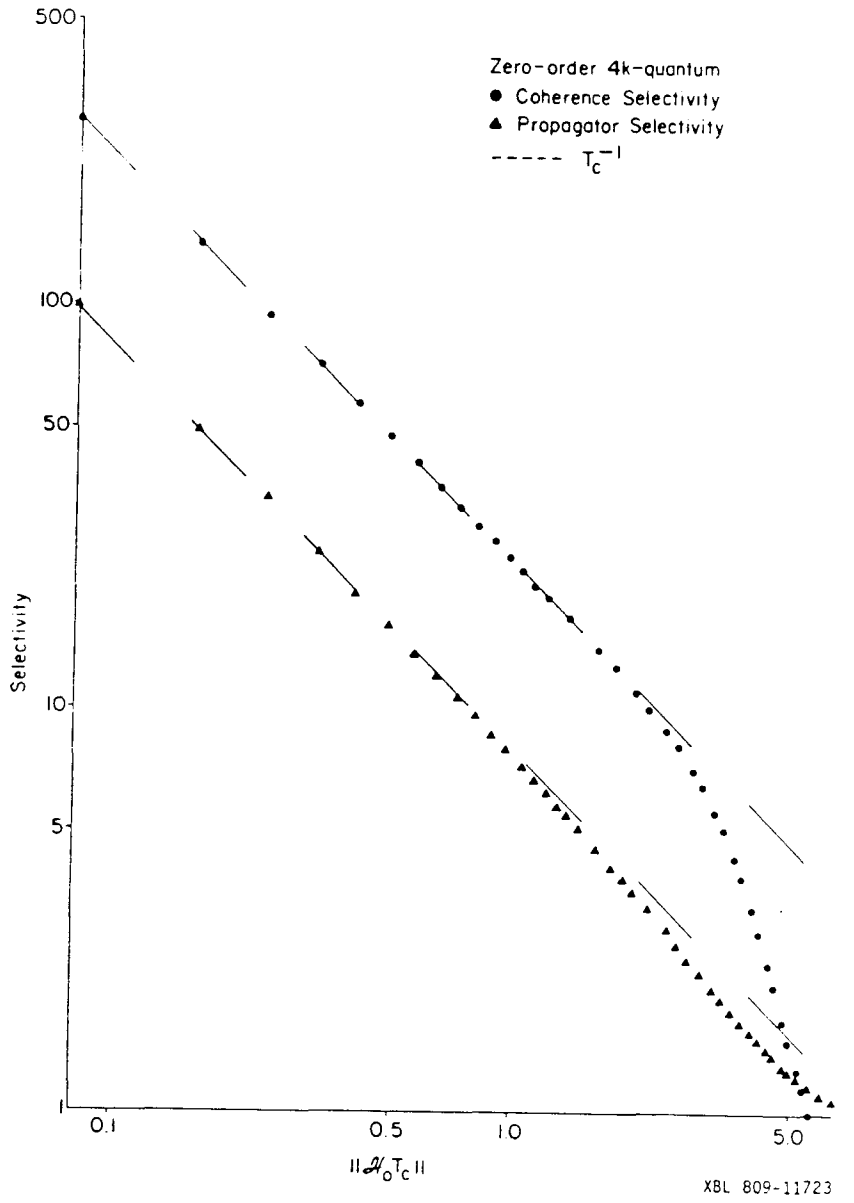

Figure IV.2. The propagator selectivity and coherence selectivity of one cycle of a zero-order 4k-quantum selective sequence. Both selectivities are proportional to T_c^{-1} for short cycle times, which indicates that $\bar{\mathcal{R}}^{(1)}$ does not vanish.

However, $(\bar{\mathcal{H}}^{(1)})_{nns}$ can be estimated using Theorem II of section 3.2.1:

$$(\bar{\mathcal{H}}^{(1)})_{nns} = (-\frac{1}{t_c}\int_0^{t_c} dt_2 \int_0^{t_2} dt_1 \; \mathcal{H}_{\phi(t_2)} \; \mathcal{H}_{\phi(t_1)})_{nns} \qquad \text{(IV.4)}$$

Since there are only four subintervals, there are only ten operators $\mathcal{H}_{\phi(t_2)}\mathcal{H}_{\phi(t_1)}$, and the sum with $\phi(t_2) = \phi(t_1)$ is 4k-quantum selective. If matrix elements for the remaining 6 operators add randomly

$$\|\bar{\mathcal{H}}^{(1)}{}_{t_c}\|_{nns} \sim \sqrt{6}\,\langle\|\mathcal{H}_{\phi(t_2)}\mathcal{H}_{\phi(t_1)}\Delta\tau_p^2\|\rangle_{nns}$$

$$\sim \frac{\sqrt{6}}{16}\;\|\mathcal{H}_{o\,t_c}\|^2 \sim .54\;\|\bar{\mathcal{H}}^{(0)}{}_{t_c}\|^2 \qquad \text{(IV.5)}$$

A typical matrix element of $\bar{\mathcal{H}}^{(0)}$ is 5.6 times larger than a typical matrix element of $\|\bar{\mathcal{H}}^{(1)}\|_{nns}$ when $\|\bar{\mathcal{H}}^{(1)}\|_{nns}/\|\bar{\mathcal{H}}^{(0)}\| \sim ((256-72)/72)^{1/2}$ $(5.6)^{-1} = 0.29$, and plugging this into equation (IV.5) gives $\|\bar{\mathcal{H}}^{(0)}{}_{t_c}\|$ ~ 0.53. The agreement with computer calculations is quite good, particularly since $\bar{\mathcal{H}}^{(1)}$ also has some 4k-quantum selective terms, which implies that this estimate of the critical value of $\|\bar{\mathcal{H}}^{(0)}{}_{t_c}\|$ should be slightly low.

Figure IV.2 also shows the ratio of the magnitude of a typical four-quantum coherence in the final density matrix to the magnitude of a typical one-, two-, or three-quantum coherence, as a function of the cycle time. This ratio will be called the coherence selectivity. The coherence selectivity is experimentally observable if the signal-to-noise ratio is sufficiently good, so it is more useful than the propagator selectivity. However, it cannot be readily calculated from coherent averaging theory. Even if the effective Hamiltonian $\bar{\mathcal{H}}$ is

completely known, the coherence selectivity requires calculation of $\exp(-i\bar{\mathcal{H}}t_c)I_z \exp(i\bar{\mathcal{H}}t_c)$, which is difficult to evaluate by hand for any reasonably sized system unless $\|\bar{\mathcal{H}}t_c\|$ is small.

Fortunately, the coherence selectivity is usually larger than the selectivity of the effective Hamiltonian. This can be readily seen by expanding ρ in powers of t_c, as in section 2.3:

$$\rho = I_z - it_c[\bar{\mathcal{H}},I_z] + \sigma(t_c^{\,2}) \tag{IV.5}$$

$$[\bar{\mathcal{H}},I_z]_{jk} = (\bar{\mathcal{H}})_{jk}(M_j-M_k) \tag{IV.6}$$

M_j-M_k is larger for the four-quantum transition than for any other transition, so the coherence selectivity is strengthened in the lowest order term. In fact, since there are 8 three-quantum transitions, 28 two-quantum transitions, and 56 one-quantum transitions, $\langle\Delta M\rangle_{nns} = 1.48$, and the coherence selectivity should be roughly 2.7 times larger than the effective Hamiltonian selectivity on the average; in Figure IV.2 the ratio for small t_c is 2.95, but this value depends on the choice of matrix elements for U_o. Thus, since the selectivity from coherent averaging theory provides an underestimate for the coherence selectivity, it is still a useful test for convergence.

4.3.1.2 Signal Intensities

Figure IV.3 shows the observable signal intensity for the four-quantum transition (the square of the coherence magnitude, from equation (II.34)) as a function of the cycle time, in units of β. (For simplicity $C = -1$ is assumed in equation (II.20)). The total available signal $\beta\mathrm{Tr}(I_z^{\,2}) = 16\,\beta$, and there are 256 matrix elements,

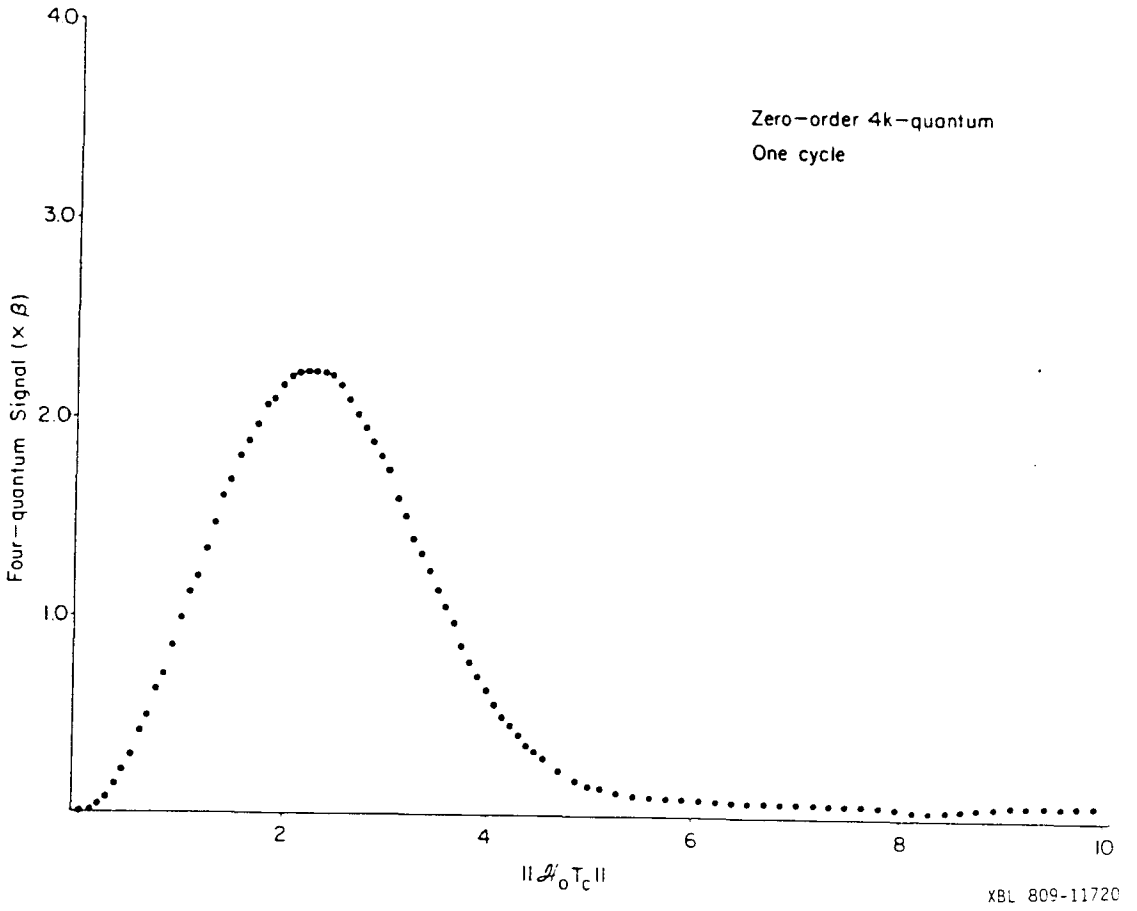

Figure IV.3. The signal produced by one cycle of a zero-order 4k-quantum selective sequence as a function of the cycle time. The maximum attained signal is 2.22 β, which represents a gain of 36 relative to nonselective excitation.

so the expectation value of the signal from nonselective excitation is .0625 β. The maximum possible value for the four-quantum signal is 4 β, from equations (III.29-33), so the possible gain is a factor of 64. The largest signal from Figure IV.3, however, is 2.22 when $\|\bar{\mathcal{H}}^{(0)} t_c\| =$ 2.1. At the peak, the propagator selectivity is only 3.40, so the selectivity disappears before the true maximum can be reached. This is not surprising, since the first maximum corresponds to a selective 90° pulse between the two extreme levels, so the coefficient of the four-quantum operator in $\bar{\mathcal{H}}^{(0)}$ must be at least $\pi/4$ (see equation (III.32) and section 3.5.1). We then expect $\|\bar{\mathcal{H}}^{(0)} t_c\| \gtrsim 1.66$ if all 72 4k-quantum operators are pumped equally, and $\|\mathcal{H}_o t_c\| \sim 3.14$. This is well outside of the expected range of convergence; in fact, the propagator selectivity is only 1.74 for this cycle time.

Several approaches can be taken to improve the selectivity. The first, and simplest, is to decrease the cycle time and increase the number of cycles. For convenience define T_c as the number of cycles times the cycle time; T_c is then the total duration. If two cycles are used, for example, $\|\mathcal{H}_o T_c\| \sim 3.14$ for the whole sequence when $\|\mathcal{H}_o t_c\| \sim 1.57$ for each cycle. Thus larger signals should be attainable, and this is illustrated in Figure IV.4; the maximum is now 3.19 at $\|\mathcal{H}_o T_c\| = 2.75$. The signal can be further increased by adding more cycles. With 16 cycles, the signal follows a $\sin^2$ curve for several oscillations, as expected from equation (II.36), and the theoretical maximum gain is achieved when $\|\mathcal{H}_o T_c\| = 3.2$, as shown in Figure IV.5; the oscillations die away as the selectivity disappears. If enough cycles are applied, the oscillations can be prolonged indefinitely.

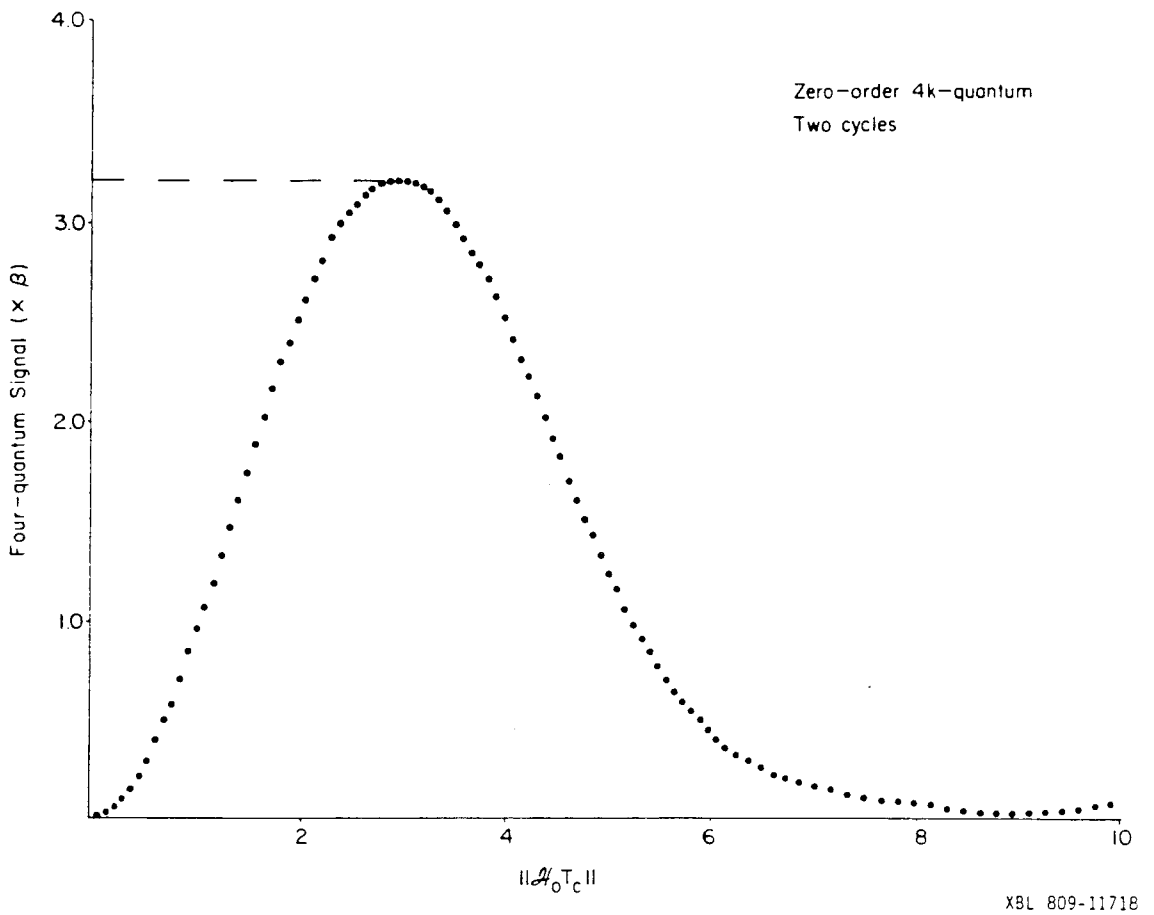

Figure IV.4. The signal produced by two cycles of a zero-order 4k-quantum selective sequence. The maximum attained signal is 3.19 β, which represents a gain of 51 relative to nonselective excitation.

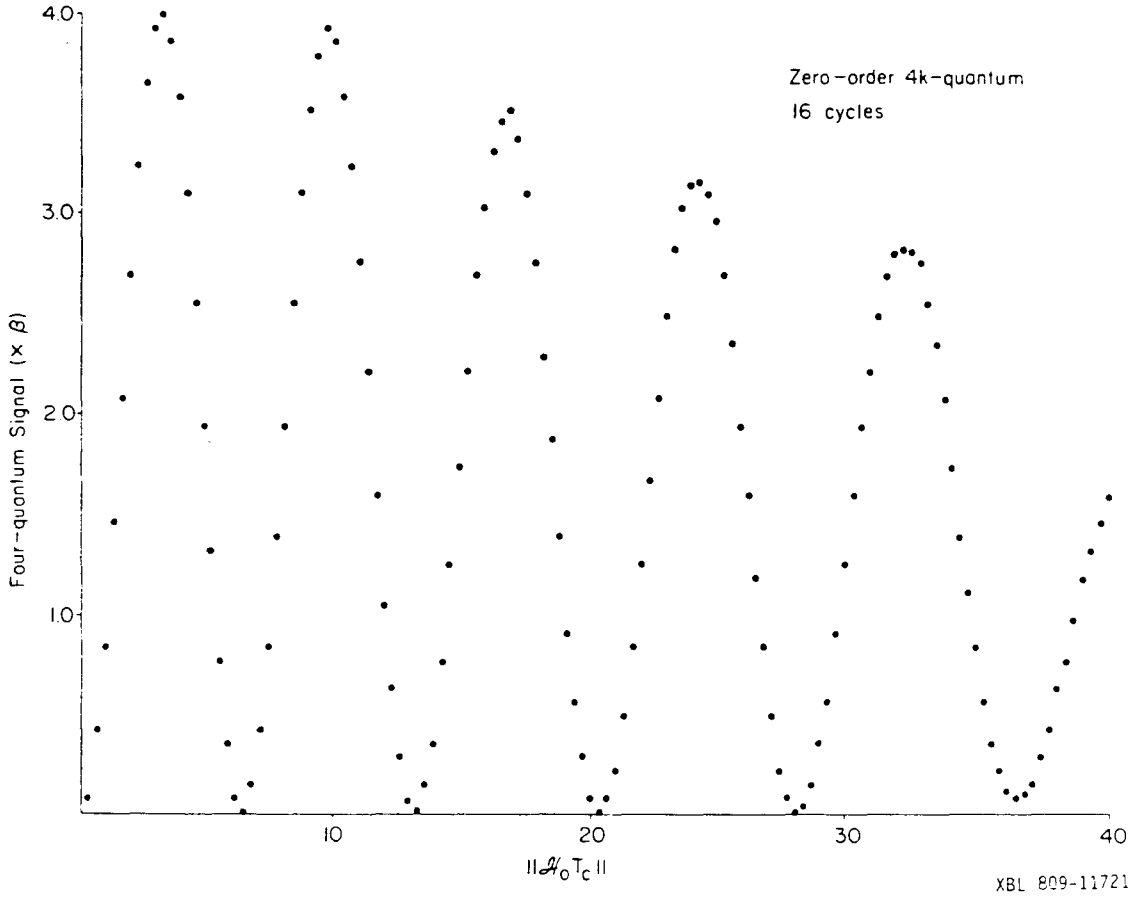

Figure IV.5 The signal produced by 16 cycles of a zero-order 4k-quantum selective sequence. The signal follows a $\sin^2$ pattern for several oscillations, and reaches the theoretical maximum of 4.00 for a gain of 64.

Any arrangement of the four phases is equivalent as far as $\bar{\mathcal{H}}^{(0)}$ is concerned. However, some arrangements might be superior in cancelling the largest terms in $(\bar{\mathcal{H}}^{(1)})_{nns}$. All of the 24 possible permutations can be related to one of the sequences (0, 90, 180, 270), (0, 180, 90, 270), or (0, 90, 279, 180), by adding a constant amount to each phase or reversing the order of the phases; thus only these three groups need be analyzed. Table IV.1 gives the maximum four-quantum signal from one cycle of zero-order 4k-quantum selection for each of these combinations. For all of these calculations $\mathcal{H}_o$ had equal matrix elements everywhere; the different runs correspond to different sets of random phases for these elements. The maximum signal is 2.22 ± 0.18 for (0, 90, 180, 270), 1.72 ± 0.09 for (0, 180, 90, 270), and 1.98 ± 0.14 for (0, 90, 270, 180). However, no single permutation is superior for all five sets of couplings, and these small differences have no practical significance. It can be concluded that there is no a priori reason to prefer any particular permutation.

4.3.2 Lower-Quantum Selection

The N-quantum transition in a N-spin system has no dipolar information, as explained in section 1.4. The (N-1)-quantum and lower-quantum transitions are therefore more important. The potential signal gain from selection is smaller (see equation (III.34)) but still substantial; for (N-1)-quantum selection, it is roughly 2^N if $N >> 1$.

As an example, Figure IV.6 shows the signal obtainable from 5k-quantum selection or 4k-quantum selection on a five-spin system. The five-quantum signal follows the normal $\sin^2$ pattern of Nk-quantum selection in a N-spin system; the maximum signal is equal to the

Table IV.1 Effect of Permutation of Phases on Zero-Order 4k-Quantum Selection.

	Maximum Four-Quantum Signal		
Trial #	(0,90,180,270)	(0,180,90,270)	(0,90,270,180)
1	1.839	1.558	1.837
2	1.979	1.913	2.293
3	2.871	1.608	2.201
4	1.910	2.020	2.128
5	2.521	1.508	1.444
	2.22 ± 0.18	1.72 ± 0.09	1.98 ± 0.14

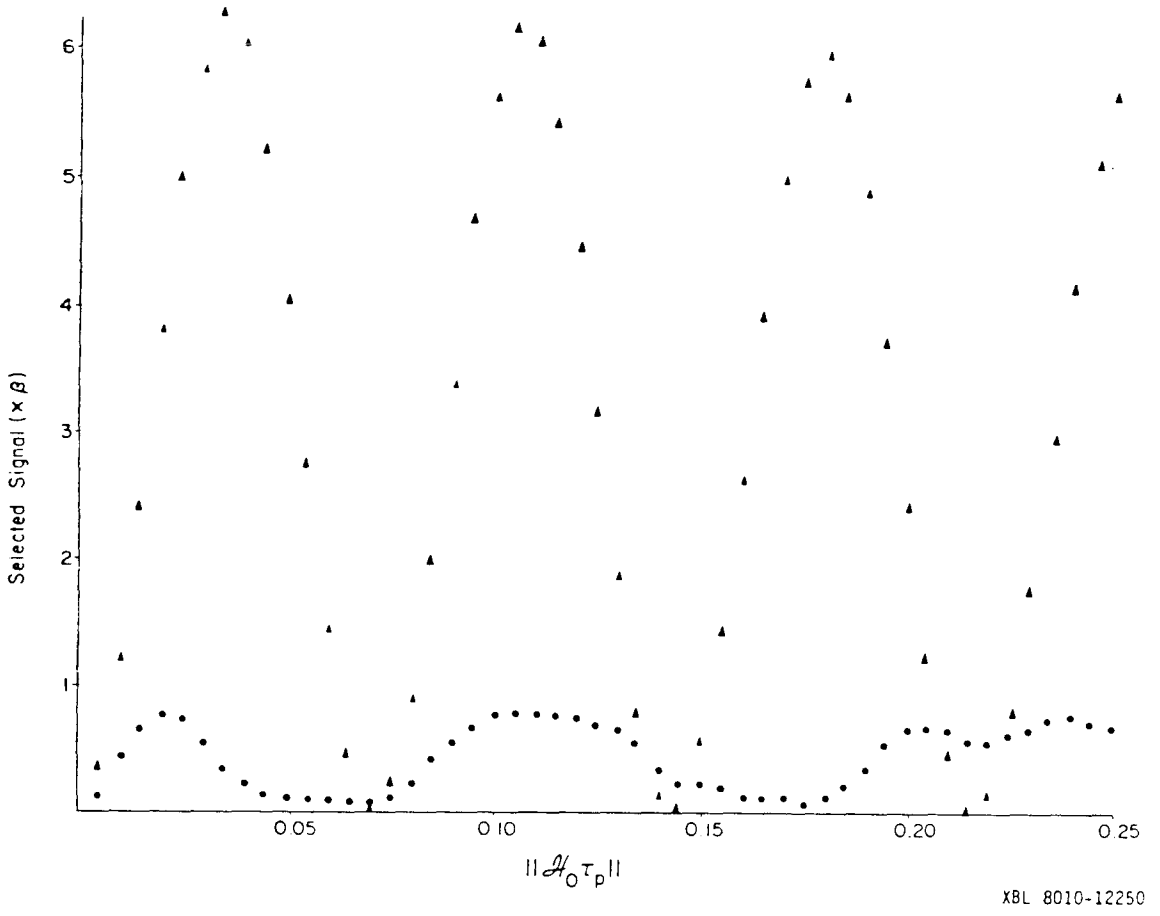

Figure IV.6 The signal produced by 4k-quantum selection (circles) or 5k-quantum selection (triangles) on a 5-spin system. The gain for 5k-quantum selection is much larger than the gain for 4k-quantum selection.

value of βI_z^2 for the extreme states, which is 6.25 β; and the gain is $N2^N = 160$. The gain is much smaller for 4k-quantum selection, because zero-quantum coherences cannot be completely suppressed, as explained in section 3.5.1. The maximum signal attained from this sequence is 0.80, which corresponds to a gain of 20.5. The average signal from $\|\mathcal{H}_o t_c\| = 10$ to $\|\mathcal{H}_o t_c\| = 20$ is 0.40, for a gain of 10.3. The estimated gain from (III.34) is 14.5.

Figure IV.7 shows the signal obtainable from 6k-quantum or 4k-quantum selection in the benzene A_1 manifold. These results will be compared in Chapter V to actual experiments. The maximum observed gain for the four-quantum signal is 7.50, when $\|\mathcal{H}_o t_c\| = 1.92$. This selective sequence was applied to five different random $\mathcal{H}_o$ operators, and does not correspond to any particular arrangement of pulses and delays, so these values are best interpreted as estimates. Thus, if the actual pulse sequence for $\mathcal{H}_o$ is the sequence of Figure III.2(a), the optimum value for $\|\mathcal{H}_z \Delta\tau_p'\|$ is on the order of 0.5 if one cycle is applied, 0.25 if 2 cycles are applied, and so forth; this would make $\|\mathcal{H}_o T_c\| \sim 2$.

4.4 Higher-Order Selective Sequences

4.4.1 Nk-Quantum Selection

Another approach to improving selectivity is to use high-order selective sequences, as explained in section 3.3.2. Two different principles (nesting phase cycles and symmetrizing phase cycles) were used to design j-order nk-quantum selective sequences for arbitrary j; if j is odd, such sequences require $(2n)^{(j+1)/2}$ subcycles. Thus, the higher the order of selectivity, the longer the cycle time. This

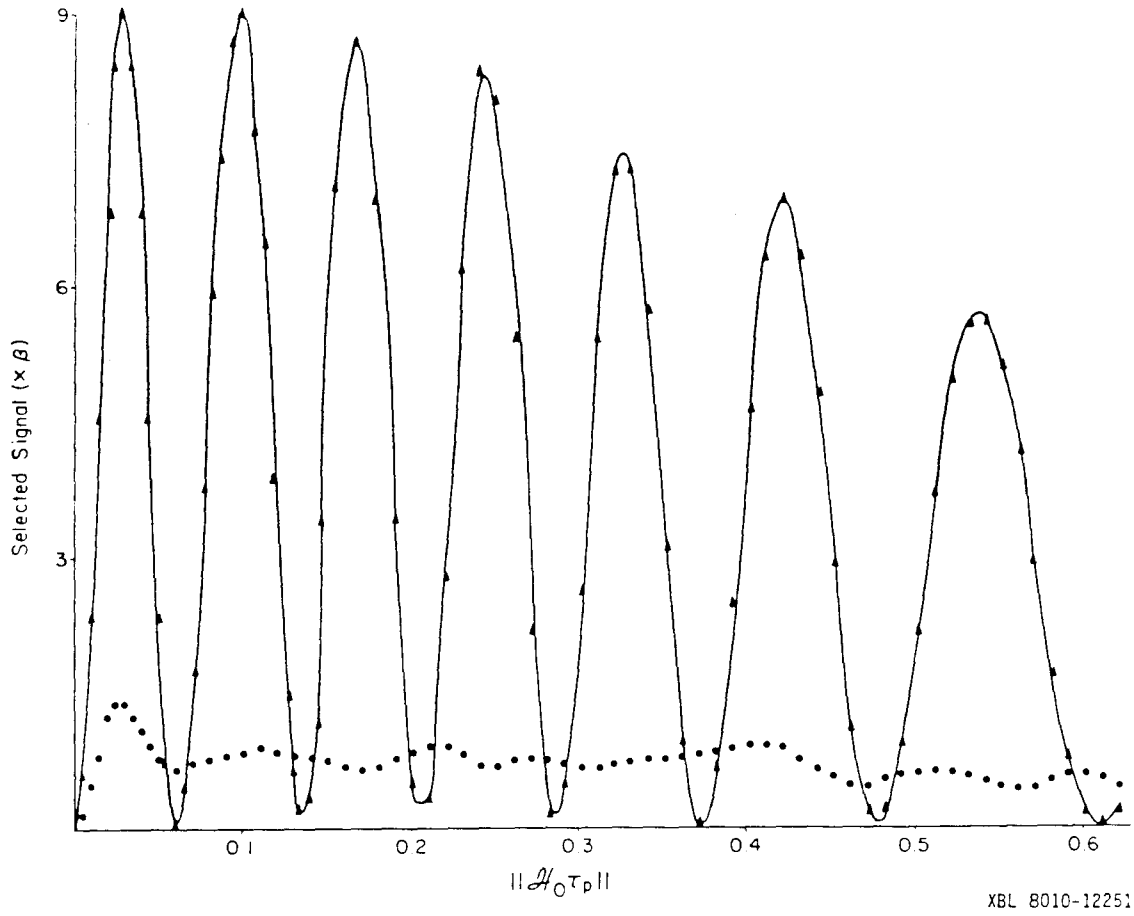

Figure IV.7 The signal produced by 4k-quantum selection (circles) or 6k-quantum selection (triangles) on the A_1 manifold of oriented benzene (13 states; see Figure V.1 for the distribution). The maximum 6-quantum enhancement is a factor of 47.5. The maximum 4-quantum enhancement is a factor of 7.50.

makes average Hamiltonian calculations much more complicated. For example, a third-order 4k-quantum selective sequence has a cycle time 16 times longer than a zero-order 4k-quantum sequence, so it is not obvious that $\|\bar{\mathcal{H}}^{(4)} t_c\|_{nns}$ for the former is always smaller than $\|\bar{\mathcal{H}}^{(1)} t_c\|_{nns}$ is for the latter. In fact, it was shown in section 4.1 that high-order selection is useless if t_c is large. If t_c is small, however, higher-order selection must be beneficial; in this example, the first nonselective operator in the propagator for the zero-order sequence is proportional to t_c^2, but the first nonselective operator for the third-order sequence is proportional to t_c^5. Thus an important question is how large t_c can be before high-order selection becomes useless.

Figure IV.8 compares the propagator selectivity of two cycles of zero-order 5k-quantum selection with one cycle of first-order 4k-quantum selection. As expected the first-order sequence is far superior for short cycle times. At $\|\mathcal{H}_o T_c\| = 4.0$ the two curves cross, and for all later times the zero-order sequence is superior. However, the crossing point is about 25% larger than the theoretical position of the first maximum (see Figure IV.5), and the improved selectivity of the first-order sequence near that maximum produces a larger four-quantum signal, as shown in Figure IV.9.

For larger values of $\|\mathcal{H}_o T_c\|$ both the first-order and the repeated zero-order sequence have little selectivity, so the repeated zero-order sequence is never significantly superior. By contrast, Figure IV.10 shows the signal from a third-order 4k-quantum selective sequence. This should be compared with 16 cycles of a zero-order sequence, shown in Figure IV.7. Again the high-order sequence is much more selective

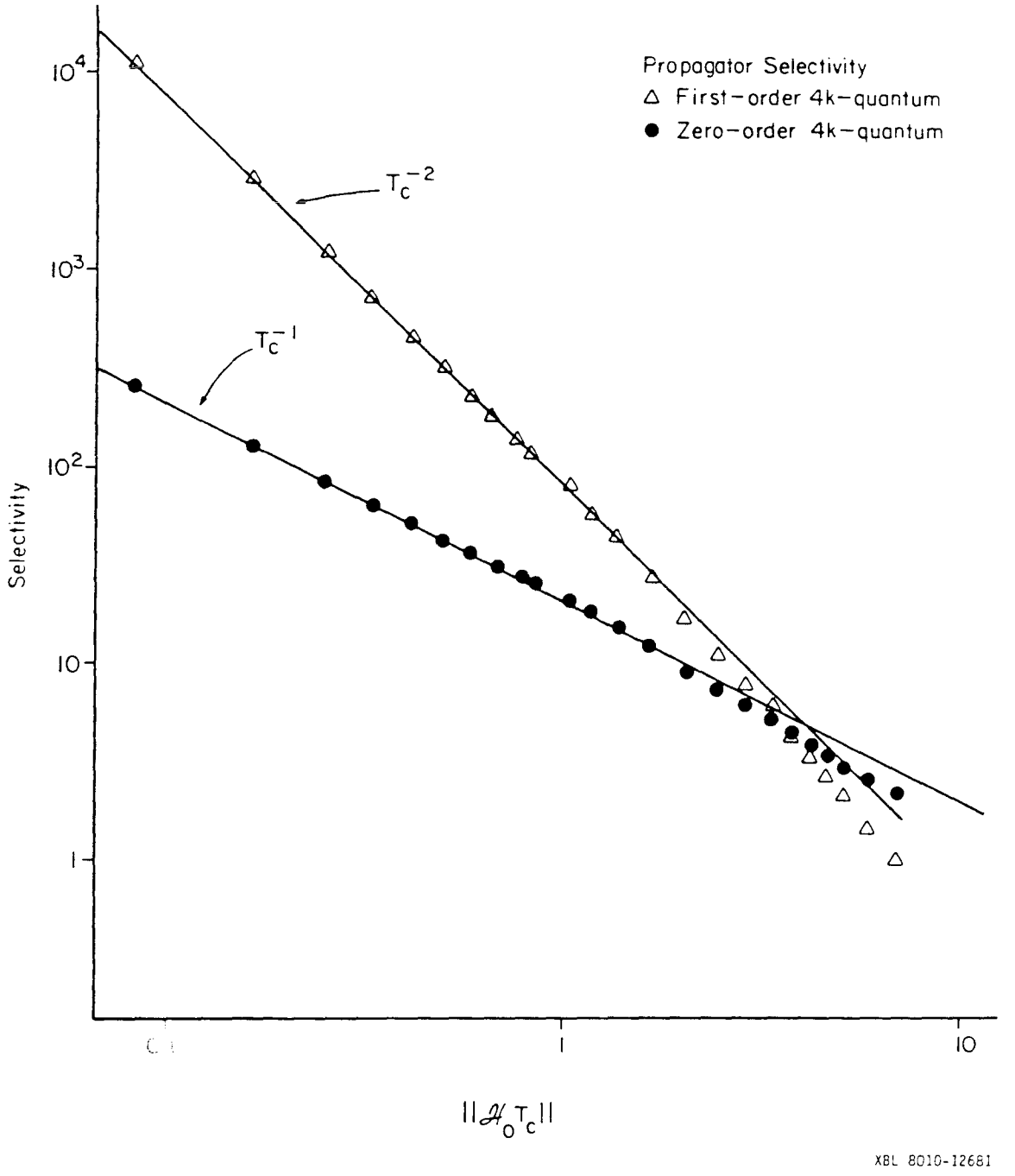

Figure IV.8 The propagator selectivity of two cycles of zero-order 4k-quantum selection, versus one cycle of first-order 4k-quantum selection. The first-order selection is superior for short cycle times.

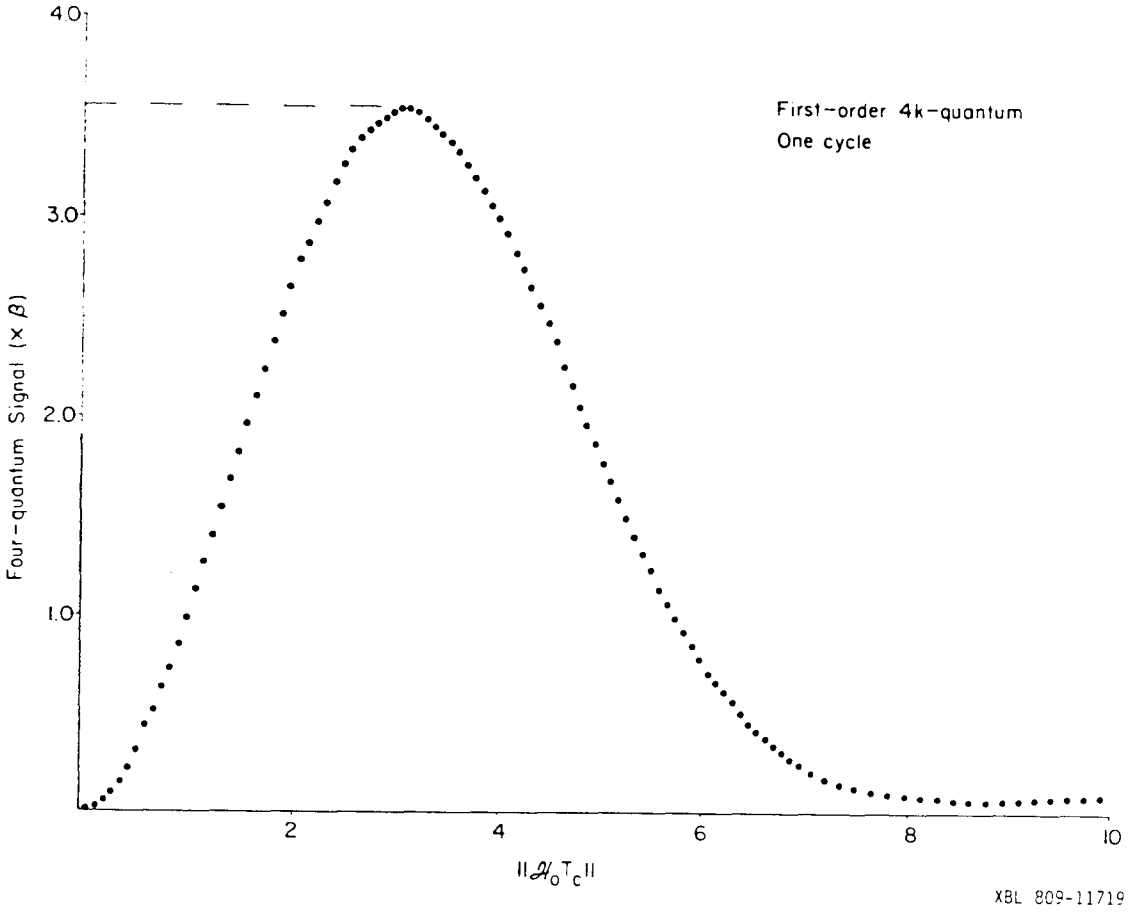

Figure IV.9 The signal produced by one cycle of a first-order 4k-quantum selective sequence. The selectivity is higher for this sequence in the region of the signal maximum than it was for two cycles of a zero-order sequence, so the maximum signal of 3.6 is larger.

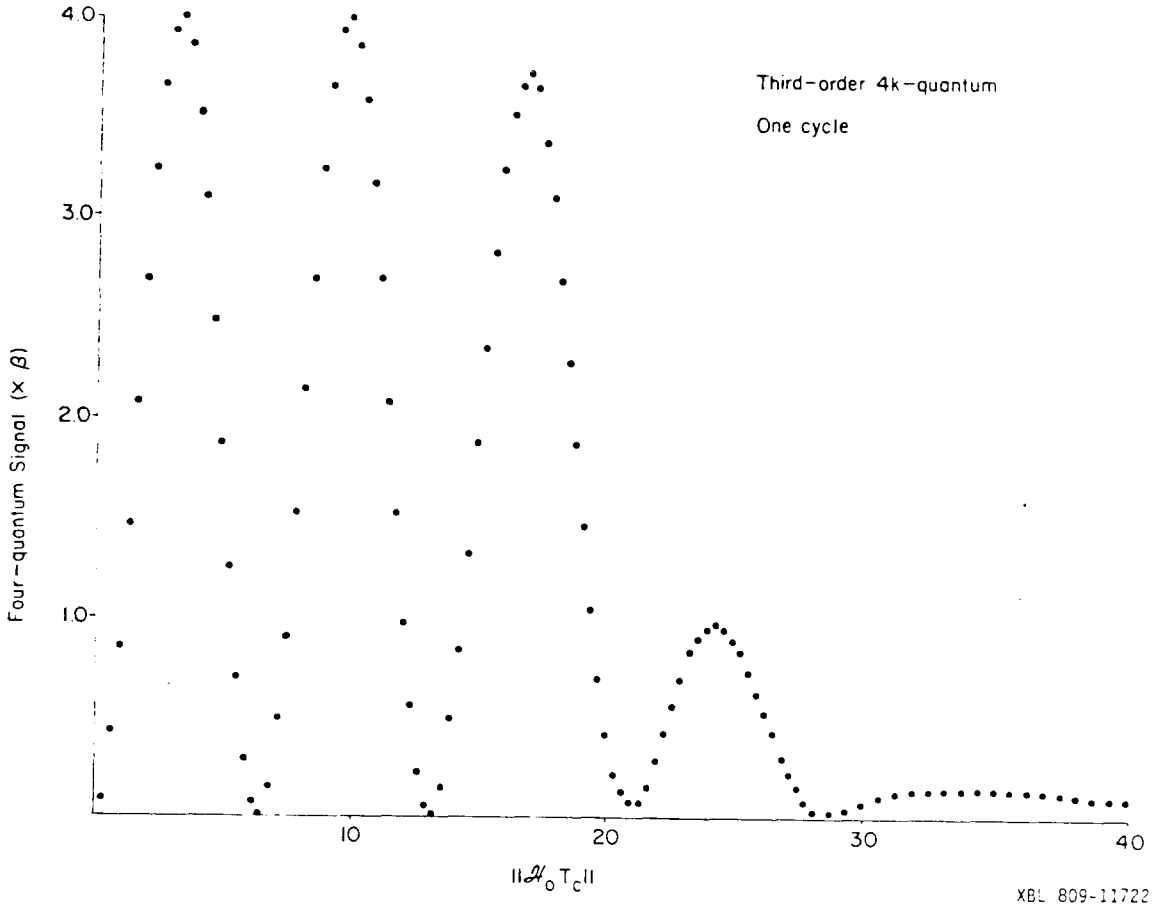

Figure IV.10 The signal produced by one cycle of third-order 4k-quantum selection. Comparison with Figure IV.5 (16 cycles of zero-order selection) shows that the high-order sequence is superior for short cycle times but inferior for long cycle times, as predicted in section 4.1.

for short cycle times; the selectivities are equal at 8.1 when $\|\mathcal{H}_o t_c\| =$ 14.7, and the zero-order sequence is superior after that. At the first maximum, the propagator selectivity of the third order sequence is 1103, compared to only 44 for the zero-order sequence. However, both of these numbers satisfy the criterion for maximum signal from equation (III.51), $S \gg 5.6$, so the signals are very nearly equal. At the second maximum the selectivities are 21.3 and 12.0, and these numbers are small enough to make the third-order sequence perceptibly better. At the third maximum the selectivities are almost equal. After the third maximum the selectivity of the third-order sequence dies away rapidly, but the repeated zero-order sequence remains partially selective for several oscillations.

Figure IV.11 shows the propagator selectivity of the third-order sequence, plotted on a log-log scale. For small values of t_c ($\|\mathcal{H}_o t_c\| \lesssim 5$) the selectivity is proportional to t_c^{-4} (the solid line in the figure) as expected when $\bar{\mathcal{H}}^{(4)}$ is the dominant nonselective term and $\bar{\mathcal{H}}^{(0)}$ is the dominant 4k-quantum selective term. The selectivity begins to deviate from the line around $\|\mathcal{H}_o t_c\| \sim 6$. The slope initially decreases, which must reflect another selective term, presumably $\bar{\mathcal{H}}^{(2)}$. In fact, the selectivity between $\|\mathcal{H}_o t_c\| = 10$ and $\|\mathcal{H}_o t_c\| = 20$ is proportional to t_c^{-2} (the dotted line in the figure), which would be expected if the dominant selective term were $\bar{\mathcal{H}}^{(2)}$. For $\|\mathcal{H}_o t_c\| > 20$ the selectivity falls off rapidly, which probably indicates that $\bar{\mathcal{H}}^{(6)}$ and higher-order non-selective terms cannot be neglected.

The convergence criterion $\|(\bar{\mathcal{H}}^{(0)} t_c)^2\| < F(n)^{-1}$ is equivalent to $\|\mathcal{H}_o t_c\| < 6.8$ if the eigenvalues have a Gaussian distribution. This

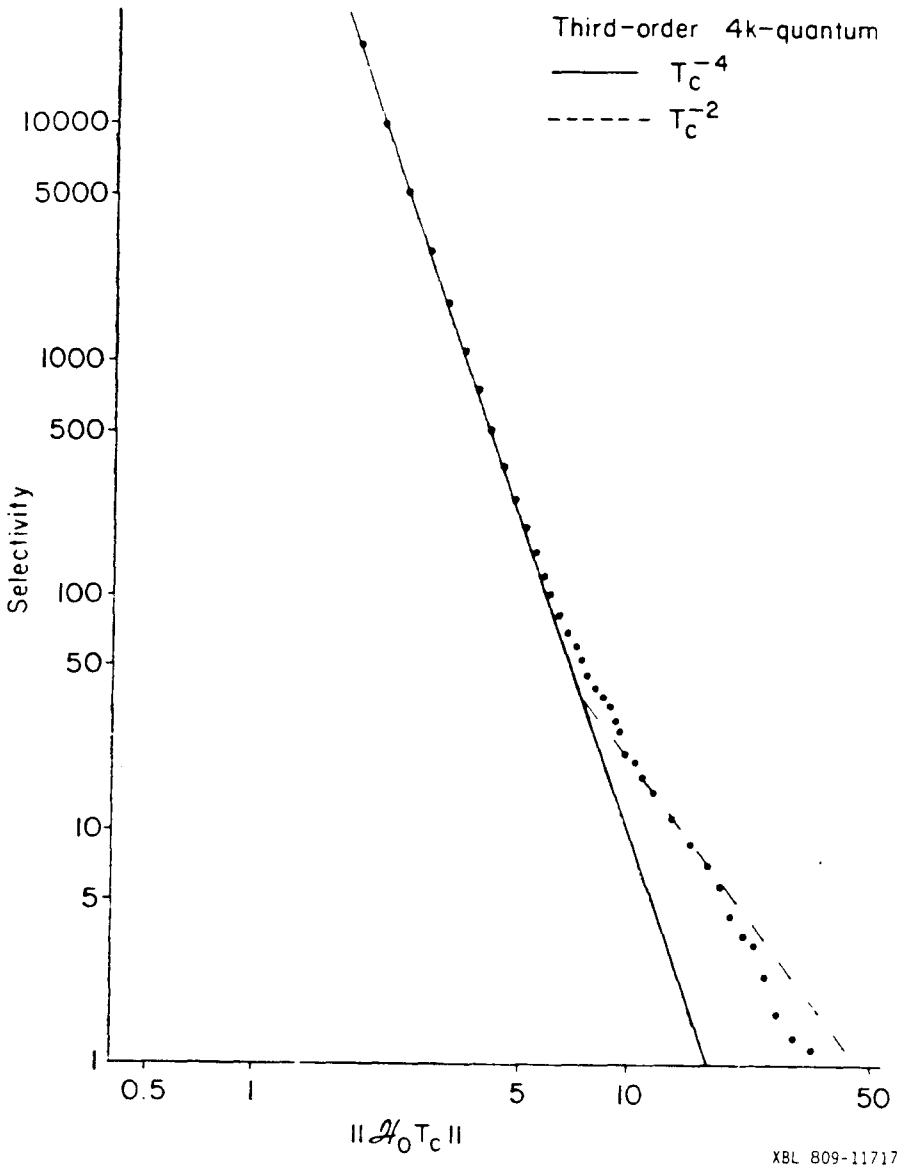

Figure IV.11 The propagator selectivity of a third-order 4k-quantum selective sequence. The selectivity is proportional to T_c^{-4} for short values of the cycle time. Deviations from this line occur in the region predicted by the convergence criteria of section 3.6.

was derived by finding the value of the cycle time which would make the first nns term from a j-order nk-quantum selective sequence (in this case, $\|\bar{\mathcal{H}}^{(4)}\|_{nns}$) equal to the first nns term of a (j-2)-order sequence repeated 2n times. Calculation of the propagator selectivity of 8 repetitions of a first-order 4k-quantum selective sequence shows that it intercepts the selectivity of this third-order sequence at $\|\mathcal{H}_o t_c\| =$ 5.1. The agreement is good, particularly since the convergence criterion is merely an estimate based on random addition of nonselective terms (see section 3.6) and a four-spin system is fairly small for such as assumption. It can be concluded that equation (III.38) is a reasonable criterion for convergence of the average Hamiltonian expansion. In fact, it is a conservative estimate; the selectivity is still around 100 when $\|\mathcal{H}_o t_c\| = 6.8$.

4.4.2 Lower-Quantum Selection

High-order selective sequences are of course also useful for (N-1)-quantum and lower-quantum transitions. In fact, the calculation of the selectivity in section 3.6 does not depend on the number of spins in the system. Computer calculations verify that the number of spins is not important. For example, the propagator selectivity of a third-order 4k-quantum selective sequence on benzene deviates by less than 10% from the selectivity in Figure IV.11 throughout the region of convergence $\|\mathcal{H}_o t_c\| \lesssim 5$. The signal from a third-order 4k-quantum sequence is identical to the signal from sixteen zero-order 4k-quantum sequences (shown in Figure IV.6) through the first maximum; is slightly larger on average through $\|\mathcal{H}_o T_c\| \sim 12.8$, where the propagator selectivities of both sequences are equal; and is smaller on average for larger

values of T_c. Four-quantum selection in five-spin systems shows similar results.

Thus, high-order selective sequences can increase the signal in the selective experiment. They are expected to become even more important for larger systems, where the required selectivity for maximum signal is greater. Since the agreement between average Hamiltonian theory and exact calculations is extremely good for the systems in this section, it is very likely that the average Hamiltonian calculations are valid for larger systems that cannot be exactly analyzed.

4.5 Suppression of Zero-Quantum Operators

It was suggested in section 3.6 that zero-quantum operators should be suppressed from $\bar{\mathcal{H}}^{(0)}$ to achieve the maximum possible gain in large systems. An average matrix element of $\bar{\mathcal{H}}^{(0)} t_c$ cannot be made comparable to 1 without violating the convergence criterion (III.38) unless the number of selected operators is small. Fortunately, the results of the last section show that the convergence criterion is an under estimate. Therefore, while zero-quantum suppression is still expected to be necessary in very large systems, it is not required in systems of moderate size (such as those that can be readily studied by computer).

Nonetheless, some of the effects of zero-quantum suppression can be seen even in these small systems. The calculation is straightforward, if a sequence such as the one in Figure (III.9a) is assumed. Replacing $\Delta\tau_p'$ with $-\Delta\tau_p'$ changes U to $U^\dagger$. Thus, the propagator for the second subcycle is $U_\phi^\dagger = \exp(i\phi I_z)\, U_o^\dagger \exp(-i\phi I_z)$, and the propagators for each subcycle are multiplied together to produce the total propagator,

as before.

Density matrices corresponding to several values of $\|\bar{\mathcal{H}}^{(0)}t_c\|$ for a third-order 4-quantum selective sequence on a four-spin system are given in Appendix C. These matrices show that the first nonselective coherences produced by the 4-quantum sequence all involve one of the states with M = ± 2. By contrast, the density matrices produced by third-order 4k-quantum selection do not show any pattern to the non-selected coherences. $(\bar{\mathcal{H}}^{(4)})_{nns}$ contains only terms such as $(\bar{\mathcal{H}}^{(0)})^2$ $(\bar{\mathcal{H}}_i^{(2)})_{nns}$, as explained in section 3.6, and if zero-quantum operators are suppressed $\bar{\mathcal{H}}^{(0)}$ only connects the states with M = ± 2; if zero-quantum operators are not suppressed, $\bar{\mathcal{H}}^{(0)}$ has matrix elements for all values of M. Thus, the sequence of Figure (III.9) does suppress zero-quantum operators from $\bar{\mathcal{H}}^{(0)}$.

4.6 The Importance of Time Reversal

In all of the computer calculations discussed so far, the exact form of $\mathcal{H}_o$ was assumed, not calculated. Thus, some unspecified pulse sequence creates multiple-quantum coherences with a propagator U_o and effective Hamiltonian $\mathcal{H}_o$, and these two operators contain equal amounts of multiple-quantum operators corresponding to all values of ΔM. This form is quite reasonable. For example, if the actual sequence for $\mathcal{H}_o$ is the sequence of Figure (III.2(a)), and if $\|\mathcal{H}_p T\| \gtrsim 1$ is all that is specified, this random $\mathcal{H}_o$ would be the best guess.

The key to producing an effective Hamiltonian with $\|\mathcal{H}_o \Delta\tau_p\| << 1$ and multiple-quantum operators is time reversal, if the sequence in Figure (III.2(a)) is used. If the time reversal is essentially perfect, $\|\mathcal{H}_o \Delta\tau_p\|$ can be made arbitrarily small by this sequence; if it is not perfect, there will be a lower bound to $\|\mathcal{H}_o \Delta\tau_p\|$. This means that the

sequences for $\mathcal{H}_p$ and $\mathcal{H}'_p$ must have short cycle times, yet must be repeated many times, so the selective sequence involves many pulses (thousands of pulses are typical, as will be shown in Chapter V). This generally implies problems with sample heating and stability of the pulse trains. In addition, there are important applications in which perfect time reversal for $\mathcal{H}_p$ is not even theoretically possible, such as in isotropic systems; there $\|\mathcal{H}_J T\| \gtrsim 1$ for $\mathcal{H}_p$ to have multiple-quantum coherences, as explained in section 2.3, but $\mathcal{H}_K$ cannot be time reversed with broadband irradiation since it is a zero-rank tensor.

In this section, the assumption of time reversal will be discarded. Specific pulse sequences will be applied to systems with known Hamiltonians. These Hamiltonians sometimes correspond to specific molecules, and sometimes are random. These calculations show that time reversal, while useful, is not essential to the design of selective sequences.

4.6.1 Simple Selective Sequences

The simplest possible cyclic pulse sequence for $\mathcal{H}_o$ would be two pulses with a delay between them. If the pulses are assumed to have phase y and $\bar{y}$ and flip angle $\pi/2$, then $\mathcal{H}_o = \mathcal{H}_x$, where $\mathcal{H}_x$ is given in equation (II.32). $\mathcal{H}_x$ is the operator which generates multiple-quantum coherences in the nonselective experiment. It only has 0-quantum, 1-quantum, and 2-quantum operators; in the nonselective experiment high-quantum operators are generated by the complex exponential in the propagator. However, higher-quantum operators must be present in $\mathcal{H}_o$ if zero-order selection is to work. Thus, a zero-order 4k-quantum

selective sequence is not expected to produce much four-quantum signal.

The general form of $\bar{\mathcal{H}}^{(j)}$ can be calculated readily from equations (III.2-4). $\mathcal{H}_{int}(t)$ is restricted to four possible operators: if $\phi = 0$, $\tilde{\mathcal{H}}_{int}(t) = \mathcal{H}_x$; if $\phi = \pi/2$, $\tilde{\mathcal{H}}_{int}(t) = \mathcal{H}_y$; if $\phi = \pi$, $\tilde{\mathcal{H}}_{int}(t) = \mathcal{H}_{xx} + \mathcal{H}_J + (\Sigma\, \sigma_i I_{xi} - \Delta\omega I_x) \equiv \mathcal{H}_{-x}$; and if $\phi = 3\pi/2$, $\mathcal{H}_{int}(t) = \mathcal{H}_{yy} + \mathcal{H}_J + (\Sigma\, \sigma_i I_{yi} - \Delta\omega I_y) \equiv \mathcal{H}_{-y}$. Since all of these operators are at most bilinear, $\bar{\mathcal{H}}^{(1)}$ involves at most three spins, and cannot have four-quantum operators. $\bar{\mathcal{H}}^{(2)}$ can have four-quantum operators, so a second-order or third-order 4k-quantum selective sequence might be useful. Unfortunately, short cycle times imply a small $\bar{\mathcal{H}}^{(2)}$, and $\bar{\mathcal{H}}^{(0)}$ does not vanish ($\bar{\mathcal{H}}^{(0)} = -1/2\, \mathcal{H}_{zz} + \mathcal{H}_J$). If the cycle time becomes long enough to make $\| \bar{\mathcal{H}}^{(2)} T_c \| \sim 1$, the convergence criterion is violated. As a result, even high-order selective sequences do not provide much signal enhancement, as shown in Figure IV.12.

The obvious solution is to suppress the zero-quantum coherences, or at least suppress the zero-quantum coherences in $\bar{\mathcal{H}}^{(0)}$. One way to do this, by analogy with Figure (III.9a), is to produce $-\mathcal{H}_x$ as well as $\mathcal{H}_x$. The largest term in $\mathcal{H}_x$ is $\mathcal{H}_{xx}$, and $-1/2\, \mathcal{H}_{xx}$ can be produced by a time reversing sequence.[77] Such a sequence would not reverse $(\Sigma\, \sigma_i I_{xi} + \Delta\omega I_x)$, but these operators could be suppressed from both $\mathcal{H}_x$ and $-\mathcal{H}_x$ (by echo pulses in $\mathcal{H}_x$, and by a suitably chosen time reversal sequence in $-\mathcal{H}_x$). $\mathcal{H}_J$ would be unaffected, but since it is very small compared to $\mathcal{H}_{xx}$ this would not pose an important limitation.

4.6.2 Use of Line Narrowing Sequences

A simpler solution is to use a line narrowing sequence for $\mathcal{H}_o$, as suggested in section 3.4.4 . For example, a WAHUHA sequence might be used. For clarity in later discussions the average Hamiltonian for

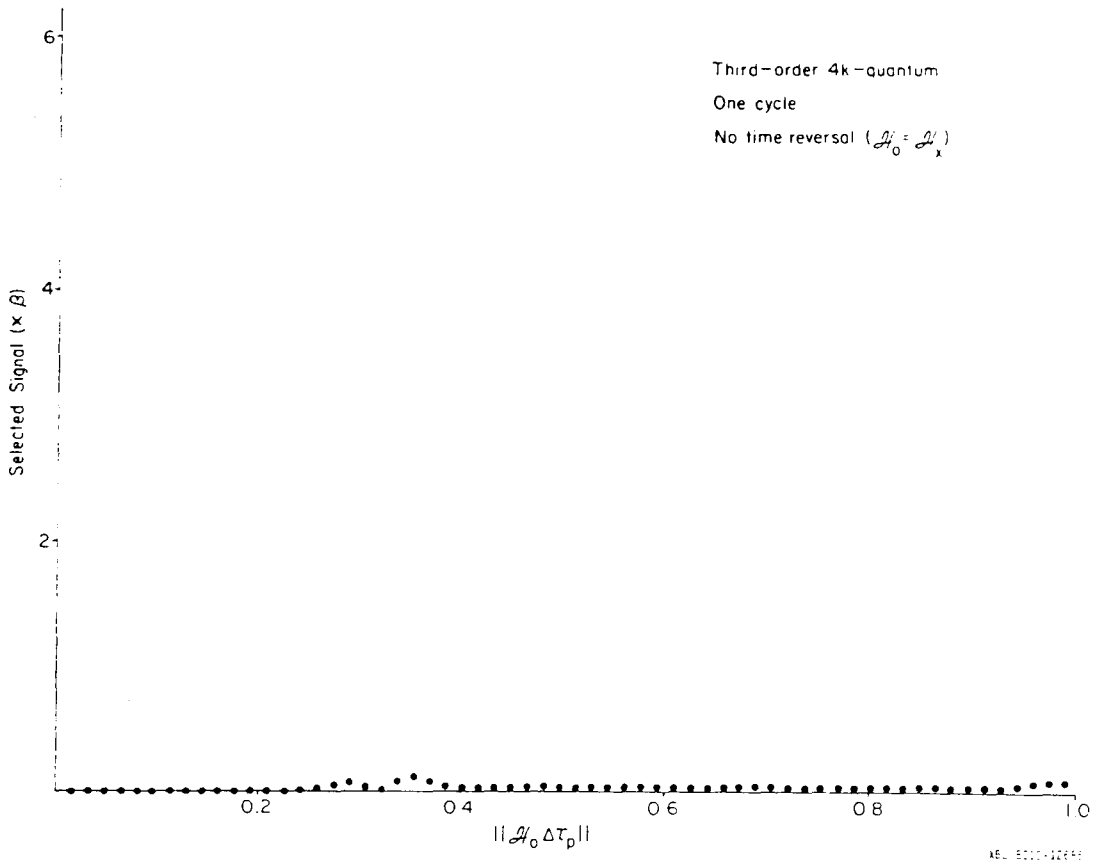

Figure IV.12 The signal produced by one cycle of third-order 4k-quantum selection without time reversal ($\mathcal{H}_0 = \mathcal{H}_x$). $\bar{\mathcal{H}}^{(0)}$ is large but does not have four-quantum operators, so the convergence criteria are violated before the four-quantum operators in $\bar{\mathcal{H}}^{(2)}$ become significant. As a result, not much signal is produced. Compare this to the time reversal case in Figure IV.6.

this sequence will be written with a small h. Pure dipolar interactions are suppressed in $\bar{h}_D^{(0)}$ and $\bar{h}_D^{(1)}$. Chemical shift and resonance offset terms are not suppressed, but these operators are generally much smaller than $\mathcal{H}_{zz}$. The operator $\bar{h}_D^{(2)}$ is given by:

$$\bar{h}_D^{(2)} = \frac{1}{648} t_c^2 \, [\mathcal{H}_{xx}-\mathcal{H}_{zz}, [\mathcal{H}_{xx},\mathcal{H}_{yy}]] \qquad \text{(IV.7)}$$

which can be readily shown to contain four-quantum operators. There is a range of values for T (the short delay between the pulses) such that $\|\mathcal{H}_z\| >> \|\bar{h}_D^{(2)}\| >> \|\mathcal{H}_{cs}\|, \|\mathcal{H}_J\|$, and if T is in this range a WAHUHA sequence can be used for $\mathcal{H}_o$ if four-quantum selection is desired. The theory of Chapter III applies, as long as T is considered to be a fixed parameter; thus, $\Delta\tau_p$ in Figure (III.2(a)) is changed by changing the number of WAHUHA cycles in $\mathcal{H}_o$.

If T is not a fixed parameter, the analysis is more complicated. Figure IV.13 shows the effect on the selectivity of varying T in a WAHUHA sequence for $\mathcal{H}_o$. The sequence is incorporated into a zero-order 4k-quantum selective sequence on a four-spin system. When T is small, the largest term in $\mathcal{H}_o$ is $\bar{h}_{cs}^{(0)} = (-1/3)\ (\Sigma\ \sigma_i(I_{xi}+I_{yi}+I_{zi}))$; zero-order selection suppresses the nonsecular part of this, but creates a nonselective $\bar{\mathcal{H}}^{(1)}$. Thus, the coherence selectivity goes to 0 as $\Delta\tau_p \to 0$; the propagator selectivity becomes very large because of the secular terms in $\bar{\mathcal{H}}^{(0)}$, but these terms will not produce coherences. If T is small, the largest nns operator in $\mathcal{H}_o$ is proportional to T; the largest 4-quantum selective operator is proportional to T^2, so the selectivity is proportional to T (in contrast to all the examples in sections 3.2.3-5, in which the selectivities were proportional to

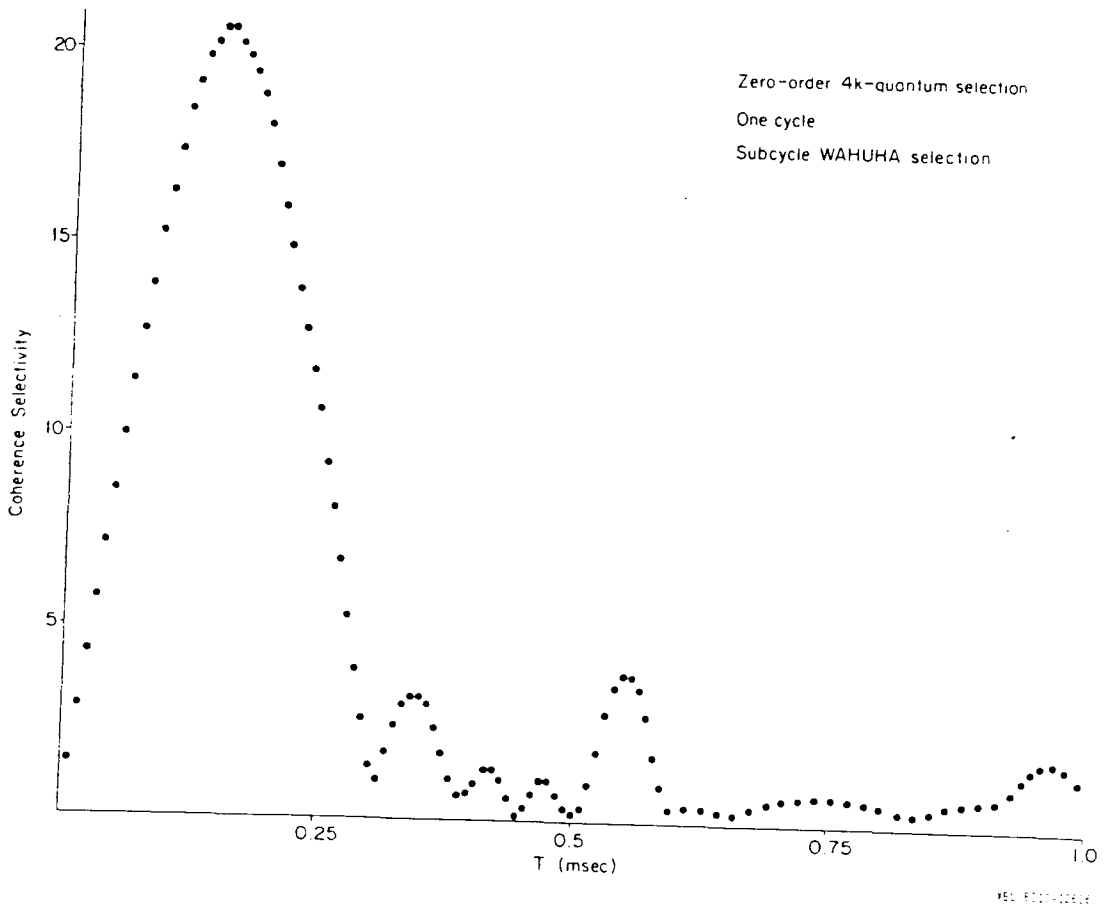

Figure IV.13 The selectivity for one cycle of zero-order 4k-quantum selection using a WAHUHA sequence for $\mathcal{H}_o$. The selectivity is proportional to T for short cycle times, because $\bar{\mathcal{H}}^{(1)}$ is nonselective and $\bar{\mathcal{H}}^{(2)}$ has 4k-quantum operators. In the region of interest $\|\bar{\mathcal{H}}^{(2)}\| \gg \|\bar{\mathcal{H}}^{(1)}\|, \|\bar{\mathcal{H}}^{(3)}\|$.

negative powers of T). When $\|\mathcal{H}_{zz}T\| \sim 1$, $\|\mathcal{H}_{cs}T\| << 1$, so $\bar{h}_{cs}^{(0)}$ and $\bar{h}_{cs}^{(1)}$ are still small; $\bar{h}_D^{(2)}$ is the dominant term in $\mathcal{H}_o$. The zero-order selective sequence still works well, since $\|\mathcal{H}_o \Delta\tau_p\| << 1$ so the coherence selectivity is good. As T is further increased, $\bar{\mathcal{H}}^{(1)}$ increases, and the selectivity falls off as T^{-1}.

Figure (IV.14) shows the signal produced by this sequence. When T is small, the signal is proportional to T^6. When $\|\mathcal{H}_{zz}T\| \sim 1$, the selectivity is good and the signal is large; in fact, the maximum signal (2.98 β) is substantially larger than the maximum achieved by one cycle of 4k-quantum selection using time reversal (Figure IV.3). Yet, this sequence requires only 16 pulses, so sample heating and pulse instability are much less troublesome.

The maximum signal can be increased by using high-order selection or increasing the number of cycles. Figure IV.15 shows the effect of fixing T at 120 μsec, and incrementing the number of cycles; the familiar $\sin^2$ pattern appears. The period of the oscillations is proportional to T^3, since the dominant term in $\mathcal{H}_o$ is $\bar{h}_D^{(2)}$. For this reason, the maximum may be hard to find in systems with unknown couplings.

Since $\bar{h}_D^{(2)}$ has no operators with $\Delta M > 4$, high-order selection must rely on higher order terms, and zero-order selection is ineffective. For higher-quantum selection a different line narrowing sequence may be helpful. For example, a sequence with a secular or vanishing $\bar{h}_{cs}^{(0)}$ will have smaller nonselective terms. Also, sequences which suppress $\bar{h}_D^{(2)}$ might be useful. Thus, for example, the 72-pulse sequence of Burum and Rhim[75] has 6-quantum operators in its leading dipolar term $\bar{h}_D^{(4)}$, and would be a good candidate for $\mathcal{H}_o$ in a 6k-quantum

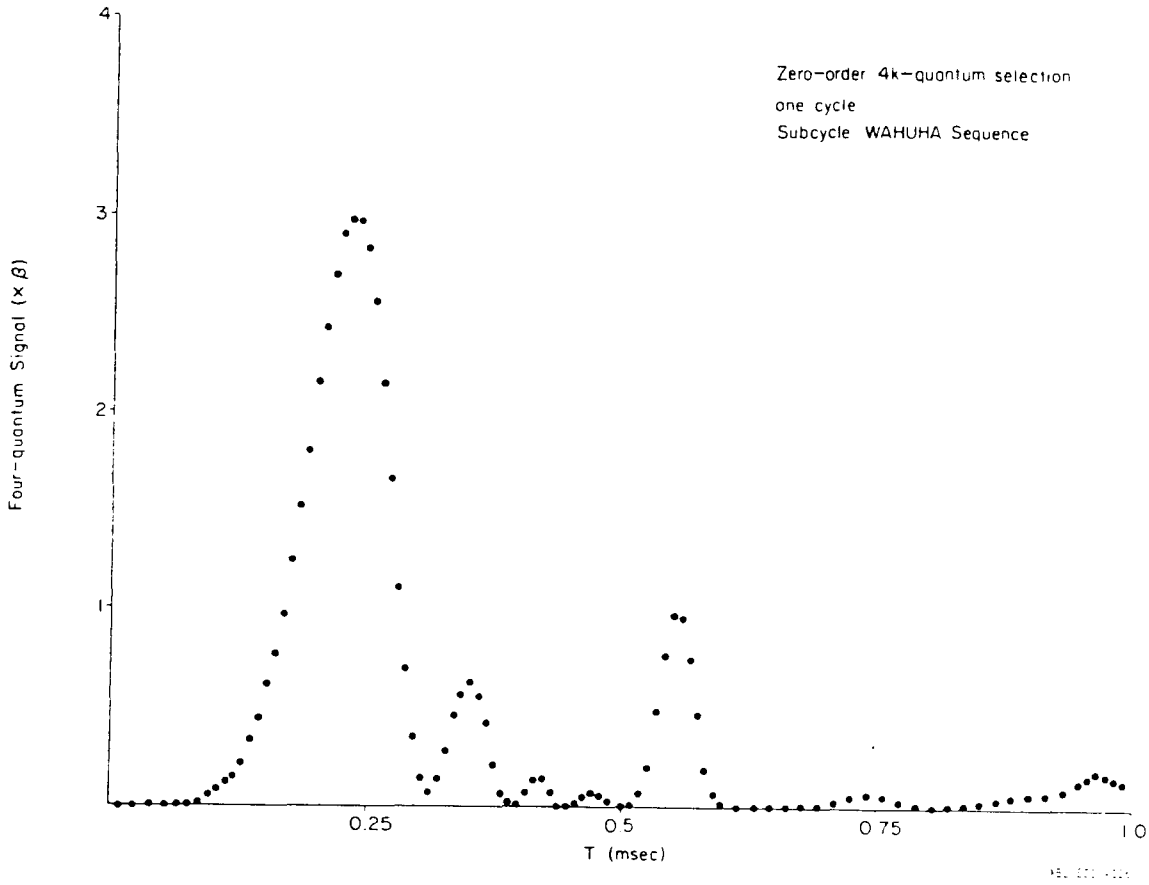

Figure IV.14 The signal produced by one cycle of zero-order 4k-quantum selection on a four-spin system, using a WAHUHA sequence for $\mathcal{H}_o$.

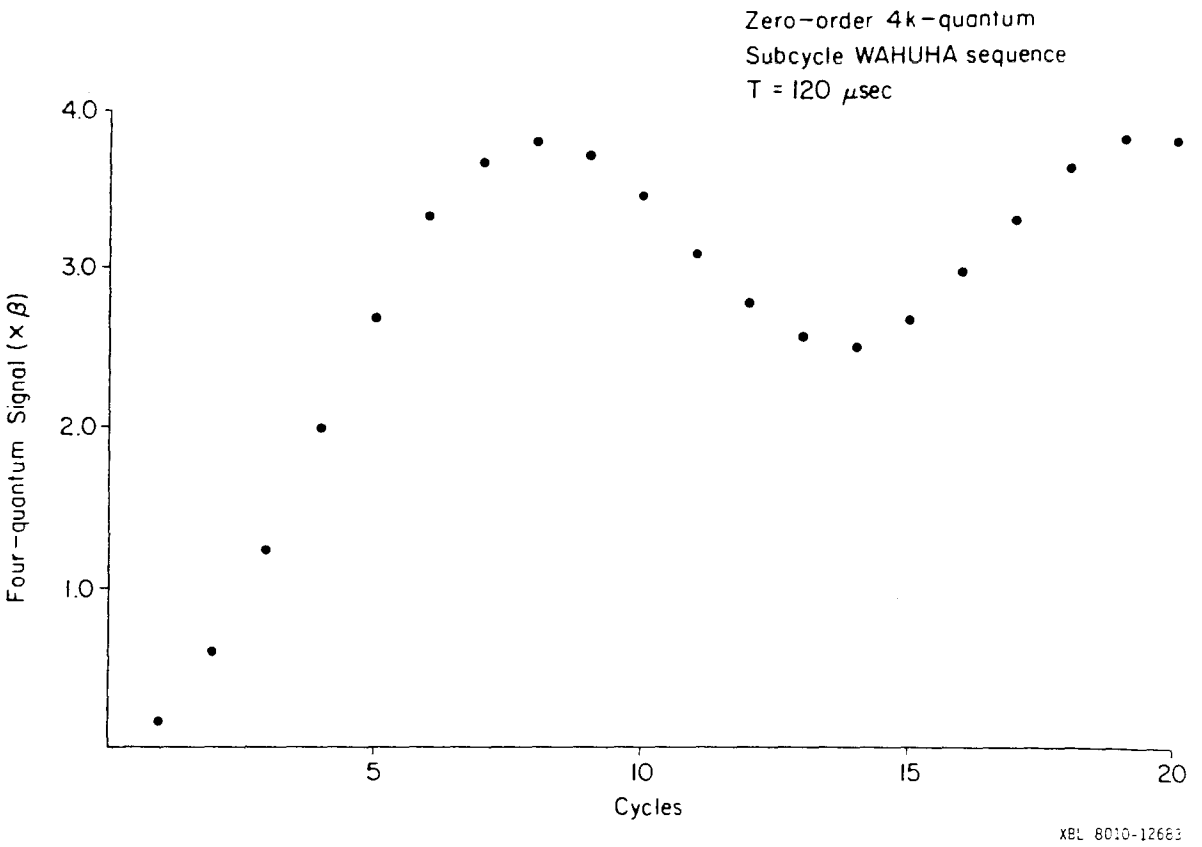

Figure IV.15 The effect of fixing T at 120 μsec in a WAHUHA sequence for $\mathcal{H}_o$ and incrementing the number of cycles of zero-order 4k-quantum selection. Signal intensities that are as large as in the time reversal experiment can be obtained.

selective sequence. A 12-pulse sequence which has $\bar{h}_D^{(4)}$ as its leading dipolar term is:

$$(\tau-90_{\bar{x}}-\tau-90_y-2\tau-90_x-\tau-90_{\bar{y}}-2\tau-90_{\bar{x}}-\tau-90_y-2\tau-90_{\bar{y}}-\tau-90_x-2\tau-90_y-\tau-90_{\bar{x}}-2\tau-90_{\bar{y}}-\tau-90_x-\tau)$$

Computer calculations show that this sequence can be used for $\mathcal{H}_o$ if 6k-quantum selection is desired. It is most useful when the chemical shift differences are small; if this is not the case then the simplest modification is to insert a 180° pulse in the middle of each delay. Each of these inserted pulses should be 180° out of phase with the 90° pulse which precedes it. Clearly, the larger the number of quanta to be selected, the more complicated $\mathcal{H}_o$ becomes, and this will be a practical limitation to the technique. Nonetheless, the advantage of very low duty cycles makes the use of line narrowing sequences an attractive option for low-quantum selection.

4.6.3 Selectivity in Isotropic Systems

For the reasons discussed in section 2.3, multiple-quantum coherences are produced more slowly in isotropic systems than in anisotropic ones. In fact, $\|\mathcal{H}_J\Delta\tau_p\| \sim 1$ will be required to give $\mathcal{H}_o$ multiple-quantum coherences. $\mathcal{H}_J$ cannot be time reversed by wideband pulses; however, $\mathcal{H}_{cs}$ can be reversed, and since $\|\mathcal{H}_{cs}\| >> \|\mathcal{H}_J\|$ an appropriately chosen sequence will give selection. For example, consider the sequence in Figure III4(a) in the limit $\Delta\tau_p' \to 0$. Let $\mathcal{H}_p$ be $\mathcal{H}_x = -\Sigma\, \sigma_i I_{xi} + \sum_{i>j} J_{ij} I_i I_j$, created by the sequence 90_x-T-$90_{\bar{x}}$; and let $\mathcal{H}_p'$ be $\mathcal{H}_{-x}$, created by the sequence $90_{\bar{x}}$-T-90_x (Figure IV.16). An average Hamiltonian expansion will not converge rapidly for $\|\mathcal{H}_J T\| \sim 1$, since then $\|\mathcal{H}_{cs} T\| >> 1$. But the propagator can be expanded, using

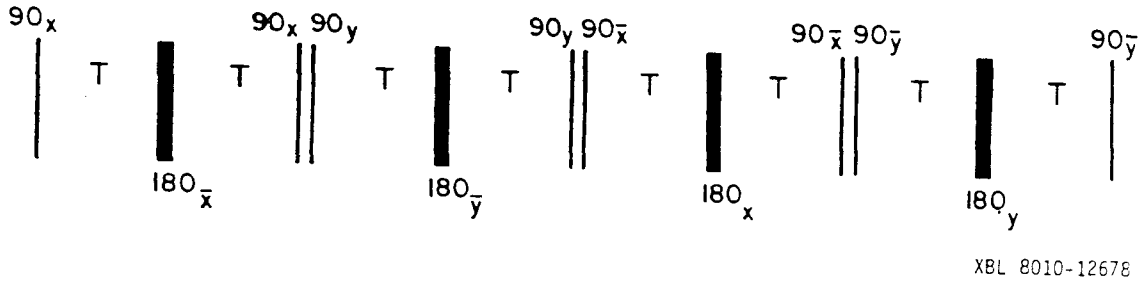

Figure IV.16 A simple pulse sequence for 4k-quantum selection in isotropic systems. The sequence for $\mathcal{H}_o$ is 90_x-T-$180_{\bar{x}}$-T-90_x, and is actually equivalent to Figure III.4(a) with $\Delta\tau_p' = 0$.

(E.10):

$$U = \exp(-i\mathcal{H}_x T)\ \exp(-i\mathcal{H}_{-x} T)$$

$$= (\exp(-i(-\Sigma\sigma_i I_{xi} + J_{ij} I_{xi} I_{xj})T) + A)(\exp(-i(\Sigma\sigma_i I_{xi} + J_{ij} I_{xi} I_{xj})T) + B)$$

$$= \exp(-2i\,\Sigma\, J_{ij} I_{xi} I_{xj} T) + A\ \exp(-i(\Sigma\sigma_i I_{xi} + J_{ij} I_{xi} I_{xj})T)$$

$$+ \exp(-i(-\Sigma\sigma_i I_{xi} + J_{ij} I_{xi} I_{xj})T)B + AB \qquad \text{(IV.9)}$$

$$A_{k\ell} = (\Sigma J_{ij}(I_{zi} I_{zj} + I_{yi} I_{yj}))_{k\ell}\ \left(\frac{\exp(-i(-\Sigma\sigma_i I_{xi} + \Sigma J_{ij} I_{xi} I_{xj})T)_{kk-\ell\ell}}{(-\Sigma\sigma_i I_{xi} + \Sigma J_{ij} I_{xi} I_{xj})_{kk-\ell\ell}}\right.$$

$$B_{k\ell} = (\Sigma J_{ij}(I_{zi} I_{zj} + I_{yi} I_{yj})_{k\ell}\ \left(\frac{\exp(-i(\Sigma\sigma_i I_{xi} + \Sigma J_{ij} I_{xi} I_{xj})_{kk-\ell\ell}}{(\Sigma\sigma_i I_{xi} + \Sigma J_{ij} I_{xi} I_{xj})_{kk-\ell\ell}}\right))$$

(IV.10)

Since $\|\mathcal{H}_{cs} T\| >> 1$, $\|A\| \sim \|B\| \sim \|\mathcal{H}_J\| / \|\mathcal{H}_{cs}\| << 1$ if the system is first order, and therefore U is close to 1. Since this sequence is cyclic, the usual ansatz $U = \exp(-i\bar{\mathcal{H}}(2T))$ can be made, and then $\|\bar{\mathcal{H}}(2T)\| << 1$. Thus, this sequence will often produce a usable $\mathcal{H}_o$.

Figure IV.17 shows the selectivity of a first-order 4k-quantum selective sequence as a function of T; the molecular parameters correspond to methanol at 270 MHz.[78] The selectivity is expected to be an extremely complicated function, because $\bar{\mathcal{H}}$ changes as T changes. Still, there is a region where the selectivity is good and $\|\mathcal{H}_o\|$ is small; if T is chosen from this region, the first-order sequence

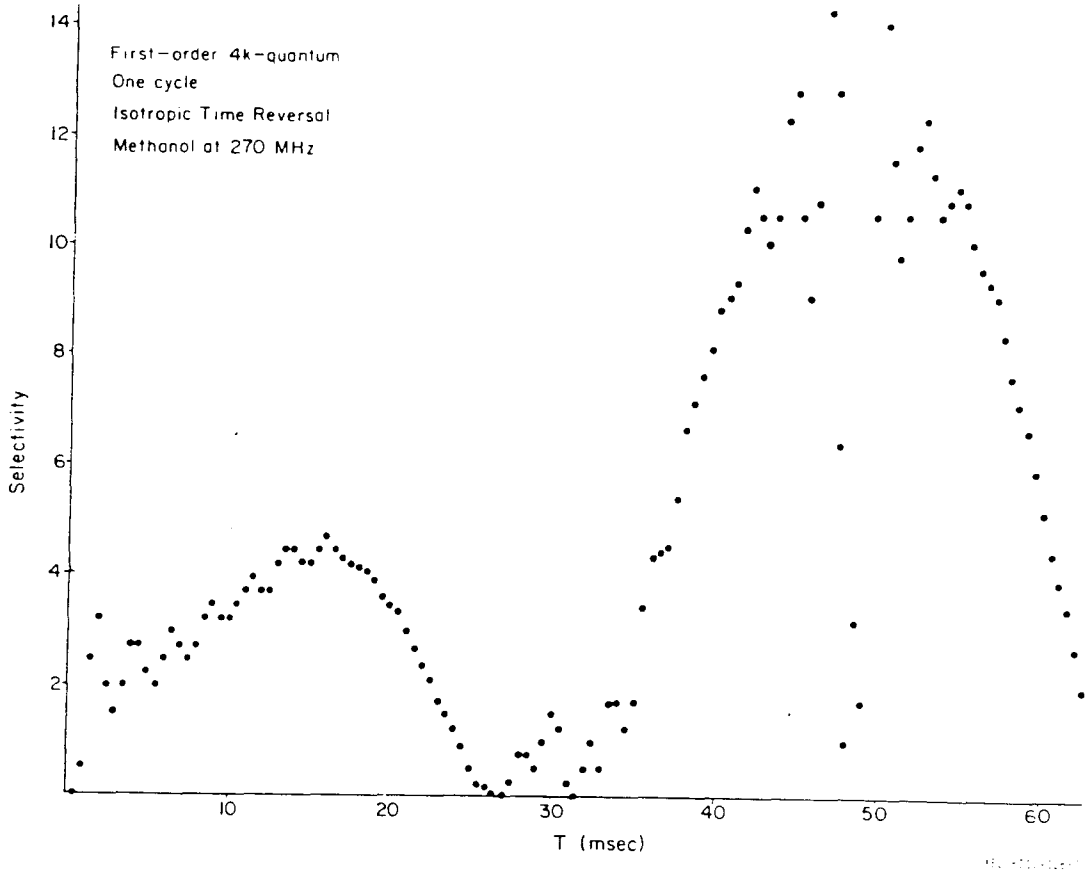

Figure IV.17 The coherence selectivity of a first-order 4k-quantum selective sequence for isotropic systems (symmetrized version of Figure IV.16). The molecular parameters correspond to methanol at 270 MHz.

can be repeated several times to give a large signal, as shown in Figure IV.18. For example, one sequence which will produce a large four-quantum signal is 3 cycles of first-order selection with T = 12.0 msec. The total duration of the sequence is 576 msec, which is short enough to neglect relaxation effects (as is implicitly done in all of these computer calculations). Higher-order selectivity is of course possible in isotropic systems as well, when relaxation times are long enough to allow many subcycles. It should be noted, however, that isotropic selective sequences are not as easy to design as anisotropic ones, and that relaxation times provide a serious constraint for protons. The J couplings are larger with other nuclei (for example, ^{13}C and ^{19}F) and therefore selectivity is simpler in those systems.

4.7 Conclusions

Computer calculations have been presented which verify the average Hamiltonian theory calculation of Chapter III. The selectivity and signal intensity have the form expected from those calculations. In additon, these calculations show that the region of convergence of the Magnus expansion agrees with earlier estimates, and that the selectivity is still good near the limits of convergence. Simplified pulse sequences for isotropic and anisotropic systems have been shown to provide signal enhancements. Since these computer calculations are exact (to the extent that the spins follow the density matrix equation of motion (II.7)) it may be concluded that selective sequences provide a practical techcique for signal enhancement.

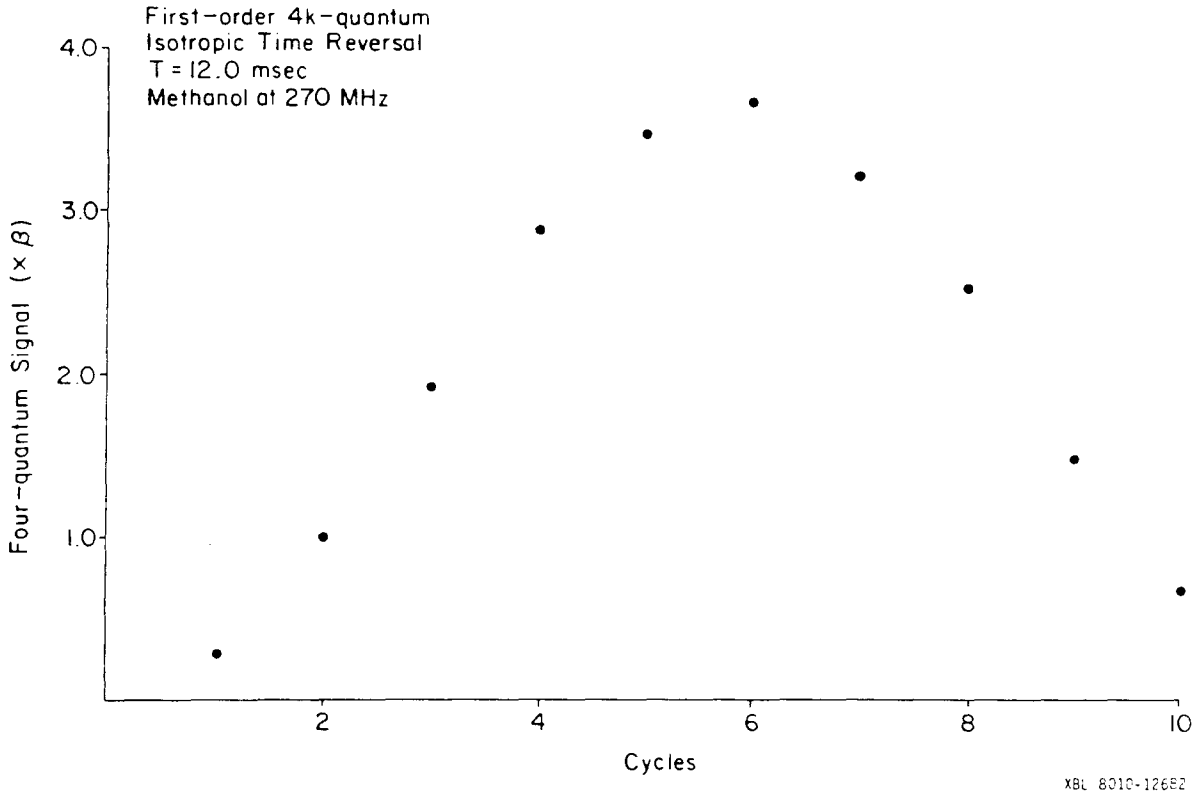

Figure IV.18 The signal produced by fixing T at 12.0 msec and incrementing the number of cycles, for 4k-quantum selection on methanol at 270 MHz.

V. Selective Experiments

5.1 The Spectrometer

The selective pulse sequences of the last two chapters require many pulses and complicated phase shifts. For this reason the sequences would not be possible with most commercial spectrometers. All of the experiments in this section were done with a homebuilt machine.

5.1.1 Magnet

The magnet is a persistent superconducting model from Bruker Instruments. It is operated at 42 kG, giving a proton resonance at 182.00 MHz. The bore is 3.5 inches in diameter. The field can be shimmed readily to 1/4 PPM over a 1 cm^3 region, and laboriously to 1/16 PPM.

5.1.2 Frequency Generation

A 10 MHz reference signal is tripled to provide an IF frequency of 30 MHz, and mixed with $\sim$ 152 MHz (generated by doubling the output of a Hewlett-Packard 3320A synthesizer and mixing it with 100 MHz) to provide the proton pulses. To ensure good isolation rf switching is done once at the IF frequency (two Summit 571 switches in series) and once at the final output frequency (one Daico 100C1281A switch). Four phases (corresponding to x, $\bar{x}$, y and $\bar{y}$) are generated at the IF frequency by commercial hybrids. The output is fed into an AR model 100 or model 200 amplifier to provide pulses of up to 200 watts. The low frequency end also operates with an IF of 30 MHz but is mixed with a lower frequency (58 MHz) to provide deuterium pulses at 28 MHz.

5.1.3 Detectors

The first stage of the detector is a commercial pre-amplifier (Avantec VTO 511 and VTO 512) with 35 dB of gain. The first stage noise figure is 2.5 dB. The signal from this is mixed and filtered to ∿ 30 MHz, amplified with a variable gain IF strip (up to 70 dB) and then mixed down to audio frequencies with two phases of the 30 MHz from the transmitter section. The recovery time after complete saturation (from pulses) is about 10 μsec.

5.1.4 Digitization

The two audio frequency signals (corresponding to M_x and M_y in the rotating frame) are fed into Datel SHM-2 S/H and Datel ADC-EH10B2 analog-to-digital converters giving 10 bits. The digitized signal is fed to a NOVA 2 computer, with a minimum acquisition time of 3 μsec. This is more than adequate for all experiments in this work.

5.1.5 Pulse Programmer

An important part of any modern NMR spectrometer is the pulse programmer. This one is microprocessor based and clocked at 10 MHz. Pulse programs may contain up to 64 simple statements (branches, compares, increments, or outputs). Pulse widths can be set to .1 μsec, and the pulses can open any one of four proton gates, any one of four low-frequency gates, and as many of eight auxiliary gates (used for temperature blanking, phase shifting, and data acquisition) as desired. The pulses can be loaded either into a 16-step FIFO or a 256-step RAM.

5.1.6 Probes

All of the experiments in this chapter require proton irradiation

only. The probe is home built with a single-tuned 8mm x 30mm solenoidal coil of uninsulated copper ribbon (11 turns). This coil is part of a tuned circuit including a homemade series turning capacitor (two copper rods with Teflon dielectric) and parallel ATC matching capacitors of various sizes. Q's of over 100 are readily achieved.

The coil is surrounded by a glass dewar to provide thermal isolation. Temperature control is achieved by passing air (or cooled N_2 gas for low temperatures) over a constantan heater coil. The temperature is constantly sampled by a copper-constantan thermocouple and compared by a digital thermometer to a reference setting. If the temperature is too low, up to 3 amps are fed into the constantan heater coil (resistance 2Ω).

All of the samples were nematic liquid crystals so pulse heating effects had to be minimized. Fortunately, the selective experiment does not require signal sampling in short windows in the pulse sequence so a high-Q circuit and low power (∿ 50W) pulses were used. Samples were sealed in 6mm O.D. x 15mm Pyrex tubes which were suspended in the center of the coil to minimize rf inhomogeneity and heating effects. The temperature-regulated air stream was focused directly on the sample to further decrease heating. Even with these precautions, relatively long delays (∿ 10 sec) were frequently required between successive shots.

5.1.7 Phase Shifting

All phase shifts are generated by a Daico 100D0898 shifter

operating at the IF frequency of 30 MHz. This device produces phase shifts in any multiple of $2\pi/256$. The phases were checked with a Hewlett-Packard 8405A vector voltmeter and found to be stable and within 1° of the stated value at all times.

The VSWR of the phase shifter depended on the phase setting. To eliminate fluctuations from this effect and from switching transients, the pulses were gained up to $\sim 3\ V_{pp}$ and passed through a series pair of crossed PIN diodes followed by a pair of crossed PIN diodes to ground. The first pair eliminates small components which are out of phase with the main pulse, and the second pair reduces fluctuations in the output voltage. The pulses were then filtered, amplified, and sent to the probe.

Increased versatility was provided by loading up to 256 phase settings into a RAM which was interfaced to the phase shifter. With this configuration third-order sequences for up to 8 spins and first-order sequences for up to 16 spins are possible.[79]

5.2 Experimental Results: Oriented Benzene

5.2.1 Four-Quantum Selection with Time Reversal

The high (D_{6h}) symmetry of benzene produces many different irreducible representations for the eigenstates (Figure V.1). This reduces the number of allowed transitions; for example, there is only one pair of five-quantum transitions, instead of the six pairs of five-quantum transitions in an unsymmetrical six spin system as mentioned in section 1.4. This molecule is small enough to be studied by nonselective sequences, and all of the theoretically allowed transitions have been observed.[28,29]

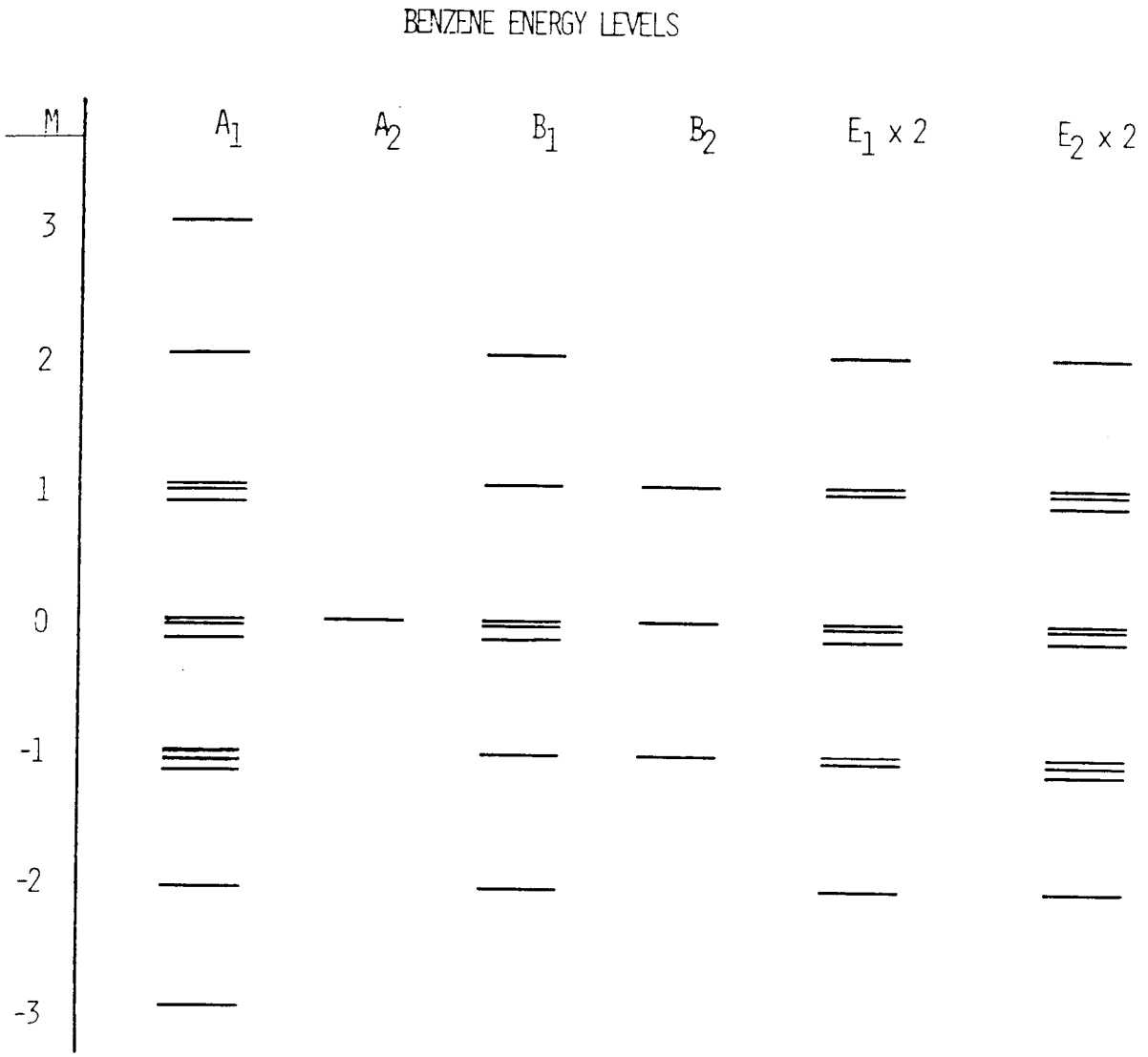

Figure V.1 Energy level diagram for benzene oriented in a liquid crystalline solvent. The assumed symmetry is C_{6v}. There is also a time reversal symmetry operation (flipping all spins) in the M = 0 manifold which is not shown. This symmetry operation affects only zero-quantum transitions.

Figure V.2(a) shows the nonselective (pulse sequence of Figure II.2(b)) multiple-quantum spectra at 24.0°C of a sample with 14 wt% benzene dissolved in Eastman liquid crystal #15320. The same sample was used for all of the benzene experiments. For this experiment $\Delta\omega$ = 500 Hz, and magnitude spectra corresponding to $t_2 = \tau$ = 4.0 msec, 6.0 msec, 8.0 msec, and 10.0 msec were averaged together. The individual lines are resolvable even in the single-quantum spectra,[17] and the three dipolar coupling constants D_{12}, D_{13} and D_{14} have been shown to be consistent with hexagonal symmetry. Figure V.2(b) shows, on the same scale, the averaged results of four spectra with 4k-quantum selection ($\phi = \pi/2$ in Figure V.3, and $\mathcal{H}_p$ is the two-quantum sequence described in section 3.4.2) and different values of T and τ. All experiments in this chapter used the same sequence for the mixing that was used for the preparation, except that one more pulse was inserted immediately before sampling, as explained in section 2.2.3.3. The four-quantum transitions are significantly enhanced, and their positions are unaffected. The nonselected orders are almost entirely under the noise level, as illustrated by the integrated intensities in Figure V.4.

Figures V.5 and V.6 present individual spectra (not averaged over any parameters in the pulse sequence) to calculate selectivity and signal gains. Each of the spectra in Figure V.5 was taken with $\phi = \pi/2$, t_p = 3.8 μsec, τ = 5.0 μsec, T = 1.5 msec, and 8 subcycles (the zero-order sequence was applied two consecutive times) to make a 4k-quantum selective sequence. The sequence was used in both the preparation and mixing periods. Immediately before detecting $\langle I_x \rangle$ and $\langle I_y \rangle$, a single additional pulse was applied as explained in Section 2.2.

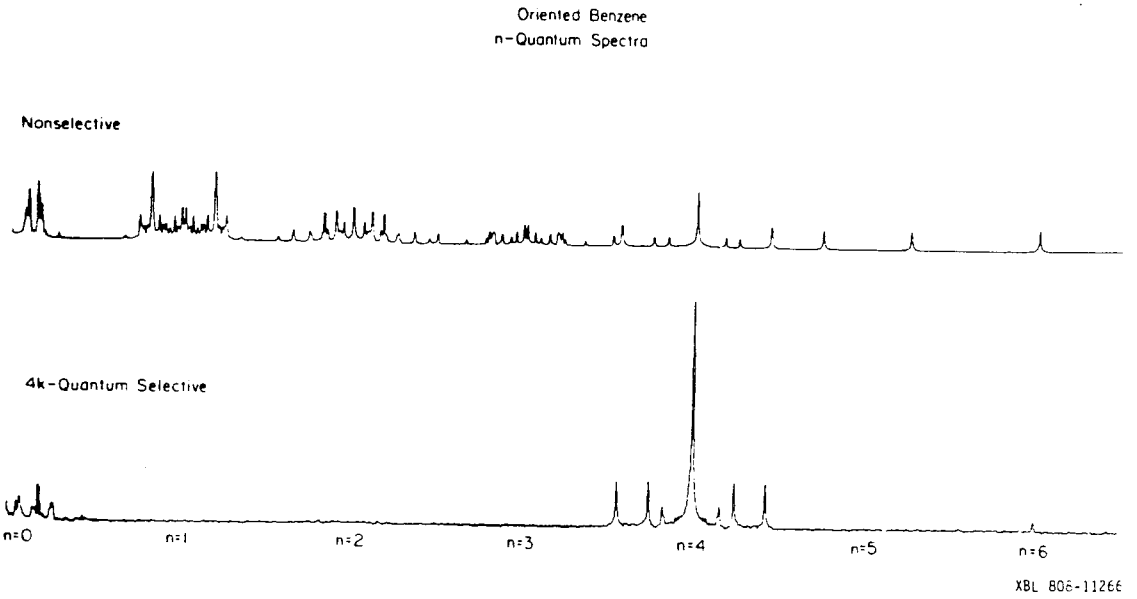

Figure V.2 Multiple-quantum ensemble averaged spectra of oriented benzene. The width of the four-quantum spectrum is 5470 ± 25 Hz. Part (a) is the nonselective spectrum (sequence of Figure II.2(b)). Part (b) is 4k-quantum selective (sequence of Figure V.3).

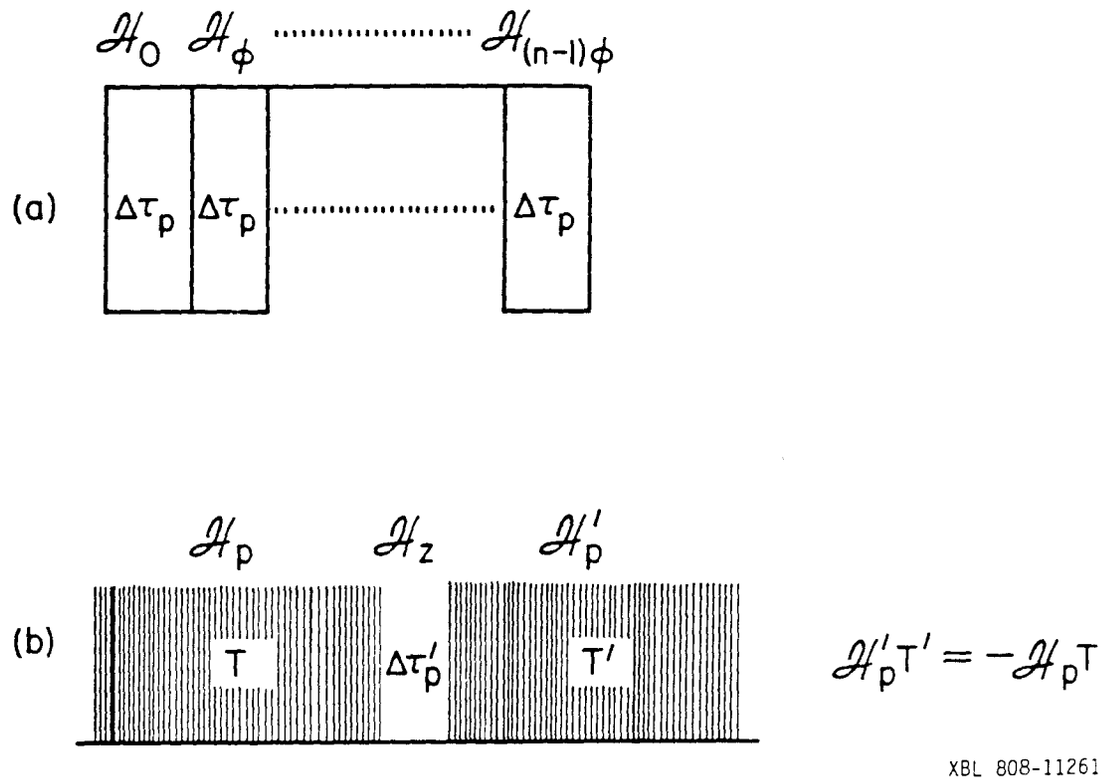

Figure V.3 General form for zero-order selective sequences. In part a) $\mathcal{H}_o$ is an arbitrary cyclic sequence of pulses and delays. All of the pulses are phase shifted by $\phi = 2\pi/n$ to produce $\mathcal{H}_o$. To lowest order, only nk-quantum coherences ($k = 0, \pm 1, \pm 2 \ldots$) survive after n shifts. Part b) is a possible sequence for $\mathcal{H}_o$ which uses dipolar time reversal to give $\mathcal{H}_o$ multiple-quantum operators yet keep $\|\mathcal{H}_o \Delta\tau_p\|$ small.

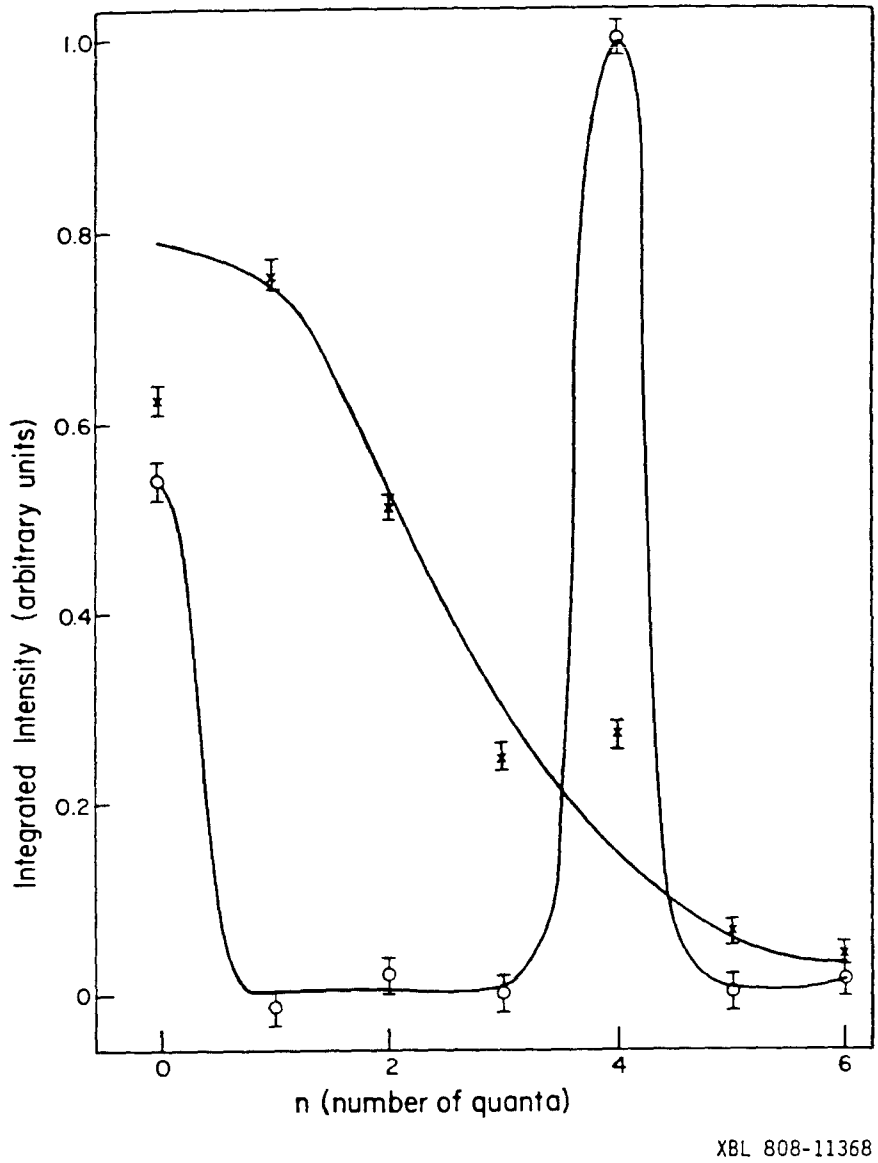

Figure V.4. Integrated intensities of the spectra in Figure V.2. The nonselective intensities for the selective spectrum are almost completely under the noise level.

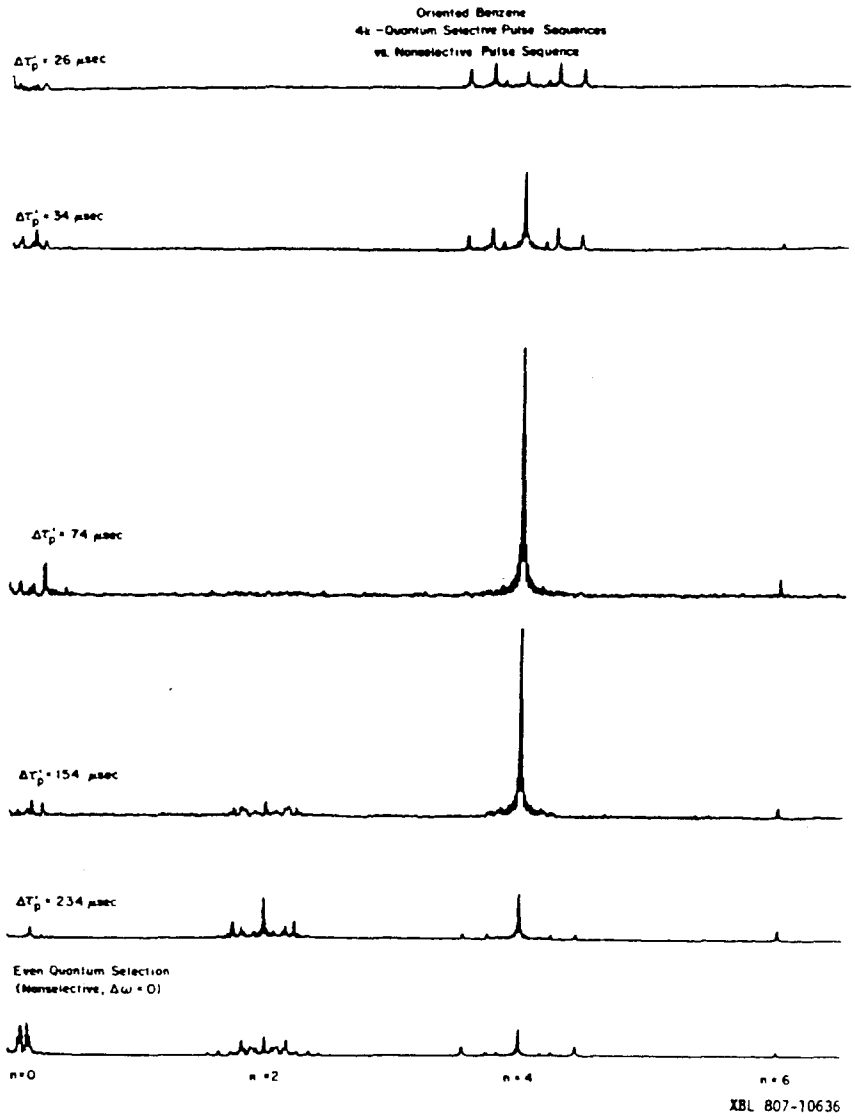

Figure V.5. The effects of varying $\Delta\tau_p'$ (see Figure V.3) in 4k-quantum selective sequences on oriented benzene. When $\Delta\tau_p'$ is long the selectivity has disappeared. The optimum value of $\Delta\tau_p'$ is expected to be longer for the central peak than for the side peaks (see text). The largest observed gains are 5.6 for the side peaks and 19 for the central peak. Pulse sequence parameters are t_p (pulse width) = 3.8 μsec, τ (delay in two-quantum sequence for $\mathcal{H}_p$) = 5.0 μsec, T = 1.5 msec. Two cycles of 4k-quantum selection were applied.

The only parameter which was varied was $\Delta\tau_p'$.

The selective terms in the average Hamiltonian are linear in $\Delta\tau_p'$. Higher order terms are nonselective, so the spectra with large values of $\Delta\tau_p'$ are expected to have substantial two-quantum and six-quantum intensity ($\mathcal{H}_o$ still has the form in equation (III.27), so no odd-quantum operators are present in the propagator). Figure V.5(e) confirms this result. If $\Delta\tau_p'$ is very small and the time reversal is good, even the linear term is small, and very little coherence is produced. Thus, there should be an optimal value (or at least an optimal range) for $\Delta\tau_p'$ to produce four-quantum coherences. One interesting feature of Figure V.5 is that the value which optimizes the central four-quantum line is much longer than the value which optimizes the side peaks. There is no reason why the optimal values should be the same; the side peaks are all A_1 transitions, whereas the central peak has contributions from every irreducible representation. In addition, diagonalizing the Hamiltonian shows that $\|\mathcal{H}_z\|$ is larger for the A_1 states than for any other representation, so equation (III.27) implies that, if one averaged over all possible operators $\mathcal{H}_p$, the A_1 transitions would peak at the smallest values of $\Delta\tau_p'$. However, this need not be true for each possible $\mathcal{H}_p$.

5.2.1.1 Signal Gains

The maximum observed signal gain for the side peaks relative to totally nonselective excitation is the gain of 5.6 in Figure V.5(b). The true maximum gain may be larger than this, since a small change in $\Delta\tau_p'$ from 34 μsec might produce a larger value. The maximum theoretical gain may be estimated by dividing up the total available intensity (which is the same as the equilibrium magnetization, $\beta\ \mathrm{Tr}(I_z^2)$)

equally among all of the pumped density matrix elements in the A_1 manifold. There are 13 A_1 states, so there are 169 matrix elements, but time-reversal symmetry in the M=0 manifold forces all 6 zero-quantum transitions in that manifold plus the three populations to vanish in the nonselective experiment. (All of the A_1 M=0 states are gerade. The density matrix in equation (II.31) only connects gerade to ungerade in the M=0 manifold, so no zero-quantum coherences are produced).[65,79] A four-quantum selective propagator will transfer some of $\beta\ \mathrm{Tr}(I_z^2)$ from ten of the populations ($M = \pm 3, \pm 2, \pm 1$) to the fourteen four-quantum coherences using only terms linear in $\Delta\tau_p'$. Only 24 matrix elements are involved, and if they are all roughly equal, the expected gain is $160/24 \sim 6.7$.

However, it is clear from the spectra in Figure V.5 that some zero-quantum coherences are also produced. This is to be expected because four-quantum operators proportional to $\Delta\tau_p'$ in the propagator imply zero-quantum and four-quantum operators proportional to $(\Delta\tau_p')^2$. There are 12 zero-quantum coherences which can be pumped, and if these are pumped as strongly as the four-quantum coherences the maximum gain falls to 4.4.

The largest enhancement observed for the four-quantum center line is the factor of 19 in Figure V.5(c). This gain cannot be readily compared to the theoretical gain because this peak corresponds to six different transitions in the different irreducible representations. In addition, the TPPI method of separating the different orders of coherence can produce artifact peaks if the phase shifts are imperfect. In this experiment, the TPPI increment was $\pi/8$ (i.e., each pulse in

the preparation period had its phase incremented by $\pi/8$ every time t_1 was incremented) and this could give artifacts only at the center of the four-quantum spectrum. The central peak has no dipolar information so a distorted intensity does not affect the analysis.

Figure V.5(f) shows an ensemble averaged nonselective experiment (using the pulse sequence in Figure II.2(b)) with $\Delta\omega=0$. $\mathcal{H}_x$ has only even-quantum coherences, so a partially selective spectrum is produced. Comparison of parts (a)-(e) with part (f) shows that the selective experiment does not distort line positions. Residual pulse errors increase the noise level of the selective experiment, but the signal-to-noise ratio of the four-quantum lines in parts (a) and (b) is still substantially better than could be achieved nonselectively in equal time.

5.2.1.2 Selectivity Improvement

The first nonselective term in the effective Hamiltonian for a zero-order selective sequence is proportional to $(\Delta\tau_p')$. If $\Delta\tau_p'$ is cut in half but the number of subcycles is doubled, this term will be cut in half. The selective term will be unaffected. Thus, the selectivity of a zero-order sequence can be made arbitrarily good by making $\Delta\tau_p'$ small and repeating the sequence many times. This is illustrated in Figures V.6(a)-(c). In this experiment t_p = 5.9 μsec, τ = 6.0 μsec, τ' = 18.2 μsec, and T = 576 μsec, so $\mathcal{H}_o$ is different from the sequences in Figure V.5. The selective term should be identical for each of the three spectra, and this is confirmed in parts (a) and (b). The four-quantum regions are virtually identical for these two spectra (this particular choice of pulse sequence parameters happens to pump two of the pairs more strongly than the

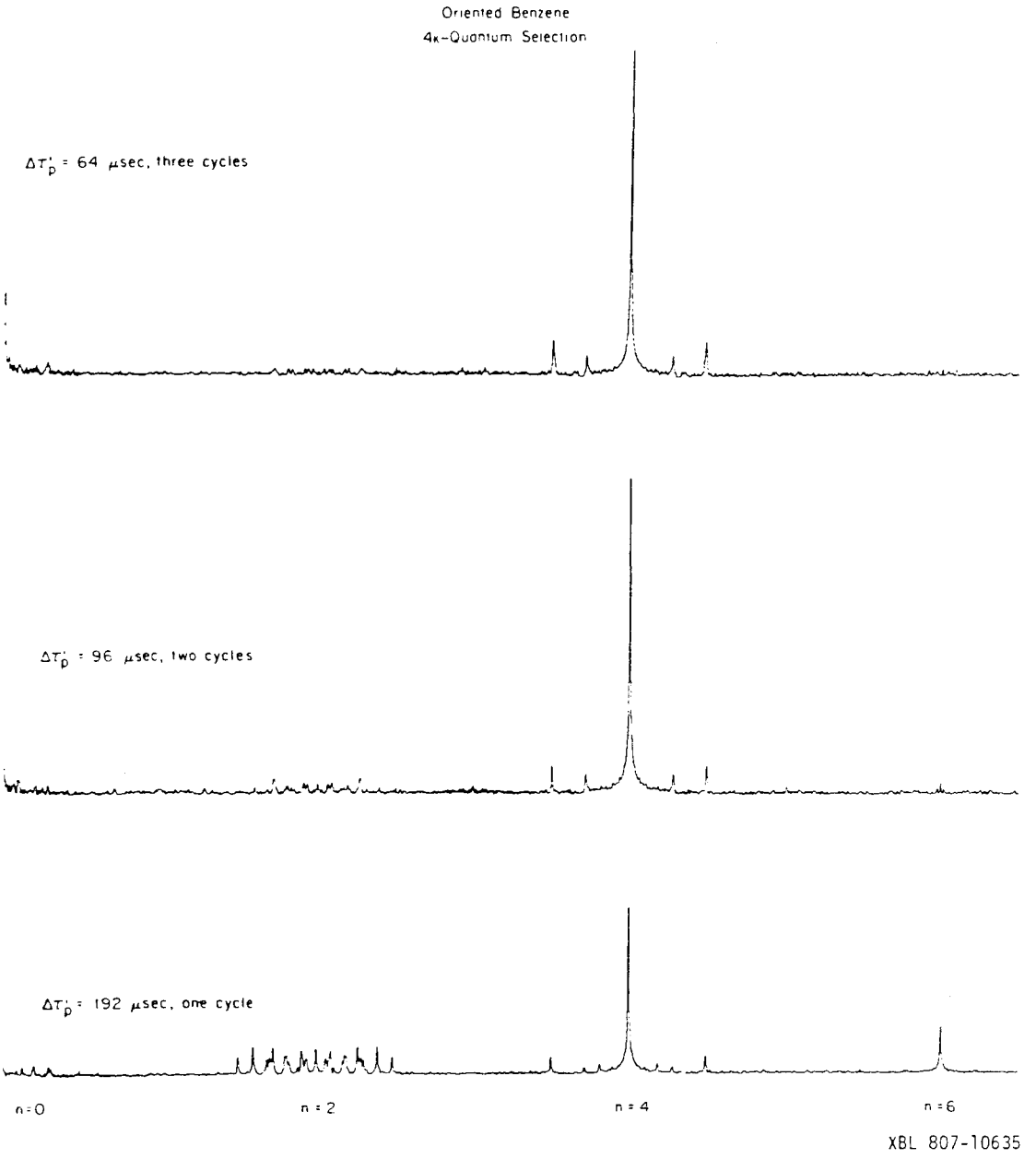

Figure V.6. The effects of increasing the cycle time and reducing the number of cycles. Average Hamiltonian theory predicts that this will not change the selective terms but will increase the nonselective terms. Pulse sequence parameters are given in the text.

the third) except that the four-quantum transitions are slightly weaker in part (b) as the reduced selectivity produces some two-quantum transitions. In part (c) the selectivity has almost disappeared.

Figures V.4-6 show that suppression of two-quantum coherences is substantially easier than suppression of six-quantum coherences. This result is expected if the phase shifts are imperfect. If the phase of the ith subcycle is $\phi_i + \varepsilon_i$ instead of the ideal value ϕ_i, a nonselected coherence ($\Delta M \neq nk$) is multiplied by $(\Sigma \exp(i(\Delta M)(\phi_i + \varepsilon_i)))/n$ instead of 0. If $\varepsilon_i << 1$ this is approximately equal in magnitude to $(\Delta M) <\varepsilon_i^2>^{1/2}/n^{1/2}$, so the error term is three times worse for $\Delta M=6$ than for $\Delta M=2$. Fortunately, most of the allowed coherences correspond to small values of ΔM and are relatively insensitive to phase errors.

5.2.2 Four-Quantum Selection with Simplified Sequences

As explained in chapters III and IV, a WAHUHA sequence (or any other line narrowing sequence) can be used for $\mathcal{H}_o$. This makes a zero-order 4k-quantum selective sequence with only 16 pulses, instead of the several hundred pulses of each sequence in Figure V.4-6. Figure V.7 shows that this selection works, and also shows that the choice of T is critical. When T = 50 μsec almost nothing is produced; T = 100 μsec is selective in all the representations; and larger values produce a large central four-quantum peak, with the selectivity slowly dying away.

5.2.3 Six-Quantum Selection; Coherent Initial Conditions

A 6k-quantum selective sequence can be generated by setting $\phi = 2\pi/6$ in Figure III.2(a). If this sequence is applied to benzene at equilibrium (initial density matrix proportional to I_z), it connects

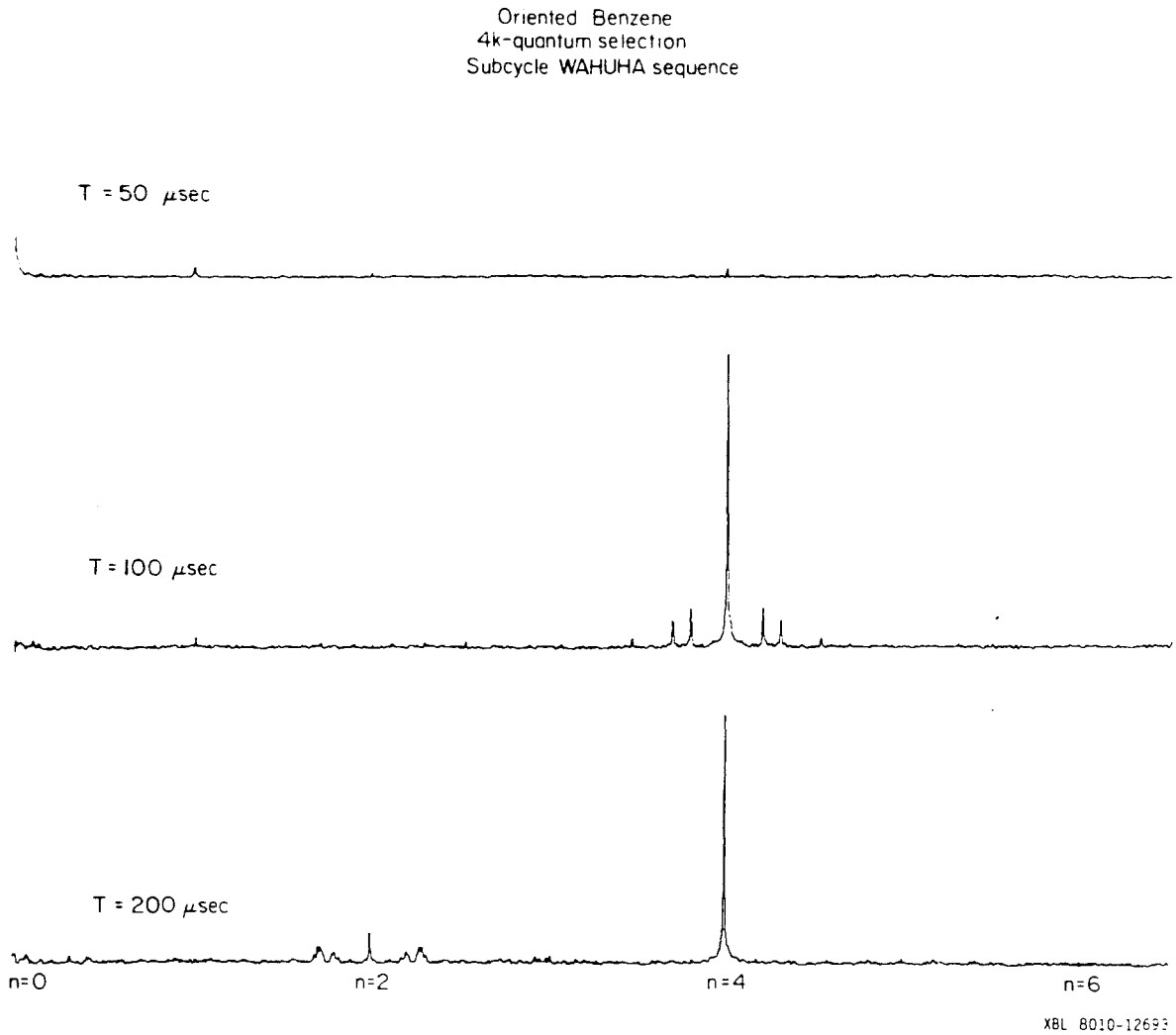

Figure V.7 Four-quantum selection without time reversal. Here $\mathcal{H}_o$ is a WAHUHA sequence, as in Figure III.4(b), with T the short interval between pulses. As expected from section 4.6 the value of T is critical. The pulse width is 5 μsec, and therefore the duty cycle is low.

only the states with $|M|=3$ and creates an effective two level system. The six-quantum spectrum which is generated has only one transition, as illustrated in Figure V.8(a). However, if the initial density matrix is made proportional to I_x by adding one pulse before the selective sequence begins, a 6k-quantum selective propagator will produce only one-quantum and five-quantum coherences. These coherences can be detected by the same 6k-quantum selective sequence if the final pulse of the sequence is removed, and the spectrum is shown in Figure V.8(b).

The residual nonselective coherences are not completely suppressed for 6k-quantum selection, because the phase shifter is a digital device which only allows shifts in exact multiples of $2\pi/256$. A zero-order sequence was approximated by ϕ values of $(0, 43\pi/128, 85\pi/128, \pi, 171\pi/128, 213\pi/128)$ instead of $(0, \pi/3, 2\pi/3, \pi, 4\pi/3, 5\pi/3)$. This approximation leaves a small amount of non-6k-quantum selective operators in the zero-order term. However, the figure shows that even with this approximate sequence fairly good selectivity can be achieved.

Figure V.9 shows the six-quantum signal as a function of $\Delta\tau_p'$. If the time reversal is perfect, the signal is zero when $\Delta\tau_p' = 0$, and follows a $\sin^2$ pattern as long as the selectivity is good. The experimental points show substantial deviations from a $\sin^2$ pattern for long values of $\Delta\tau_p'$, which have low selectivity. In addition, the nonzero value as $\Delta\tau_p' \to 0$ in the figure shows that time reversal with this sequence ($t_p = \tau = 4.5$ μ sec, $T = 672$ μ sec, six subcycles) is imperfect, yet good selectivity can still be achieved. This has great practical significance, especially in isotropic systems.

5.2.4 Symmetry Selection

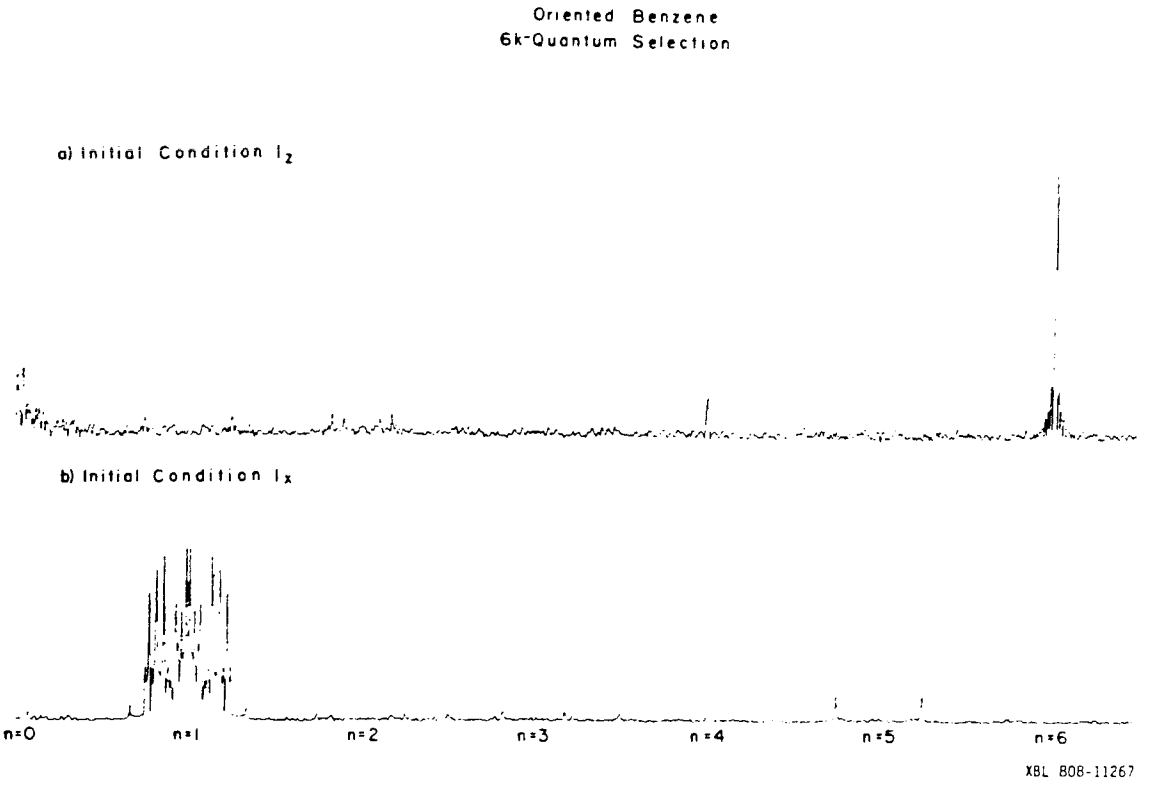

Figure V.8 Spectra with 6k-quantum selection on oriented benzene. If the initial density matrix is at equilibrium, as in part (a), only the six-quantum coherence is produced. If the initial density matrix is made proportional to I_x by one pulse as in part (b), one-quantum and five-quantum coherences are produced. In both of these cases one cycle of 6k-quantum selection was applied.

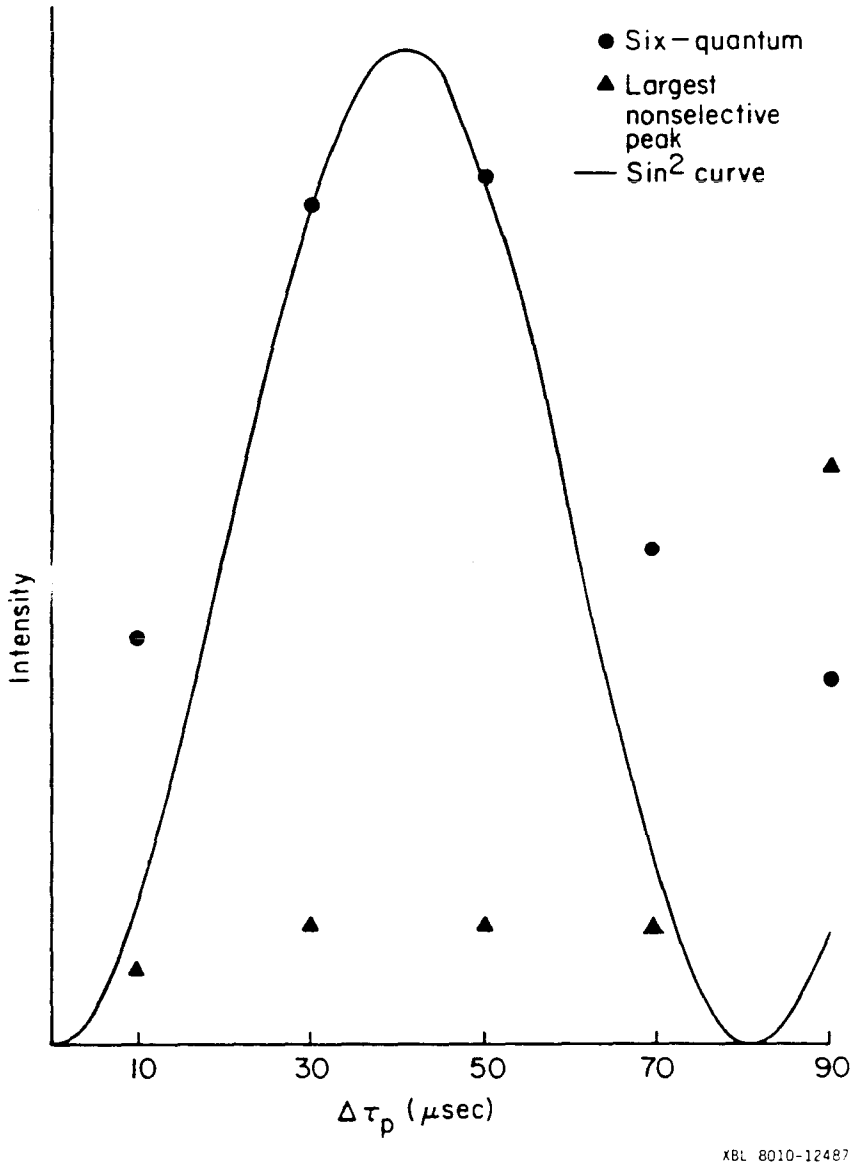

Figure V.9 The six-quantum signal magnitude as a function of $\Delta\tau_p'$. Pulse sequence parameters are t_p = 4.5 μsec, τ = 4.5 μsec, and T = 672 μsec. With perfect time reversal this should follow a $\sin^2$ pattern, as in Figure IV.7. Good selectivity is possible even without perfect time reversal.

The single six-quantum coherence in benzene has A_1 symmetry, as does the single N-quantum transition in any N-spin system. Therefore, a 6k-quantum selective sequence applied to an equilibrium density matrix perturbs only A_1 states; all other representations are unaffected. If a single pulse is applied immediately after the selective sequence, A_1 transitions corresponding to all possible values of ΔM are produced, but non-A_1 appear only if $\Delta M=1$, since the density matrix in all other representations is proportional to I_x or I_y. Such a sequence therefore selectively prepares A_1 multiple-quantum transitions, and at the end of the evolution period, a single pulse followed by a 6k-quantum selective sequence selective detects A_1 transitions. The resulting spectrum is shown in Figure V.10. One pair of non-A_1 transitions is visible in the three-quantum spectrum; this pair corresponds to two nearly degenerate sets of transitions from the E_1 and E_2 manifolds, and is fairly intense in the nonselective spectrum. Except for this pair, all of the observed lines correspond to known A_1 transitions.

Therefore 4k-quantum selection, 6k-quantum selection, and A_1 selection can be readily demonstrated in oriented benzene. Nonselective terms can be made very small, and the signal gain from selectivity is approximately equal to the theoretical predictions. The behavior as $\Delta\tau_p'$ or the number of cycles is varied is consistent with predictions from average Hamiltonian theory for a zero-order selective sequence.

5.3 Experimental Results: Oriented 1-Bromobutane

5.3.1 Four-Quantum Selection

Benzene is a small and highly symmetric molecule, so nonselective

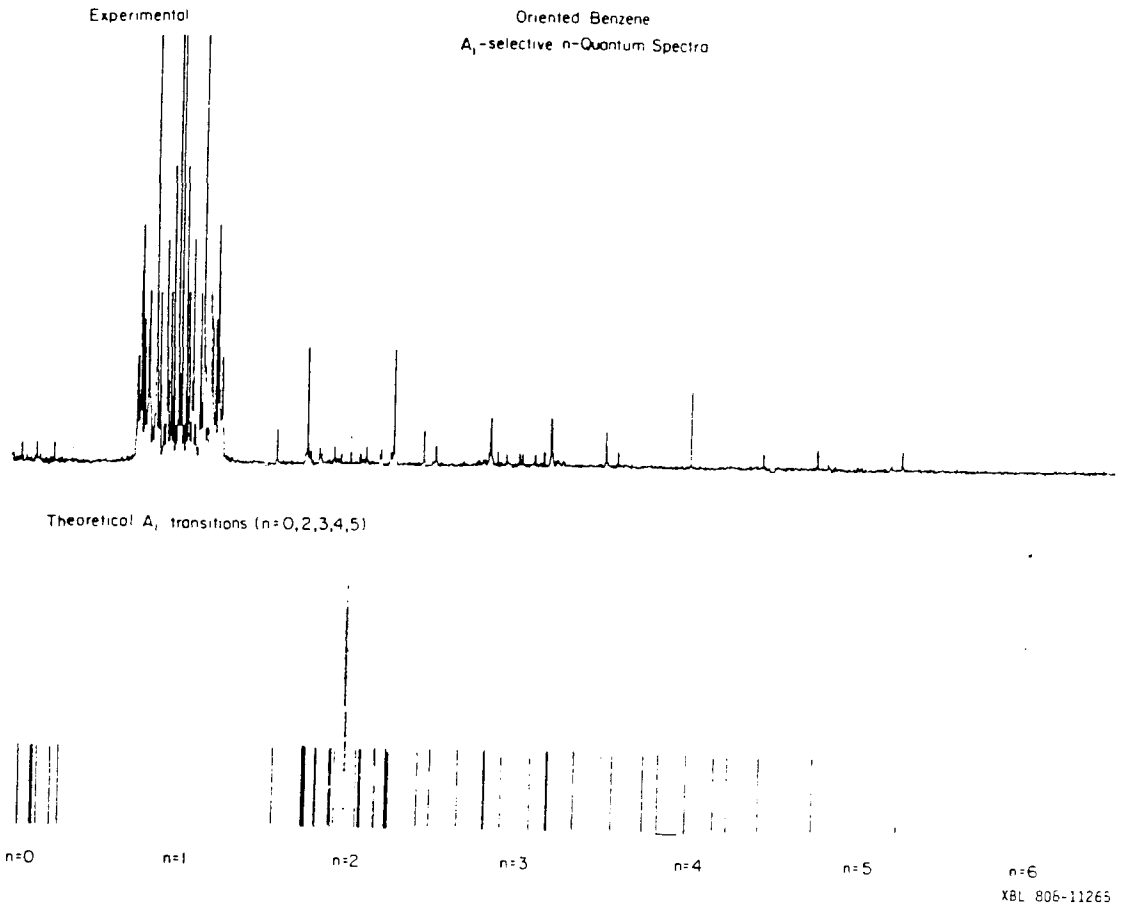

Figure V.10 A_1 symmetry selection on oriented benzene. 6k-quantum selection produces a density matrix which is at equilibrium in all manifolds except for A_1, so one additional pulse gives only single-quantum coherences in these manifolds, but multiple-quantum A_1 coherences. To detect these coherences one additional pulse is applied immediately before the mixing sequence.

multiple-quantum spectra are perfectly adequate. However, the signal available for any individual transition in the absence of molecular symmetry is proportional to 4^{-N}, where N is the number of spins in the molecule. Thus, an unsymmetrical seven-spin molecule requires 16 times as many signal measurements as does an unsymmetrical six-spin molecule to achieve the same signal-to-noise ratio.

This problem is illustrated in Figure V.11 with the nonselective multiple-quantum and eight-quantum spectra of this nine-spin system are expected to reflect internal motion of the chain.[81] However, these spectra are essentially unobservable, since there are many more transitions in the one-quantum and two-quantum spectra. Extensive averaging of nonselective spectra has confirmed that they are weak.

The energy level distribution for n-butyl bromide[80,81] is shown in Figure V.12. There are 144 A x A states, which produce four pairs of eight-quantum transitions and 19 pairs of seven-quantum transitions (there are three more pairs of seven-quantum transitions in the other representations). Nonselective excitation divides the total signal among 144^2 = 20736 matrix elements. 4k-quantum selection pumps the 16 matrix elements with $\Delta M = \pm 8$, the 1816 matrix elements with $\Delta M = \pm 4$, and the 3352 matrix elements with $\Delta M = 0$ for a gain of 4.0 in the A_1 manifold. Similar gains are found in the other manifolds. Figures V.13-14 show the results of 4k-quantum selection on this system. The actual enhancement is in fact somewhat better than 4.0, because the zero-quantum matrix elements are not strongly driven. If they are neglected, the expected gain is 10.5 (the populations cannot be neglected). The actual gain is somewhere in this range.

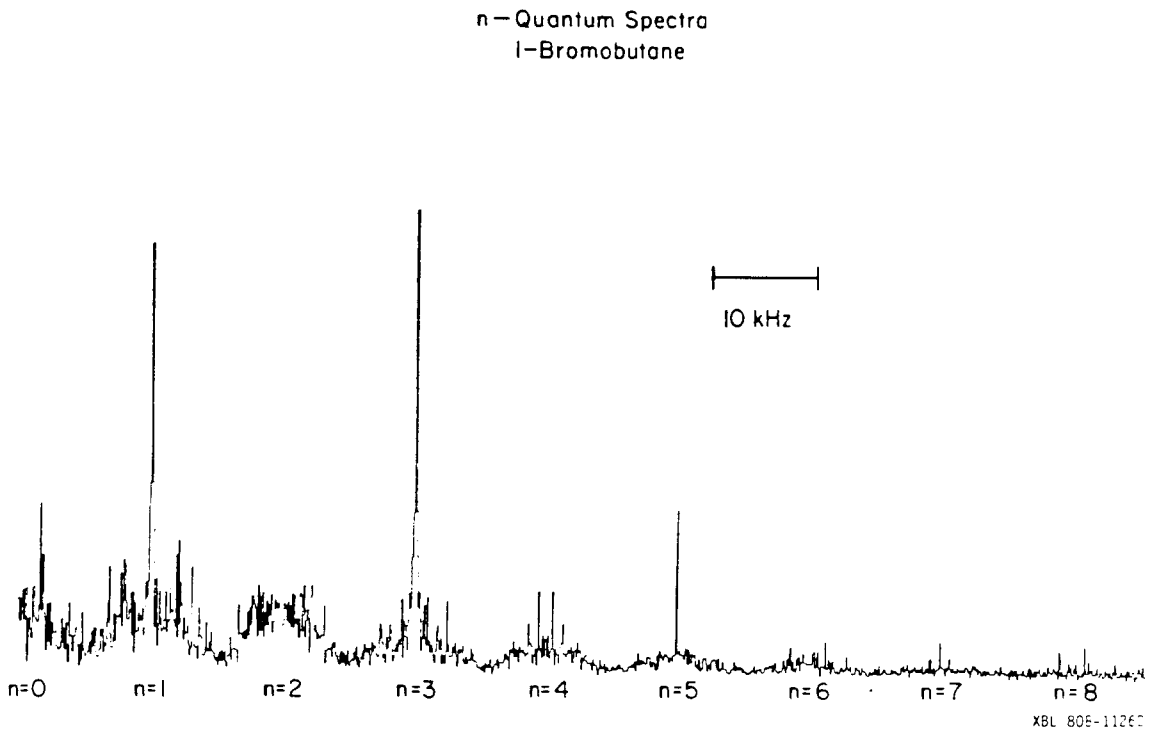

Figure V.11 Nonselective multiple-quantum spectra of 1-bromobutane. The signal intensity for the large values of ΔM is extremely small. This spectrum corresponds to $\Delta\omega=0$ and $\tau=4.0$ msec.

1-BROMOBUTANE ENERGY LEVEL DIAGRAM
SYMMETRY ADAPTED STATES

	A x A	A x B	E x A	E x B
M = 9/2	1	0	0	0
M = 7/2	4	3	2	0
M = 5/2	13	9	4	3
M = 3/2	23	19	12	9
M = 1/2	31	25	19	16
M = -1/2	31	25	19	16
M = -3/2	23	19	12	9
M = -5/2	13	9	4	3
M = -7/2	4	3	2	0
M = -9/2	1	0	0	0

Figure V.12 Energy level diagram for 1-bromobutane. The methyl group has A states and E states; the remaining six spins have A states and B states. There are 512 energy levels and many allowed single-quantum transitions. Note, however, that there is only one nine-quantum transition and there are only four pairs of eight-quantum transitions.

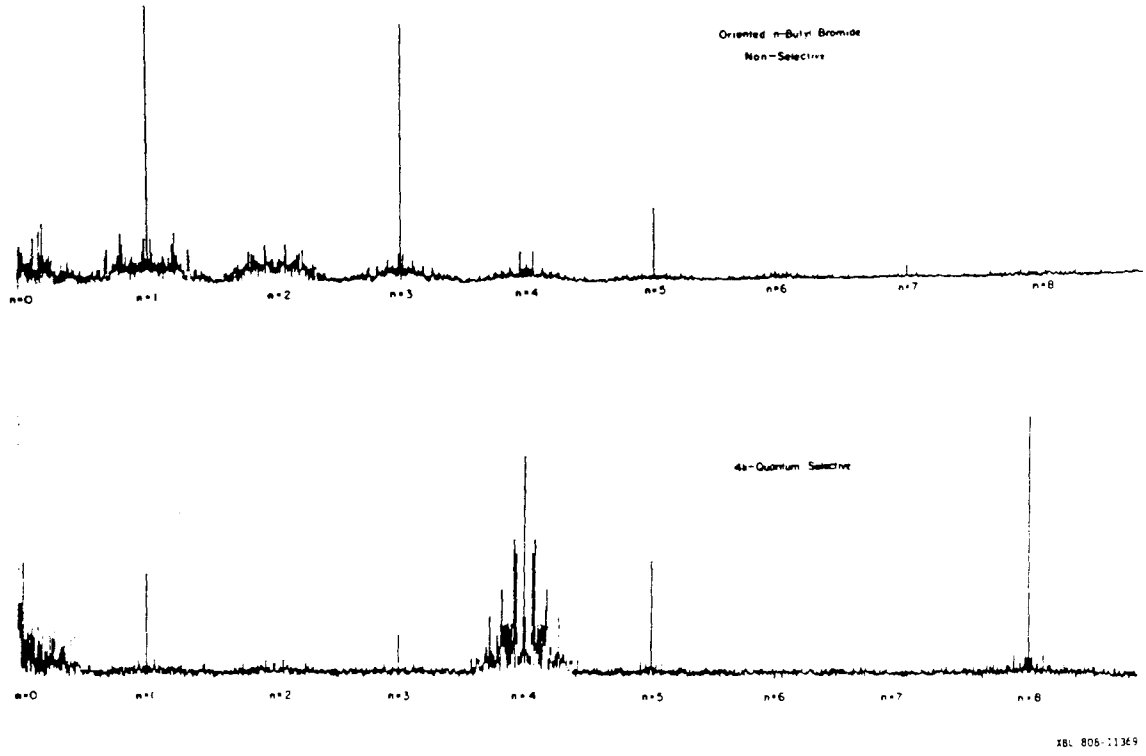

Figure V.13 Comparison of 4k-quantum selective spectra (part (b)) with the nonselective spectrum of Figure V.11 (part (a)). The four-quantum transitions are strongly enhanced.

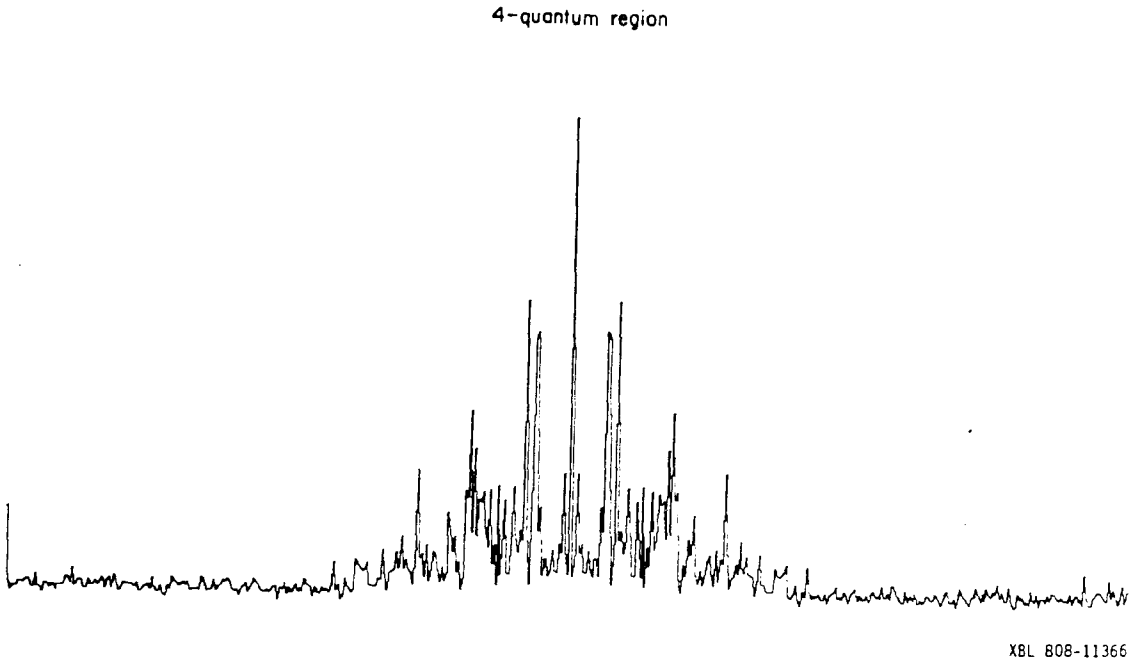

Figure V.14 Enlargement of the four-quantum region of Figure V.13(b). The pulse sequence included two cycles of 4k-quantum selection with $\Delta\tau_p' = 15$ μsec, $t_p = 3.5$ μsec, $\tau = 4.2$ μsec, $T = 720$ μsec.

5.3.2 Eight-Quantum Selection

Ideal eight-quantum selective excitation would involve only 16 eight-quantum coherences, the populations of the ten states with $|M| = 9/2$ or $|M| = 7/2$ (no other states are connected by eight-quantum operators) and 24 zero-quantum coherences for a total of 50 matrix elements. The available signal is the fraction of $\beta\ \mathrm{Tr}(I_z^2)$ in the ten selected populations, which is 33% of the total. The net result is a predicted maximum signal gain of 137, which reduces the signal accumulation time by a factor of 18,700. This tremendous gain would probably require high-order selective pulse sequences and suppression of zero-quantum coherences. Nonetheless, even a zero-order selective sequence should give a large enhancement.

Figures V.15-16 show the results of averaging only four 8k-quantum selective spectra ($\phi = \pi/4$ in Figure V.2). The TPPI increment is $\pi/16$ for these spectra so that inaccurate phase shifts are expected to produce a large central spike in the eight-quantum region. At least three of the four expected pairs can be seen. The chain has many allowed conformations, so very little information can be extracted from these few lines, and the seven-quantum spectrum will also be required. This spectrum can be obtained in two fundamentally different ways. A seven-quantum selective propagator can be designed by setting $\phi = 2\pi/7$ in Figure V.2. Since $\mathcal{H}_o$ in Figure V.2 is even-quantum selective, some change has to be made in the sequence; one possibility would be to put a 45° pulse immediately before $\Delta\tau_p'$, and another 45° pulse with opposite phase immediately after $\Delta\tau_p'$. This sequence would pump all 22 pairs of seven-quantum

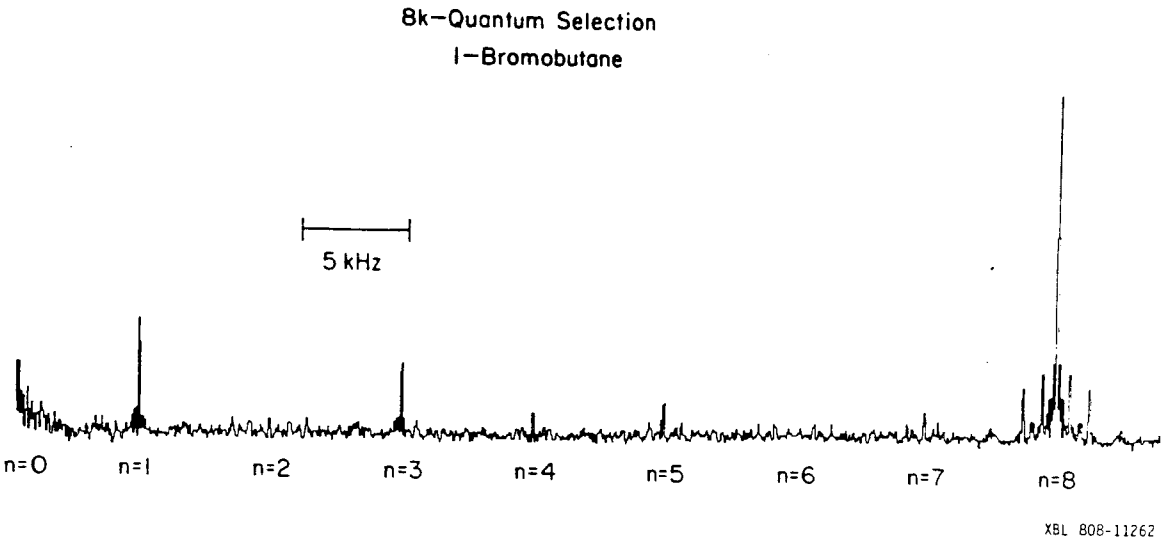

Figure V.15 The effects of 8k-quantum selection on 1-bromobutane. The signal scale is the same as in Figure V.11. Four spectra with different pulse sequence parameters were averaged together.

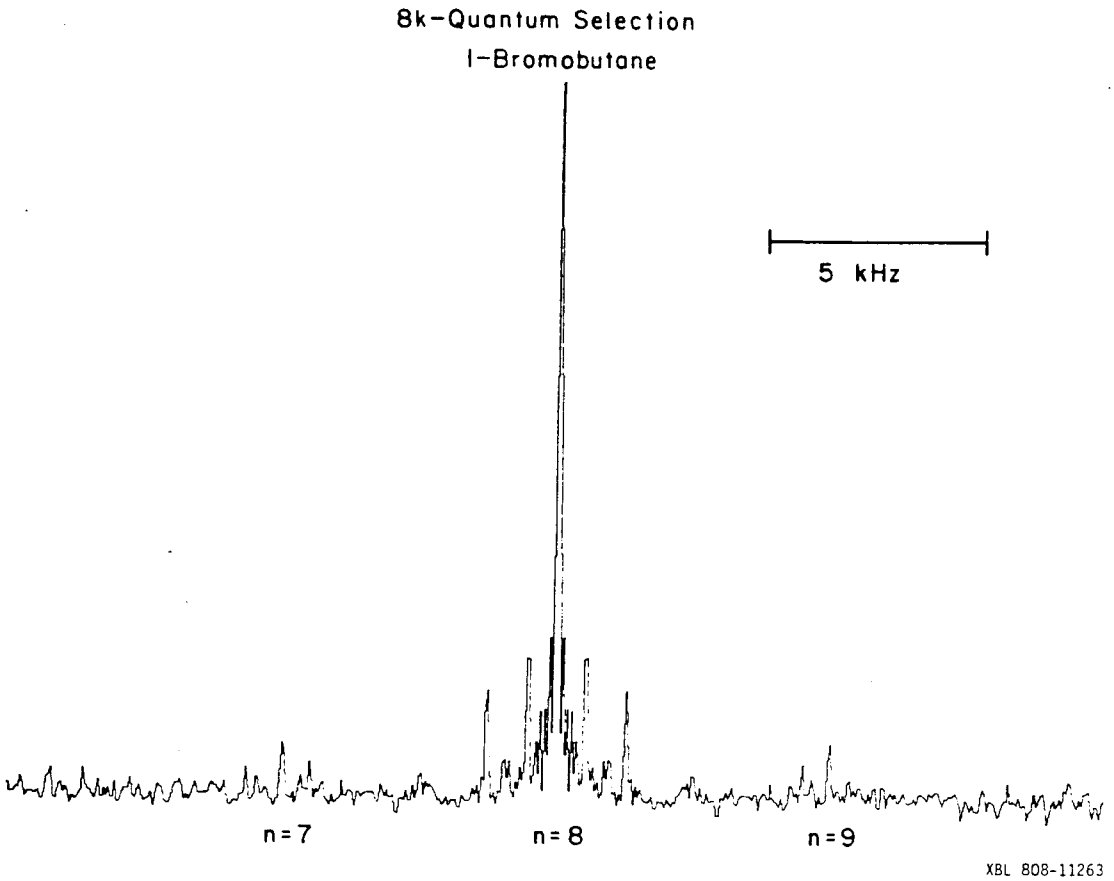

Figure V.16 The eight-quantum region of the selective 1-bromobutane spectrum of Figure V.15. At least three of the four expected pairs are visible above the noise level.

lines. An alternative approach would be to use an eight-quantum selective pulse sequence starting with a density matrix proportional to I_x instead of I_z. Since only the A_1 representation can have eight-quantum operators, only the 19 pairs of A_1 seven-quantum transitions, the single nine-quantum transition, and one-quantum transitions will be produced. The first approach will probably give the larger signal gain.

5.4 Experimental Results: Cyclopentane

Cyclopentane undergoes very rapid pseudorotation at room temperature,[82] so only an averaged structure with C_{5v} symmetry should be observable in an NMR experiment. However, the ratios of the coupling constants should reflect the amplitude of the out-of-plane displacements. The four-quantum spectrum can be obtained by selective sequences, as shown in Figure V.17. Since there are many four-quantum transitions in this ten-spin system the spectrum is not resolvable, and higher-quantum selection will be required.

5.5 Conclusions

Selective excitation sequences have been presented for four-, six-, and eight-quantum transitions. These sequences produce large signal enhancements and make multiple-quantum NMR a practical technique for a wide range of hitherto inaccessible molecules. The effects of changing pulse sequence parameters agree with predictions based on average Hamiltonian theory, which suggests that more sophisticated pulse sequences selective to higher order will be able to provide further signal enhancement.

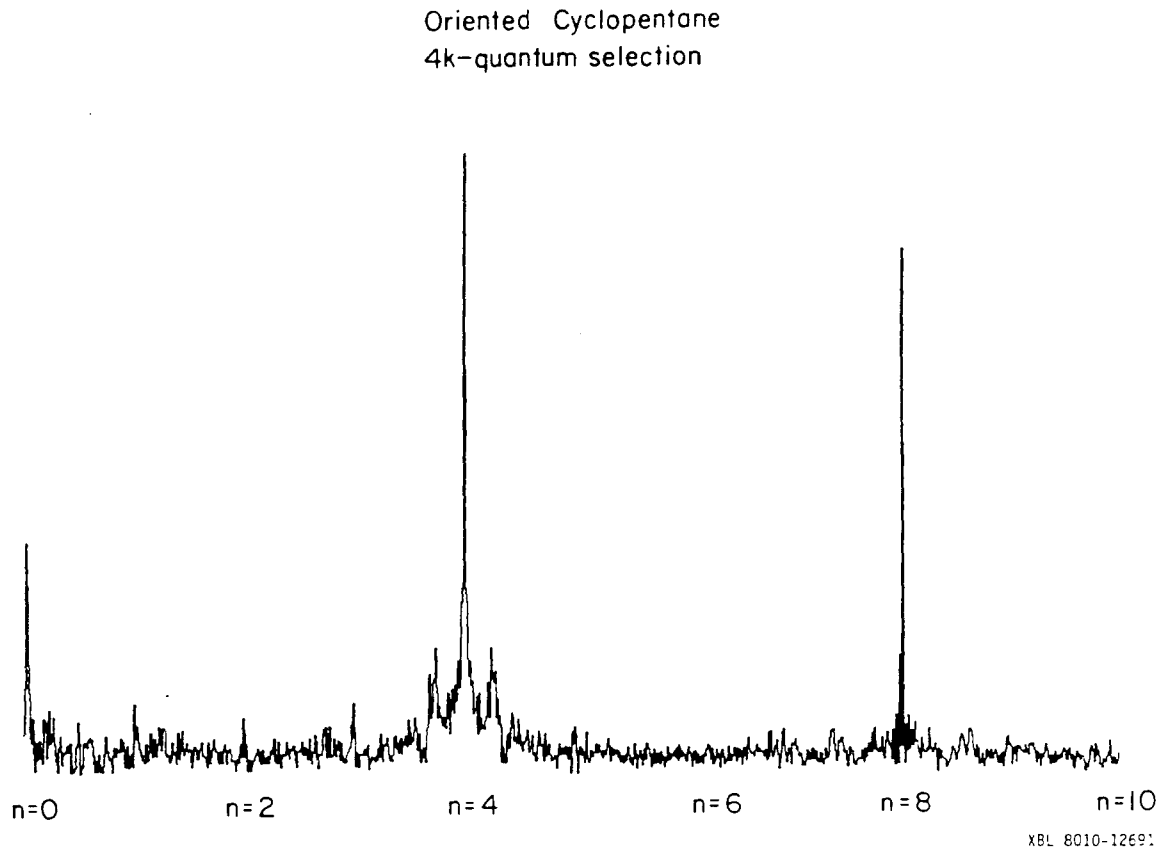

Figure V.17 Four-quantum selection on cyclopentane. The four-quantum spectrum has many allowed transitions, and therefore is not resolvable. Pulse sequence parameters are $\Delta\tau_p' = 25$ μsec, $t_p = 5.0$ μsec, $\tau = 4.7$ μsec, T = 941 μsec, and eight subcycles.

VI. Other Topics in Multiple-Quantum NMR

6.1 Two-Dimensional Techniques

Multiple-quantum NMR is just one example of a broader class of experiments, known as two dimensional spectroscopy.[32,83] A generalized two-dimensional sequence has the same preparation, evolution and mixing periods as in Chapter II and Figure II.9. However, the restriction of taking data at only one value of t_2 is dropped. Frequently, in fact, enough points are taken in t_2 to permit a second Fourier transformation. This technique has numerous applications. One example of a two-dimensional spectrum is given in Figure VI.1.[84]

In this section, two-dimensional spectroscopy will only be considered as a signal enhancement technique. Suppse that $\langle I_x \rangle$ and $\langle I_y \rangle$ are sampled at two distinct values of t_2 to produce two multiple-quantum spectra. Line positions are governed only by the evolution in t_1 so these spectra can be averaged together. Clearly the signal-to-noise ratio is no worse than if one value of t_2 were saved, and it may be better. This can of course be generalized to taking n points. The important questions are:

1. How many points should be taken?
2. Should all points be weighted equally?
3. What is the attainable signal-to-noise improvement?

The signal as a function of t_2 can be written as

$$\langle I_y(t_2) \rangle = -C\beta \mathrm{Tr}(I_x \exp(-i\mathcal{H}_z t_2) V \exp(-i\mathcal{H}_2 t_1) U I_z U^\dagger \exp(i\mathcal{H}_z t_1) V^\dagger \exp(i\mathcal{H}_2 t_2))$$

$$= -C\beta \sum_{i,j} (U I_z U^\dagger)_{ij} (V^\dagger \exp(i\mathcal{H}_z t_2) I_y \exp(-i\mathcal{H}_z t_2) V)_{ji} \, e^{i\omega_{ij} t_1} \tag{VI.2}$$

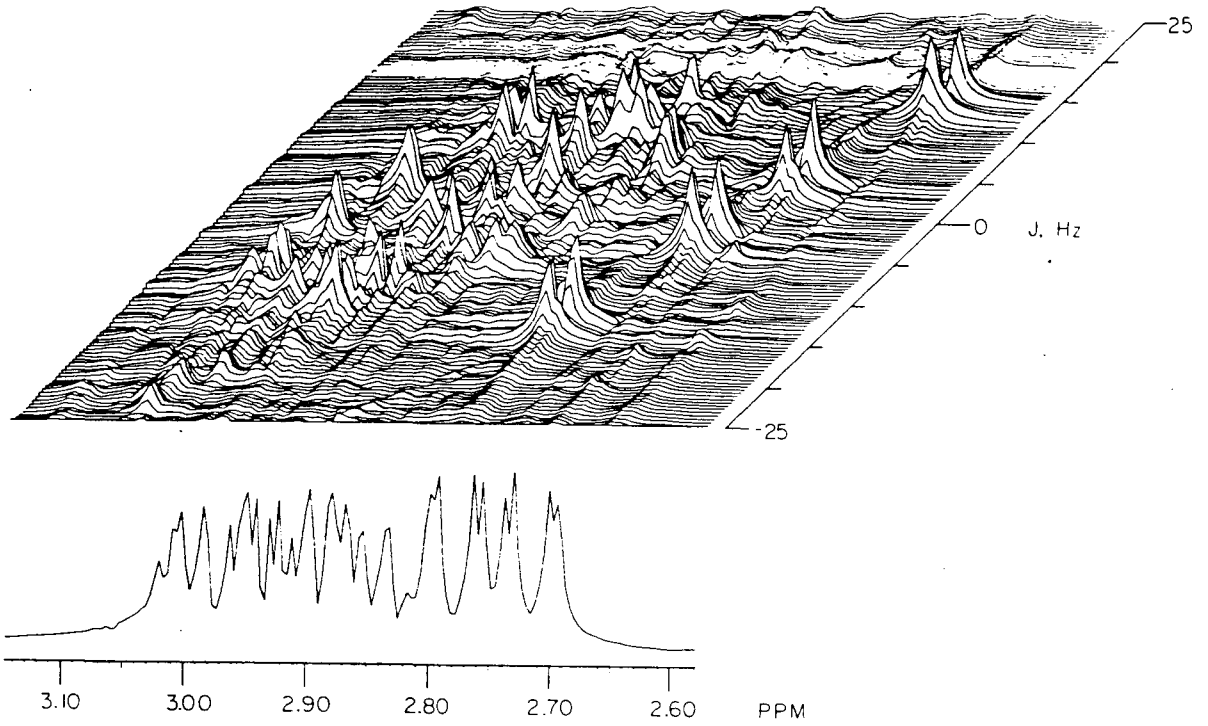

XBL 799-11391

Figure VI.1 A sample two-dimensional spectrum. This is a two-dimensional J spectrum of Cyclo-[3-(4-β-aminoethyl)phenyloxypropanoyl-L-prolyl], not a multiple-quantum spectrum, but the signal/noise arguments are exactly the same. (Figure courtesy of Drs. Willy Shih and Mel Klein).

A similar expression can be written for I_x. The differences between equations (VI.2) and (II.62) arise solely from the inclusion of the case $t_2 \neq 0$ here; if $t_2 = 0$ they are identical except for the fictitious pulse in section 2.2.3.3 which allows I_z to be sampled. The integrated intensity of the multiple-quantum transitions is maximized when $|(UI_zU^\dagger)|_{ij} = |(V^\dagger \exp(i\mathcal{H}_z t_2) I_x \exp(-i\mathcal{H}_z t_2)V|_{ji}$. For example, this condition is satisfied if

$$U = V^\dagger \exp(i\mathcal{H}_z t_2) \exp(i\pi I_y/2) \tag{VI.3}$$

but if equation (VI.3) holds for one particular value of t_2 it is violated for other values. To go any further requires some assumptions about the nature of U and V.

6.1.1 Nonselective Experiments

In the simplest nonselective experiments (Figure II.1b) $V = \exp(i\pi I_y/2)$ and $U = \exp(-i\mathcal{H}_x\tau)$. The signal is maximized if $t_2 = \pm\tau$. Time reversal does not affect the solution, so only $t_2 > 0$ will be considered. One can write:

$$\rho_{MQ}(-t_2) = V^\dagger \exp(i\mathcal{H}_z t_2) I_z \exp(-i\mathcal{H}_z t_2) V = \exp(i\mathcal{H}_x t_2) I_z \exp(-i\mathcal{H}_x t_2)$$

$$\rho_{MQ}(\tau) = UI_zU^\dagger = \exp(-i\mathcal{H}_x\tau) I_z \exp(i\mathcal{H}_x\tau) \tag{VI.4}$$

as in equation (II.34). If $\|\mathcal{H}_x(\tau-t_2)\| \ll 1$ or $\|\mathcal{H}_x(\tau+t_2)\| \ll 1$ then the magnitudes of all matrix elements of $\rho_{MQ}(-t_2)$ are very near their optimum values, and the signal is nearly as large as at $\tau = \pm t_2$. However, if $\|\mathcal{H}_x(\tau-t_2)\| \gtrsim 1$ and $\|\mathcal{H}_x(\tau+t_2)\| \gtrsim 1$ then the magnitudes of the matrix elements of $\rho_{MQ}(-t_2)$ have changed substantially. The

expressions for the signal are:

$$S(\tau \sim \pm t_2) = -C\ \beta \sum_{ij} |\rho_{MQ}(\tau)|^2_{ij} = -C\ \beta\ \mathrm{Tr}(\rho_{MQ}(\tau)^2) \tag{VI.5}$$

$$\langle S(\tau \neq \pm t_2)\rangle = -C\ \beta \sum_{ij} \langle|\rho_{MQ}(\tau)|_{ij}\rangle^2 \tag{VI.6}$$

(VI.6) is smaller than (VI.5), but generally it is not much smaller. The simplest assumption would be that the magnitude of each matrix element of $\rho_{MQ}(\tau)$ has a one-dimensional Gaussian probability distribution, which gives

$$\langle S(\tau \neq \pm t_2)\rangle = (2/\pi)\ S(\tau \sim \pm t_2) \tag{VI.7}$$

The signal is down by less than a factor of 1.6. In a large anisotropic system this random assumption is probably reasonable, since so many different operators are involved in the propagator. In fact computer calculations suggest that the situation may be even more favorable.[66] At any rate it is clearly advantageous to take many values of t_2 other than just $t_2 \sim \tau$.

Relaxation has been neglected in these calculations, but the effects are easily included if each coherence is assumed to dephase with the same value of T_2. In this case

$$\rho_{MQ}(\tau) = e^{-\tau/T_2} \exp(-i\mathcal{H}_x\tau) I_z \exp(i\mathcal{H}_x\tau) + \beta I_x(1-e^{-\tau/T_1}) \tag{VI.8}$$

$$\rho_{MQ}(-t_2) = e^{-t_2/T_2} \exp(i\mathcal{H}_x t_2) I_z \exp(-i\mathcal{H}_x t_2) + \beta I_x(1-e^{-t_2/T_1}) \tag{VI.9}$$

If $t_2 \gtrsim T_2$ the signal drops off substantially and further data points are not very useful. The optimal spacing of retained points in t_2 depends on the noise bandwidth $\Delta\omega_n$, since two data points separated by less than $1/\Delta\omega_n$ will have strongly correlated noise levels, and this correlation means that the signal-to-noise ratio is not improved by averaging them together. It is therefore reasonable to take about $(T_2\Delta\omega_n)$ data points, and the expected signal-to-noise gain is roughly

$$g_{2-D} \sim (1 + .4\ T_2\ \Delta\omega_n)^{1/2} \qquad \text{(VI.10)}$$

assuming equation (VI.7). The optimum value for $\Delta\omega_n$ is the single-quantum spectral width, so the gain is about the square root of the ratio of the width of the spectrum to the width of a single transition.

6.1.2 The Second Fourier Transformation; Optimal Filtering

The discussion so far has centered around the signal gain obtainable by averaging together multiple-quantum spectra corresponding to several different values of t_2. In a true two-dimensional experiment, such as the one illustrated in Figure VI.1, a second Fourier transform is applied with respect to t_2. The phases of the peaks in the two-dimensional spectrum vary enormously, and therefore are presented in magnitude mode or corrected by adding together several spectra with phase shifted pulses.[32,83]

Suppose that data accumulation in t_2 begins at $t_2 = \tau$. Then the normal (i.e., only $t_2=\tau$) multiple-quantum spectrum correspond to an integral over ω_2 in the uncorrected two-dimensional spectrum. Since the peaks are not in phase most of the intensity cancels out. If all values of ω_2 correspond to equal amounts of signal, and all the

phases are random, then magnitude correction followed by integration over ω_2 would be expected to increase the signal/noise ratio by the square root of the number of points in ω_2, which agrees with the estimate in (VI.10).

In fact, not all values of ω_2 are equally good. For example, if the single-quantum spectrum contains resolved lines, then values of ω_2 which do not correspond to those lines have no signal. This can be seen in Figure VI.1. The optimum signal/noise ratio can be shown to be produced when each value of ω_2 is assigned a weighting factor equal to the total signal intensity of that value. This is equivalent to applying an optimal filter in t_2, instead of merely setting the filtering bandwidth equal to the single-quantum spectral width. Most large molecules will not have much structure in the single-quantum spectrum, and therefore this process does not improve the signal/noise ratio substantially.

It should be noted that there are cases for which two-dimensional spectroscopy is not very useful in improving signal/noise ratios. For example, it will not be very useful when the dominant noise factor is spectrometer instabilities over the long interval which separates points in t_1. In addition, there are some systems which do not have signal for $t_2 \neq \pm\tau$ that is as large as shown in equation (VI.7). For example, the expression for the N-quantum coherence magnitude of an isotropic first-order system with N spins-1/2 (equation (II.55)) gives

$$<|\rho_{MQ}(\tau)|^2>_{N/2,-N/2} = (\frac{\pi^2}{8})^N \quad <|\rho_{MQ}(\tau)|>^2_{N/2,-N/2} \qquad \text{(VI.11)}$$

so that if N is large, $t_2 = \pm\tau$ can be much better than $t_2 \neq \pm\tau$, and

the expected gain is reduced. The N-quantum coherence in a system with A_N symmetry (equation (II.57)) presents a slightly more favorable case; for a 10-spin system the ratio is 3.44.

6.1.3 Selective Experiments

Suppose U and V in Figure (II.9) are selective propagators, so that the gain compared to nonselective excitation is G when $t_2 = 0$. If the filters are set so that the noise bandwidth $\Delta\omega_n \sim \|\mathcal{H}_z\|$ then values of t_2 with $\|\mathcal{H}_z t_2\| \lesssim 1$ have strongly correlated noise and do not enhance the signal/noise ratio. However, if $\|\mathcal{H}_z t_2\| \gtrsim 1$ the selective propagator V is multiplied by a large nonselective propagator $\exp(i\mathcal{H}_z t_2)$ (see equation (VI.2)). This dramatically reduces the selective matrix elements. If $\|\mathcal{H}_z t_2\| >> 1$, the operator $V^\dagger \exp(i\mathcal{H}_z t_2) I_y \exp(-i\mathcal{H}_z t_2) V$ is nonselective, and the signal is about $\sqrt{G}$ smaller than at $t_2 = 0$. These smaller blocks of signal produce a gain of

$$g_{2D} \sim (1 + (T_2 \Delta\omega_n / G))^{1/2} \tag{VI.12}$$

and if G is large g_{2D} is negligible. For example, 9-quantum selection in a ten-spin system gives $G \sim 512$, and if $T_2 = 1$ sec and $\Delta\omega_n = 5$ KHz, the gain is only about 3 if 5000 data points have been saved in t_2 instead of one point.

Selective excitation makes two-dimensional signal enhancement techniques unnecessary, since almost all of the signal is present at $t_2 = 0$, and this implies that the phase of any individual transition in the two-dimensional spectrum is independent of ω_2. However, data manipulations in ω_2 may be useful to provide improved noise filtering.

As mentioned in chapter III, the signal should generally be sampled as close as possible to the last pulse in V, but if the receiver section is filtered no signal will be seen when $t_2 << \Delta\omega_n$. The filters are therefore opened wider than would be necessary in the nonselective experiment, to sample earlier. The additional noise this lets in could be removed by taking many points in t_2, Fourier transforming, zeroing the regions of ω_2 that do not correspond to single-quantum transitions (and perhaps weighting the regions that do) and integrating over t_2. The signal at $t_2 = 0$ is retained, but the noise is reduced. Just as in the nonselective case, this is only useful if spectrometer instabilities are not the dominant noise source.

6.1.4 Conclusions

Two-dimensional techniques will often improve the signal-to-noise ratios of nonselective spectra, at the expense of enormously increased data manipulations. However, selective excitation techniques make it possible to choose only a single point in t_2 without significant signal loss. Thus, two-dimensional techniques are expected to have limited applications in large spin systems, whereas the enormous gains of selective excitation are extremely important for this case.

6.2 Multiple-Quantum NMR in Exchanging Systems

6.2.1 Density Matrix Equations of Motion

In all of the preceding chapters the internal Hamiltonian has been written in an implicitly time independent form. In fact, the terms $\mathcal{H}_Q$, $\mathcal{H}_J$, $\mathcal{H}_D$ and $\mathcal{H}_{cs}$ all depend on molecular structure or electronic configuration, and even at absolute zero some motions occur.

The effects of these motions on the NMR spectrum depends on their

timescale relative to terms in the Hamiltonian. For example, vibrational motions distort the structure of any molecule away from its equilibrium value and may instantaneously destroy symmetry elements. The period of these motions ($\sim 10^{14}$ Hz) is so short compared to the frequency spread in $\mathcal{H}_z$ that only the time averaged structure matters.[85] Thus the couplings D_{ij} in $\mathcal{H}_D$ are proportional to $\langle r_{ij}^{-3} \rangle$ as shown in equation (I.12), and this implies that symmetry elements of a vibrationally averaged structure do not exactly dictate ratios of coupling constants (i.e., the hexagonal symmetry of benzene does not imply that D_{12}/D_{14} is exactly 8, but it is nearly so.[44]) At the other extreme, motions which only change the molecular structure over intervals which are much longer than T_2 will not substantially affect linewidths or line positions.

The interesting case occurs when the period of motions that substantially distort the molecular structure is comparable to terms in $\mathcal{H}_z$. The density matrix equation of motion for this case was derived several years ago.[86,87] The simplest case is a discrete process (for example, exchange between two equivalent sites) which obeys Markovian statistics. The motion is assumed to change the density matrix from ρ to $R\rho R^{\dagger}$, and if the frequency of this motion is $1/\tau_m$ then

$$\dot{\rho}(t)_{ii} = i[\rho(t),\mathcal{H}]_{ii} + \left(\frac{R\rho R^{\dagger}-\rho}{\tau_m}\right)_{ii} - \left(\frac{\rho+\beta I_z}{T_1}\right)_{ii} \qquad \text{(VI.13)}$$

$$\dot{\rho}(t)_{ij} = i[\rho(t),\mathcal{H}]_{ij} + \left(\frac{R\rho R^{\dagger}-\rho}{\tau_m}\right)_{ij} - \frac{\rho_{ij}}{T_2} \qquad \text{(VI.14)}$$

These equations of motion are readily solved for continuous wave irradiation by setting $\dot{\rho} = 0$ as in section 2.2.1.[88] This solution

also gives the spectrum after a one-pulse sequence.

More complicated pulse sequences, such as the nonselective multiple-quantum sequence of Figure II.1(b), are more troublesome. If $[R,H] \neq 0$ then $\rho(t)$ and $\rho(0)$ are not related by a unitary transformation, and in this framework the time evolution must be recalculated every time t_1 is changed. An alternative approach is to use a superoperator formalism,[60,89] in which ρ is written as a column vector. The evolution under the Hamiltonian is governed by the Liouville operator L:

$$L_{ij,k\ell} = \mathcal{H}_{ik}\,\delta_{j\ell} - \delta_{ki}\,\mathcal{H}_{\ell j} \tag{VI.15}$$

and the exchange term is represented by the operator R:

$$R_{ij,k\ell} = \frac{1}{\tau_m}\left(R_{ik}R^{\dagger}_{\ell j} - \delta_{ik}\delta_{\ell j}\right) \tag{VI.16}$$

The equation of motion is

$$\dot{\rho}(t) = -i\,L\,\rho(t) + R\,\rho(t)$$

$$\rho(t) = \exp((-iL+R)t)\rho(0) \tag{VI.17}$$

The evolution can be solved exactly, but if ρ is a n x n matrix it must be written as a 1 x n^2 column vector, and the matrices L and R are n^2 by n^2. Therefore, calculations of the effects of exchange are likely to be difficult in large spin systems. However, it is clear that the multiple-quantum spectra have fewer lines than does the single-quantum spectrum. Therefore large exchanging systems, which cannot be easily analyzed by conventional NMR because the single-quantum spectrum is unresolvable, should give resolvable multiple-quantum spectra.

6.2.2 Signal Size and Enhancement Techniques for General Exchanging Systems

The nonselective pulse sequences of Figure II.2 can all be used in exchanging systems. If $\|\mathcal{K}_z\tau_m\| \gg 1$ (slow exchange) then it is possible to choose $\tau, t_2 \ll \tau_m$ yet still pump multiple-quantum transitions and in this limit the signal size is essentially the same as in the static case (equation (II.61)). A similar result holds if $\|\mathcal{K}_z\tau_m\| \ll 1$ (fast exchange). If $\|\mathcal{K}_z\tau_m\| \sim 1$, however, $\tau, t_2 \sim \tau_m$ will be required to pump multiple-quantum operators, and the signal will be degraded; the exchange makes coherent pumping difficult.

6.2.2.1 Two-dimensional Techniques

The exchange process generally broadens most or all of the single-quantum transitions. This reduces the gain from two-dimensional techniques, derived in section 6.1; the formula for the gain (equation (VI.10)) must have T_2 replaced by the reciprocal of the average linewidth. If $\|\mathcal{K}_z\tau_m\| \sim 1$ the gain falls to essentially unity, if all the single-quantum transitions are affected.

6.2.2.2 Selective Techniques

The average Hamiltonian expansions of chapter III are only valid if the rate of exchange is much slower than the cycle time; otherwise the nonselective matrix elements of $\mathcal{K}_\circ$, $\mathcal{K}_\phi$ and so forth will not cancel. This implies that if $\|\mathcal{K}_z\tau_m\| \sim 1$ selective sequences will not be possible.

6.2.3 One Example--Cyclooctatetraene (COT)

6.2.3.1 Theoretical Multiple-Quantum Spectra

The bond shift process in cyclooctatetraene (C_8H_8) was described in qualitative terms in section 1.4, and theoretical spectra for the

rapid exchange and slow exchange limits were drived by symmetry arguments (Figure I.7). The intermediate exchange regime will be discussed here. Recall from section 1.4 that the bond shift can be viewed as a pseudo-rotation; spin 1 becomes spin 2, spin 2 becomes spin 3, and so forth. The matrix elements of R can be written in the spin product (SP) basis set:

$$M = 4: \quad R(\prod_i \alpha_i) = (\prod_i \alpha_i) \qquad R = 1$$

$$M = 3: \quad R(\beta_j \prod_{i \neq j} \alpha_i) = \beta_{j+1} \prod_{i \neq j} \alpha_{i+1}$$

$$R = \begin{matrix} 0 & 1 & 0 & 0 & 0 & 0 & 0 & 0 \\ 0 & 0 & 1 & 0 & 0 & 0 & 0 & 0 \\ 0 & 0 & 0 & 1 & 0 & 0 & 0 & 0 \\ 0 & 0 & 0 & 0 & 1 & 0 & 0 & 0 \\ 0 & 0 & 0 & 0 & 0 & 1 & 0 & 0 \\ 0 & 0 & 0 & 0 & 0 & 0 & 1 & 0 \\ 0 & 0 & 0 & 0 & 0 & 0 & 0 & 1 \\ 1 & 0 & 0 & 0 & 0 & 0 & 0 & 0 \end{matrix} \qquad \text{(VI.18)}$$

and so forth. R is secular and orthogonal (real valued and unitary). $R^8 = 1$, so $R^{-1} = R^7$. The M=4 state is clearly not affected by bond shifts. In fact, despite the form of (VI.18), not all of the M=3 states are affected by the bond shift process. This can be seen by generating symmetry adapted states. The symmetry operations of this molecule are shown in Table VI.1. In the slow exchange limit the point group is D_{2d}, which gives the symmetry adapted states and

Table VI.1 Symmetry Operations of Cyclooctatetraene

C_2:	$1 \leftrightarrow 5,\ 2 \leftrightarrow 6,\ 3 \leftrightarrow 7,\ 4 \leftrightarrow 8$
$2S_4$:	$1 \rightarrow 3,\ 2 \rightarrow 4,\ 3 \rightarrow 5,\ 4 \rightarrow 6,\ 5 \rightarrow 7,\ 6 \rightarrow 8,\ 7 \rightarrow 1,\ 8 \rightarrow 2$
	$1 \rightarrow 7,\ 2 \rightarrow 8,\ 3 \rightarrow 1,\ 4 \rightarrow 2,\ 5 \rightarrow 3,\ 6 \rightarrow 4,\ 7 \rightarrow 5,\ 8 \rightarrow 6$
$2C_2'$:	$1 \leftrightarrow 6,\ 3 \leftrightarrow 4,\ 7 \leftrightarrow 8,\ 2 \leftrightarrow 5$
	$1 \leftrightarrow 2,\ 5 \leftrightarrow 6,\ 3 \leftrightarrow 8,\ 4 \leftrightarrow 7$
$2\sigma_D$:	$1 \leftrightarrow 4,\ 2 \leftrightarrow 3,\ 5 \leftrightarrow 8,\ 6 \leftrightarrow 7$
	$1 \leftrightarrow 8,\ 2 \leftrightarrow 7,\ 3 \leftrightarrow 6,\ 4 \leftrightarrow 5$
R:	$1 \rightarrow 2,\ 2 \rightarrow 3,\ 3 \rightarrow 4,\ 4 \rightarrow 5,\ 5 \rightarrow 6,\ 6 \rightarrow 7,\ 7 \rightarrow 8,\ 8 \rightarrow 1$

numbers of transitions shown in Table VI.2. The symmetry adapted states for M = ±4 and M = ±3 are given in Table VI.3. In this basis R for M = ±3 is given by:

$$R = \begin{matrix} 1 & 0 & 0 & 0 & 0 & 0 & 0 & 0 \\ 0 & -1 & 0 & 0 & 0 & 0 & 0 & 0 \\ 0 & 0 & 0 & -1 & 0 & 0 & 0 & 0 \\ 0 & 0 & 1 & 0 & 0 & 0 & 0 & 0 \\ 0 & 0 & 0 & 0 & \frac{1}{2} & -\frac{1}{2} & -\frac{1}{2} & -\frac{1}{2} \\ 0 & 0 & 0 & 0 & \frac{1}{2} & \frac{1}{2} & \frac{1}{2} & -\frac{1}{2} \\ 0 & 0 & 0 & 0 & \frac{1}{2} & \frac{1}{2} & -\frac{1}{2} & \frac{1}{2} \\ 0 & 0 & 0 & 0 & -\frac{1}{2} & \frac{1}{2} & -\frac{1}{2} & -\frac{1}{2} \end{matrix} \qquad \text{(IV.19)}$$

The A_1 and A_2 states are invariant, but all other states are affected. In fact it can readily be seen that the M = ±4, ±3 A_1 states and M = ±3, ±2 A_2 states are the only ones which are invariant to the bond shift process,[24] so any transition may be affected unless both the initial and final states are among these ten. The number of invariant transitions for each value of ΔM is given in Table VI.2. The seven-quantum and eight-quantum spectra have no dynamical information. However, the six-quantum spectra has six fewer transitions in the rapid exchange limit than in the slow exchange limit (R becomes a symmetry operation with rapid exchange), as noted in section 1.4.

At any exchange rate $[R^2,\mathcal{H}] = [R^2,\rho] = 0$, because R^2 is equivalent to S_4. There is therefore no problem with the assumption of a pseudo-rotation which increases the index of each spin by one; of course a pseudorotation which decreases each index by one is equally

Table VI.2 Symmetry States for Cyclooctatetraene

M	Number of Symmetry Adapted States					
	A_1	A_2	B_1	B_2	E	Total
±4	1	0	0	0	0	1
±3	1	1	1	1	2x2	8
±2	6	2	4	4	6x2	28
±1	7	7	7	7	14x2	56
0	13	7	9	9	16x2	70
						256

	Allowed Nondegenerate Transitions	Unaffected by bond shifts
ΔM=1	1430	6
ΔM=2	995	0
ΔM=3	546	0
ΔM=4	225	2
ΔM=5	70	4
ΔM=6	15	0
ΔM=7	2	2
ΔM=8	1	1

Table VI.3 Wavefunctions (D_{2d} point group)

ψ	Symmetry Group	$R\psi$	Symmetry Group
	M = +4		
αααααααα	A_1	αααααααα	A_1
	M = +3		
	"1" ≡ βαααααα, etc.		
1+2+3+4+5+6+7+8	A_1	2+3+4+5+6+7+8+1	A_1
1-2+3-4+5-6+7-8	A_2	2-3+4-5+6-7+8-1	A_2
1+2-3-4+5+6-7-8	B_1	2+3-4-5+6+7-8-1	B_2
1-2-3+4+5-6-7+8	B_2	2-3-4+5+6-7-8+1	B_1
1+2+3+4-5-6-7-8	$E_a^{(1)}$		
1+2-3-4-5-6+7+8	$E_b^{(1)}$	Linear combinations of E states	
1-2+3-4-5+6-7+8	$E_a^{(2)}$		
1-2-3+4-5+6+7-8	$E_b^{(2)}$		

valid, but since $R\rho R^7 = R^7\rho R$ the same density matrix is produced. This means that the pseudorotation is basically a two-site problem. The behavior under exchange of the six-quantum transitions is:

1. The A_1 and A_2 transitions from M = +3 to M = -3 are not affected by the exchange. Both of these transitions appear at $\omega = 0$.

2. The B_1 and B_2 transitions from M = +3 to M = -3 are mixed by the exchange. Both of these transitions also appear at $\omega = 0$, so $L = 0$ in equation (VI.17), and the exchange merely broadens the line.

3. The E transitions from M = +3 to M = -3 can be described by 16 x 16 matrices L and R, and the A_1 transitions from M = ±4 to M = -2 can be described by 36 x 36 matrices. The transitions from M = ±2 to M = -4 just make the spectrum symmetric, so their evolution does not need to be independently calculated. All of these transitions can broaden at different rates. In the slow exchange limit, Alexander[84] has shown that the linewidths are given by:

$$1/T_2 - 1/T_2^{o} = (1-R_{mm}R_{nn})/\tau_m \qquad \text{(VI.20)}$$

where m and n are the initial and final states.

The intensities of the peaks cannot be calculated unless the preparation and mixing periods are also analyzed. In this case R and L are 64 k x 64 k matrices.

6.2.3.2 Experimental Spectra

As explained in section 6.2.2, most of the signal enhancement techniques available are of limited use in exchanging systems, so nonselective multiple-quantum spectra were observed. The signal level depended critically on τ_m. Figures VI.2-4 show the multiple-

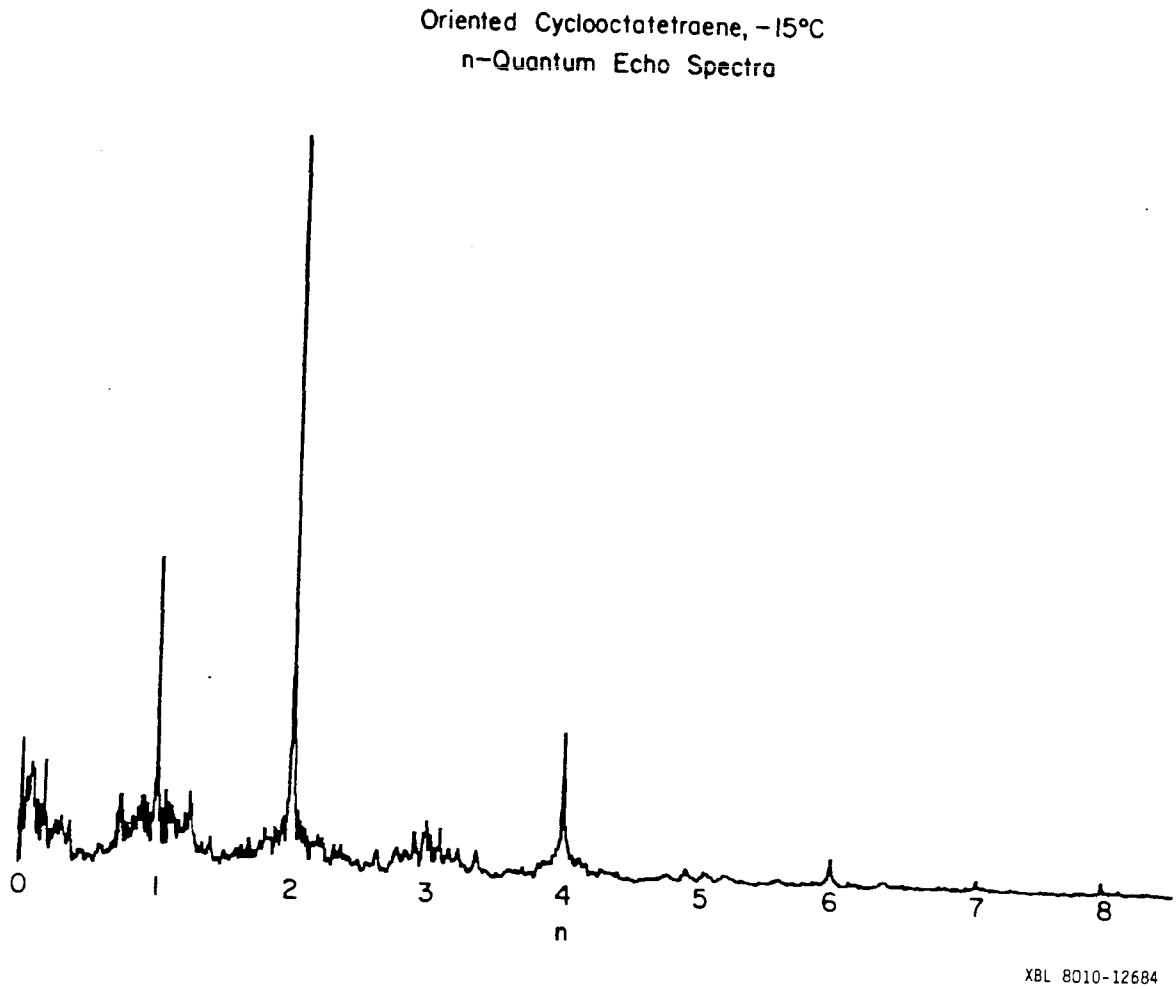

Figure VI.2 Nonselective multiple-quantum magnitude spectra of 12 wt% cyclooctatetraene in Phase V liquid crystal at -15.0°C.

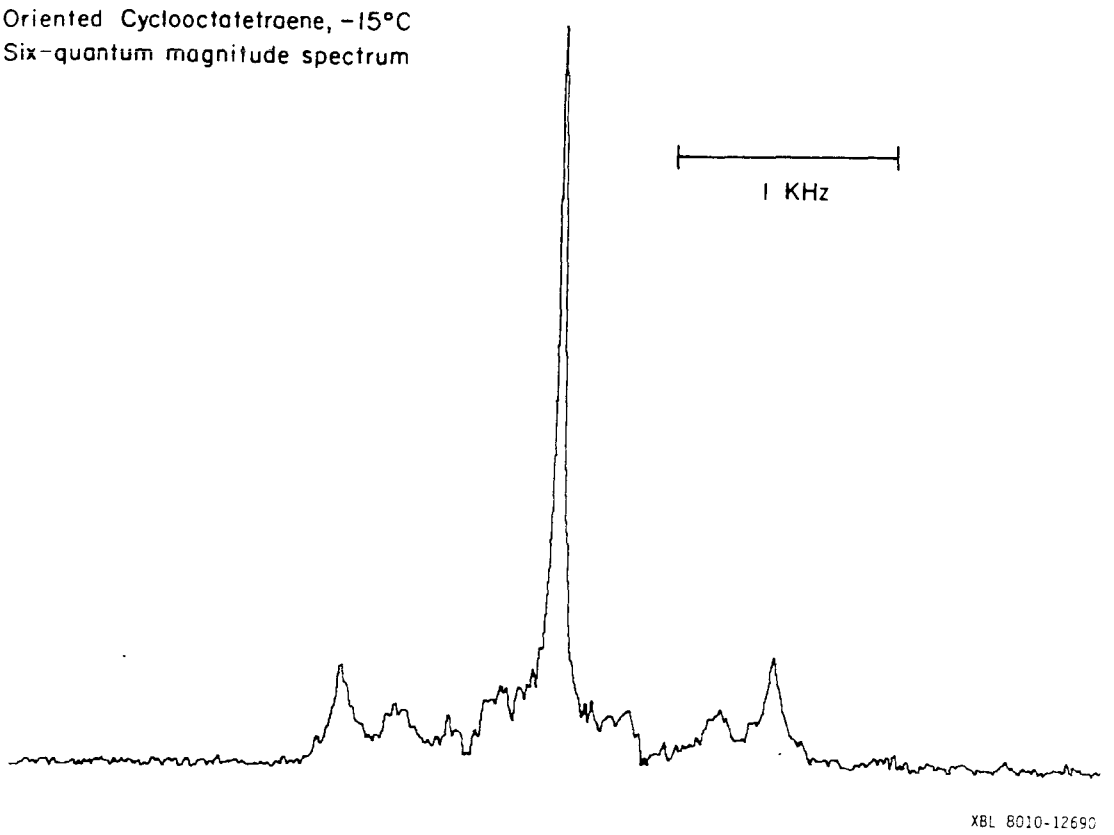

Figure VI.3 Six-quantum region of the spectrum of Figure VI.2. All transitions except for the central one are broadened by exchange.

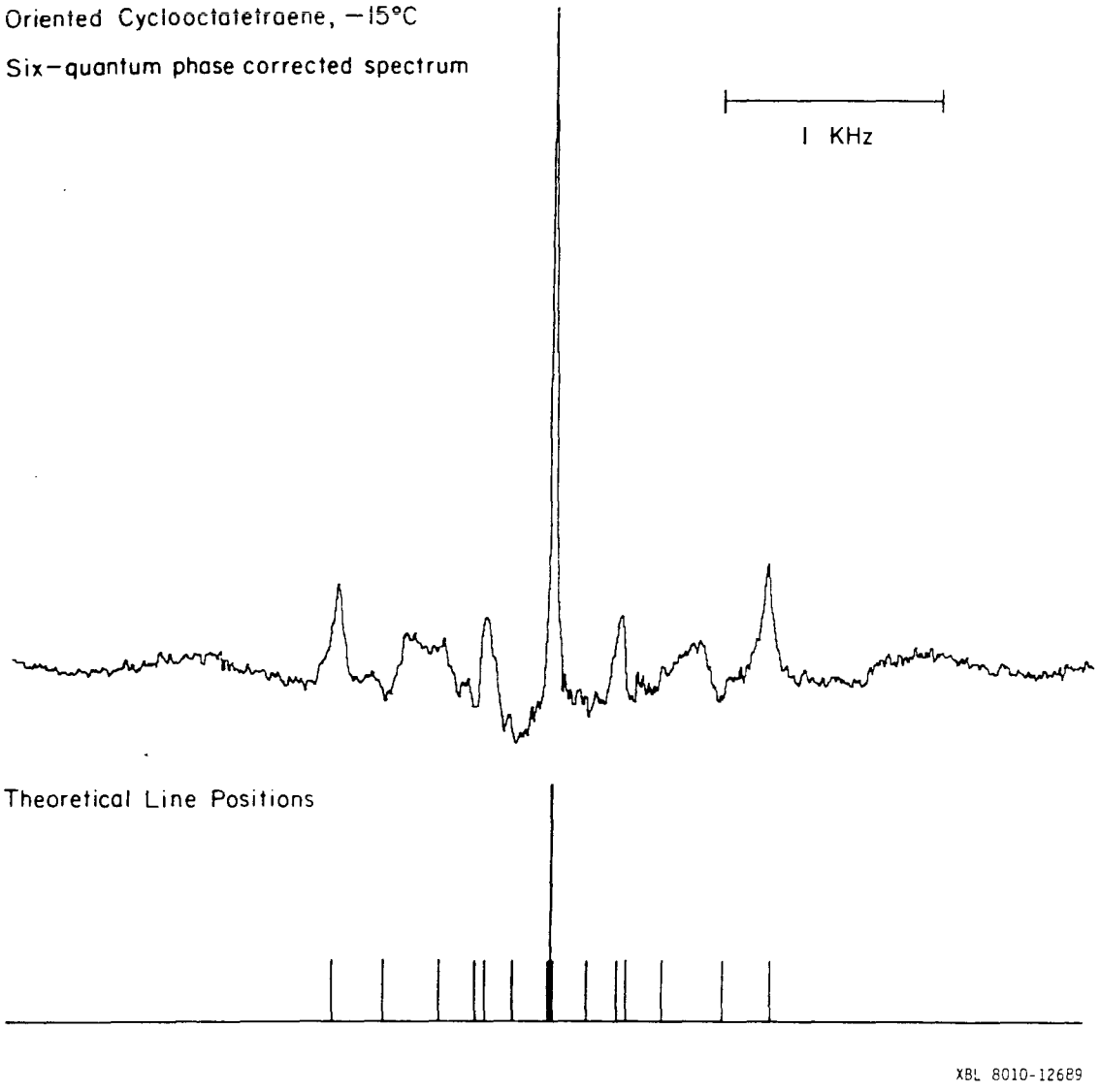

Figure VI.4 Same as Figure VI.3, except that the spectrum is phase corrected instead of magnitude. The theoretical transitions from the couplings in reference (24) are also shown. The implied exchange rate from the line widths is about 33 Hz.

quantum spectra at -15°C of a sample with 12 wt% COT in Phase V; data accumulation time was roughly 15 hours. At higher temperatures no six-quantum signal was observable. In addition, the linewidths increased as the temperature was lowered past this point. This effect has been attributed to increasing viscosity.[24]

Since the slow exchange limit was not observed assignment of the dipolar couplings was not possible from the spectra alone. However, if the dipolar coupling constants from reference (24) are assumed the exchange rate can be calculated from linewidths in the six-quantum spectra. Of the seven allowed pairs of transitions, only one is isolated enough and intense enough to measure a linewidth. That transition has a full width at half maximum of 75 ± 12 Hz, and $(1-R_{mm}R_{nn})$ for that transition is 0.84. The central six-quantum peak is 20±12Hz wide, so the estimated exchange rate is τ_m^{-1} = 33 ± 10 Hz, which is somewhat smaller than the rate τ_m^{-1} = 55 ± 22 Hz found in reference (24).

6.2.4 Multiple Pulse Techniques to Measure Exchange

It is clear from the last several subsections that multiple-quantum NMR spectra in exchanging systems will generally be weak and fairly difficult to analyze. The fundamental problem is that the equation of motion in (VI.13-14) has two noncommuting terms. It is easily solved if either of these two terms vanishes, but not otherwise.

In particular, if $\mathcal{H} = 0$ then

$$\dot{\rho}(t) = \frac{R\rho(t)R^{\dagger}-\rho(0)}{\tau_m}$$

$$\rho(t) = \rho(0) + \frac{1}{2}(R\rho(0)R^{\dagger}-\rho(0))(1-e^{-2\tau/\tau_m}) \qquad \text{(VI.21)}$$

and if $R\rho(0)R^{\dagger}$ is substantially different from $\rho(0)$ a pure exponential

decay results.

One sequence which uses this simple evolution to determine the exchange rate is shown in Figure VI.5. The density matrix at the end of the first interval t_2 is

$$\rho(t_2) = -\beta \exp(-i\mathcal{H}_z t_2) I_y \exp(i\mathcal{H}_z t_2) \tag{VI.22}$$

If $\|\mathcal{H}_z \tau_m\| \gtrsim 1$ then it is possible to choose t_2 such that $\rho(t_2)$ has substantial components which do not commute with R. The pulse sequence during t_1 removes $\mathcal{H}_z$; several choices are possible, including the two-quantum pulse sequence of Figure III.9c, repeated with a 90° pulse shift.

Assuming that $t_2 \ll \tau_m$, the signal for $t_1 = 0$ is:

$$A = \mathrm{Tr}(\exp(-2i\mathcal{H}_z t_2) I_y \exp(2i\mathcal{H}_z t_2) I_y) \tag{VI.23}$$

and the signal for $T_2 > t_1 \gg \tau_m$ is (A+B)/2 where B is

$$B = \mathrm{Tr}(R \exp(-i\mathcal{H}_z t_2) I_y \exp(i\mathcal{H}_z t_2) R^{\dagger} \exp(i\mathcal{H}_z t_2) I_y \exp(-i\mathcal{H}_z t_2)) \tag{VI.24}$$

Matrix elements $\rho(t_2)_{mn}$ which are not affected by the exchange (i.e., $(R\rho(t_2)R^{\dagger})_{mn} = \rho(t_2)_{mn}$) do not contribute to the signal difference. But if $\rho(t_2)_{mn}$ oscillates at frequency ω_1 and $(R\rho(t_2)R^{\dagger})_{mn}$ oscillates at frequency ω_2 (assuming two-site exchange) then the signal difference becomes large when $\langle|(\omega_2-\omega_1)t_2|\rangle \gtrsim 1$.

In general, this sequence will not work for $\tau_m \gtrsim \|\mathcal{H}_z\|$, because in this case $\|[R,\rho(t_2)]\| \ll \|\rho(t_2)\|$. On the other hand, if $\tau_m \sim \|\mathcal{H}_J\|$ the sequence to suppress $\mathcal{H}_z$ will not be good enough to give an accurate measurement. Nonetheless for a typical dipolar system this gives τ_m a

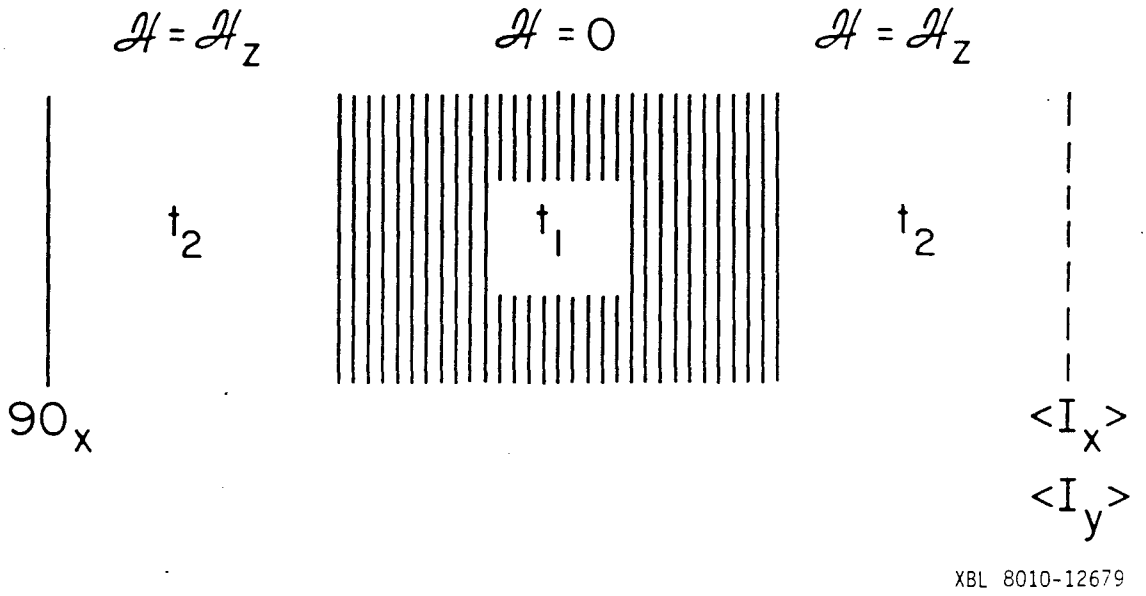

Figure VI.5 Multiple-pulse sequence for measuring exchange rates. If the line narrowing sequence is good the signal is proportional to $\exp(-2t_1/\tau_m)$.

measurable range of several orders of magnitude. The technique is quite general and should be applicable to a wide range of exchanging systems.

6.3 An Information Theory Treatment of Multiple-Quantum Coherence

6.3.1 Introduction

The high multiple-quantum spectra of large spin systems are of great interest because the single-quantum spectrum is often intractable, as explained in Chapter I. Unfortunately the increased simplicity of the high multiple-quantum spectra is accompanied by a large decrease in intensity if nonselective excitation is used. For example, Figure (II.7) shows the integrated intensity of each order of transitions in a typical experiment on oriented benzene, compared to an extremely simple model in which all transitions are assumed to have the same intensity making the total intensity of each order proportional to the number of transitions in that order. The experimental results agree fairly well with this simple theory; in fact, despite the high degree of molecular symmetry, group theoretical restrictions do not dramatically change the intensity pattern.

Given a specific pulse sequence and a specific Hamiltonian (including, for example, all dipolar coupling constants and chemical shifts), the exact non-linear evolution of the spin density matrix can be determined by the equation of motion and thus the exact spectrum can be calculated. For large spin systems, however, this approach rapidly becomes prohibitively time-consuming. In addition, it requires detailed advance knowledge about the Hamiltonian, which in fact might be the information that the experiment is designed to provide.

In this section a more general approach to describing multiple-quantum coherences will be used. Given only limited information about pulse sequences and the Hamiltonian, one would like to make predictions about the integrated intensity pattern as a function of the number of quanta. In other words, if this approach is applied to oriented benzene, it should reproduce Figure II.7, but is not expected to reproduce exact spectra such as Figure II.4. The predictions obtained are nonetheless important, for several reasons. For large spin systems, they should point to a description of multiple-quantum coherence that is essentially statistical, and allow the testing of different models for a "pumping operator" to represent the evolution of coherences. In addition, they should predict how difficult it will be to pump high order multiple-quantum coherences in complicated systems. The intensity pattern is predicted here by information theory, which determines the most probable density matrix consistent with assumed mechanisms for pumping multiple-quantum coherences. Section 6.3.2 develops the concept of the statistical coherence limit, corresponding to the most random but coherent density matrix. Calculations using different pumping mechanisms are compared to exact dynamical calculations for small systems in section 6.3.3. These calculations show that an information theory treatment agrees fairly well with experiment, and give some insight into the evolution of multiple-quantum coherences for general anisotropic systems.

6.3.2 Statistical Calculations

6.3.2.1 Information Theory

A complete specification of the density operator for a system with N states requires measuring the expectation values of N^2-1 linearly

independent operators.[90] If fewer measurements are performed, there may be more than one density operator which correctly reproduces the measured results. To select a particular density operator one adopts from information theory[91] and quantum statistical mechanics [92] the entropy, given in dimensionless units by

$$S[\rho] = -\mathrm{Tr}(\rho \ln \rho) \tag{VI.25}$$

as a measure of missing information. The required density operator is selected from amongst those consistent with the known constraints as the one of maximal entropy.[90-99] The resulting density operator is consistent with the data and is otherwise as random as possible. It is the least committal (or most conservative) induction that is warranted by the data at hand.

Given the expectation values of m operators A_r,

$$\langle A_r \rangle = \mathrm{tr}(\rho A_r) \qquad r = 1, 2, \ldots, m \tag{VI.26}$$

the normalized ($\mathrm{Tr}\,\rho = 1$) density operator which is consistent with the m mean values in (VI.26) and has maximal entropy is given by[94,98]

$$\rho = \exp(-\lambda_0 + \sum_{r=1}^{m} \lambda_r A_r) \tag{VI.27}$$

The (m+1) parameters, λ_0 and the λ_r's, in ρ are determined by the M+1 operator expectation values that are consistent with the data. The solution for the λ values is unique, provided that the operators are linearly independent.

6.3.2.2 The Statistical Coherence Limit

As a first application consider the specification of a density

matrix when all that is known is that it is not incoherent, which means that, in the basis of interest the off-diagonal matrix elements of ρ, (ρ_{ji}, $i \neq j$), are not necessarily zero. The constraints are therefore normalization and finite coherence,

$$\sum_{i=1}^{N} \rho_{ii} = 1$$

$$\sum_{i} \sum_{j \neq i} \rho_{ji} = C \tag{VI.28}$$

For algebraic reasons it is convenient to add the first and second constraints and rewrite as

$$\sum_{i} \sum_{j} H_{ij}\rho_{ji} \equiv \mathrm{Tr}(\underset{\sim}{H}\underset{\sim}{\rho}) = (C+1)/N \tag{VI.29}$$

Here $\underset{\sim}{H}$ is the N x N matrix whose every element is 1/N so that

$$\underset{\sim}{H}^2 = \underset{\sim}{H} \quad . \tag{VI.30}$$

The density matrix $\underset{\sim}{\rho}$ of maximal entropy subject to the two commuting constraints of mean $\underset{\sim}{H}$ and mean $\underset{\sim}{I}$ is given by

$$\underset{\sim}{\rho} = \exp[-\lambda_0 \underset{\sim}{I} - \lambda \underset{\sim}{H}] \quad . \tag{VI.31}$$

Recalling that an exponential of a matrix is defined by a power series expansion and using (VI.30) repeatedly,

$$\underset{\sim}{\rho} = \exp(-\lambda_0) \{\underset{\sim}{I} + [\exp(-\lambda) - 1]\underset{\sim}{H}\} \quad . \tag{VI.32}$$

Therefore, if all that is known is that $\underset{\sim}{\rho}$ is coherent, then the most reasonable inference is that all the off-diagonal elements of $\underset{\sim}{\rho}$ are of equal magnitude. The diagonal elements are also all equal

and exceed the magnitude of the off-diagonal ones. If the coherence is not imposed as a constraint ($\lambda \equiv 0$) then (VI.31) properly reduces to the familiar microcanonical statistical limit $\underset{\sim}{\rho} = \underset{\sim}{I}/N$, a density matrix of random phases and equal probabilities.

One can readily relate the values of λ_0 and λ to those of the constraints

$$\exp(-\lambda_0) = 1/[N+\exp(-\lambda) - 1]$$

$$\exp(-\lambda) = (N-1)(C+1)/[N-C-1] \quad , \qquad \text{(VI.33)}$$

which shows that the problem is well posed only if $\mathrm{Tr}(\underset{\sim}{H}\underset{\sim}{\rho}) = (C+1)/N < 1$. This is as it should be since $\underset{\sim}{H}$ is a projection matrix (cf. (VI.30)) whose expectation value must be between zero and unity.

The density matrix $\underset{\sim}{\rho}$ is typically that of a mixed state,

$$\mathrm{Tr}(\rho^2) = (1+(C^2/N-1))/N \qquad \text{(VI.34)}$$

It tends to a pure state, $\underset{\sim}{\rho} = \underset{\sim}{H}$, only in the strong coherence limit when $C = N-1$; then $\underset{\sim}{\rho}$ is an eigenmatrix of the projection $\underset{\sim}{H}$, so that $\mathrm{Tr}(\underset{\sim}{H}\underset{\sim}{\rho}) = 1$. In the opposite extreme $C = 0$ and $\rho = \underset{\sim}{I}/N$, the most chaotic (i.e., maximal entropy) mixed state that is possible. The magnitude of λ increases monotonically as C increases, starting at zero when $C = 0$ and tending to infinity as $C \to N-1$.

The object of this theory is to reproduce some of the general features of the nonselective multiple-quantum spectrum. As explained in sections 2.2.2.2 and 6.1, the ensemble averaged intensity of the transition from $|i\rangle$ to $|j\rangle$ is $-C\beta \langle|\rho_{MQ}(\tau)|\rangle^2_{ij}$ (or $-C\beta \langle|\rho^2_{MQ}(\tau)|_{ij}\rangle$ if $t_2 = \pm\tau$ is assumed.) It was shown in section 6.1 that the difference

between these two expressions is generally small. This averaging over τ is the key to a statistical approach. Say the different values of τ are indexed by r, r = 1,2, ..., m, so that altogether m measurements were taken. Let A_r be the operator whose value was measured at the r'th time. The spectrum would be reproduced by a density matrix which is consistent with the m measured values. Invoking the maximum entropy formalism, the result is given by (VI.31).

Two points are important to note. The first is that the density operator (VI.31) will not necessarily reproduce any of the individually measured spectra, nor is it meant to. All that it is geared to do is to account for the average spectra, obtained after many samplings, corresponding to different values of τ. The second and technical point is that (VI.31) does not have the form expected from stochastic theories of lineshape.[94] The reason is the differences in the physics of the problem. There, one is dealing with a Hamiltonian which contains random elements (e.g., an impurity can find itself in a variety of host environments.)[100] To determine the evolution of the system, it is thus necessary to average ρ over the distribution of the random elements. Here however we are dealing with a single system, with an exceedingly complex Hamiltonian which we prefer not to have to look at. To make the problem manageable for a simple theory we thus have to collect considerable data on the system, which is achieved by repeated sampling. The net result, (VI.31), looks like it is the logarithm of ρ rather than ρ itself that has been 'averaged'. The conclusion is inevitable, and is essentially the key theme of the maximum entropy approach. The way to incorporate data in the least biased manner is by minimizing the

average deviance of $\ln \rho$ from the weighted constraints

$$<-\ln \rho + \sum_r \lambda_r A_r> = \min \quad . \tag{VI.35}$$

The magnitudes of the Lagrange parameters serve as the weights.

6.3.3 Forms for the Pumping Operator

Clearly the choice of the constraint operators is extremely important. The information theory framework implies that these should be operators whose expectation values are given. Obviously, if the expectation values for all the (N^2-1) coherences and populations are known, the density matrix is known, but the theory then has no predictive value. The constraints should thus be kept to a minimum.

All of the following properties are known about $\rho_{MQ}(\tau)$:

1. $Tr(\rho_{MQ}(\tau)) = 1$. This constraint is easily satisfied since $\lambda_0 I$ in equation (VI.31) can be factored out of the exponential, and then it becomes a normalization constant.

2. $\rho_{MQ}(\tau)$ is related to $1-\beta I_z$ by a unitary transformation. This important constraint cannot be readily expressed in the information theory framework.

3. In the limit of small τ, $\rho_{MQ}(\tau)$ can be written as:

$$\rho_{MQ}(\tau) = -\beta(I_z + i[I_z,\mathcal{H}_x]\tau + \mathcal{O}(\tau^2)) \tag{VI.36}$$

Thus small values of τ produce two-quantum coherences (and one-quantum coherences if chemical shifts are present), as explained in section 2.2.2.2. The expectation value $<i[I_z,\mathcal{H}_x]>$ is known for small values of τ:

$$\mathrm{Tr}(\rho_{MQ}(\tau)i[I_z,\mathcal{H}_x]) = -\beta(\tau\ \mathrm{Tr}((i[I_z,\mathcal{H}_x])^2) + O(\tau^3))$$

$$i[I_z,\mathcal{H}_x] = -\sum_{i>j} D_{ij}(3I_{xi}I_{yj}+3I_{yi}I_{xj}) - \Delta\omega\ I_y + \Sigma\ \sigma_i I_{yi}$$

$$= \Sigma\ D_{ij}(+\frac{3i}{2})(I_i^+I_j^+-I_i^-I_j^-) - \frac{i}{2}\ \Sigma(\sigma_i-\Delta\omega)(I_i^+-I_i^-)$$

$$\mathrm{Tr}(i[I_z,\mathcal{H}_x]^2) = (\frac{9}{8})(2^{N-1})\sum_{i>j} D_{ij}^2 + 2^{N-2}\ \Sigma_i(\sigma_i-\Delta\omega)^2 \qquad \text{(VI.37)}$$

It can be confirmed by substitution that the term proportional to τ^2 vanishes. Higher-order terms must tend to cancel the τ term since the expectation value cannot grow indefinitely.

The operator $i[I_z,\mathcal{H}_x]$ reflects any molecular symmetry, and if $\Delta\omega = \sigma_i = 0$ for all i it is even-quantum. A most probable density matrix of the form

$$\rho[\lambda] = \exp(i\lambda[I_z,\mathcal{H}_x])/\mathrm{Tr}(\exp(i\lambda[I_z,\mathcal{H}_x]))$$

$$\equiv \exp(\lambda P)/\mathrm{Tr}(\exp(\lambda P)) \qquad \text{(VI.38)}$$

will also have these properties, so this operator may be a good choice for a pumping operator. The important test, of course, is how well equation (VI.38) agrees with experiments.

Figure VI.6 shows how $\langle P\rangle$ behaves as a function of λ. The expectation value is initially proportional to λ, but for large λ it approaches a maximum value. It can be shown that this maximum is simply the largest eigenvalue of P by transforming to a basis set which diagonalizes $\rho[\lambda]$. As λ increases the fraction of high multiple-quantum coherence increases monotonically, as shown in

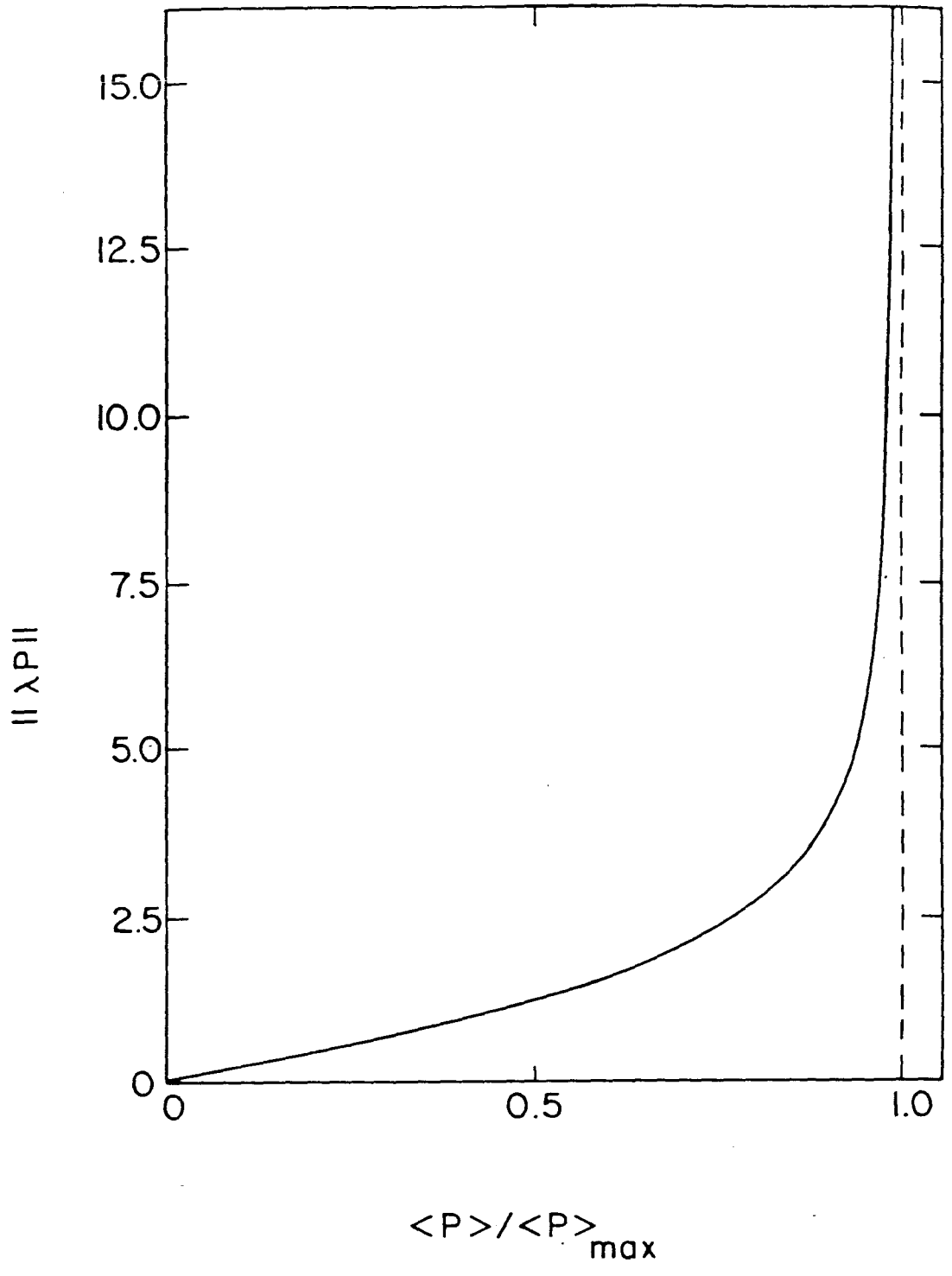

Figure VI.6 The expectation value of $\langle P\rangle = Tr(\rho P)$ as a function of λ. For large λ it approaches a maximum value equal to the largest eigenvalue of P.

Figure VI.7 for benzene with $\Delta\omega = 0$, and finally converges to what will be called the strong pumping limit. Physically the strong pumping limit corresponds to values of τ such that $\|\mathcal{H}_z\tau\| >> 1$ but $\tau << T_2$.

The multiple-quantum intensity distribution is compared to the exact dynamical solution (i.e., the average over many values of τ) for several different systems in Figures VI. 8-11. If only dipolar terms are present, both the exact solution and the information theory solution are purely even-quantum. The eigenstates decompose into two disconnected groups (for example, for a four-spin system states with $M = 0, \pm 2$ are not connected to states with $M = \pm 1$) and the matrix elements of these two groups should be separately normalized in the information theory treatment. If this is done the agreement with the exact dynamics is quite good, as shown in Figures VI. 8-10. For example, the four-quantum transition in a four-spin system is substantially stronger when all the coupling constants have the same sign than it is when the couplings have different signs, as shown in Figures VI. 8 and VI. 9.

Attempts to introduce a resonance offset were less successful. This is to be expected, because the main effect of a resonance offset is to generate a term proportional to $\sin(\Delta\omega\tau)$ which has odd-quantum elements only (equation (II.60)). If the pumping operator has only even-quantum elements so will the density matrix, but it is unlikely that any form for a pumping operator will give only odd-quantum elements for all values of λ. Similarly, the effects of chemical shifts were not readily reproduced. Figure IV.11 shows the intensity pattern generated for a typical five-spin system with chemical shifts; the information theory prediction tends to be too large for the large

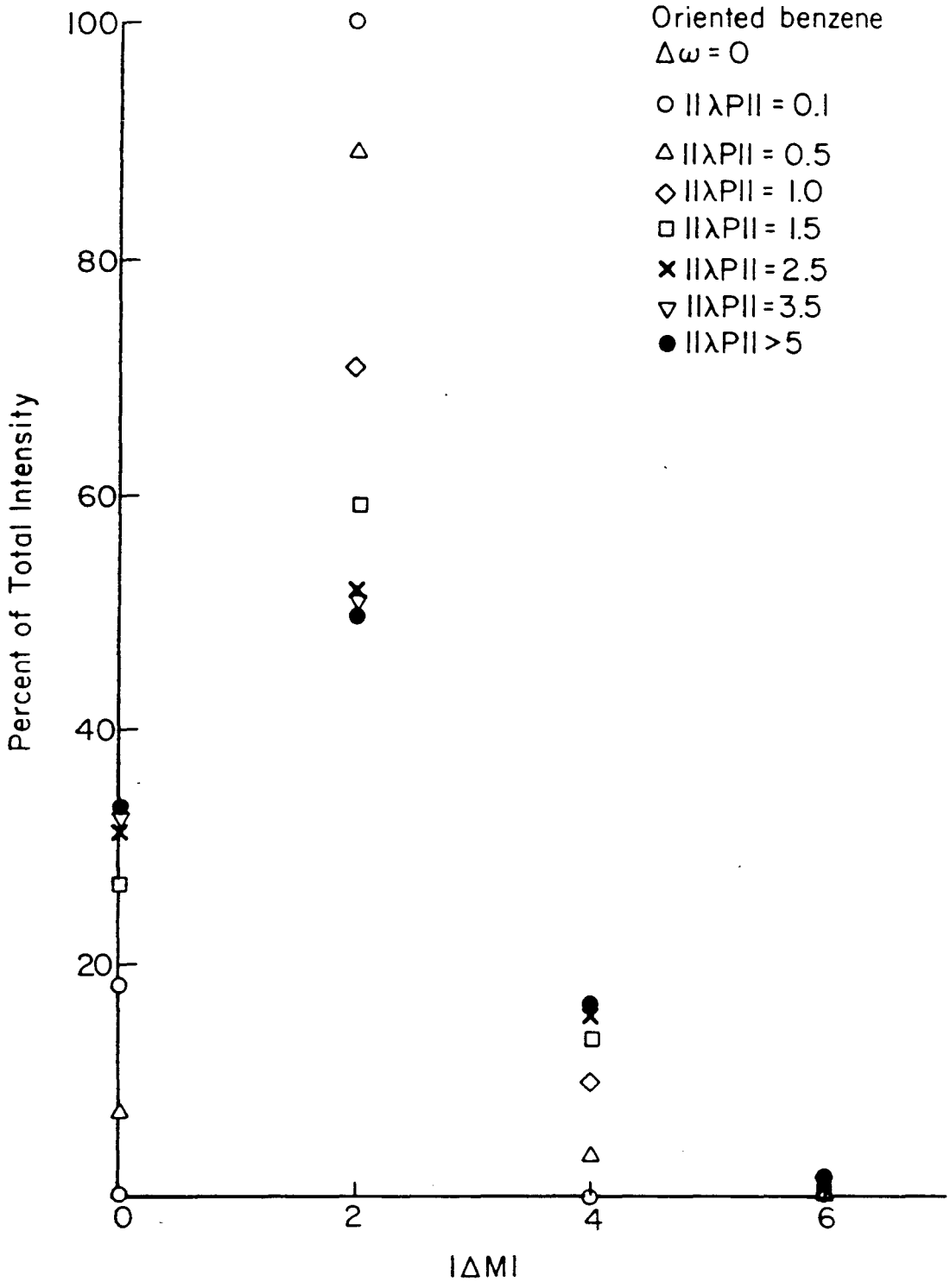

XBL 8010-12680

Figure VI.7 The intensity pattern as a function of λ for benzene with Δω = 0. The pattern converges to what will be called the strong pumping limit for large λ.

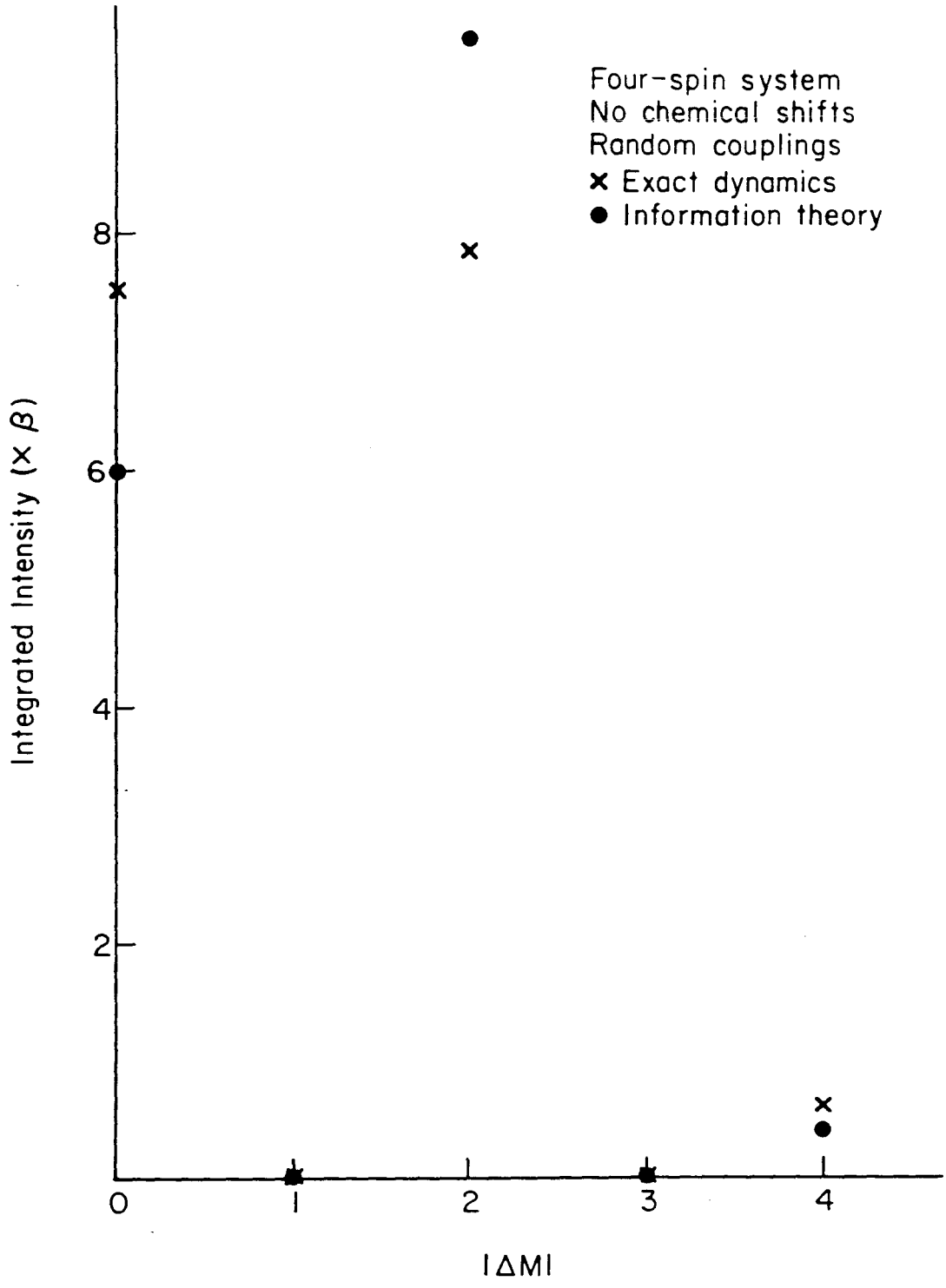

XBL 8010-12491

Figures VI.8-11 The intensity patterns for several different molecules in the strong pumping limit, versus an exact dynamical calculation (the average intensity pattern over many values of τ).

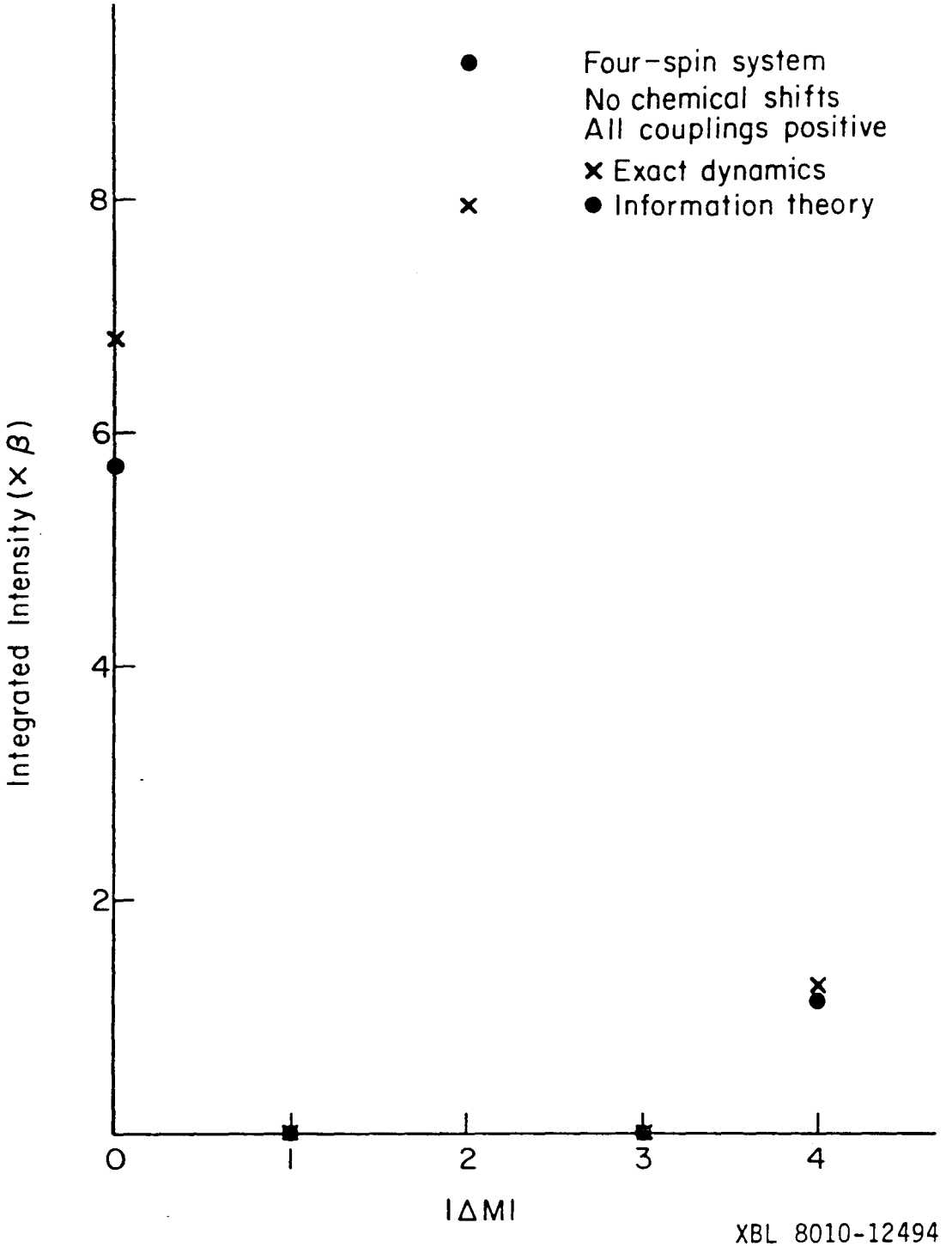
Four-spin system
No chemical shifts
All couplings positive
× Exact dynamics
● Information theory
Integrated Intensity (× β)
8
6
4
2
0
1
2
3
4
|ΔM|
XBL 8010-12494

Figure VI.9.

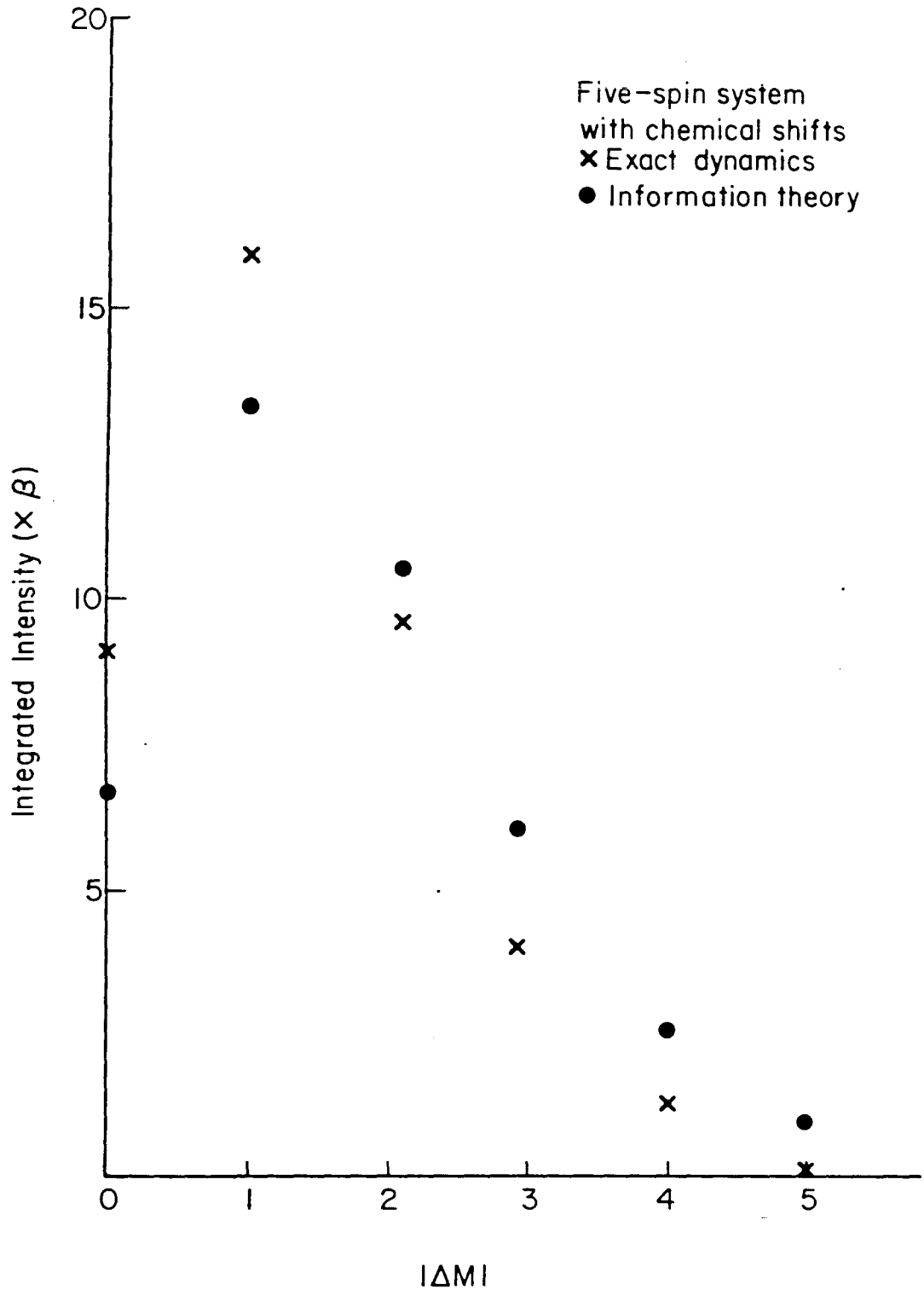

XBL 8010-12490

Figure VI.10.

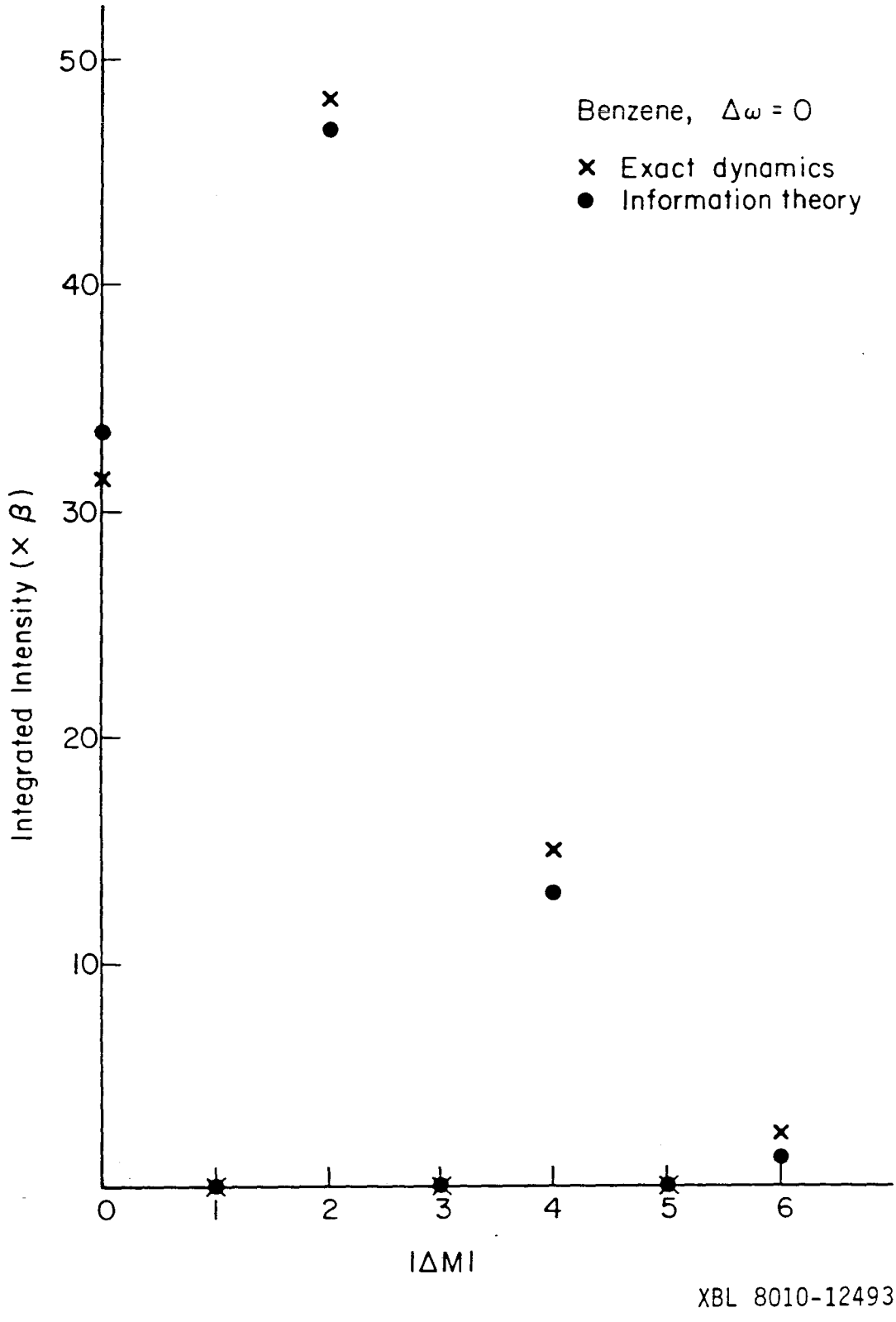
Benzene, Δω = 0
× Exact dynamics
● Information theory
Integrated Intensity (× β)
50
40
30
20
10
0
1
2
3
4
5
6
|ΔM|
XBL 8010-12493

Figure VI.11.

values of ΔM.

6.3.4 Density Matrix Reduction Schemes: Coherence Versus Incoherent Pumping

Figures (VI.10-12) show that equation (VI.38) gives good qualitative agreement with experiment, at least for systems with only dipolar couplings. In fact, the formalism can be further simplified. Specifying the entire density matrix (i.e., the magnitude and phase of every element) is probably only necessary to describe the fine structure of the spectrum. Therefore a reduced density matrix can be employed where each level is assigned a degeneracy g_i corresponding to the number of different eigenstates in the original manifold. Each element ρ_{if} of the reduced matrix corresponds therefore to a block of $g_i g_f$ states in the initial matrix. Thus, for example, the density operator and the pumping operator for benzene (which are expressed as 64 x 64 matrices) are reduced to 7 x 7 matrices.

The best method for reduction of a block of elements in the full matrices to a single number depends on the form of the pumping operator. The exponential in (VI.38) can be expanded:

$$(\rho[\lambda])_{ij} \sim (1 + (\lambda P) + \frac{1}{2}(\lambda P)^2 + \frac{1}{6}(\lambda P)^3 + \ldots)_{ij}$$

$$(P^N)_{ij} = \sum_{\alpha,\beta,\gamma\ldots} P_{i\alpha} P_{\alpha\beta} \ldots P_{\gamma j} \qquad \text{(VI.39)}$$

In the reduced matrix $P_{i\alpha}$ is a single number; in the full matrix it is a block of $g_i\, g_\alpha$ numbers. Thus, a typical matrix element of $P_{i\alpha}P_{\alpha\beta}$ is a sum of g_α terms.

Two simple cases can be distinguished:

1. Coherent pumping. If all of the matrix elements of P have the same phase then one expects a typical matrix element of $P_{i\alpha} P_{\alpha\beta}$ to be g_α times larger than $\langle P_{i\alpha}\rangle\langle P_{\alpha\beta}\rangle$. The appropriate reduction scheme in this case is:

$$P_{ij} \xrightarrow[\text{reduction}]{\text{coherent}} \sqrt{g_i g_j}\ \langle P_{ij}\rangle$$

block, $g_i x g_j$ one number

The signal intensity $g_i g_j \langle P_{ij}^2\rangle$ is desired at the end of the calculation, so after $\exp(\lambda P)/\mathrm{Tr}(\exp(\lambda P))$ is calculated each matrix element must be squared.

2. Incoherent pumping. If the matrix elements of P have random phases then one expects the square of a typical matrix element of $P_{i\alpha}P_{\alpha\beta}$ to be g_α times larger than $\langle P_{i\alpha}^2\rangle\langle P_{\alpha\beta}^2\rangle$. The appropriate reduction in this case is:

$$P_{ij} \xrightarrow[\text{reduction}]{\text{incoherent}} \sqrt{g_i g_j}\ \langle P_{ij}^2\rangle$$

block, $g_i x g_j$ one number

When $\exp(\lambda P)/\mathrm{Tr}(\exp(\lambda P))$ is calculated the signal intensity automatically appears, so no squaring is necessary. However, each element in the final matrix must be multiplied by $\sqrt{g_i g_j}$.

Figure VI.12 compares the coherent and incoherent reduction schemes for a four-spin system with only positive couplings. Only the coherent reduction agrees with a full information theory treatment. In fact this can also be seen by examining the form of the pumping operator

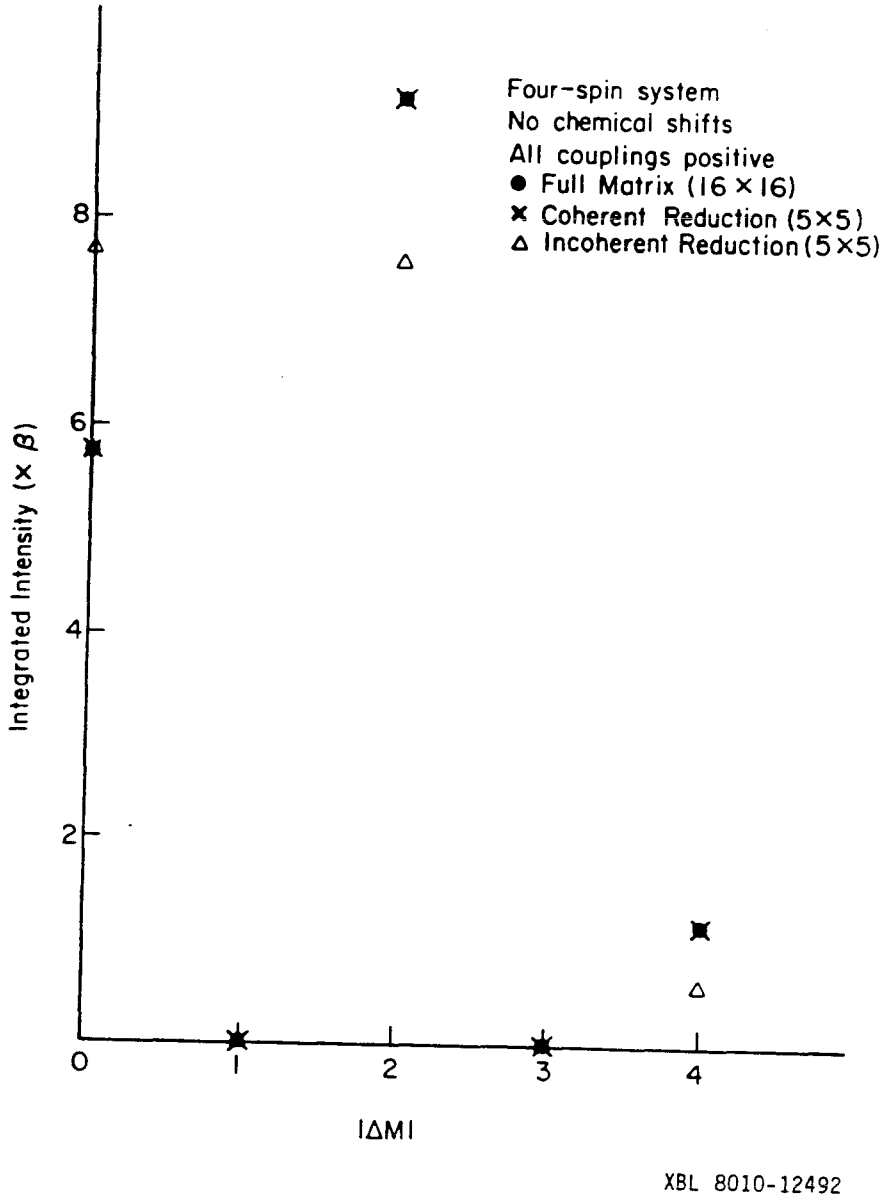

Figure VI.12 Comparison of coherent and incoherent reduction schemes for a four-spin molecule with positive couplings. The coherent reduction agrees with the full information theory treatment, showing that the different pathways to high-quantum operators reinforce.

in (VI.38); rotation of $-\pi/4$ about the spin z axis produces an operator with only positive matrix elements. Thus for this operator all of the pathways to high values of ΔM reinforce. On the other hand, if the couplings have both positive and negative values as in Figure VI.13, the four-quantum coherence agrees with an incoherent reduction, but neither reduction scheme describes the overall intensity pattern well. In fact there is no basis set in which all of the matrix elements of P are positive; however, some terms will still add coherently (for example, all the terms in the diagonal will). This is therefore a mixed case.

6.3.5 Conclusions

An information theory approach to predicting the intensities of multiple-quantum transitions gives good qualitative agreement with experiment for dipolar systems. In this framework the high multiple-quantum transitions are predicted to be enhanced when the couplings all have the same sign, since this case corresponds to coherent pumping. Exact dynamical calculations verify this enhancement. In general, however, the distribution of intensities is approximately statistical.

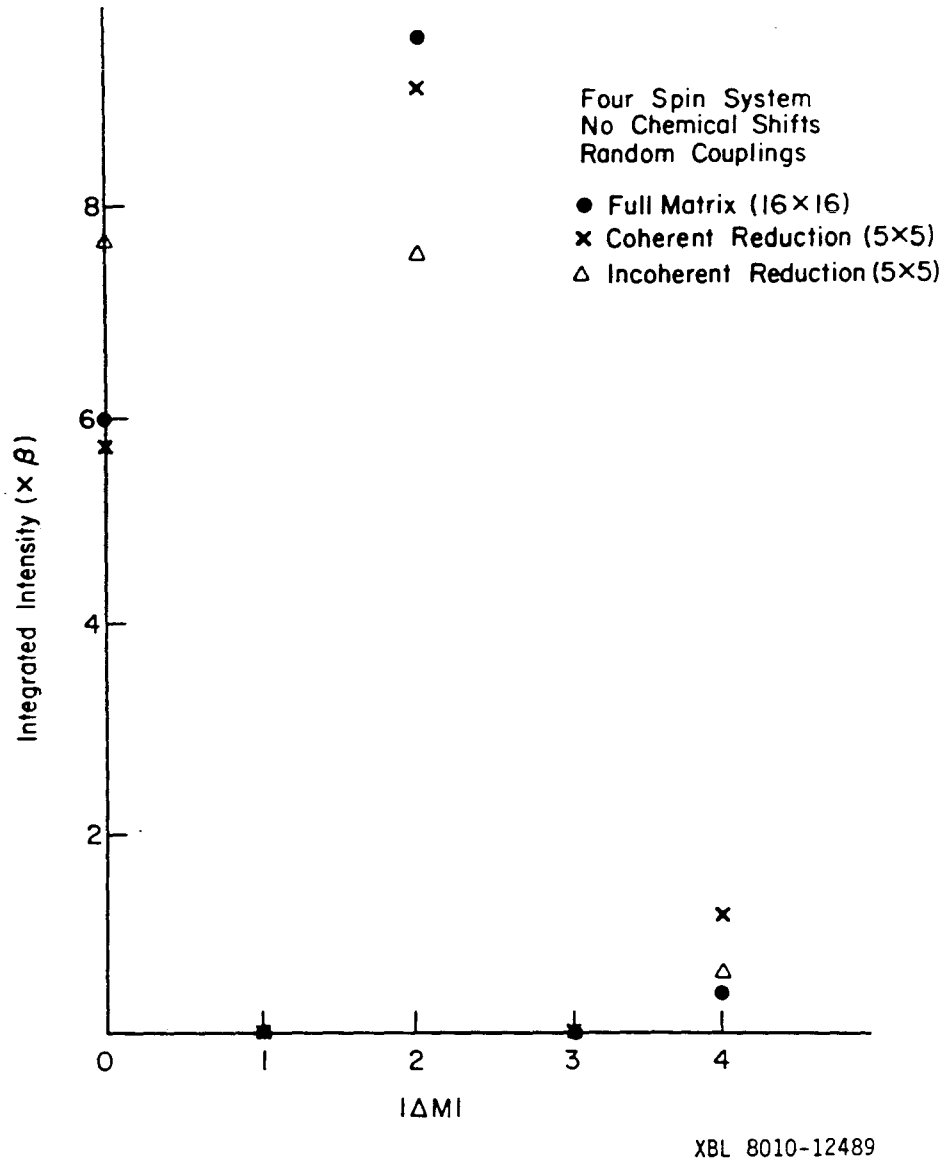

Figure VI.13 Comparison of coherent and incoherent reduction schemes for a four-spin molecule with random couplings. Neither the coherent nor the incoherent reduction agrees well with the full information theory treatment, so the different pathways to high-quantum operators do not reinforce. The intensity of the four-quantum transition is therefore lower than in Figure VI.12.

Appendix A. Counting Schemes for (N-2)-quantum and lower-quantum transitions

As explained in section 1.4, (N-2)-quantum transitions fall into three distinct groups: $M = N/2 \rightarrow M = -((N/2)-2)$, $M = (N/2)-2 \rightarrow M = -N/2$, and $M = ((N/2)-1) \rightarrow M = -((N/2)-1)$. The first two cases are easily handled, because all of those transitions have A_1 symmetry. The number of states with A_1 symmetry for $M = (N/2)-2$ is just the number of distinct pairs of spins, and the same is true for $M = -((N/2)-2)$. Thus each unique pair (ab) of spins generates one pair of transitions in the first two cases.

The third case is more complicated. In general, the transitions from $M = (N/2)-1$ to $M = -((N/2)-1)$ can have any symmetry. The situation can be somewhat simplified for systems with only bilinear couplings, because then the energies and eigenstates for these two manifolds are identical, and the number of transitions (and line positions) will be exactly the same as the spectrum of the zero-quantum transitions in the $M = (N/2)-1$ manifold. In the spin product basis each of these states has one unique spin, and each matrix element can be written as $(a) \rightarrow (b)$, where the label in parentheses specifies that spin. In the most general case, n^2-n of these elements can evolve independently.

If the system has symmetry operations, then the number of independent matrix elements is immediately reduced to the number of unique pairs (ab). In addition, if there exists a symmetry operation $a \leftrightarrow b$ then the matrix element for $(a) \rightarrow (b)$ equals the element for $(b) \rightarrow (a)$. They are also complex conjugates of each other because the density matrix is Hermitian. Thus they are real, and the number of possibly independent matrix elements with imaginary parts is at most equal to the number of pairs (ab) such that $a \not\leftrightarrow b$. If there are m different frequencies for transitions in the

eigenbasis then there will be m independent matrix elements in any other basis, so this gives the number of zero-quantum transitions. Combining this result with the counting arguments for the other groups of (N-2)-quantum transitions shows that there is at most one pair of transitions for each unique ordered pair (ab).

If all of the symmetry operations of the system can be written in terms of permutations of pairs of nuclei, then the number of transitions will be exactly equal to the number of ordered pairs. This will be true whenever the symmetry operations do not include C_n axes ($n \geq 3$) or when the C_n axes are accompanied by mirror planes to raise the group to C_{nv}. Thus, the counting arguments work for all of the examples of section 1.4, and for all other common molecules; one case for which these are fewer transitions than would be predicted is the case of two inequivalent correlated methyl groups.

The arguments can be extended to (N-3)-quantum transitions. Each unique triplet (abc) could generate at most eight transitions: one with $M = N/2 \rightarrow M = -((N/2)-3)$, three with $M = (N/2)-1 \rightarrow M = -((N/2)-2)$ ((a) → (bc), (b) → (ac), (c) → (ab)), three with $M = (N/2)-2 \rightarrow M = -((N/2)-1)$, ((ab) → (c), (ac) → (b), (bc) → (a)), and one with $M = (N/2)-3 \rightarrow M = -N/2$.

Additional symmetry elements will make some of these degenerate. For example, an isolated methyl group will only generate four distinct transitions, and an isoceles triangle ($D_{ab} = D_{bc} \neq D_{ac}$) will generate six distinct transitions. There are also matrix elements of the form (ab) → (a); the number of these is exactly equal to the number of unique ordered pairs of spins.

Appendix B. Listings of Computer Programs

Selective Sequences:

Program	SELECT
Subroutines	HEIGEN, LBINO, NUMSORT, DEFILE, HARDMAT

Information Theory:

Program	INFORM

```
                    27-Oct-1982 13:11:14     VAX-11 FORTRAN IV-PLUS V1.3-22
                                             GSTIN.FOR.12

0001                program select
          c
          c         This program tests selective sequences of arbitrarily high
          c         order.  The parameter 'irev' specifies the construction of the
          c         first subcycle:
          c           0:No time reversal.  This is equivalent to the pulse
          c             sequence (90_x -T-90_x) for the subcycle.
          c
          c           1:Random subcycle Hamiltonian.  The effective Hamiltonian is
          c             assumed to have equal matrix elements everywhere, with
          c             random phases (subject to the constraint that the matrix
          c             be Hermitian).
          c           2:Subcycle WAHUHA sequence. The subcycle pulse sequence is
          c             (T-90_x -T-90_y -2T-90_y -T-90_x -T), which suppresses the dipolar
          c             Hamiltonian to first and second order in the average
          c             Hamiltonian expansion.
          c           3:Isotropic time reversal.  This is equivalent to the
          c             pulse sequence (90_x -T-180_x -T-90_x) for the subcycle.
          c
          c           4:Suppression of zero-quantum operators. If this option is
          c             specified the phase cycling eliminates zero-quantum operators
          c             using phase shifts of (pi/n) instead of (pi/2n), and alter-
          c             nating between H and -H.
          c           12:Subcycle 12-pulse sequence. This pulse sequence eliminates
          c             the dipolar Hamiltonian to two higher orders than does the
          c             WAHUHA sequence. In the compressed notation commonly used
          c             for complicated sequences the states of the Hamiltonian are
          c             (ZYX)(YZX)(XYZ)(ZXY)(YZX)(XYZ).
          c               The 12-pulse sequence is useful for six-quantum selection.
          c             This version of the selective program can only handle systems
          c             with six spins or less, but that can be changed by expanding
          c             the arrays.
          c
0002                complex expiz(4096),u(4096),s(4096),dr(128),r(64),q,ss,ww(64)
0003                complex ca,cphse
0004                dimension ititle(72),c(64),rat(131),avrat(131),ist(64),rho(131),
          1          avdmrat(131),dmrat(131),iflip(2),numb(2,64),avnqco(131)
0005                dimension ist1(2,64),haz(4096),expiy(4096),es(64),d(15)
0006                dimension cj(15),ist(20),ntc(7),isp(6),h(20,20),istart(5)
0007                real inc, iz(64),nqco(131)
0008                common twopi,n
          c
0009                data iz/3.0,2.0,3*1.0,3*0.0,3*-1.0,-2.0,-3.0,51*0.0/
0010                indx(i,j)=nst*(j-1) + i
          c
0011      730       format(21f)
          c
0012                open(unit=21,name='qexhex.dat',type='old')
0013                read(1,632) n,irev,insel,ncyc,nord,nsym,nt,icyc,incwho,nh,ll,mm,tt,dt
0014      632       format(12(i6./),2(e14.6,/))
0015                close(unit=21)
0016                print 632
0017      600       format(///////,11x,'Consider a 2**n by 2**n effective Hamiltonian',
          1          /,11x,'H describing an n spin 1/2 system. Matrix elements are '
          2          /,11x,'pumped in the time available (if coupling constants are',
```

```
                3   /,11x,'given) or assumed to be everywhere equal in magnitude',
                3   /,11x,'with random phases. Phase shifts create a sequence which',
                3   /,11x,'is n-quantum selected to any desired order. This program',
                4   /,11x,'calculates the density matrix which is produced as a ',
                5   /,11x,'function of t, the propagator and coherence selectiv- ',
                6   /,11x,'ities, and the n-quantum signal magnitude.',///)
0018    755     print 601
0019    601     format(11x,'Enter 1 for time reversal, 0 otherwise: ')
0020            print 850
0021    850     format(11x,'(2 gives WAHUHA,3 gives isotropic selection,4 removes')
0022            print 851
0023    851     format(11x,'zero-quantum,and 12 gives the 12 pulse sequence)')
0024            print 799,irev
0025    799     format (11x,i4)
0026            print 602
0027    602     format(11x,'Enter the number of spins (0 implies benzene): ', $)
0028            print 702,n
0029    702     format(i2)
0030            ibenz=0
0031            if(n.eq.0) ibenz = 1
0032            if(ibenz.eq.1) n = 6
0033            nst=2**n
0034            if(ibenz.eq.1) nst = 13
0035            print 623
0036    623     format(11x,'Enter the order of coherence which is selected: ',$)
0037            print 799,insel
0038            jnsel=insel
0039            if(irev.eq.4) insel=insel*2
0040    723     format(i2)
0041    421     print 402
0042    402     format(11x,'Enter the number of cycles, the order of the se-'
                1   /,11x,'quence, and 1 if symmetrization is desired: ',$)
0043            nerd= =1 +(nsym+1)*nerd
0044            print 798,ncyc,nerd,nsym
0045    798     format (11x,3i6)
0046    403     format (3i4)
0047            if(nsym.ne.1) nsym = 0
0048            nsym=nsym + 1
0049            print 604
0050    604     format(11x,'how many different values do you want?(.le.125)',$)
0051            print 799,nt
0052            nprop = nt /12
0053            if (nprop.lt.1) nprop = 1
0054            print 625
0055    625     format(11x,'Enter the initial value for time, in .1 msecs: ',$)
0056    704     format (f8.4)
0057            print 797,tt
0058    797     format (11x,f8.4)
0059            print 640
0060    640     format(11x,'Enter 1 to increment time, 2 to increment cycles:',$)
0061            print 799,incwho
0062    641     format (i2)
0063            if (incwho.ne.1) go to 650
0064            print 605
0065    636     format(11x,'Enter the time increment: ',$)
0066            print 797,dt
```

```
0267            go to 550
0068    650     print 651
0069    651     format (11x,'Enter the cycle increment: ',$)
0070            print 799,icyc
0071    662     print 607
0072    607     format(/,11x,'how many H''s should be averaged over, to minimize',
                1  /,11x,'any peculiarities due to a particular choice of random',
                2  /,11x,'phases ? ',$)
0073            print 799,nh
0074            print 608
0075    608     format(/,11x,'Enter any two positive integers < 32763 : ',$)
0076            print 798,ll,mm
        c
        c
0077            pi=4.0*atan(1.0)
0078            twopi=2.0*pi
0079            inc=twopi/insel
0080            do 10 i=1,101
0081            avnqec(i)=0.0
0082            avdmrat(i)=0.0
0083    10      avrat(i)=0.0
        c
        c       for each state, assign the number of spins "up"
        c
0084            if(iden2.eq.1) go to 645
0085            kk=0
0086            np1=n+1
0087            do 15 im=1,np1
0088            nup=im - 1
0089            mst=lbino(n,nup)
0090            do 12 k=1,mst
0091            kk=kk+1
0092            lst(kk)=nup
0093            iz(kk)=(n - 2*nup) / 2.0
0094    12      continue
0095    15      continue
        c       open(unit=21,name='ret.dat',type='new')
        c       open(unit=22,name='dmrat.dat',type='new')
        c       open(unit=23,name='nqeo.dat',type='new')
        c
        c
0096    645     continue
0097            do 300 ih=1,nh
        c
0098            t=tt
        c
        c       set up the initial matrix:
        c
0099            n212=2
0100            i012=n
0101            if((irev.ne.1).and.(irev.ne.4)) go to 20
0102            do 100 j=1,nst
0103            do 100 i=1,j
0104            phse=ran(ll,mm) * twopi
0105            ij=indx(i,j)
0106            if(i .eq. j) go to 50
```

```
0107            ji=indx(j,i)
0108            nq=int(abs(iz(j) - iz(i)))
0109            a(ij)=0.0
0110            if(nq.le.1012) n212=n212 + 2
0111            if(nq.le.1212) a(ij)=cexp(cmplx(0.0,phse))
0112            a(ji)=conjg(a(ij))
0113            go to 100
0114    50      n212=n212 + 1
0115            a(ij)=sign(1.0,pi - phse)
0116            if (i.eq.nst) a(ij)=a(1)
0117    100     continue
0118            go to 111
        c
0119    20      do 31 i=1,nst
0120            do 31 j=1,nst
0121    31      hzz(indx(i,j))=0.0
0122            call defile('mole',6,1)
0123            read(1,6121) ititle
0124            read(1,6122) n,ncp
0125            read(1,6123) voff,(d(i),i=1,ncp),(cj(i),i=1,ncp),(cs(i),i=1,n)
0126    6121    format(72a1)
0127    6122    format i14)
0128    6123    format(e16.9)
0129            close(unit=21)
        c
0130            nmr=n
0131            nm1=n-1
0132            np1=n+1
0133            print 5221, ititle
0134    5001    format(1h1,///////,11x,72a1,////)
0135            print 5003,voff
0136    5003    format 11x,'offset freq. = ',f7.1,1x,'Hz',//)
0137            voff=voff/2.0
0138            print 5004
0139    5004    format'11x,'dipolar and J couplings (in Hz)',/,11x,31(1h-),/)
0140            k=0
0141            do 5012 i=1,nm1
0142            ip1=i+1
0143            do 5012 j=ip1,n
0144            k=k+1
0145            print 5225,i,j,d(k),i,j,cj(k)
0146    5035    format(11x,'d(',i1,',',i1,') =',f9.2,5x,'J(',i1,',',i1,') =',
              1 f6.2)
0147            d(k)=d(k)/4.0
0148            cj(k)=cj(k)/4.0
0149    5012    continue
0150            print 5026
0151    5026    format(//,11x,'chemical shifts in Hz',/,11x,21(1h-),/)
0152            print 5007,(cs(i), i=1,n)
0153    5007    format(11x,8f9.1)
0154            do 5215 i=1,6
0155    5015    cs(i)=cs(i)/2.0
        c
        c
0156            ans=2.0
0157            do 32 i=1,n
```

```
0158    32      acs=acs + cs(i)
0159            ecp=2.0
0160            do 35 i=1,ncp
0161    35      ecp=ecp + d(i) + cj(i)
0162            hzz(1)=-n*voff + ecp - acs
0163            hzz(indx(nst,nst))=n*voff + ecp + acs
0164            mst0=1
0165            mmst2=2
0166            call numsort(numb,n,nst)
0167            lst1(1,1)=numb(1,nst)
0168            lst1(2,1)=numb(2,nst)
0169            lst1(1,nst)=numb(1,1)
0170            lst1(2,nst)=numb(2,1)
0171            kkk=1
        c
        c
0172            do 113 js=1,nm1
        c
0173            istart(js)=mmst2
0174            is=n - js
0175            itsp=2*is - n
0176            kk=0
0177            do 42 j=1,nst
0178            if(numb(2,j) .ne. is) go to 40
0179            kk=kk+1
0180            kkk=kkk+1
0181            ist(kk)=numb(1,j)
0182            lst1(1,kkk)=numb(1,j)
0183            lst1(2,kkk)=is
0184    42      continue
0185            mst=kk
0186            nbc(js+1)=kk
0187            l=2
        c
0188            do 80 m=1,mst
0189            do 82 l=1,mst
0190            if(l .ne. m) go to 82
0191            msk=1
0192            do 51 k=1,n
0193            isp(k)=-1
0194            if((ist(l) .and. msk) .ne. 0) isp(k)=1
0195            msk=msk + msk
0196    51      continue
0197            h(l,m)= -voff*itsp
0198            kk=2
0199            do 55 i=1,nm1
0200            ip1=i+1
0201            do 55 j=ip1,n
0202            kk=kk+1
0203            h(l,m)=h(l,m)  +  (d(kk) + cj(kk)) * isp(j) * isp(i)
0204    55      continue
0205            do 57 i=1,n
0206    57      h(l,m)=h(l,m) - cs(i)*isp(i)
0207            go to 80
        c
0208    60      jw=1
```

```
      jsp=2
      h(1,m)=0.0
      msk=1
      do 75 k=1,n
      if((ist(1) .and. msk) - (ist(m) .and. msk)) 70,75,70
70    jsp=jsp+1
      iflip(jw)=k
      jw=2
75    msk=msk * 2
      if(jsp .ne. 2) go to 80
      k5= (2*n - iflip(1))*(iflip(1) - 1)/2 - iflip(1) + iflip(2)
      h(1,m)= -d(k5) + 2.0*cj(k5)
80    continue
      do 105 m=1,mst
      do 105 l=1,mst
      hzz(indx(mst0+l,mst0+m))=h(1,m)
105   continue
      mst0=mst0 + mst
110   continue
c
c
c     generation of the pulse propagator.....
c
      aaa=(1.0 / sqrt(2.0)) ** n
      do 2100 i=1,nst
      do 2100 j=1,nst
      expiy(indx(i,j))=aaa
      ksp=1
      msk=1
      do 2000 k=1,n
      if((ist1(i,k) .and. msk) .le. (ist1(i,j) .and. msk)) go to 2000
      ksp=-ksp
2000  msk=msk * msk
      if(ksp .lt. 0) expiy(indx(i,j))=-aaa
2100  continue
c
c     diagonalize and get the energies.....
c
      do 2144 i=1,nst
      do 2142 j=1,nst
      rss=0.0
      do 2141 k=1,nst
      ik=indx(i,k)
      kj=indx(k,j)
2141  rss=rss + expiy(ik)*hzz(kj)
2142  r(j)=cmplx(rss,0.0)
      do 2143 j=1,nst
      ij=indx(i,j)
2143  e(ij)=r(j)
2144  continue
      do 2244 i=1,nst
      do 2242 j=1,nst
      ss=0.0
      do 2241 k=1,nst
      ik=indx(i,k)
      jk=indx(j,k)
```

```
2241          ss=ss + a(ik)*expiy(jk)
2242          r(j)=ss
              do 2243 j=1,nst
              ij=indx(i,j)
2243          a(ij)=r(j)
2244          continue
              tss=0.0
              do 2250 i=1,nst
              do 2250 j=1,nst
2250          tss=tss+a(indx(i,j))*conjg(a(indx(i,j)))/(nst*nst)
              do 2255 i=1,nst
              do 2255 j=1,nst
2255          a(indx(i,j))=a(indx(i,j))/sqrt(tss)
c             call rmat(bzz)
c             call rmat(expiy)
111           call heigen(a,u,nst)
              do 122 i=1,nst
              if((irev.eq.1).or.(irev.eq.4))tscale=sqrt(float(nst)/float(n212))
              if ((irev.ne.1 ).and.(irev.ne.4)) tscale=ni*sqrt(tss)/5000
              ii=indx(i,i)
122           e(i)=a(ii)
c
c
c             now for the time-dependent portion of this program.....
c
c
              do 222 it=1,nt
              if ((it.gt.1).and.(inowho.ne.1)) go to 522
c
c             first calculate exp(-iEt)....
c
              do 140 j=1,nst
              q=cexp(cmplx(0.0,-e(j)*t*tscale))
              ww(j)=q
              do 142 i=1,nst
              ij=indx(i,j)
142           a(ij)=w(ij) * q
d             print 923
c
d             print 924, (ww(j), j=1,nst)
924           format(2f15.5)
c
              do 144 i=1,nst
              do 142 j=1,nst
              ss=0.0
              do 141 k=1,nst
              ik=indx(i,k)
              jk=indx(j,k)
141           ss=ss + a(ik)*conjg(u(jk))
142           r(j)=ss
              do 143 j=1,nst
              ij=indx(i,j)
              dm(ij)=r(j)
143           a(ij)=r(j)
144           continue
              if(irev.eq.2) go to 2300
```

```
0300            if(irev.eq.3) go to 2412
0301            if(irev.eq.12) go to 2320
0302            go to 300
        c       make a WAHUHA sequence...this part makes exp(iHzz T)
0303    2320    do 2344 i=1,nst
0304            do 2342 j=1,nst
0305            ss=0.0
0306            do 2341 k=1,nst
0307            ki=indx(k,i)
0308            kj=indx(k,j)
0309            jk=indx(j,k)
0310    2341    ss=ss + expiy(ki)*a(kj)
0311    2342    r(j)=ss
0312            do 2343 j=1,nst
0313            ij=indx(i,j)
0314    2343    dm(ij)=r(j)
0315    2344    continue
0316            do 2354 i=1,nst
0317            do 2352 j=1,nst
0318            ss=0.0
0319            do 2351 k=1,nst
0320            ik=indx(i,k)
0321            kj=indx(k,j)
0322            jk=indx(j,k)
0323    2351    ss=ss + dm(ik)*expiy(kj)
0324    2352    r(j)=ss
0325            do 2353 j=1,nst
0326            ij=indx(i,j)
0327    2353    dm(ij)=r(j)
0328    2354    continue
0329            do 2355 i=1,nst
0330            do 2355 j=1,nst
0331    2355    expiz(indx(i,j))=dm(indx(i,j))
        c       now multiply by exp(iHxx T)
0332            do 2364 i=1,nst
0333            do 2362 j=1,nst
0334            ss=0.0
0335            do 2361 k=1,nst
0336            ik=indx(i,k)
0337            kj=indx(k,j)
0338            jk=indx(j,k)
0339    2361    ss=ss + dm(ik)*a(kj)
0340    2362    r(j)=ss
0341            do 2363 j=1,nst
0342            ij=indx(i,j)
0343    2363    dm(ij)=r(j)
0344    2364    continue
0345            do 2374 i=1,nst
0346            do 2372 j=1,nst
0347            ss=0.0
0348            do 2371 k=1,nst
0349            ik=indx(i,k)
0350            kj=indx(k,j)
0351            cphse=cexp(cmplx(0.0,pi*(iz(k)-iz(j))/2))
0352            jk=indx(j,k)
0353    2371    ss=ss + dm(ik)*a(kj)*cphse
```

```
2354    2372    r(j)=ss
2355            do 2373 j=1,nst
2356            ij=indx(i,j)
2357    2373    dm(ij)=r(j)
2358    2374    continue
2359            do 2354 i=1,nst
2360            do 2352 j=1,nst
2361            ss=0.0
2362            do 2351 k=1,nst
2363            ik=indx(i,k)
2364            kj=indx(k,j)
2365            cphse=cexp(cmplx(0.0,pi*(iz(k)-iz(j))/2))
2366            jk=indx(j,k)
2367    2351    ss=ss + dm(ik)*a(kj)*cphse
2368    2352    r(j)=ss
2369            do 2353 j=1,nst
2370            ij=indx(i,j)
2371    2353    dm(ij)=r(j)
2372    2354    continue
2373            if(irev.eq.12) go to 10020
2374            do 2390 i=1,nst
2375            do 2392 j=1,nst
2376            ss=0.0
2377            do 2391 k=1,nst
2378            ik=indx(i,k)
2379            kj=indx(k,j)
2380            jk=indx(j,k)
2381    2391    ss=ss - dm(ik)*a(kj)
2382    2392    r(j)=ss
2383            do 2393 j=1,nst
2384            ij=indx(i,j)
2385    2393    dm(ij)=r(j)
2386    2394    continue
2387            do 2424 i=1,nst
2388            do 2422 j=1,nst
2389            ss=0.0
2390            do 2421 k=1,nst
2391            ik=indx(i,k)
2392            kj=indx(k,j)
2393            jk=indx(j,k)
2394    2421    ss=ss + dm(ik)*expiz(kj)
2395    2422    r(j)=ss
2396            do 2423 i=1,nst
2397            ij=indx(i,j)
2398    2423    a(ij)=r(j)
2399    2424    continue
        c       call hardmat(dm)
        c       now give the average Hamiltonian high-order terms...
2400            go to 500
2401    2410    do 804 i=1,nst
2402            do 802 j=1,nst
2403            ss = 0.0
2404            do 821 k=1,nst
2405            ij=indx(i,j)
2406            kj=indx(k,j)
2407            ik=indx(i,k)
```

```
0408    801     ss = ss + (a(ik)*a(kj)*cexp(cmplx(0.0,(iz(k)-iz(j))*twopi/2.0)))
0409    802     r(j)=ss
0410            do 823 j=1,nst
0411            ij=indx(i,j)
0412            dm(ij)=r(j)
0413    823     continue
0414    824     continue
0415            do 810 i=1,nst
0416            do 813 j=1,nst
0417            ij=indx(i,j)
0418    810     a(ij)=dm(ij)
        c       multiply by exp(iHzzT)....
0419            go to 999
0420    10000   do 10004 i=1,nst
0421            do 10002 j=1,nst
0422            ss=0.0
0423            do 10001 k=1,nst
0424            ik=indx(i,k)
0425            kj=indx(k,j)
0426            jk=indx(j,k)
0427    10001   ss=ss + dm(ik)*expiz(kj)
0428    10002   r(j)=ss
0429            do 10003 j=1,nst
0430            ij=indx(i,j)
0431    10003   dm(ij)=r(j)
0432    10004   continue
        c       now multiply by exp(iHxx T)
0433            do 10014 i=1,nst
0434            do 10012 j=1,nst
0435            ss=0.0
0436            do 10011 k=1,nst
0437            ik=indx(i,k)
0438            kj=indx(k,j)
0439            jk=indx(j,k)
0440    10011   ss=ss + dm(ik)*a(kj)
0441    10012   r(j)=ss
0442            do 10013 j=1,nst
0443            ij=indx(i,j)
0444    10013   dm(ij)=r(j)
0445    10014   continue
        c       now multiply by exp(iHxx T)
0446            do 10024 i=1,nst
0447            do 10022 j=1,nst
0448            ss=0.0
0449            do 10021 k=1,nst
0450            ik=indx(i,k)
0451            kj=indx(k,j)
0452            jk=indx(j,k)
0453    10021   ss=ss + dm(ik)*a(kj)
0454    10022   r(j)=ss
0455            do 10023 j=1,nst
0456            ij=indx(i,j)
0457    10023   dm(ij)=r(j)
0458    10024   continue
        c       multiply by exp(iHyyT)....
0459            do 10034 i=1,nst
```

```
      do 10032 j=1,nst
      ss=2.0
      do 10031 k=1,nst
      ik=indx(i,k)
      kj=indx(k,j)
      cphse=cexp(cmplx(0.0,pi*(iz(k)-iz(j))/2))
      jk=indx(j,k)
10031 ss=ss + dm(ik)*a(kj)*cphse
10032 r(j)=ss
      do 10033 j=1,nst
      ij=indx(i,j)
10033 dm(ij)=r(j)
10034 continue
c     multiply by exp(iEzzT)....
      do 10044 i=1,nst
      do 10042 j=1,nst
      ss=2.0
      do 10041 k=1,nst
      ik=indx(i,k)
      kj=indx(k,j)
      jk=indx(j,k)
10041 ss=ss + dm(ik)*expiz(kj)
10042 r(j)=ss
      do 10043 j=1,nst
      ij=indx(i,j)
10043 dm(ij)=r(j)
10044 continue
c     multiply by exp(iEzzT)....
      do 10054 i=1,nst
      do 10052 j=1,nst
      ss=2.0
      do 10051 k=1,nst
      ik=indx(i,k)
      kj=indx(k,j)
      jk=indx(j,k)
10051 ss=ss + dm(ik)*expiz(kj)
10052 r(j)=ss
      do 10053 j=1,nst
      ij=indx(i,j)
10053 dm(ij)=r(j)
10054 continue
c     multiply by exp(iHyyT)....
      do 10064 i=1,nst
      do 10062 j=1,nst
      ss=2.0
      do 10061 k=1,nst
      ik=indx(i,k)
      kj=indx(k,j)
      cphse=cexp(cmplx(0.0,pi*(iz(k)-iz(j))/2))
      jk=indx(j,k)
10061 ss=ss + dm(ik)*a(kj)*cphse
10062 r(j)=ss
      do 10063 j=1,nst
      ij=indx(i,j)
10063 dm(ij)=r(j)
10064 continue
```

```
        c       now multiply by exp(iHxx T)
        10      do 10074 i=1,nst
                do 10072 j=1,nst
                ss=0.0
                do 10071 k=1,nst
                ik=indx(i,k)
                kj=indx(k,j)
                jk=indx(j,k)
        10071   ss=ss + dm(ik)*a(kj)
        10072   r(j)=ss
                do 10073 j=1,nst
                ij=indx(i,j)
        10073   dm(ij)=r(j)
        10074   continue
        c       now multiply by exp(iHyy T)
                do 10084 i=1,nst
                do 10082 j=1,nst
                ss=0.0
                do 10081 k=1,nst
                ik=indx(i,k)
                kj=indx(k,j)
                jk=indx(j,k)
        10081   ss=ss + dm(ik)*a(kj)
        10082   r(j)=ss
                do 10083 j=1,nst
                ij=indx(i,j)
        10083   dm(ij)=r(j)
        10084   continue
        c       multiply by exp(iHzzT)....
                do 10094 i=1,nst
                do 10092 j=1,nst
                ss=0.0
                do 10091 k=1,nst
                ik=indx(i,k)
                kj=indx(k,j)
                jk=indx(j,k)
        10091   ss=ss + dm(ik)*expiz(kj)
        10092   r(j)=ss
                do 10093 j=1,nst
                ij=indx(i,j)
        10093   dm(ij)=r(j)
        10094   continue
        c       multiply by exp(iHyyT)....
                do 10104 i=1,nst
                do 10102 j=1,nst
                ss=0.0
                do 10101 k=1,nst
                ik=indx(i,k)
                kj=indx(k,j)
                cphse=cexp(cmplx(0.0,pi*(iz(k)-iz(j))/2))
                jk=indx(j,k)
        10101   ss=ss + dm(ik)*a(kj)*cphse
        10102   r(j)=ss
                do 10103 j=1,nst
                ij=indx(i,j)
        10103   dm(ij)=r(j)
```

```
SELECT          27-Oct-1982 18:11:14     VAX-11 FORTRAN IV-PLUS V1.3-22
                                         GSPIN.FOR.12

      10124     continue
      c         multiply by exp(iEyyT)....
                do 10114 i=1,nst
                do 10112 j=1,nst
                ss=0.0
                do 10111 k=1,nst
                ik=indx(i,k)
                kj=indx(k,j)
                cphse=cexp(cmplx(0.0,pi*(iz(k)-iz(j))/2))
                jk=indx(j,k)
      10111     ss=ss + dm(ik)*a(kj)*cphse
      10112     r(j)=ss
                do 10113 j=1,nst
                ij=indx(i,j)
      10113     dm(ij)=r(j)
      10114     continue
      c         now multiply by exp(iExx T)
                do 10124 i=1,nst
                do 10122 j=1,nst
                ss=0.0
                do 10121 k=1,nst
                ik=indx(i,k)
                kj=indx(k,j)
                jk=indx(j,k)
      10121     ss=ss + dm(ik)*a(kj)
      10122     r(j)=ss
                do 10123 j=1,nst
                ij=indx(i,j)
      10123     dm(ij)=r(j)
      10124     continue
      c         multiply by exp(iEzzT)....
                do 10134 i=1,nst
                do 10132 j=1,nst
                ss=0.0
                do 10131 k=1,nst
                ik=indx(i,k)
                kj=indx(k,j)
                jk=indx(j,k)
      10131     ss=ss + dm(ik)*expiz(kj)
      10132     r(j)=ss
                do 10133 j=1,nst
                ij=indx(i,j)
      10133     a(ij)=r(j)
      10134     continue
      399       continue
      c         decide how many times to cycle propagator
      c         if(mod(it,nprop).ne.1) go to 146
      c         if(it.ne.1) go to 146
      c         if(nst.gt.16) go to 146
      c         print 145,t
      c         format (/'The nonselected propagator for t = ',f8.4,1x,'is:' /)
      c         call hardmat (a)
                if (nord.eq.0) go to 520
                do 515 i3=1,nord
                do 450 i=1,nst
                do 450 j=1,nst
```

```
0611            ij=indx(i,j)
0612            dm(ij)=0.0
0613      450   if (i.eq.j) dm(ij)=1.0
0614            imsel=imsym*insel
0615            do 510 i1=1,imsel
0616            if (i1.le.insel) phse=inc * (i1-1)
0617            if (i1.gt.insel) phse=inc * (imsel-i1)
        c       multiply by last propagator
0618            if(nsym.eq.1) nz=(-1)**(min(i1-1,imsel-i1))
0619            if(nsym.ne.1) nz=(-1)**(i1+1)
0620            if(irev.ne.4) nz=1
0621            do 505 i=1,nst
0622            do 503 j=i,nst
0623            ss=0.0
0624            do 502 k=1,nst
0625            ik=indx(i,k)
0626            kj=indx(k,j)
0627            jk=indx(j,k)
0628            if(nz.eq.1) ca=a(kj)
0629            if(nz.ne.1) ca=conjg(a(jk))
0630      502   ss=ss+dm(ik)*ca*cexp(cmplx(0.0,(iz(k)-iz(j))*phse))
0631      503   r(j)=ss
0632            do 504 j=1,nst
0633            ij=indx(i,j)
0634      504   dm(ij)=r(j)
0635      505   continue
0636      510   continue
        d       call hardmat (dm)
0637            do 513 i=1,nst
0638            ss=0.0
0639            do 511 j=1,nst
0640            ij=indx(i,j)
0641      511   ss=ss + (dm(ij)*conjg(dm(ij)))
0642            do 512 j=1,nst
0643            ij=indx(i,j)
0644            dm(ij)=dm(ij)/csqrt(ss)
0645            if (incwho.ne.1) u(ij)=dm(ij)
0646      512   a(ij)=dm(ij)
0647      513   continue
0648      515   continue
        d       call hardmat (dm)
0649      520   if (ncyc.eq.1) go to 550
0650            do 551 ns=2,ncyc
0651            do 529 i=1,nst
0652            do 527 j=1,nst
0653            ss=0.0
0654            do 526 k=1,nst
0655            ik=indx(i,k)
0656            kj=indx(k,j)
0657            if(incwho.ne.1) dm(kj)=u(kj)
0658      526   ss=ss+(a(ik)*dm(kj))
0659      527   r(j)=ss
0660            do 528 j=1,nst
0661            ij=indx(i,j)
0662      528   a(ij)=r(j)
0663      529   continue
```

```
0664    681     continue
0665    550     continue
        c       find averages of propagator selected and non selected elements....
        c
0666            nsel=0
0667            nnon=0
0668            avsel=0.0
0669            avnon=0.0
0670            do 160 j=1,nst
0671            do 160 i=1,nst
0672            if(i .eq. j) go to 160
0673            ij=indx(i,j)
0674            nq=int(abs(iz(j) - iz(i)))
0675    101     format (1x,'  ',i2,$)
0676            if(mod(nq,jnsel) .ne. 0) go to 150
0677            if(irev.eq.4.and.nq.eq.0) go to 160
0678            avsel=avsel + cabs(a(ij)*a(ij))
0679            nsel=nsel + 1
0680            go to 160
0681    150     avnon=avnon + cabs(a(ij)*a(ij))
0682            nnon=nnon + 1
0683    160     continue
        c
        c       the long-awaited propagator ratio at last....
        c
        d       print 101,nsel
0684            if(avsel.ne.0) avsel=sqrt(avsel/ nsel)
0685            if(avnon.ne.0) avnon=sqrt(avnon/ nnon)
0686            if (avnon.ne.0) rat(it)=avsel / avnon
0687            if(avnon.eq.0) rat(it)=0
        c
        c
        c       now calculate exp(-iHt) Iz exp(iHt)
        c
0688            do 170 j=1,nst
0689            do 170 i=1,nst
0690            ij=indx(i,j)
0691    170     dm(ij)=a(ij) * iz(j)
        c
0692            do 194 i=1,nst
0693            do 182 j=1,nst
0694            ss=0.0
0695            do 181 k=1,nst
0696            ik=indx(i,k)
0697            jk=indx(j,k)
0698    181     ss=ss + dm(ik)*conjg(a(jk))
0699    182     r(j)=ss
0700            do 183 j=1,nst
0701            ij=indx(i,j)
0702    183     dm(ij)=r(j)
0703    184     continue
0704            if(mod(it,nprop).ne.1) go to 147
0705            if(ik.ne.1) go to 147
0706            if(nst.gt.16) go to 147
0707            print 148,t
0708    148     format ('1The density matrix for t = ',g11.4,1x,'is:',/)
```

```
0709            call berimat (dm)
          c     calculate trace rho squared
0710      147   rho2=0.0
0711            do 785 i=1,nst
0712            do 785 j=1,nst
0713            ij=indx(i,j)
0714            rho2=rho2+cabs(dm(ij)*dm(ij))
0715      785   continue
0716            rho(it)=rho2
          c     find the magnitude of the n-quantum coherence and the average
          c     magnitude of the non-selected elements of exp(-iHt) Iz exp(iHt) ....
          c
0717            nsel=0
0718            avsel=0.0
0719            nnon=0
0720            avnon=0.0
0721            do 192 j=2,nst
0722            jm1=j-1
0723            do 192 i=1,jm1
0724            ij=indx(i,j)
0725            nq=int(abs(iz(i) - iz(j)))
0726            if(mod(nq,jnsel).ne. 0) go to 185
0727            if(nq .eq. 0) go to 192
0728            avsel=avsel+cabs(dm(ij)*dm(ij))
0729            nsel=nsel + 1
0730            go to 192
0731      185   avnon=avnon + cabs(dm(ij)*dm(ij))
0732            nnon=nnon + 1
0733      192   continue
          c     ..
          c     the n-quantum coherence/non-selected ratio for the transformed Iz.....
          c
0734            if(avsel.ne.0)avsel=sqrt(avsel/nsel)
0735            nqco(it)=avsel*avsel
0736            if(avnon.ne.0) avnon=sqrt(avnon/ nnon)
0737            if (avnon.ne.0)dmrat(it)=avsel / avnon
0738            if(avnon.eq.0) dmrat(it)=0
          c
          c     increment time....
          c
0739            if (incwho.eq.1) t=t + dt
0740            if (incwho.ne.1) ncyc=icyc+1
0741      200   continue
          c
          c
0742            if(nh .eq. 1) go to 250
0743            if(nh .gt. 5) go to 210
0744            print 610,ih
0745      610   format(//,11x,'data for initial matrix ',i2,':',/)
0746            print 611
0747      611   format(3x,'propagator selected/non-selected ratios....',/)
0748            print 615, (rat(i), i=1,nt)
0749      615   format(13x,5g12.1)
0750            print 612
0751      612   format(//,3x,'the n-quantum coherence/non-selected coherence',
                1  11x,'ratio....',/)
```

```
0752            print 615, (dmrat(i), i=1,nt)
0753            print 613
0754      613   format(/,3x,'n quantum signal (coherence squared)...'/)
0755            print 615, (nqco(i), i=1,nt)
0756            go to 222
0757      210   print 616, ih
0758      616   format(11x,'initial matrix #',i3,11x,' completed')
0759      222   continue
          c     if(ih .le. 10) write(1,620) (rat(i), i=1,nt)
          c     if(ih .le. 10) write(2,620) (dmrat(i), i=1,nt)
          c     if(ih .le. 10) write(3,620) (nqco(i), i=1,nt)
0760      620   format(f15.5)
          c
0761      250   do 260 i=1,nt
0762            avnqco(i)=avnqco(i) + nqco(i)
0763            avdmrat(i)=avdmrat(i) + dmrat(i)
0764      260   avrat(i)=avrat(i) + rat(i)
0765      320   continue
          c
          c
          c
0766            do 320 i=1,nt
0767            avnqco(i)=avnqco(i) / nh
0768            avdmrat(i)=avdmrat(i) / nh
0769      320   avrat(i)=avrat(i) / nh
          c
          c     close(unit=21)
          c     close(unit=22)
          c     close(unit=23)
0770            open(unit=21,name='avrat.dat',type='new')
0771            write(1,620) (avrat(i), i=1,nt)
0772            close(unit=21)
0773            open(unit=21,name='avdmrat.dat',type='new')
0774            write(1,620) (avdmrat(i), i=1,nt)
0775            close(unit=21)
0776            open(unit=21,name='avnqco.dat',type='new')
0777            write(1,620) (avnqco(i), i=1,nt)
0778            close(unit=21)
          c
0779            print 621
0780      621   format(1h1,//////,11x,'AVERAGE propagator selectivity...',/)
0781            print 615, (avrat(i), i=1,nt)
          c     print 722
          c.    format(11x,'Graph of AVERAGE propagator ratios:',/)
0782            call wcvplot(avrat,nt,5)
          c
          c     print 736
          c     format('1TYPICAL values of trace rho squared...',/)
          c     print 615, (rho(i), i=1,nt)
0783            print 622
0784      622   format(1h1,//////,11x,'AVERAGE coherence selectivity...',/)
0785            print 615, (avdmrat(i), i=1,nt)
          c     print 721
          c     format(11x,'Graph of AVERAGE coherence ratios:',/)
0786            call wcvplot(avdmrat,nt,5)
0787            print 623
```

```
SELECT          27-Oct-1980 13:11:14     VAX-11 FORTRAN IV-PLUS V1.3-22
                                         ESTIM.FOR;12

2758    823     format(1h1,///////,11x,'AVERAGE n-quantum signal magnitude.. .'./)
2759            print 815, (avnqco(i), i=1,nt)
2760            aimbig=r * n / 4.0
        c       print 725
        c       format '11x,'Graph of AVERAGE n-quantum signal magnitude:',/)
2791            call wowplot(avnqco,nt,aimbig)
2792            end
```

27-Oct-1980 18:13:24 VAX-11 FORTRAN IV-PLUS V1.3-22

```
              c
              c
              c
              c
0221                subroutine wowplot(avdat,nt,s)
              c
              c     displays data on the crt
              c
0222                dimension avdat(125),my(126),lx(126)
              c
0223                print 723
0224          723   format (1h1)
0225                qt=nt
0226                nt1=nt+1
0227                amax=2.0
0228                do 410 i=1,nt
0229          410   amax=amax1(avdat(i),amax)
0210                amax=amax1(s,amax)
0211                if(amax.eq.0) amax=1
0212                do 420 i=1,nt
0213          420   my(i)=53.3 * (amax - avdat(i)) / amax  +  1.5
0214                ms=53.3 * (amax - s) / amax  +  1.5
              c
0215                do 436 l=1,59
0216                if(l .eq. 59) go to 427
0217                do 425 i=2,126
0218          425   lx(i)=1h
0219                lx(1)=1h|
0220                if(l .eq. ms) lx(1)=1hs
0221                go to 429
0222          427   do 426 i=2,126
0223          426   lx(i)=1h-
0224                lx(1)=1h+
0225          429   do 432 k=1,nt
0226                kx=125.2 * k/qt  +  1.5
0227          432   if(l .eq. my(k)) lx(kx)=1h*
0228                print 630, (lx(i), i=1,126)
0229          435   continue
              c
0230          630   format(1x,126a1)
0231                print 631,amax
0232          631   format(5x,'y-axis range: 0 to ',f15.5)
0233                return
0234                end
```

```
0001          subroutine heigen(h,u,nm)
        c
        c     this subroutine diagonalizes an nm by nm hermitian matrix h by
        c     the Jacobi method and outputs h and the unitary transformation
        c     matrix u.  the procedure is adapted from subroutine  eigen
        c     in the IBM system/360 scientific subroutine package.
        c
0002          complex h(nm,nm),u(nm,nm),ull,ulm,uml,umm,th,tu
0003          nnm=nm-1
0004          qn=nm
0005          range=5.2e-11
0006          do 20 i=1,nm
0007          do 10 j=1,nm
0008    10    u(i,j)=0.0
0009    20    u(i,i)=1.0
        c
0010          anorm=0.0
0011          do 32 i=1,nnm
0012          ii=i+1
0013          do 30 j=ii,nm
0014    30    anorm=anorm + real(h(i,j)*conjg(h(i,j)))
0015          if(anorm .le. range) return
0016          anorm=sqrt(2.0 * anorm)
0017          anormx=anorm * range / qn
0018          ind=0
0019          thr=anorm
        c
0020    40    thr=thr/qn
        c
0021    50    do 80 l=1,nnm
0022          ll=l+1
0023          do 80 m=ll,nm
0024          if( cabs(h(l,m)) .lt. thr ) go to 80
        c
0025          ind=1
0026          diff=real( h(m,m) - h(l,l) )
0027          if(diff .eq. 0.0) diff=1.0e-15
0028          ar=0.5 * atan( 2.0 * real(h(l,m)) / diff )
0029          ai=0.5 * atan( 2.0 * aimag(h(l,m)) / diff )
0030          sini=sin(ai)
0031          cosi=cos(ai)
0032          sinr=sin(ar)
0033          cosr=cos(ar)
0034          ull=cmplx( cosr*cosi, sinr*sini )
0035          ulm=cmplx(-sinr*cosi,-cosr*sini )
0036          uml=cmplx( sinr*cosi,-cosr*sini )
0037          umm=cmplx( cosr*cosi,-sinr*sini )
        c
0038          do 60 j=1,nm
0039          th=     ull*h(l,j) + ulm*h(m,j)
0040          h(m,j)=uml*h(l,j) + umm*h(m,j)
0041          h(l,j)=th
0042    60    continue
        c
0043          do 70  i=1,nm
0044          th=     umm*h(i,l) - uml*h(i,m)
```

```
0245          b(i,m)=-ulm*b(i,1) + ull*b(i,m)
0246          b(i,1)=tn
0247          tu=      umm*u(i,1) - uml*u(i,m)
0248          u(i,m)=-ulm*u(i,1) + ull*u(i,m)
0249          u(i,1)=tu
0250    70    continue
        c
0251    80    continue
        c
0252          if(ind .eq. 0) go to 100
0253          ind=0
0254          go to 50
        c
0255    100   if(thr .gt. anormx) go to 40
0256          return
0257          end
```

```
0001          function lbino(n,m)
        c
        c     computes the binomial coefficient for n "things" taken m at a time
        c
0002          lbino=1
0003          if(m .le. 0) return
0004          if(m .ge. n) return
0005          mm=m
0006          if(m .gt. n/2) mm=n-m
0007          lbino=n
0008          if(mm .eq. 1) return
0009          mm1=mm-1
0010          id=1
0011          do 20 i=1,mm1
0012          lbino=lbino*(n-i)
0013          id=id*(i+1)
0014    20    continue
0015          lbino=lbino/id
0016          return
0017          end
```

```
0001          subroutine numsort(numb,n,nn)
        c
        c     tatulates the number of 'ones' in the binary representation
        c     of integers
        c
0002          dimension numb(2,nn)
0003          do 23 j=1,nn
0004          jj=j-1
0005          numb(1,j)=jj
0006          kk=1
0007          ll=0
0008          do 12 k=1,n
0009          if((jj .and. kk) .ne. 0) ll=ll+1
0010          kk=kk+kk
0011    12    continue
0012          numb(2,j)=ll
0013    23    continue
0014          return
0015          end
```

```
0001          subroutine defile(name,kk,io)
        c
        c     opens a file on the disk
        c             io=1 for input
        c             io=0 for output
        c
0002          dimension m(3)
0003          m(1)=name
0004          m(2)=4hb0.da
0005          m(3)=0
        c
0006          m21=4hi.da
0007          inc=m21 - m(2)
0008          m(2)=m(2) + kk*inc
        c
0009          if(io .eq. 0) open(unit=01,name=m,type='new',err=900)
0010          if(io .eq. 1) open(unit=01,name=m,type='old',err=900)
0011          return
        c
        c
0012    900   type 901,kk
0013    901   format(//,' open error for file ',i1,/)
0014          return
0015          end
```

```
      subroutine hardmat(p)
c
c     displays complex matrices (up to 16x16) or one page
c
      complex p(256)
      dimension mag(16),iph(16),lst(16)
      common twopi,n
c
      indx(i,j)=(j-1)*nst1 + i
c
      nst=2**n
      if(n.gt.4) nst = 16
      if(n.eq.3) nst = 13
      nst1=nst
      if(nst.eq.16) nst1=2**n
      rad=twopi/360.
c
      kk=0
      np2=n
      if(nst.ge.10) np2 = 4
      np1=np2-1
d     print 103,nst,n,np2,np1
      do 15 im=1,np1
      nup=np1 - im
      nst=lshift(np2,nup)
      do 12 k=1,nst
      kk=kk+1
      lst(kk)=nup
12    continue
15    continue
c
c
      print 125, (lst(j), j=1,nst)
125   format(1h0,//,3x,16(' |',i1,' up>'))
      print 112
112   format(1x,132(1h-))
c
c     calculate phase and magnitude for each matrix element, then print....
c
      do 50 i=1,nst
      do 42 j=1,nst
      ij=indx(i,j)
      xx=real(p(ij))
      yy=aimag(p(ij))
      zz=cabs(p(ij))
      if(zz .lt. 0.001) go to 35
      if(xx) 34,31,34
31    if(yy) 33,32,32
32    iph(j)=90
      go to 40
33    iph(j)=-90
      go to 40
34    ph=atan2(yy,xx) / rad
      iph(j)=ph + sign(0.5,ph)
      go to 42
35    iph(j)=0
```

```
BARDMAT          27-Oct-1984 19:27:21     VAX-11 FORTRAN IV-PLUS V1.3-22
                                          SUBS.FOR;1

0045     62      mag(j)=1.00, * aa - sign(0.5,aa)
0046             print 115, lst(1),(mag(j), j=1,nst)
0047     115     format(1h2,'c',i1,' mp|',16i7)
0048             print 116, (ipk(j), j=1,nst)
0049     116     format(7c,16i7)
0050     50      continue
         c
0051             return
0052             end
```

```
0001          program inform
        c
        c     This program is designed to go where no man has gone before
        c     with information theory--into multiple-quantum NMR.  It derives
        c     from 'Espin' (and from some of Jim Murdoch's programs) the
        c     operators Ezz and Exx.  It will use these operators to produce
        c     exp(Hxx T) and exp([Hxx,Iz] T).
        c
0222          complex trace(25),dm(4096),r(64),q,ss,e(64),pump(4096),u(4096)
0223          complex sum,ee(19),dmred(361),ured(361),pumpred(361)
0224          complex ee1(19),dmred1(361),ured1(361),pumpred1(361)
0225          dimension ititle(72),lst(64),count(19,19),avred(19,19),
            1 iflip(2),numb(2,64),ave1(19,19),ave(19,19),hzx(4096),rr(64)
0226          dimension s2(19), lst1(2,64),hzz(4096),expiy(4096),cs(6),d(15)
0227          dimension cj(15),ist(22),nbs(7),isp(6),k(22,22),istart(5)
0228          dimension facpl(20),degen(20)
0229          real iro,ix(64,64),rho(25),iz(64)
0212          common twopi n
        c
0211          data iz/3.2,2.0,3*1.0,3*0.2,3*-1.0,-2.0,-3.0,51*0.0/
0212          irdx(i,j)=(n+1)*(j-1) + i
0213          indx(i,j)=nst*(j-1) + i
        c
        c
0214          open(unit=61,name='inform.dat',type='old')
0215          read(1,622) n,nt,icomm,tt,csave,dijave,dt
0216          tscale=1.2/(max(dijave,csave,1.0))
0217          npl=n-1
0218          print 622
0219    623   format(/,' This program uses information theory to predict ',
            1  /,' the most probable density matrix. The pumping operator ',
            2  /,' can have any one of several different forms.',/,//)
0220          print 602
0221    622   format(' Enter the number of spins (.le. 4): ', $)
0222          print 799,n
0223    799   format(1x,i4)
0224    722   format(i4)
0225          nst=2**n
0226          print 623
0227    623   format(' What is the form of the pumping operator:')
0228          print 623
0229    602   format('     1:Pumping operator Exx',/,'     2:Pumping op',
            1  'erator [Exx,Iz]')
0230          print 799,icomm
0231    723   format(i2)
0232          print 624
0233    624   format(' How many different values do you want ? (.le. 25) ',$)
0234          print 799,nt
0235          print 635
0236    635   format(' Enter the initial value for time: ',$)
0237    797   format (1x,g11.4)
0238          print 797,tt
0239          print 636
0240    606   format(' Enter the time increment: ',$)
0241          print 797,dt
0242          if(n.le.6) go to 7999
```

```
0243            print 7978
0244    7978    format(' Enter the r.m.s. dipolar coupling and chemical shift:')
0245            print 7979,dijave,csave
0246    7979    format(' ',g13.4,'  ',g13.4)
        c
0247    620     format(3'16,/),4(e14.6,/))
0248    7980    close(unit=21)
        c
0249            nst=2**n
0250            pi=4.0*atan(1.0)
0251            do 8212 i=3,npl
0252            facpl(1)=1
0253            facpl(2)=1
0254    8210    facpl(i)=(i-1)*facpl(i-1)
0255            do 8220 i=1,npl
0256    8220    degen(i)=facpl(npl)/(facpl(i)*facpl(npl+1-i))
0257            twopi=2.0*pi
0258            if(n.gt.6) go to 8000
        c
        c       for each state, assign the number of spins 'up'
        c
0259            kk=0
0260            npl=n+1
0261            do 15 im=1,npl
0262            nup=im - 1
0263            nst=ibinc(n,nup)
0264            do 12 k=1,nst
0265            kk=kk+1
0266            lst(kk)=nup
0267            iz(kk)=(n - 2*nup) / 2.0
0268    12      continue
0269    15      continue
0270            do 31 i=1,nst
0271            do 31 j=1,nst
0272    31      hze(index(i,j))=0.0
0273            call defile('role',9,1)
0274            read(1,6101) ititle
0275            read(1,6102) n,ncp
0276            read(1,6103) voff,(d(i),i=1,ncp),(cj(i),i=1,ncp),(cs(i),i=1,n)
0277    6101    format(72a1)
0278    6102    format(i14)
0279    6103    format(e16.8)
0280            close(unit=31)
        c
0281            nnn=n
0282            nm1=n-1
0283            npl=n+1
0284            print 5202, ititle
0285    5202    format(1a1,'/',1x,72a1,////)
0286            print 5203,voff
0287    5203    format(6x,'offset freq. = ',f7.1,' Hz',//)
0288            voff=voff/2.0
0289            print 5204
0290    5204    format(6x,'dipolar and J couplings (in Hz)',/,6x,31(1h-),/)
0291            k=0
0292            do 5010 i=1,nm1
```

```
0093            ip1=i+1
0094            do 5010 j=ip1,n
0095            k=k+1
0096            print 5025,i,j,d(k),i,j,cj(k)
0097      5025  format(6x,'d(',i1,',',i1,') =',f9.2,5x,'J(',i1,',',i1,') =',
                1  f6.2)
0098            d(k)=d(k)/4.0
0099            cj(k)=cj(k)/4.0
0100      5010  continue
0101            print 5026
0102      5026  format(//,6x,'chemical shifts in Hz',/,6x,21(1h=),/)
0103            print 5027,(cs(i), i=1,n)
0104      5027  format(6x,6f8.1)
0105            csave=0
0106            do 5015 i=1,6
0107            if(cs(i).ne.0) csave=1
0108      5015  cs(i)=cs(i)/2.0
        c
        c
0109            acs=0.0
0110            do 32 i=1,n
0111      32    acs=acs - cs(i)
0112            ecp=0.0
0113            do 35 i=1,ncp
0114      35    ecp=ecp + d(i) - cj(i)
0115            hz2(1)=-n*voff + ecp - acs
0116            hz2(ind(nst,nst))=n*voff + ecp + acs
0117            mst0=1
0118            mmst0=0
0119            call numsort(numb,n,nst)
0120            lst1(1,1)=numb(1,nst)
0121            lst1(2,1)=numb(2,nst)
0122            lst1(1,nst)=numb(1,1)
0123            lst1(2,nst)=numb(2,1)
0124            kkk=1
        c
        c
0125            do 110 js=1,nm1
        c
0126            istart(js)=mmst0
0127            is=n - js
0128            itsp=2*is - n
0129            kk=0
0130            do 40 j=1,nst
0131            if(numb(2,j) .ne. is) go to 40
0132            kk=kk+1
0133            kkk=kkk+1
0134            ist(kk)=numb(1,j)
0135            lst1(1,kkk)=numb(1,j)
0136            lst1(2,kkk)=is
0137      40    continue
0138            mst=kk
0139            ktc(js+1)=kk
0140            lm=0
        c
0141            do 80 m=1,mst
```

```
      do 33 l=1,mst
      if(l .ne. m) go to 60
      msk=1
      do 51 k=1,n
      isp(k)=-1
      if((ist(l) .and. msk) .ne. 0) isp(k)=1
      msk=msk + msk
51    continue
      h(l,m)= -voff*itsp
      kk=0
      do 55 i=1,nm1
      ip1=i+1
      do 55 j=ip1,n
      kk=kk+1
      h(l,m)=h(l,m) + (d(kk) * cj(kk)) * isp(j) * isp(i)
55    continue
      do 57 i=1,n
57    h(l,m)=h(l,m) - cs(i)*isp(i)
      go to 33
c
60    jw=1
      jsp=0
      h(l,m)=2.0
      msk=1
      do 75 k=1,n
      if((ist(l) .and. msk) - (ist(m) .and. msk.) 73,75,73
73    jsp=jsp+1
      iflip(jw)=k
      jw=2
75    msk=msk * 2
      if(jsp .le. 2) go to 33
      k5= (2*n - iflip(1))*(iflip(1) - 1)/2  -  iflip(1)  +  iflip(2)
      h(l,m)= -c(k5) + 2.0*cj(k5)
82    continue
      do 125 m=1,mst
      do 125 l=1,mst
      h2(indx(mst3+l,mst3+m))=h(l,m)
125   continue
      mst3=mst3 + mst
110   continue
c
c
c     generation of the pulse propagator.....
c
      aaa=(1.2 / sqrt(2.0)) ** n
      do 2100 i=1,nst
      do 2100 j=1,nst
      expiy(indx(i,j))=aaa
      ksp=1
      msk=1
      do 2000 k=1,n
      if((lst1(1,i) .and. msk) .le. (lst1(1,j) .and. msk)) go to 2000
      ksp=-ksp
2000  msk=msk + msk
      if(ksp .lt. 3) expiy(indx(i,j))=-aaa
2100  continue
```

```
        c       generation of Iz....
2193            do 2130 i=1,nst
2194            do 2130 j=1,nst
2195            sp=0
2196            msk=1
2197            do 2230 k=1,n
2198            if((ist1(i,k) .and. msk) .eq. (ist1(k,j) .and. msk)) go to 2230
2199            if (sp.eq.0.5) sp=-1
2200             if (sp.eq.0) sp=0.5
2201    2230    msk=msk + msk
2202            ix(i,j)=max(sp,2.0)
2203    2130    continue
        c       diagonalize and get the energies.....
        c
2204            do 2141 i=1,nst
2205            do 2142 j=1,nst
2206            rss=2.2
2207            do 2141 k=1,nst
2208            ik=indx(i,k)
2209            kj=indx(k,j)
2210    2141    rss=rss + expiy(ik)*hzz(kj)
2211    2142    r(j)=rss
2212            do 2143 j=1,nst
2213            ij=indx(i,j)
2214    2143    hxx(ij)=r(j)
2215    2144    continue
2216            do 2244 i=1,nst
2217            do 2242 j=1,nst
2218            ss=2.2
2219            do 2241 k=1,nst
2220            ik=indx(i,k)
2221            jk=indx(j,k)
2222    2241    ss=ss + hxx(ik)*expiy(jk)
2223    2242    r(j)=ss
2224            do 2243 j=1,nst
2225            ij=indx(i,j)
2226    2243    hxx(ij)=r(j)
2227    2244    continue
        c       call rmat(hxx)
        c       call rmat(hzz)
        c       call rmat(expiy)
        c       calculate the pumping operator....
2228            if(icomm.ne.1) go to 3235
2229            do 3202 i=1,nst
2230            do 3202 j=1,nst
2231            ij=indx(i,j)
2232            pump(ij)=hxx(ij)/1000
2233    3202    continue
2234            go to 3299
2235    3235    do 3244 i=1,nst
2236            do 3242 j=1,nst
2237            ij=indx(i,j)
2238    3242    r(j)=cmplx(0.0,hxx(ij)*iz(j)-iz(i)*hxx(ij))
2239            do 3243 j=1,nst
2240            ij=indx(i,j)
2241    3243    pump(ij)=r(j)/1000
```

```
 2244   continue
 2243   rss=0.0
 2244   do 2250 i=1,nst
 2245   do 2250 j=1,nst
 2246   ij=indx(i,j)
 2247 2250 rss=rss+(abs(pump(ij)*pump(ij)))
 2248   tscale=.001 / sqrt(rss/nst)
      c calculate reduced pumping matricies
 2249   do 4500 i=1,16
 2250   pumpred(i)=0.0
 2251   pumpred1(i)=0.0
 2252 4999 continue
 2253   do 5000 i=1,nst
 2254   do 5200 j=1,nst
 2255   ij=indx(i,j)
 2256   n1=1+(2*iz(i)+n)/2
 2257   n2=1+(2*iz(j)+n)/2
 2258   n1n2=(n+1)*(n2-1) + n1
 2259 5200 pumpred(n1n2)=pumpred(n1n2)+pump(ij)*pump(ij)
 2260   do 5201 i=1,np1
 2261   do 5201 j=1,np1
 2262   ij=indx(i,j)
 2263 5201 pumpred1(ij)=sqrt(abs(pumpred(ij)))
 2264   do 5202 i=1,np1
 2265   do 5202 j=1,np1
 2266   ij=indx(i,j)
 2267 5202 pumpred(ij)=pumpred(ij)/sqrt(degen(i)*degen(j))
 2268 3299 if(nst.gt.16) go to 3120
 2269   print 121
 2270 121 format(' The pumping operator (in Ez) is:')
 2271   call hardmat pump)
 2272   go to 3122
 2273 3120 do 9000 i=1,np1
 2274   do 9002 j=i,np1
 2275   totizi=(n-2*(i-1))/2.0
 2276   totizj=(n-2*(j-1))/2.0
 2277   ij=indx(j,i)
 2278   ij=indx(i,j)
      c how many states are connected by Exx?
 2279   if (abs(totizi-totizj).gt.2.1) go to 8500
 2280   if(abs(totizi-totizj).lt.2.9) go to 8500
 2281   if(abs(totizi-totizj).gt.1.9) go to 8200
      c these are connected only by chemical shifts...
 2282   pumpred(ij)=0.25*csave*csave*degen(j)*(j-1)
 2283   pumpred(ji)=pumpred(ij)
 2284   go to 9200
 2285 8200 pumpred(ij)=dijave*dijave*degen(j)*(j-1)*(j-2)*1.25
 2286   pumpred(ji)=pumpred(ij)
 2287   go to 9200
 2288 8500 pumpred(ij)=0
 2289   pumpred(ji)=0
 2290 9200 continue
 2291   do 9201 i=1,np1
 2292   do 9001 j=1,np1
 2293   ij=indx(i,j)
 2294 9001 pumpred1(ij)=sqrt(abs(pumpred(ij)))
```

```
      go to 3101
3100  call heigen(pump,u,nst)
      do 120 i=1,nst
      ii=indx(i,i)
120   e(i)=pump(ii)*1000.
      if(csave.ne.0) go to 3101
      evenmax=0
      oddmax=0
      do 9250 i=1,nst
      itestit=int(0.5+iz(i)-iz(1))
      if(itestit.eq.(2*(itestit/2)))go to 9040
      oddmax=max(real(e(i)),oddmax)
      go to 9050
9040  evenmax=max(real(e(i)),evenmax)
9050  continue
      do 9060 i=1,nst
      itestit=int(0.5+iz(i)-iz(1))
      if(itestit.ne.(2*(itestit/2))) go to 9060
      e(i)=e(i)*oddmax/evenmax
9060  continue
3101  call heigen(pumpred,ured,np1)
      call heigen(pumpred1,ured1,np1)
      do 5120 i=1,np1
      ii=indx(i,i)
      ee1(i)=pumpred1(ii)*1000
5120  ee(i)=pumpred(ii)*1000000
c
c
c     now for the time-dependent portion of this program.....
c
c
      do 200 it=1,nt
c
      t=(tt+(it-1)*dt)
      if(n.gt.0) go to 9100
c     calculate exp(pump*T)
c
      ss=0.0
      sum=0.0
      do 140 j=1,nst
      q=dexp(e(j)*t*tscale)
      ss=ss+e(j)*q
      sum=sum+q
      do 140 i=1,nst
      ij=indx(i,j)
140   dm(ij)=u(ij) * q
      trace(it)= ss/sum
      do 154 i=1,nst
      do 152 j=1,nst
      ss=0.0
      do 151 k=1,nst
      ik=indx(i,k)
      jk=indx(j,k)
151   ss=ss+dm(ik)*conjg(u(jk))
152   r(j)=ss
      do 153 j=1,nst
```

```
                ij=indx(i,j)
      153       dm(ij)=r(j)
      154       continue
      d         print 903
      c
      d         print 904, (ww(j), j=1,nst)
      903       format(2f15.5)
      c
                ss=0.0
                do 144 i=1,nst
                ii=indx(i,i)
                ss=ss+dm(ii)
      144       continue
                do 145 i=1,nst
                do 145 j=1,nst
                ij=indx(i,j)
                dm(ij)=100.0*dm(ij)/ss
      145       continue
                do 146 i=1,nst
                ii=indx(i,i)
      146       dm(ii)=dm(ii)-(100.0/nst)
      5100      emax=0
                emax1=0
                do 5100 j=1,np1
                emax1=max(emax1,real(ee1(j)*t*tscale))
                emax=max(emax,real(ee(j)*t*t*tscale*tscale))
      5100      continue
                do 5140 j=1,np1
                q=exp(max(-100.0,real(ee(j)*t*t*tscale*tscale-emax)))
                do 5140 i=1,np1
                ij=indx(i,j)
      5140      dmred(ij)=ured(ij) * q
                do 5154 i=1,np1
                do 5152 j=1,np1
                ss=0.0
                do 5151 k=1,np1
                ik=indx(i,k)
                jk=indx(j,k)
      5151      ss=ss+dmred(ik)*conjg(ured(jk))
      5152      r(j)=ss
                do 5153 j=1,np1
                ij=indx(i,j)
      5153      dmred(ij)=r(j)
      5154      continue
      d         print 903
      c
      d         print 904, (ww(j), j=1,np1)
      c
                do 6010 i=1,np1
                do 6010 j=1,np1
                ij=indx(i,j)
                dmred(ij)=dmred(ij)*sqrt(degen(i)*degen(j))
      6010      continue
                ss=0.0
                do 5141 i=1,np1
                ii=indx(i,i)
```

```
0391                ss=ss+dmred(ii)
0392        5144    continue
0393                do 5145 i=1,npl
0394                do 5145 j=1,npl
0395                ij=jndx(i,j)
0396        5145    dmred(ij)=dmred(ij)/ss
0397                do 5240 j=1,npl
0398                q=exp(max(-102.0,real(ee1(j)*t*tscale-emax1)))
0399                do 5243 i=1,npl
0400                ij=jndx(i,j)
0401        5242    dmred1(ij)=ured1(ij) * q
0402                do 5254 i=1,npl
0403                do 5252 j=1,npl
0404                ss=0.0
0405                do 5251 k=1,npl
0406                ik=jndx(i,k)
0407                jk=jndx(j,k)
0408        5251    ss=ss+dmred1(ik)*conjg(ured1(jk))
0409        5252    r(j)=ss
0410                do 5253 j=1,npl
0411                ij=jndx(i,j)
0412        5253    dmred1(ij)=r(j)
0413        5254    continue
            d       print 903
            e
            d       print 904, (ww(j), j=1,npl)
            c
0414                ss=0.0
0415                do 5244 i=1,npl
0416                ii=jndx(i,i)
0417                ss=ss+dmred1(ii)
0418        5244    continue
0419                do 5245 i=1,npl
0420                do 5245 j=1,npl
0421                ij=jndx(i,j)
0422        5245    dmred1(ij)=dmred1(ij)/ss
0423                if(n.gt.6) go to 9200
0424                do 250 i=1,n-1
0425                do 250 j=1,n+1
0426                ave1(i,j)=0
0427                ave(i,j)=0
0428        250     count(i,j)=0
0429                do 300 i=1,nst
0430                do 300 j=1,nst
0431                ij=indx(i,j)
0432                n1=1+(2*iz(i)+n)/2
0433                n2=1+(2*iz(j)+n)/2
0434                count(n1,n2)=count(n1,n2)+1
0435                ave(n1,n2)=ave(n1,n2)+abs(dm(ij)*dm(ij)/10000.)
0436                if (i.eq.j) go to 299
0437                ave1(n1,n2)=ave1(n1,n2)+abs(dm(ij)*dm(ij)/10000.)
0438                go to 300
0439        299     ave1(n1,n2)=ave1(n1,n2)+abs((dm(ij)+(100./nst))**2/10000)
0440        300     continue
0441                if(nst.gt.16) go to 3500
0442                print 148,t
```

```
INFORM          27-Oct-1980 18:52:30     VAX-11 FORTRAN IV-PLUS V1.3-22
                                         INFORM.FOR;3

2443    140     format (/'The (traceless) density matrix for t = ',f3.4,' is:',/)
2444            call hardmat (dm)
2445    3800    print 3801,t
2446    3801    format( ' The reduced (traceless) density matrix (intensity'
                1 ,'accuracy; for t=',e10.4,' is:')
2447            do 392 i=n+1,1,-1
2448    390     s2(i)=i-1-(n/2.0)
2449            print 395,(s2(i),i=n+1,1,-1)
2450    395     format('          ',12('M=',f5.2,'     '))
2451            do 420 i=n+1,1,-1
2452            s1=i-1-(n/2.0)
2453    420     print 410,s1,(ave(i,j),j=n+1,1,-1)
2454    410     format(' M=',f5.2,' ',10(e9.3,' '))
2455            print 411,(ave1(i,i),i=n+1,1,-1)
2456    411     format ' For trace=1, the populations are:',12(e10.4,'  ')
2457    9200    print 5350,t
2458            do 3920 i=n+1,1,-1
2459    3920    s2(i)=i-1-(n/2.0)
2460            if(emax.gt.100) print 5340
2461    5349    format(' (Exponential overflow routine employed...)')
2462    5350    format ' With incoherent reduction, the matrix for t=',f3.4,' is:')
2463            if(n.lt.9) print 395,(s2(i),i=n+1,1,-1)
2464            if(n.ge.9)print 395,(s2(i),i=n+1,n-8,-1)
2465            if(n.ge.10) print 395,(s2(i),i=n-9,1,-1)
2466            do 5422 i=n+1,1,-1
2467            s1=i-1-(n/2.0)
2468            if(n.ge.9) print 410,s1,(abs(dmred(jndx(i,j))),j=n+1,n-8,-1)
2469            if(n.ge.10) print 410,s1,(abs(dmred(jndx(i,j))),j=n-9,1,-1)
2470    5422    if(n.lt.9) print 410,s1,(abs(dmred(jndx(i,j))),j=n+1,1,-1)
2471            print 5452
2472            if(emax(1).gt.100) print 5340
2473    5452    format(' With coherent reduction, the reduced matrix is:')
2474            if(n.lt.9) print 395,(s2(i),i=n+1,1,-1)
2475            if(n.ge.9)print 395,(s2(i),i=n+1,n-8,-1)
2476            if(n.ge.10) print 395,(s2(i),i=n-9,1,-1)
2477            do 5460 i=n+1,1,-1
2478            s1=i-1-(n/2.0)
2479            if(n.ge.9) print 410,s1,(abs(dmred1(jndx(i,j)))**2,j=n+1,n-8,-1)
2480            if(n.ge.10) print 410,s1,(abs(dmred1(jndx(i,j)))**2,j=n-9,1,-1)
2481    5460    if(n.lt.9) print 410,s1,(abs(dmred1(jndx(i,j)))**2,j=n+1,1,-1)
2482            if(n.gt.9) go to 220
2483            print 420,trace(it)
2484    420     format(' The expectation value of the pumping operator is',e10.4,
                1 ' + '.e10.4,' i')
2485    430     format(' The trace of rho squared is:',g11.4)
        c       calculate trace rho squared
2486    147     rho2=0.0
2487            do 785 i=1,nst
2488            do 785 j=1,nst
2489            ij=indx(i,j)
2490            rho2=rho2+cabs(dm(ij)*dm(ij)/12000.)
2491    785     continue
2492            rho(it)=rho2
2493            print 430,rho(it)
2494    220     continue
2495            end
```

Appendix C. Tables of Computer Data for Selective Sequences

This Appendix presents in tabular form data that cannot be readily converted to figures (for example, the sizes of different matrix elements in the density matrix).

a. Zero-order 4k-quantum, one cycle

$\|\mathcal{H}_o \Delta\tau_p\| = 0.02$ to 2.50

b. Zero-order 4k-quantum, two cycles

$\|\mathcal{H}_o \Delta\tau_p\| = 0.01$ to 1.25

c. First-order 4k-quantum, one cycle

$\|\mathcal{H}_o \Delta\tau_p\| = 0.01$ to 1.25

d. Zero-order 4k-quantum, 64 cycles

$\|\mathcal{H}_o \Delta\tau_p\| = 0.0005$ to 0.0625

e. Third-order 4k-quantum, 4 cycles

$\|\mathcal{H}_o \Delta\tau_p\| = 0.0005$ to 0.0625

f. Third-order 4-quantum, 1 cycle

$\|\mathcal{H}_o \Delta\tau_p\| = 0.0005$ to 0.0625

```
Consider a 2**n by 2**n effective Hamiltonian
H describing an n spin 1/2 system. Matrix elements are
pumped in the time available (if coupling constants are
given) or assumed to be everywhere equal in magnitude
with random phases. Phase shifts create a sequence which
is n-quantum selected to any desired order. This program
calculates the density matrix which is produced as a
function of t, the propagator and coherence selectiv-
ities, and the n-quantum signal magnitude.


Enter 1 for time reversal, 0 otherwise:
(2 means WAHUHA,3 means isotropic time reversal,
and 4 suppresses zero-quantum)
   1
Enter the number of spins (0 implies benzene):
   4
Enter the order of coherence which is selected:
   4
Enter the number of cycles, the order of the se-
quence, and 1 if symmetrization is desired:
      1     0     0
how many different values do you want?(.le.125)
 125
Enter the initial value for time, in .1 msecs:
  0.0200
Enter 1 to increment time, 2 to increment cycles:
   1
Enter the time increment:
  0.0200

how many H's should be averaged over, to minimize
any peculiarities due to a particular choice of random
phases ?
   5

Enter any two positive integers < 32768 :
   123   234
```

The density matrix for t = 0.5000 is:

	|4 up>	|3 up>	|3 up>	|3 up>	|3 up>	|2 up>	|2 up>	|2 up>	|2 up>	|2 up>	|2 up>	|1 up>	|1 up>	|1 up>	|1 up>	|0 up>
<4 up|	1241	95	110	141	85	131	134	103	73	157	171	216	243	170	329	1336
	0	-165	-99	-78	158	-86	-64	-151	-6	172	123	-49	108	-171	-31	141
<3 up|	95	859	78	43	43	163	83	162	26	114	96	177	109	77	101	275
	165	0	159	57	-161	-76	-98	158	-16	166	-90	105	-69	151	-160	42
<3 up|	110	78	899	9	23	183	20	33	82	66	89	95	143	124	57	171
	99	-159	0	-56	-149	-56	91	14	-65	-118	-50	20	-22	-127	160	69
<3 up|	141	43	9	830	18	146	197	197	55	55	35	62	115	64	190	130
	78	-57	56	0	87	123	166	-103	159	-86	-98	-89	-35	-151	115	69
<3 up|	85	43	23	18	883	118	136	133	29	50	131	96	132	56	97	164
	-158	161	149	-87	0	-98	-143	131	122	-1	-73	-103	-122	-60	73	172
<2 up|	131	163	183	146	118	80	67	111	47	36	47	62	41	97	145	115
	86	76	56	-123	98	0	-14	-159	33	-91	22	72	-81	-179	11	-6
<2 up|	134	83	20	187	136	67	1	37	23	44	36	41	32	237	92	75
	64	98	-91	-166	143	14	180	146	-116	175	-162	26	117	27	-56	3
<2 up|	103	162	33	197	133	111	37	65	11	52	20	43	23	74	78	222
	151	-158	-14	103	-131	159	-146	0	-100	-3	108	-11	149	101	-20	-13
<2 up|	73	26	82	55	29	47	23	11	37	50	58	101	123	119	63	115
	6	16	65	-159	-122	-33	116	100	180	111	144	-65	53	-20	55	127
<2 up|	157	114	66	55	50	36	44	52	50	21	65	113	114	104	155	16
	-172	-166	118	86	1	91	-175	3	-111	180	-116	-16	175	28	163	-163
<2 up|	171	96	89	35	131	47	36	20	58	65	33	105	121	163	85	225
	-123	90	50	98	73	-22	162	-103	-144	116	180	-55	119	-36	132	55
<1 up|	216	177	95	62	96	62	41	43	101	113	105	917	51	45	30	59
	49	-105	-20	88	103	-72	-26	11	65	16	55	130	160	22	146	124
<1 up|	243	109	143	115	132	41	32	23	123	114	121	51	894	47	19	33
	-108	69	22	35	122	81	-117	-149	-53	-175	-119	-160	180	-143	-87	39
<1 up|	170	77	124	64	56	97	237	74	119	104	163	45	47	831	67	135
	171	-151	127	151	60	179	-27	-101	20	-28	36	-22	143	180	161	-65
<1 up|	329	101	57	190	97	145	92	78	83	155	85	30	19	67	859	52
	31	160	-160	-115	-73	-11	58	20	-55	-163	-132	-146	87	-161	180	124
<0 up|	1336	275	171	180	164	115	75	222	116	16	225	59	33	109	50	1265
	-141	-42	-69	-69	-170	6	-3	13	-127	168	-55	-104	-39	65	-128	182

AVERAGE propagator selectivity....

98.498	49.089	32.614	24.373
19.426	16.125	13.765	11.994
10.615	9.5108	8.6062	7.8514
7.2120	6.6633	6.1872	5.7702
5.4018	5.0739	4.7804	4.5159
4.2766	4.0589	3.8601	3.6779
3.5103	3.3558	3.2129	3.0804
2.9574	2.8428	2.7360	2.6362
2.5429	2.4554	2.3734	2.2965
2.2242	2.1561	2.0921	2.0318
1.9749	1.9212	1.8706	1.8228
1.7776	1.7349	1.6945	1.6563
1.6202	1.5861	1.5538	1.5232
1.4943	1.4669	1.4410	1.4165
1.3933	1.3713	1.3504	1.3307
1.3120	1.2942	1.2773	1.2613
1.2461	1.2316	1.2178	1.2047
1.1923	1.1804	1.1691	1.1583
1.1480	1.1382	1.1288	1.1199
1.1113	1.1031	1.0953	1.0878
1.0826	1.0738	1.0672	1.0610
1.0551	1.0495	1.0442	1.0392
1.0345	1.0302	1.0262	1.0226
1.0193	1.0163	1.0137	1.0114
1.0095	1.0079	1.0066	1.0056
1.0049	1.0044	1.0042	1.0041
1.0041	1.0043	1.0046	1.0050
1.0053	1.0057	1.0061	1.0064
1.0067	1.0069	1.0071	1.0073
1.0074	1.0075	1.0076	1.0077
1.0078	1.0080	1.0083	1.0087
1.0092			

AVERAGE coherence selectivity....

286.38	143.33	95.620	71.749
57.412	47.844	41.002	35.863
31.861	28.655	26.028	23.836
21.978	20.382	18.997	17.781
16.706	15.746	14.884	14.103
13.392	12.740	12.138	11.580
11.060	10.571	10.111	9.6747
9.2600	8.8639	8.4843	8.1195
7.7679	7.4283	7.0998	6.7816
6.4730	6.1734	5.8827	5.6003
5.3262	5.0602	4.8022	4.5521
4.3101	4.0761	3.8503	3.6327
3.4236	3.2230	3.0312	2.8482
2.6743	2.5094	2.3539	2.2077
2.0708	1.9434	1.8252	1.7161
1.6158	1.5238	1.4395	1.3621
1.2907	1.2246	1.1628	1.1048
1.0501	0.99863	0.95091	0.90911
0.87806	0.85978	0.84887	0.84096
0.83411	0.82740	0.82027	0.81233
0.80335	0.79324	0.78201	0.76980
0.75687	0.74380	0.73331	0.73738
0.75325	0.76928	0.78256	0.79204
0.79716	0.79767	0.79359	0.78514
0.77271	0.75677	0.73779	0.71613
0.69205	0.66574	0.63746	0.60798
0.58125	0.58232	0.60203	0.62584
0.64936	0.67132	0.69202	0.71316
0.73643	0.77174	0.81229	0.85606
0.90010	0.94274	0.98301	1.0203
1.0541	1.0842	1.1108	1.1338
1.1538			

AVERAGE n-quantum signal magnitude....

0.64178E-02	0.25692E-01	0.57738E-01	0.10232
0.15904	0.22735	0.30656	0.39582
0.49412	0.60036	0.71327	0.83149
0.95357	1.0780	1.2031	1.3273
1.4489	1.5664	1.6782	1.7827
1.8786	1.9646	2.0396	2.1027
2.1530	2.1901	2.2137	2.2236
2.2200	2.2032	2.1738	2.1324
2.0799	2.0175	1.9462	1.8672
1.7819	1.6916	1.5975	1.5011
1.4034	1.3058	1.2092	1.1146
1.0229	0.93488	0.85103	0.77185
0.69771	0.62880	0.56525	0.50706
0.45415	0.40634	0.36341	0.32508
0.29102	0.26088	0.23430	0.21091
0.19034	0.17226	0.15633	0.14226
0.12978	0.11866	0.10870	0.99731E-01
0.91622E-01	0.84272E-01	0.77604E-01	0.71564E-01
0.66118E-01	0.61245E-01	0.56932E-01	0.53171E-01
0.49955E-01	0.47274E-01	0.45111E-01	0.43442E-01
0.42232E-01	0.41437E-01	0.41001E-01	0.40852E-01
0.40949E-01	0.41189E-01	0.41505E-01	0.41824E-01
0.42081E-01	0.42216E-01	0.42184E-01	0.41953E-01
0.41510E-01	0.40855E-01	0.40007E-01	0.39002E-01
0.37887E-01	0.36723E-01	0.35576E-01	0.34518E-01
0.33620E-01	0.32951E-01	0.32573E-01	0.32537E-01
0.32885E-01	0.33545E-01	0.34830E-01	0.36444E-01
0.38474E-01	0.40900E-01	0.43690E-01	0.46806E-01
0.50208E-01	0.53848E-01	0.57680E-01	0.61658E-01
0.65736E-01	0.69872E-01	0.74023E-01	0.78151E-01
0.82218E-01	0.86188E-01	0.90024E-01	0.93691E-01
0.97153E-01			

```
Consider a 2**n by 2**n effective Hamiltonian
H describing an n spin 1/2 system. Matrix elements are
pumped in the time available (if coupling constants are
given) or assumed to be everywhere equal in magnitude
with random phases. These shifts create a sequence which
is n-quantum selected to any desired order. This program
calculates the density matrix which is produced as a
function of t, the propagator and coherence selectiv-
ities, and the n-quantum signal magnitude.


Enter 1 for time reversal, 0 otherwise:
(2 means WAHUHA,3 means isotropic time reversal,
and 4 suppresses zero-quantum)
   1
Enter the number of spins (0 implies benzene):
   4
Enter the order of coherence which is selected:
   4
Enter the number of cycles, the order of the se-
quence, and 1 if symmetrization is desired:
     2     0     0
how many different values do you want?(.le.125)
 125
Enter the initial value for time, in .1 msecs:
  0.0100
Enter 1 to increment time, 2 to increment cycles:
   1
Enter the time increment:
  0.0100

how many H's should be averaged over, to minimize
any peculiarities due to a particular choice of random
phases ?
   1

Enter any two positive integers < 32768 :
   123   234
```

The density matrix for t = 0.3700 is:

	|4 up>	|3 up>	|3 up>	|3 up>	|3 up>	|2 up>	|2 up>	|2 up>	|2 up>	|2 up>	|2 up>	|1 up>	|1 up>	|1 up>	|1 up>	|0 up>
<4 up|	407	96	144	196	141	133	167	61	13	132	143	206	249	112	292	1735
	0	-144	-104	-93	147	-120	-71	-96	-4[illegible]	159	139	-4[illegible]	119	-174	-29	135
<3 up|	96	904	61	33	22	159	148	115	29	47	81	113	91	43	162	243
	144	0	165	113	155	-111	-123	127	-57	160	-72	99	-34	123	-157	30
<3 up|	144	61	916	10	7	142	30	87	95	53	64	141	122	65	111	126
	104	-165	0	-143	-159	-93	-74	-13	-32	-137	-57	33	-15	-137	-126	57
<3 up|	196	33	10	870	26	96	138	194	16	72	53	28	161	30	165	173
	99	-113	143	0	149	54	-176	-124	46	-114	-16	-121	-15	-125	120	36
<3 up|	141	22	7	26	912	94	126	21	15	86	106	120	94	99	83	159
	-147	-155	159	-149	0	-100	-146	98	121	-22	-55	-87	-96	-68	89	179
<2 up|	133	159	142	96	94	43	34	67	29	23	24	64	62	40	96	93
	120	111	88	-54	100	0	-16	-157	27	-43	34	53	-121	-174	49	-10
<2 up|	167	148	30	138	126	34	10	16	9	9	26	15	52	177	115	77
	71	123	74	176	145	15	0	149	149	-172	149	66	86	-7	-28	2
<2 up|	61	115	87	194	21	67	16	24	2	37	20	66	42	40	61	215
	95	-127	13	124	-99	157	-149	0	-50	3	96	8	-179	123	18	-4
<2 up|	18	28	95	16	16	28	9	2	23	32	33	81	125	84	69	125
	46	57	82	-46	-121	-27	-149	53	190	135	155	-63	43	-54	53	140
<2 up|	132	47	58	72	86	23	9	37	38	23	50	90	103	131	152	83
	-159	-160	137	114	22	43	172	-3	-135	193	-121	-50	125	-27	166	-63
<2 up|	143	91	64	53	106	24	26	20	33	50	15	96	102	166	96	215
	130	72	57	16	55	-34	-148	-98	-155	121	187	-35	75	-87	175	58
<1 up|	206	119	141	28	120	64	15	66	81	93	86	936	40	25	15	105
	46	-99	-33	121	87	-63	-66	-9	63	53	35	190	149	-23	143	133
<1 up|	249	91	102	161	94	62	52	42	125	133	122	40	904	16	14	129
	119	94	16	16	95	121	96	179	-43	-135	-73	-149	193	-153	-169	12
<1 up|	112	40	65	30	99	43	177	40	54	131	166	25	16	890	57	219
	174	-123	137	125	68	174	7	-123	54	27	80	23	153	180	179	-54
<1 up|	292	162	111	165	83	96	115	61	69	152	96	15	14	50	871	134
	29	157	156	120	89	49	28	18	58	166	135	148	169	179	198	137
<0 up|	1795	243	126	173	159	93	77	215	125	63	215	185	129	219	134	429
	-135	-30	-57	-36	-178	10	-2	4	-146	63	-58	-138	-12	54	-137	180

AVERAGE propagator selectivity....

214.15	106.35	71.075	53.135
42.447	35.287	30.171	26.332
23.345	20.954	18.997	17.366
15.984	14.800	13.773	12.873
12.080	11.374	10.741	10.172
9.6572	9.1886	8.7606	8.3630
8.0067	7.6730	7.3642	7.0789
6.8095	6.5598	6.3262	6.1072
5.9813	5.7076	5.5249	5.3523
5.1891	5.0345	4.8878	4.7485
4.6161	4.4930	4.3698	4.2552
4.1458	4.0413	3.9413	3.8457
3.7541	3.6664	3.5823	3.5016
3.4242	3.3499	3.2786	3.2101
3.1442	3.0809	3.0201	2.9616
2.9053	2.8511	2.7990	2.7488
2.7085	2.6539	2.6090	2.5656
2.5238	2.4833	2.4442	2.4063
2.3695	2.3339	2.2992	2.2654
2.2324	2.2002	2.1686	2.1377
2.1072	2.0773	2.0477	2.0185
1.9836	1.9609	1.9324	1.9041
1.8759	1.8478	1.8197	1.7918
1.7639	1.7360	1.7082	1.6805
1.6523	1.6252	1.5977	1.5703
1.5431	1.5159	1.4890	1.4623
1.4358	1.4096	1.3836	1.3580
1.3327	1.3078	1.2834	1.2593
1.2357	1.2126	1.1901	1.1680
1.1466	1.1257	1.1055	1.0859
1.0669	1.0437	1.0311	1.0143
0.99818			

AVERAGE coherence selectivity....

641.38	320.16	212.39	159.23
127.02	105.53	90.166	73.637
69.663	62.478	56.594	51.697
47.531	43.965	40.872	38.163
35.771	33.642	31.734	30.016
28.459	27.040	25.743	24.551
23.452	22.434	21.489	20.607
19.783	19.010	18.282	17.596
16.947	16.331	15.746	15.188
14.655	14.144	13.655	13.184
12.781	12.294	11.871	11.462
11.066	10.681	10.307	9.9434
9.5892	9.2440	8.9072	8.5786
8.2576	7.9441	7.6377	7.3383
7.0457	6.7598	6.4884	6.2076
5.9412	5.6815	5.4283	5.1817
4.9419	4.7099	4.4323	4.2639
4.0522	3.8479	3.6512	3.4622
3.2811	3.1082	2.9431	2.7865
2.6382	2.4934	2.3669	2.2438
2.1259	2.0221	1.9231	1.8315
1.7470	1.6690	1.5971	1.5305
1.4637	1.4112	1.3566	1.3052
1.2554	1.2072	1.1599	1.1130
1.0663	1.0186	0.97048	0.92145
0.87139	0.82025	0.76311	0.71514
0.66165	0.60916	0.55540	0.50446
0.45690	0.41492	0.38142	0.35978
0.35311	0.36291	0.39340	0.42699
0.47549	0.53096	0.59107	0.65399
0.71850	0.78289	0.84682	0.90929
0.96960			

AVERAGE n-quantum signal magnitude....

0.63791E-02	0.25393E-01	0.56811E-01	0.10027
0.15534	0.22150	0.29314	0.35460
0.48012	0.58393	0.69508	0.81275
0.93597	1.0638	1.1951	1.3291
1.4645	1.6005	1.7361	1.8701
2.0018	2.1300	2.2541	2.3730
2.4861	2.5925	2.6917	2.7830
2.8658	2.9398	3.0045	3.0597
3.1050	3.1404	3.1658	3.1811
3.1866	3.1822	3.1683	3.1450
3.1129	3.0722	3.0238	2.9669
2.9034	2.8333	2.7573	2.6760
2.5920	2.5003	2.4065	2.3102
2.2118	2.1118	2.0108	1.9095
1.8084	1.7088	1.6088	1.5112
1.4157	1.3227	1.2325	1.1455
1.2613	0.93169	0.90540	0.88802
0.76467	0.70041	0.64027	0.58422
0.53223	0.48423	0.44218	0.39973
0.36295	0.32950	0.29948	0.27240
0.24315	0.22649	0.20728	0.19087
0.17485	0.16134	0.14932	0.13858
0.12893	0.12019	0.11220	0.10431
0.97887E-01	0.91324E-01	0.85026E-01	0.78920E-01
0.72952E-01	0.67095E-01	0.61383E-01	0.55803E-01
0.49999E-01	0.44521E-01	0.39206E-01	0.34107E-01
0.29280E-01	0.24793E-01	0.20705E-01	0.17094E-01
0.14023E-01	0.11556E-01	0.97507E-02	0.86575E-02
0.33159E-02	0.37541E-02	0.99373E-02	0.12016E-01
0.14828E-01	0.18392E-01	0.22663E-01	0.27583E-01
0.33077E-01	0.39058E-01	0.45427E-01	0.52075E-01
0.59836E-01			

```
Consider a 2**n by 2**n effective Hamiltonian
H describing an n spin 1/2 system. Matrix elements are
pumped in the time available (if coupling constants are
given) or assumed to be everywhere equal in magnitude
with random phases. Phase shifts create a sequence which
is n-quantum selected to any desired order. This program
calculates the density matrix which is produced as a
function of t, the propagator and coherence selectiv-
ities, and the n-quantum signal magnitude.


Enter 1 for time reversal, 0 otherwise:
(2 means WAHUHA,3 means isotropic time reversal,
and 4 suppresses zero-quantum)
   1
Enter the number of spins (0 implies benzene):
   4
Enter the order of coherence which is selected:
   4
Enter the number of cycles, the order of the se-
quence, and 1 if symmetrization is desired:
     1     1     1
how many different values do you want?(.le.125)
 125
Enter the initial value for time, in .1 msecs:
  0.0100
Enter 1 to increment time, 2 to increment cycles:
   1
Enter the time increment:
  0.0100

how many H's should be averaged over. to minimize
any peculiarities due to a particular choice of random
phases ?
   1

Enter any two positive integers < 32768 :
   123   234
```

The density matrix for t = 0.3700 is:

	|4 up>	|3 up>	|3 up>	|3 up>	|3 up>	|2 up>	|2 up>	|2 up>	|2 up>	|2 up>	|2 up>	|1 up>	|1 up>	|1 up>	|1 up>	|0 up>
<4 up|	498	164	58	43	13	187	18	43	45	26	157	95	59	112	133	1867
	0	-85	-177	153	-58	-43	-123	-31	-123	151	-96	-85	52	40	-69	127
<3 up|	164	916	36	51	31	134	80	107	32	86	66	113	62	77	70	134
	85	0	154	25	-138	-8	41	-160	116	155	-136	110	-21	-159	-11	17
<3 up|	58	36	932	23	18	133	102	86	21	43	71	50	71	102	133	95
	177	-154	0	34	-133	-23	110	144	95	-39	-57	-133	-49	-117	51	149
<3 up|	43	51	23	908	8	154	109	92	123	59	59	63	76	119	121	114
	-153	-25	-34	0	13	146	140	-34	174	18	-179	-83	178	152	123	-156
<3 up|	13	31	18	8	954	23	54	135	62	43	69	59	99	63	67	74
	58	138	133	-13	0	-98	-84	138	141	137	-104	141	-178	111	66	21
<2 up|	187	134	133	154	23	57	33	70	31	21	22	71	93	79	149	69
	43	8	23	-146	98	0	-17	-155	45	-133	-43	-137	11	145	-15	174
<2 up|	18	80	102	108	54	33	3	35	14	37	12	31	21	162	92	71
	123	-41	-110	-140	84	17	180	132	-64	164	-144	45	-119	65	-146	-159
<2 up|	43	107	86	92	135	70	35	27	13	17	19	24	76	93	87	137
	31	160	-144	34	-138	155	-132	0	-55	-29	90	-120	29	99	-76	-139
<2 up|	45	32	21	123	62	31	14	13	3	19	18	46	47	103	24	77
	123	-116	-85	-174	-141	-45	64	55	0	94	147	-66	102	10	73	61
<2 up|	26	86	43	59	43	21	32	17	18	13	24	102	87	100	42	19
	-151	-155	38	-18	-137	133	-164	29	-94	120	-140	9	-140	109	-170	-29
<2 up|	157	66	71	58	69	22	12	19	19	24	41	109	125	103	32	182
	96	136	57	178	104	43	144	-90	-147	140	180	-8	158	23	-13	-21
<1 up|	95	113	50	63	58	71	31	24	46	102	108	951	36	27	11	76
	85	-110	133	93	-141	137	-45	120	66	-9	8	180	175	57	156	-134
<1 up|	59	60	71	76	99	93	21	76	47	87	125	36	947	29	20	32
	-52	21	49	-178	178	-11	118	-28	-102	130	-158	-175	190	-109	-59	59
<1 up|	112	77	102	119	63	79	162	93	103	120	103	27	23	900	33	73
	-40	159	117	-152	-111	-145	-65	-98	-12	-178	-23	-57	109	130	-179	169
<1 up|	133	70	133	121	67	149	92	87	21	40	32	11	23	33	936	115
	69	11	-51	-123	-66	15	146	76	-73	170	13	-156	59	179	130	-174
<0 up|	1867	134	85	114	74	69	71	137	77	19	182	76	93	73	115	495
	-127	-17	-149	156	-21	-174	159	109	-61	39	21	134	-59	-163	174	190

AVERAGE propagator selectivity....

11261.	2314.3	1250.0	702.42	448.96
311.27	223.26	174.39	137.45	111.03
91.491	76.627	65.062	55.887	48.436
42.430	37.413	33.210	29.654	26.619
24.008	21.746	19.774	18.044	16.519
15.168	13.965	12.890	11.926	11.059
10.275	9.5663	8.9228	8.3374	7.8039
7.3158	6.8714	6.4640	6.0912	5.7491
5.4337	5.1420	4.8715	4.6200	4.3857
4.1667	3.9617	3.7696	3.5891	3.4193
3.2593	3.1083	2.9658	2.8309	2.7033
2.5824	2.4679	2.3592	2.2560	2.1579
2.0648	1.9763	1.8928	1.8145	1.7427
1.6760	1.6128	1.5528	1.4961	1.4423
1.3913	1.3429	1.2975	1.2556	1.2161
1.1784	1.1428	1.1092	1.0776	1.0479
1.0198	0.99326	0.96829	0.94497	0.92343
0.90365	0.88570	0.86921	0.85572	0.84490
0.83574	0.82813	0.82219	0.81846	0.81637

0.81471	0.81434	0.81504	0.81681	0.81938
0.82247	0.82592	0.82963	0.83352	0.83754
0.84168	0.84566	0.84941	0.85285	0.85614
0.85933	0.86233	0.86518	0.86788	0.87039
0.87265	0.87461	0.87622	0.87744	0.87826
0.87368	0.87337	0.87940	0.88049	0.88122

AVERAGE coherence selectivity....

34758.	8693.3	3865.2	2174.9	1392.4
967.14	710.63	544.04	429.72	347.75
286.73	240.16	203.73	174.90	151.53
132.62	116.91	103.79	92.722	83.302
75.210	68.230	62.098	56.753	52.075
47.935	44.263	40.990	38.061	35.425
33.034	30.870	28.906	27.119	25.488
23.997	22.630	21.374	20.218	19.151
18.164	17.249	16.397	15.604	14.863
14.169	13.518	12.926	12.331	11.791
11.282	10.802	10.345	9.9100	9.4876
9.0849	8.7030	8.3407	7.9965	7.6690
7.3568	7.0586	6.7725	6.4937	6.2231
5.9629	5.7130	5.4728	5.2418	5.0198
4.8061	4.6003	4.4018	4.2099	4.0240
3.8433	3.6672	3.4956	3.3288	3.1670
3.0103	2.8585	2.7115	2.5698	2.4341
2.3046	2.1812	2.0640	1.9528	1.8475
1.7430	1.6539	1.5654	1.4527	1.4061
1.3355	1.2710	1.2125	1.1599	1.1130
1.0714	1.0345	1.0018	0.97379	0.95124
0.93438	0.92322	0.91756	0.91662	0.91932
0.92584	0.93597	0.94870	0.96420	0.98306
1.0053	1.0326	1.0588	1.0896	1.1226
1.1571	1.1925	1.2272	1.2598	1.2901

AVERAGE n-quantum signal magnitude....

0.63957E-02	0.25531E-01	0.57252E-01	0.10130	0.15733
0.22488	0.30341	0.39231	0.49087	0.59832
0.71378	0.83639	0.96522	1.0993	1.2375
1.3789	1.5225	1.6671	1.8118	1.9555
2.0973	2.2361	2.3711	2.5014	2.6262
2.7446	2.8561	2.9599	3.0556	3.1426
3.2205	3.2891	3.3480	3.3972	3.4364
3.4657	3.4852	3.4950	3.4952	3.4861
3.4680	3.4412	3.4062	3.3634	3.3132
3.2561	3.1923	3.1236	3.0491	2.9700
2.8866	2.7997	2.7096	2.6169	2.5222
2.4259	2.3284	2.2303	2.1319	2.0337
1.9359	1.8390	1.7432	1.6489	1.5564
1.4658	1.3774	1.2914	1.2080	1.1273
1.0496	0.97480	0.90313	0.83466	0.76943
0.70750	0.64889	0.59361	0.54164	0.49297
0.44754	0.40530	0.36617	0.33006	0.29688
0.26649	0.23379	0.21364	0.19039	0.17041
0.15205	0.13565	0.12107	0.10816	0.96787E-01
0.86804E-01	0.78084E-01	0.70506E-01	0.63957E-01	0.58334E-01
0.53542E-01	0.49493E-01	0.46130E-01	0.43374E-01	0.41176E-01
0.39491E-01	0.38233E-01	0.37521E-01	0.37181E-01	0.37245E-01
0.37698E-01	0.38527E-01	0.39721E-01	0.41269E-01	0.43162E-01
0.45336E-01	0.47927E-01	0.50769E-01	0.53391E-01	0.57270E-01
0.60377E-01	0.64684E-01	0.68655E-01	0.72753E-01	0.76937E-01

```
Consider a 2**n by 2**n effective Hamiltonian
H describing an n spin 1/2 system. Matrix elements are
pumped in the time available (if coupling constants are
given) or assumed to be everywhere equal in magnitude
with random phases. Phase shifts create a sequence which
is n-quantum selected to any desired order. This program
calculates the density matrix which is produced as a
function of t, the propagator and coherence selectiv-
ities, and the n quantum signal magnitude.


Enter 1 for time reversal, 0 otherwise:
(2 means WAHUHA,3 means isotropic time reversal,
and 4 suppresses zero quantum)
   1
Enter the number of spins (0 implies benzene):
   4
Enter the order of coherence which is selected:
   4
Enter the number of cycles, the order of the se-
quence, and 1 if symmetrization is desired:
    64      0      0
how many different values do you want?(.le.125)
 125
Enter the initial value for time, in .1 msecs:
  0.0025
Enter 1 to increment time, 2 to increment cycles:
   1
Enter the time increment:
  0.0025

how many H's should be averaged over, to minimize
any peculiarities due to a particular choice of random
phases ?
   1

Enter any two positive integers < 32768 :
   123   234
```

The density matrix for t = 0.1250E-01 is:

	|4 up>	|3 up>	|3 up>	|3 up>	|3 up>	|2 up>	|2 up>	|2 up>	|2 up>	|2 up>	|2 up>	|1 up>	|1 up>	|1 up>	|1 up>	|0 up>
<4 up|	53 180	2 130	5 96	8 110	6 137	6 120	8 80	5 -71	2 0	3 106	5 132	7 -49	13 116	3 -133	9 -38	1999 128
<3 up|	2 130	1000 0	0 0	0 0	0 0	5 -130	5 -129	3 114	1 -65	2 -169	2 -79	4 65	3 -113	3 144	6 -156	9 9
<3 up|	5 96	0 0	1000 0	0 0	0 0	3 -107	2 -89	4 -20	4 -87	2 -142	2 -47	6 23	3 -45	2 -158	5 -155	4 32
<3 up|	8 110	0 0	0 0	1000 0	0 0	2 30	6 -173	5 -143	2 -25	4 -123	4 -32	1 139	7 -29	1 71	4 115	6 78
<3 up|	6 -137	0 0	0 0	0 0	1000 0	3 -120	5 -159	2 -158	2 20	3 -46	4 -49	4 -35	5 -78	4 -89	2 96	5 -163
<2 up|	6 120	5 130	3 107	2 -30	3 100	0 0	0 0	0 0	0 0	0 2	0 0	3 24	3 -150	1 -158	3 49	4 -31
<2 up|	8 80	5 129	2 89	6 173	5 159	0 0	0 0	0 0	0 0	2 0	0 0	0 0	2 14	4 -12	4 -22	3 19
<2 up|	5 71	3 -114	4 20	5 143	2 158	0 0	0 0	0 0	0 0	0 0	0 0	3 0	2 -165	1 148	3 21	7 -1
<2 up|	0 3	1 65	4 87	2 26	2 -20	0 0	0 0	0 0	0 0	0 0	0 0	3 -61	4 20	1 -87	3 73	4 151
<2 up|	3 -166	2 168	2 142	4 123	3 46	0 0	0 0	0 0	0 0	0 0	0 0	2 -69	3 105	3 -55	4 157	4 -43
<2 up|	5 132	2 79	2 47	4 32	4 49	0 0	0 2	0 0	0 0	0 3	0 3	3 -22	2 83	6 -103	4 112	7 52
<1 up|	7 49	4 -65	6 -23	1 -139	4 65	3 -24	0 0	3 0	3 61	2 69	3 82	1000 190	0 0	0 0	2 0	6 143
<1 up|	10 116	3 113	3 45	7 29	5 78	3 150	2 -14	2 165	4 -20	3 -105	2 -83	0 0	1000 190	0 0	0 2	6 -5
<1 up|	3 138	3 -144	2 158	1 -71	4 89	1 158	4 12	1 -148	1 67	3 55	6 103	0 0	0 0	1000 190	2 0	7 -50
<1 up|	8 38	5 156	5 155	4 -115	2 -96	3 43	4 22	3 -21	3 73	4 -157	4 -112	0 0	0 2	0 0	1000 190	7 141
<0 up|	1999 -128	9 -9	4 -32	6 -78	5 163	4 31	3 -19	7 1	4 -151	4 43	7 -52	6 -140	6 5	7 50	7 -141	53 0

The density matrix for t = 0.6050E-01 is:

	|4 up>	|3 up>	|3 up>	|3 up>	|3 up>	|2 up>	|2 up>	|2 up>	|2 up>	|2 up>	|2 up>	|1 up>	|1 up>	|1 up>	|1 up>	|0 up>
<4 up|	352 0	26 140	33 126	44 170	46 162	19 121	5 -78	32 -34	23 80	29 128	23 175	25 41	72 159	46 120	52 52	1962 129
<3 up|	25 140	997 0	0 0	0 0	1 101	12 -67	8 -51	30 93	15 -34	23 140	4 46	2 -44	11 -42	22 115	14 -57	18 63
<3 up|	33 120	0 0	997 0	0 0	1 128	27 -66	18 -39	13 -121	12 -141	14 -103	13 -51	2 19	33 157	15 -120	20 -135	34 42
<3 up|	44 -170	0 0	0 0	997 0	2 158	9 130	3 49	9 -85	9 -93	21 167	14 25	17 7	29 27	22 -59	12 171	49 107
<3 up|	46 -162	1 -101	1 103	2 -158	996 0	12 -97	15 -158	11 128	19 -52	12 -65	11 8	7 133	12 -93	40 -125	24 128	63 164
<2 up|	19 121	12 67	27 66	9 -130	12 97	1 0	1 0	1 177	0 0	1 0	0 0	7 -81	23 -123	9 -167	3 -173	52 -52
<2 up|	5 -75	9 51	19 89	3 -49	15 158	1 0	0 0	0 0	0 2	0 0	0 0	14 0	8 51	4 -36	15 27	11 -19
<2 up|	32 34	30 -93	13 121	9 85	11 -103	1 -177	0 0	0 0	0 0	1 0	0 0	9 -45	19 -122	19 177	4 49	17 -23
<2 up|	23 80	15 34	12 141	9 83	19 50	0 0	0 0	0 0	1 0	1 0	0 0	5 -23	9 62	18 -77	7 41	27 126
<2 up|	29 -128	23 -140	14 103	21 -167	12 65	1 0	0 0	1 0	1 0	1 0	0 0	11 -15	19 -169	21 19	7 -162	15 73
<2 up|	28 175	4 46	13 51	14 25	11 3	0 0	0 0	0 0	2 0	0 0	0 0	22 -165	5 128	7 110	10 72	9 169
<1 up|	25 -41	2 44	2 -162	17 -7	7 -133	7 81	14 -6	9 45	5 23	11 15	22 165	998 180	1 2	1 0	1 0	30 82
<1 up|	72 153	14 42	33 150	28 27	12 99	23 123	8 51	19 122	9 67	19 166	6 123	1 0	996 130	1 28	1 122	45 52
<1 up|	46 120	22 -115	15 100	22 59	40 125	8 167	4 86	19 -177	13 77	21 -19	7 -140	1 0	1 -23	997 180	2 -157	34 -71
<1 up|	52 50	14 57	28 135	19 191	24 128	3 173	15 77	4 49	7 11	7 162	10 -72	1 0	1 123	2 152	997 199	39 90
<0 up|	1962 -129	16 -63	34 -40	46 -107	63 -164	32 52	11 18	17 23	27 -126	15 -73	9 -109	30 -82	45 50	34 71	39 -90	951 190

AVERAGE preparater selectivity....

4291.4	2145.3	1429.9	1072.1
857.46	714.29	612.01	535.26
475.55	427.76	388.63	356.00
328.37	304.66	284.10	266.08
250.15	235.97	223.26	211.80
201.39	191.91	183.22	175.22
167.53	160.97	154.53	148.62
143.03	137.79	132.84	128.18
123.77	119.60	115.65	111.90
108.35	104.99	101.80	98.789
95.912	93.253	90.717	88.325
86.071	83.946	81.941	80.049
78.261	76.566	74.958	73.423
71.968	70.570	69.227	67.933
66.681	65.465	64.231	63.123
61.988	60.872	59.774	58.690
57.621	56.566	55.526	54.502
53.496	52.511	51.550	50.614
49.729	48.835	47.996	47.194
46.431	45.706	45.022	44.378
43.773	43.206	42.677	42.183
41.722	41.292	40.890	40.514
40.160	39.826	39.509	39.205
38.912	38.626	38.344	38.064
37.794	37.502	37.215	36.924
36.628	36.328	36.024	35.719
35.415	35.114	34.820	34.536
34.266	34.014	33.782	33.573
33.391	33.235	33.108	33.010
32.948	32.895	32.876	32.878
32.888	32.931	32.972	33.216
33.057			

AVERAGE coherence selectivity....

12365.	6431.3	4236.7	3213.3
2569.7	2139.9	1832.7	1601.9
1422.1	1277.9	1159.6	1060.6
976.47	903.93	840.63	784.79
735.22	692.25	649.65	612.53
578.33	546.59	516.94	489.06
462.67	437.56	413.52	392.37
368.00	346.29	325.14	304.46
284.13	264.27	244.69	225.39
206.39	187.66	169.21	151.05
133.19	115.65	98.447	81.607
65.153	49.103	33.480	18.305
3.5941	13.637	24.378	37.592
50.234	62.437	74.032	85.054
95.462	105.30	114.49	123.22
130.96	139.00	144.41	150.06
154.98	159.00	162.25	164.69
166.28	167.06	167.24	166.22
164.64	162.34	159.36	155.75
151.55	146.81	141.59	135.94
129.62	123.56	116.91	110.03
102.94	95.678	88.286	80.793
73.226	65.614	57.932	50.355
42.753	35.214	27.749	20.384
13.143	6.0437	0.87612	7.6084
14.128	23.415	26.453	32.221
37.727	42.397	47.781	52.350
56.599	60.523	64.117	67.384
70.352	72.934	75.223	77.191
78.864	80.184	81.216	81.944
82.372	82.536	82.348	81.901
81.172			

AVERAGE n-quantum signal magnitude....

0.16363E-01	0.55163E-01	0.14560	0.26634
0.39555	0.56096	0.74987	0.95916
1.1354	1.4249	1.6732	1.9290
2.1833	2.4355	2.6806	2.9146
3.1387	3.3342	3.5129	3.6673
3.7940	3.3917	3.9537	3.9937
3.9964	3.9660	3.9048	3.2121
3.6900	3.5404	3.3658	3.1692
2.9535	2.7225	2.4797	2.2292
1.9750	1.7213	1.4721	1.2315
1.0333	0.79134	0.59991	0.42915
0.23432	0.16320	0.81185E-01	0.25159E-01
0.13042E-02	0.98939E-02	0.49232E-01	0.12091
0.22279	0.35327	0.51024	0.69115
0.39304	1.1127	1.3466	1.5909
1.3417	2.2949	2.3465	2.5925
3.3243	3.0313	3.2577	3.4435
3.6059	3.7425	3.8511	3.9299
3.9778	3.9339	3.9730	3.9304
3.8520	3.7438	3.6277	3.4459
3.2616	3.0559	2.3346	2.0937
2.3538	2.1234	1.8513	1.6015
1.3591	1.1352	0.93573	0.73392
0.52288	0.36491	0.23314	0.12938
2.55306E-01	0.12342E-01	0.25964E-03	0.25123E-01
0.71280E-01	0.15289	0.26367	0.42178
0.56524	0.75231	0.95616	1.1773
1.4122	1.6557	1.9043	2.1541
2.4013	2.6417	2.8717	3.0877
3.2362	3.4641	3.6136	3.7472
3.3460	3.9194	3.9634	3.9702
3.9487			

Consider a 2**n by 2**n effective Hamiltonian
H describing an n spin 1/2 system. Matrix elements are
pumped in the time available (a typical coupling is (12/
0.25 Khz) or assumed to be everywhere equal in magnitude
with random phases. Phase shifts create a sequence which
is n-quantum selected to any desired order. This program
calculates the density matrix which is produced as a
function of t, the propagator and coherence selectiv-
ities, and the n-quantum signal magnitude.

```
Enter 1 for a random propagator:
   1
Enter the number of spins (0 implies benzene):
   4
Enter the order of coherence which is selected:
   4
Enter the number of cycles, the order of the se-
quence, and 1 if symmetrization is desired:
     4     3     1
how many different values do you want?(.le.125)
 125
Enter the initial value for time, in .1 msecs:
  0.0025
Enter 1 to increment time, 2 to increment cycles:
   1
Enter the time increment:
  0.0005

how many H's should be averaged over, to minimize
any peculiarities due to a particular choice of random
phases ?
   1

Enter any two positive integers < 32768 :
   123   234
```

The density matrix for t = 0.0125 is:

	|4 up>	|3 up>	|3 up>	|3 up>	|3 up>	|2 up>	|2 up>	|2 up>	|2 up>	|2 up>	|2 up>	|1 up>	|1 up>	|1 up>	|1 up>	|0 up>
<4 up|	58 180	0 0	0 0	0 0	0 0	0 0	0 0	0 0	0 0	0 0	0 0	0 0	0 0	0 0	0 0	1999 128
<3 up|	0 0	1000 0	0 0	0 0	0 0	0 0	0 0	0 0	0 0	0 0	0 0	0 0	0 0	0 0	0 0	0 0
<3 up|	0 0	0 0	1000 0	0 0	0 0	0 0	0 0	0 0	0 0	0 0	0 0	0 0	0 0	0 0	0 0	0 0
<3 up|	0 0	0 0	0 0	1000 0	0 0	0 0	0 0	0 0	0 0	0 0	0 0	0 0	0 0	0 0	0 0	0 0
<3 up|	0 0	0 0	0 0	0 0	1000 0	0 0	0 0	0 0	0 0	0 0	0 0	0 0	0 0	0 0	0 0	0 0
<2 up|	0 0	0 0	0 0	0 0	0 0	0 0	0 0	0 0	0 0	0 0	0 0	0 0	0 0	0 0	0 0	0 0
<2 up|	0 0	0 0	0 0	0 0	0 0	0 0	0 0	0 0	0 0	0 0	0 0	0 0	0 0	0 0	0 0	0 0
<2 up|	0 0	0 0	0 0	0 0	0 0	0 0	0 0	0 0	0 0	0 0	0 0	0 0	0 0	0 0	0 0	0 0
<2 up|	0 0	0 0	0 0	0 0	0 0	0 0	0 0	0 0	0 0	0 0	0 0	0 0	0 0	0 0	0 0	0 0
<2 up|	0 0	0 0	0 0	0 0	0 0	0 0	0 0	0 0	0 0	0 0	0 0	0 0	0 0	0 0	0 0	0 0
<1 up|	0 0	0 0	0 0	0 0	0 0	0 0	0 0	0 0	0 0	0 0	0 0	1000 1[illegible]2	0 0	0 0	0 0	0 0
<1 up|	0 0	0 0	0 0	0 0	0 0	0 0	0 0	0 0	0 0	0 0	0 0	0 0	1000 132	0 0	0 0	0 0
<1 up|	0 0	0 0	0 0	0 0	0 0	0 0	0 0	0 0	0 0	0 0	0 0	0 0	0 0	1000 1[illegible]	0 0	0 0
<1 up|	0 0	0 0	0 0	0 0	0 0	0 0	0 0	0 0	0 0	0 0	0 0	0 0	0 0	0 0	1000 190	0 0
<0 up|	1999 -128	0 0	0 0	0 0	0 0	0 0	0 0	0 0	0 0	0 0	0 0	0 0	0 0	0 0	0 0	58 0

The density matrix for t = 0.0005 is:

	|4 up>	|3 up>	|3 up>	|3 up>	|3 up>	|2 up>	|2 up>	|2 up>	|2 up>	|2 up>	|2 up>	|1 up>	|1 up>	|1 up>	|1 up>	|0 up>
<4 up|	280	0	0	1	0	1	0	1	0	0	2	1	1	1	1	1993
	0	0	0	0	0	0	0	0	0	0	0	0	0	135	0	123
<3 up|	0	1000	0	0	0	7	3	8	3	2	1	1	1	1	0	1
	0	0	0	0	0	-135	-162	59	-66	-3	0	0	0	0	0	0
<3 up|	0	0	1000	0	0	4	1	3	1	1	1	0	0	1	0	0
	0	0	0	0	0	-106	-101	56	-33	0	140	0	0	0	0	0
<3 up|	1	0	0	1000	0	7	4	7	4	2	1	1	1	1	1	0
	0	0	0	0	0	33	-2	-151	85	-177	0	0	0	0	0	0
<3 up|	0	0	0	0	1000	4	2	5	2	2	1	0	0	1	1	0
	0	0	0	0	0	180	124	-5	-130	-57	0	0	0	0	0	0
<2 up|	1	7	4	7	4	0	0	0	0	0	0	3	2	6	3	1
	0	135	103	-30	-180	0	0	0	0	0	0	-15	-147	61	164	0
<2 up|	0	3	1	4	2	0	0	0	0	0	0	5	4	7	2	1
	0	162	101	0	-124	0	0	0	0	0	0	-164	25	-96	-15	0
<2 up|	1	8	3	7	5	0	0	0	0	0	0	2	2	3	1	0
	0	-59	-85	151	5	0	0	0	0	0	0	97	-70	102	-164	0
<2 up|	0	3	1	4	2	0	0	0	0	0	0	5	4	5	3	0
	0	66	38	-65	130	0	0	0	0	0	0	116	-43	-178	-39	0
<2 up|	0	2	1	2	2	0	0	0	0	0	0	5	5	9	3	0
	0	3	0	177	57	0	0	0	0	0	0	-78	117	-11	60	0
<2 up|	0	1	1	1	1	0	0	0	0	0	0	3	0	1	2	1
	0	0	-140	0	0	0	0	0	0	0	0	-107	24	-107	-47	0
<1 up|	1	1	0	1	0	3	5	2	5	5	3	1000	0	0	0	0
	0	0	0	0	0	13	164	-97	-116	75	157	153	0	0	0	0
<1 up|	1	1	0	1	0	2	4	2	4	5	3	0	1000	0	0	1
	0	0	0	0	0	147	-25	70	43	-117	-24	0	160	0	0	0
<1 up|	1	1	1	1	1	6	7	3	3	9	4	0	0	1000	0	1
	-135	0	0	0	0	-61	96	-162	175	11	127	0	0	150	0	51
<1 up|	1	0	0	1	1	3	2	1	3	3	2	0	0	0	1000	1
	0	0	0	0	0	-164	15	164	96	-36	47	0	0	0	132	0
<0 up|	1983	1	0	0	0	1	1	0	0	0	1	0	1	1	1	253
	-123	0	0	0	0	0	0	0	0	0	0	0	0	-51	0	133

AVERAGE propagator selectivity....

0.9181E+11	0.6534E+10	0.1283E+10	0.4082E-09	0.1684E+09
0.3153E+08	0.4435E+08	0.2010E+08	0.1647E+08	0.1091E+08
0.7531E+07	0.5362E+07	0.3960E+07	0.2889E+07	0.2337E+07
0.1810E+07	0.1455E+07	0.1155E+07	0.9793E+06	0.8209E+06
0.6974E+06	0.6000E+06	0.5225E+06	0.4625E+06	0.4178E+06
0.3707E+06	0.3354E+06	0.3125E+06	0.2918E+06	0.2752E+06
0.2615E+06	0.2493E+06	0.2369E+06	0.2221E+06	0.2032E+06
0.1799E+06	0.1542E+06	0.1289E+06	0.1064E+06	0.8751E+05
0.7222E+05	0.6007E+05	0.5045E+05	0.4282E+05	0.3674E+05
0.3186E+05	0.2791E+05	0.2470E+05	0.2205E+05	0.1987E+05
0.1806E+05	0.1654E+05	0.1528E+05	0.1422E+05	0.1333E+05
0.1259E+05	0.1198E+05	0.1145E+05	0.1105E+05	0.1076E+05
0.1051E+05	0.1033E+05	0.1018E+05	0.1005E+05	9911.
9729.	9407.	8971.	8395.	7712.
6987.	6222.	5520.	4887.	4332.
3854.	3446.	3099.	2806.	2557.
2346.	2166.	2014.	1885.	1775.
1682.	1603.	1541.	1489.	1445.
1417.	1396.	1384.	1380.	1383.
1392.	1402.	1409.	1405.	1377.
1322.	1232.	1122.	996.1	873.0
759.4	659.2	573.2	500.5	439.4
388.1	344.9	308.4	277.5	251.2
228.7	209.2	192.4	177.8	165.0
153.8	143.8	135.0	127.2	122.2

AVERAGE coherence selectivity....

0.3391E+12	0.2500E+11	0.4913E+10	0.1566E+10	0.6463E+09
0.3133E+09	0.1725E+09	0.1207E+09	0.5343E+08	0.4210E+08
0.2910E+08	0.2082E+08	0.1533E+08	0.1158E+08	0.8943E+07
0.7040E+07	0.5638E+07	0.4536E+07	0.3764E+07	0.3163E+07
0.2676E+07	0.2239E+07	0.1979E+07	0.1727E+07	0.1522E+07
0.1352E+07	0.1211E+07	0.1093E+07	0.9916E+06	0.9035E+06
0.8243E+06	0.7516E+06	0.6832E+06	0.6079E+06	0.5329E+06
0.4557E+05	0.3793E+05	0.3275E+05	0.2437E+05	0.1895E+05
0.1450E+06	0.1094E+06	0.8108E+05	0.5878E+05	0.4122E+05
0.2737E+05	0.1640E+05	7665.	675.0	4973.
9565.	0.1334E+05	0.1647E+05	0.1911E+05	0.2137E+05
0.2324E+05	0.2509E+05	0.2668E+05	0.2814E+05	0.2951E+05
0.3079E+05	0.3198E+05	0.3305E+05	0.3394E+05	0.3457E+05
0.3452E+05	0.3457E+05	0.3375E+05	0.3234E+05	0.3040E+05
0.2812E+05	0.2561E+05	0.2309E+05	0.2067E+05	0.1842E+05
0.1637E+05	0.1454E+05	0.1292E+05	0.1148E+05	0.1021E+05
9093.	8103.	7226.	6444.	5745.
5116.	4543.	4031.	3556.	3115.
2733.	2315.	1941.	1577.	1218.
857.5	493.5	125.1	229.5	590.2
936.0	1166.	1356.	1473.	1527.
1531.	1501.	1452.	1387.	1315.
1246.	1176.	1107.	1041.	977.4
917.6	861.1	807.7	757.5	710.1
665.4	623.2	583.4	545.7	510.1

AVERAGE n-quantum signal magnitude....

0.1636E-01	0.6519E-01	0.1457	0.2565	0.3958
0.5814	0.7535	0.9621	1.157	1.427
1.676	1.930	2.186	2.439	2.684
2.918	3.135	3.338	3.517	3.671
3.798	3.895	3.961	3.995	3.997
3.965	3.902	3.805	3.664	3.533
3.356	3.157	2.942	2.707	2.462
2.216	1.955	1.722	1.451	1.210
0.9819	0.7707	0.5796	0.4116	0.2696
0.1558	0.7221E-01	0.2024E-01	0.1943E-05	0.1298E-01
0.5820E-01	0.1351	0.2424	0.3734	0.5403
0.7270	0.9340	1.158	1.396	1.644
1.898	2.153	2.426	2.652	2.888
3.109	3.312	3.493	3.650	3.731
3.882	3.953	3.992	3.999	3.973
3.915	3.825	3.707	3.568	3.388
3.194	2.980	2.750	2.503	2.253
2.004	1.750	1.499	1.257	1.027
0.8130	0.6131	0.4455	0.2983	0.1726
0.5837E-01	0.2917E-01	0.1907E-02	0.6995E-02	0.4435E-01
0.1134	0.2129	0.3413	0.4966	0.6761
0.8771	1.096	1.330	1.574	1.826
2.082	2.332	2.582	2.815	3.043
3.250	3.438	3.603	3.741	3.852
3.933	3.982	4.020	3.985	3.939

Consider a 2**n by 2**n effective Hamiltonian H describing an n spin 1/2 system. Matrix elements are pumped in the time available (if coupling constants are given) or assumed to be everywhere equal in magnitude with random phases. Phase shifts create a sequence which is n-quantum selected to any desired order. This program calculates the density matrix which is produced as a function of t, the propagator and coherence selectivities, and the n-quantum signal magnitude.

```
Enter 1 for time reversal, 0 otherwise:
(2 means WAHUEA,3 means isotropic time reversal,
and 4 suppresses zero-quantum)
   4
Enter the number of spins (0 implies benzene):
   4
Enter the order of coherence which is selected:
   4
Enter the number of cycles, the order of the se-
quence, and 1 if symmetrization is desired:
     1     3     1
how many different values do you want?(.le.125)
 125
Enter the initial value for time, in .1 msecs:
  2.0005
Enter 1 to increment time, 2 to increment cycles:
   1
Enter the time increment:
  0.0005

how many H's should be averaged over, to minimize
any peculiarities due to a particular choice of random
phases ?
   1

Enter any two positive integers < 32768 :
   123   234
```

The density matrix for t = 0.1250E-01 is:

	|4 up>	|3 up>	|3 up>	|3 up>	|3 up>	|2 up>	|2 up>	|2 up>	|2 up>	|2 up>	|2 up>	|1 up>	|1 up>	|1 up>	|1 up>	|0 up>
<4 up|	58 180	0 0	0 0	0 0	0 0	0 0	0 0	0 0	0 0	0 0	0 0	0 0	0 0	0 0	0 0	1999 128
<3 up|	0 0	1000 0	0 0	0 0	0 0	0 0	0 0	0 0	0 0	0 0	0 0	0 0	0 0	0 0	0 0	0 0
<3 up|	0 0	0 0	1000 0	0 0	0 0	0 0	0 0	0 0	0 0	0 0	0 0	0 0	0 0	0 0	0 0	0 0
<3 up|	0 0	0 0	0 0	1000 0	0 0	0 0	0 0	0 0	0 0	0 0	0 0	0 0	0 0	0 0	0 0	0 0
<3 up|	0 0	0 0	0 0	0 0	1000 0	0 0	0 0	0 0	0 0	0 0	0 0	0 0	0 0	0 0	0 0	0 0
<2 up|	0 0	0 0	0 0	0 0	0 0	0 0	0 0	0 0	0 0	0 0	0 0	0 0	0 0	0 0	0 0	0 0
<2 up|	0 0	0 0	0 0	0 0	0 0	0 0	0 0	0 0	0 0	0 0	0 0	0 0	0 0	0 0	0 0	0 0
<2 up|	0 0	0 0	0 0	0 0	0 0	0 0	0 0	0 0	0 0	0 0	0 0	0 0	0 0	0 0	0 0	0 0
<2 up|	0 0	0 0	0 0	0 0	0 0	0 0	0 0	0 0	0 0	0 0	0 0	0 0	0 0	0 0	0 0	0 0
<2 up|	0 0	0 0	0 0	0 0	0 0	0 0	0 0	0 0	0 0	0 0	0 0	0 0	0 0	0 0	0 0	0 0
<2 up|	0 0	0 0	0 0	0 0	0 0	0 0	0 0	0 0	0 0	0 0	0 0	0 0	0 0	0 0	0 0	0 0
<1 up|	0 0	0 0	0 0	0 0	0 0	0 0	0 0	0 0	0 0	0 0	0 0	1000 180	0 0	0 0	0 0	0 0
<1 up|	0 0	0 0	0 0	0 0	0 0	0 0	0 0	0 0	0 0	0 0	0 0	0 0	1000 180	0 0	0 0	0 0
<1 up|	0 0	0 0	0 0	0 0	0 0	0 0	0 0	0 0	0 0	0 0	0 0	0 0	0 0	1000 180	0 0	0 0
<1 up|	0 0	0 0	0 0	0 0	0 0	0 0	0 0	0 0	0 0	0 0	0 0	0 0	0 0	0 0	1000 180	0 0
<0 up|	1999 -128	0 0	0 0	0 0	0 0	0 0	0 0	0 0	0 0	0 0	0 0	0 0	0 0	0 0	0 0	58 0

The density matrix for t = 0.6050E-01 is:

	|4 up>	|3 up>	|3 up>	|3 up>	|3 up>	|2 up>	|2 up>	|2 up>	|2 up>	|2 up>	|2 up>	|1 up>	|1 up>	|1 up>	|1 up>	|0 up>
<4 up|	311	1	1	1	1	1	2	2	2	1	1	6	6	6	5	1976
	0	0	0	-139	136	0	-103	-44	159	8	-143	-137	22	40	-104	127
<3 up|	1	1000	0	0	0	0	0	0	0	0	0	0	0	0	0	7
	0	0	0	0	0	0	0	0	0	0	0	0	0	0	0	4
<3 up|	1	0	1000	0	0	0	0	0	0	0	0	0	0	0	0	5
	0	0	0	0	0	0	0	0	0	0	0	0	0	0	0	-88
<3 up|	1	0	0	1000	0	0	0	0	0	0	0	0	0	0	0	5
	139	0	0	0	0	0	0	0	0	0	0	0	0	0	0	-5
<3 up|	1	0	0	0	1000	0	0	0	0	0	0	0	0	0	0	5
	-136	0	0	0	0	0	0	0	0	0	0	0	0	0	0	-24
<2 up|	1	0	0	0	0	0	0	0	0	0	0	0	0	0	0	2
	0	0	0	0	0	0	0	0	0	0	0	0	0	0	0	-56
<2 up|	2	0	0	0	0	0	0	0	0	0	0	0	0	0	0	1
	103	0	0	0	0	0	0	0	0	0	0	0	0	0	0	-135
<2 up|	2	0	0	0	0	0	0	0	0	0	0	0	0	0	0	1
	44	0	0	0	0	0	0	0	0	0	0	0	0	0	0	-79
<2 up|	2	0	0	0	0	0	0	0	0	0	0	0	0	0	0	2
	-139	0	0	0	0	0	0	0	0	0	0	0	0	0	0	96
<2 up|	1	0	0	0	0	0	0	0	0	0	0	0	0	0	0	2
	-8	0	0	0	0	0	0	0	0	0	0	0	0	0	0	21
<2 up|	1	0	0	0	0	0	0	0	0	0	0	0	0	0	0	3
	143	0	0	0	0	0	0	0	0	0	0	0	0	0	0	30
<1 up|	6	0	0	0	0	0	0	0	0	0	0	1000	0	0	0	0
	137	0	0	0	0	0	0	0	0	0	0	180	0	0	0	0
<1 up|	6	0	0	0	0	0	0	0	0	0	0	0	1000	0	0	1
	-22	0	0	0	0	0	0	0	0	0	0	0	190	0	0	0
<1 up|	6	0	0	0	0	0	0	0	0	0	0	0	0	1000	0	0
	-40	0	0	0	0	0	0	0	0	0	0	0	0	190	0	0
<1 up|	5	0	0	0	0	0	0	0	0	0	0	0	0	0	1000	1
	104	0	0	0	0	0	0	0	0	0	0	0	0	0	180	0
<0 up|	1976	7	6	6	5	2	1	1	2	2	3	0	1	0	1	311
	-127	-4	88	5	24	56	135	79	-96	-21	-30	0	0	0	0	180

AVERAGE propagator selectivity....

0.7556E+12	0.3323E+11	0.6384E+10	0.1970E+10	0.7946E+09
0.3822E+09	0.2045E+09	0.1195E+09	0.7439E+08	0.4858E+08
0.3307E+08	0.2326E+08	0.1681E+08	0.1244E+08	0.9394E+07
0.7220E+07	0.5634E+07	0.4458E+07	0.3570E+07	0.2890E+07
0.2362E+07	0.1947E+07	0.1618E+07	0.1355E+07	0.1142E+07
0.9679E+06	0.8252E+06	0.7071E+06	0.6088E+06	0.5265E+06
0.4571E+06	0.3984E+06	0.3485E+06	0.3058E+06	0.2692E+06
0.2377E+06	0.2104E+06	0.1867E+06	0.1660E+06	0.1480E+06
0.1322E+06	0.1183E+06	0.1061E+06	0.9524E+05	0.8566E+05
0.7717E+05	0.6960E+05	0.6287E+05	0.5684E+05	0.5146E+05
0.4663E+05	0.4229E+05	0.3840E+05	0.3488E+05	0.3171E+05
0.2885E+05	0.2626E+05	0.2392E+05	0.2179E+05	0.1986E+05
0.1811E+05	0.1651E+05	0.1506E+05	0.1373E+05	0.1252E+05
0.1142E+05	0.1041E+05	9492.	8649.	7877.
7170.	6522.	5927.	5382.	4882.
4422.	4000.	3613.	3256.	2929.
2628.	2352.	2097.	1864.	1649.
1451.	1270.	1103.	950.2	809.6
680.7	562.5	454.2	354.9	264.2
181.2	105.4	36.31	26.63	83.85
135.8	182.9	225.4	263.8	298.2
329.1	356.7	381.2	402.8	421.9
438.5	452.8	465.1	475.4	484.0
490.9	496.1	500.4	503.2	504.7
505.2	504.7	503.3	501.1	498.0

AVERAGE coherence selectivity....

0.1065E+13	0.4573E+11	0.8744E+10	0.2683E+10	0.1079E+10
0.5166E+09	0.2750E+09	0.1597E+09	0.9371E+08	0.6397E+08
0.4317E+08	0.3007E+08	0.2150E+08	0.1573E+08	0.1173E+08
0.8893E+07	0.6839E+07	0.5326E+07	0.4192E+07	0.3331E+07
0.2669E+07	0.2154E+07	0.1750E+07	0.1430E+07	0.1174E+07
0.9677E+06	0.8006E+06	0.6643E+06	0.5525E+06	0.4604E+06
0.3840E+06	0.3206E+06	0.2676E+06	0.2232E+06	0.1860E+06
0.1546E+06	0.1280E+06	0.1056E+06	0.8660E+05	0.7047E+05
0.5676E+05	0.4512E+05	0.3522E+05	0.2530E+05	0.1965E+05
0.1359E+05	8451.	4109.	449.3	2621.
5136.	7313.	9063.	0.1049E+05	0.1163E+05
0.1253E+05	0.1322E+05	0.1372E+05	0.1407E+05	0.1429E+05
0.1439E+05	0.1438E+05	0.1429E+05	0.1413E+05	0.1390E+05
0.1362E+05	0.1330E+05	0.1293E+05	0.1253E+05	0.1211E+05
0.1166E+05	0.1120E+05	0.1072E+05	0.1023E+05	9735.
9233.	8729.	8223.	7718.	7216.
6719.	6227.	5742.	5266.	4800.
4344.	3901.	3471.	3055.	2656.
2272.	1907.	1560.	1232.	924.8
638.1	372.6	128.5	94.11	295.3
475.3	634.7	774.1	894.2	995.9
1080.	1148.	1201.	1241.	1267.
1282.	1287.	1282.	1269.	1249.
1223.	1192.	1156.	1117.	1075.
1030.	984.1	936.5	888.1	839.2

AVERAGE n-quantum signal magnitude....

0.1636E-01	0.6518E-01	0.1457	0.2565	0.3958
0.5614	0.7505	0.9601	1.187	1.426
1.676	1.930	2.186	2.439	2.684
2.918	3.137	3.338	3.517	3.671
3.797	3.895	3.961	3.995	3.997
3.966	3.903	3.808	3.685	3.534
3.357	3.159	2.942	2.709	2.465
2.213	1.958	1.704	1.454	1.213
0.9854	0.7742	0.5829	0.4147	0.2723
0.1581	0.7365E-01	0.2097E-01	0.3000E-03	0.1215E-01
0.5633E-01	0.1321	0.2382	0.3729	0.5341
0.7190	0.9247	1.148	1.385	1.632
1.884	2.139	2.391	2.637	2.873
3.094	3.298	3.481	3.639	3.772
3.875	3.948	3.990	3.999	3.977
3.922	3.836	3.721	3.578	3.410
3.219	3.008	2.781	2.542	2.294
2.042	1.768	1.538	1.296	1.065
0.8492	0.6517	0.4759	0.3246	0.2001
0.1044	0.3909E-01	0.5112E-02	0.3021E-02	0.3281E-01
0.9400E-01	0.1856	0.3061	0.4535	0.6256
0.8194	1.032	1.260	1.500	1.747
1.999	2.257	2.497	2.737	2.964
3.177	3.370	3.542	3.690	3.811
3.903	3.965	3.996	3.995	3.964

Appendix D. Residual Nonselective Terms for Selective Sequences

In this Appendix the size of the first non-nk-quantum selective operator from a j-order nk-quantum selective sequence, which is $(-i\bar{\mathcal{H}}^{(j+1)}t_c)_{nns}$, is estimated.

To simplify the calculations phase cycling and symmetrization are combined into one operation, which turns a (j-2)-order nk-quantum selective subcycle (j odd) into a j-order nk-quantum selective cycle requiring 2n subcycles (Figure III.2), assuming perfect phase shifts and no timing errors. As in earlier calculations, the propagator for the j-order nk-quantum selective sequence is expanded in powers of t_c. The first nonselective term is $i\bar{\mathcal{H}}^{(j+1)}t_c$, which is proportional to $t_c^{(j+2)}$. All other terms proportional to t_c^{j+2} are nk-quantum selective, so the only possible nns term proportional to $t_c^{(j+2)}$ is $(i\bar{\mathcal{H}}^{(j+1)}t_c)_{nns}$. The product of the propagators for the subcycles has several terms proportional to $(t_{ci})^{j+2}=(t_c/2n)^{j+2}$; they are:

$$\prod_i U(t_{ci}) = -i\sum_i \bar{\mathcal{H}}_i^{(j+1)}t_{ci} \qquad \text{(D.1)}$$

$$-\sum_{i<j}(\bar{\mathcal{H}}_i^{(0)}\bar{\mathcal{H}}_j^{(j)}+\bar{\mathcal{H}}_i^{(j)}\bar{\mathcal{H}}_j^{(0)})t_{ci}^2 \qquad \text{(D.2)}$$

$$-\frac{1}{2}\sum_i(\bar{\mathcal{H}}_i^{(0)}\bar{\mathcal{H}}_i^{(j)}+\bar{\mathcal{H}}_i^{(j)}\bar{\mathcal{H}}_i^{(0)})t_{ci}^2 \qquad \text{(D.3)}$$

$$-\sum_{i<j}(\bar{\mathcal{H}}_i^{(1)}\bar{\mathcal{H}}_j^{(j-1)}+\bar{\mathcal{H}}_i^{(j-1)}\bar{\mathcal{H}}_j^{(1)})t_{ci}^2 \qquad \text{(D.4)}$$

$$-\frac{1}{2}\sum_i(\bar{\mathcal{H}}_i^{(1)}\bar{\mathcal{H}}_i^{(j-1)}+\bar{\mathcal{H}}_i^{(j-1)}\bar{\mathcal{H}}_i^{(1)})t_{ci}^2 \qquad \text{(D.5)}$$

$$+(i\sum_{i>j>k}t_{ci}^3+(i/2)\sum_{i=j>k}t_{ci}^3+(i/2)\sum_{i>j=k}t_{ci}^3)$$
$$(\bar{\mathcal{H}}_i^{(0)}\bar{\mathcal{H}}_j^{(0)}\bar{\mathcal{H}}_k^{(j-1)}+\bar{\mathcal{H}}_i^{(0)}\bar{\mathcal{H}}_j^{(j-1)}\bar{\mathcal{H}}_k^{(0)}+\bar{\mathcal{H}}_i^{(j-1)}\bar{\mathcal{H}}_j^{(0)}\bar{\mathcal{H}}_k^{(0)}) \qquad \text{(D.6)}$$

$$+(i/6)\sum_i t_{ci}^3(\bar{\mathcal{H}}_i^{(0)}\bar{\mathcal{H}}_i^{(0)}\bar{\mathcal{H}}_i^{(j-1)}+\bar{\mathcal{H}}_i^{(0)}\bar{\mathcal{H}}_i^{(j-1)}\bar{\mathcal{H}}_i^{(0)}+\bar{\mathcal{H}}_i^{(j-1)}\bar{\mathcal{H}}_i^{(0)}\bar{\mathcal{H}}_i^{(0)}) \qquad \text{(D.7)}$$

plus terms not proportional to $(t_c)^{j+2}$. We will assume that the subcycles are themselves constructed by phase cycling and symmetrization, so that $\bar{\mathcal{H}}_i^{(j\pm 2j')} = 0$ for all j', and terms (D.2 - D.5) vanish. In addition, terms (D.1) and (D.7) are unaffected by a phase shift of $\phi = 2\pi/n$, so they are nk-quantum selective. Finally, term (D.6) contains many nk-quantum selective portions; for example $\sum_{i=j<k} \bar{\mathcal{H}}_j^{(0)}\bar{\mathcal{H}}_j^{(0)}\bar{\mathcal{H}}_k^{(j-1)}$ is nk-quantum selective of i and j are in the first half of the cycle and k is in the second half.

The construction of the subcycles implies $\bar{\mathcal{H}}_i^{(0)} = \bar{\mathcal{H}}_j^{(0)}$ and $\|\bar{\mathcal{H}}_i^{(j-1)}\| = \|\bar{\mathcal{H}}_j^{(j-1)}\|$, and therefore $\langle \|(\bar{\mathcal{H}}_i^{(0)})^2\bar{\mathcal{H}}_j^{(j-1)}\|^2 \rangle \sim \langle \|\bar{\mathcal{H}}_i^{(0)}\bar{\mathcal{H}}_j^{(j-1)}\bar{\mathcal{H}}_k^{(0)}\|\rangle^2 \sim \langle \|\bar{\mathcal{H}}_i^{(j-1)}(\bar{\mathcal{H}}_j^{(0)})^2\|^2 \rangle$. Straightforward counting arguments show that the operator $\bar{\mathcal{H}}_i^{(0)}\bar{\mathcal{H}}_j^{(0)}\bar{\mathcal{H}}_k^{(j-1)}$ occurs $(\frac{3}{2}n^2 + \frac{1}{2}n + k^2 - k - 2nk)$ times; the operator $\bar{\mathcal{H}}_i^{(0)}\bar{\mathcal{H}}_j^{(j-1)}\bar{\mathcal{H}}_k^{(0)}$ occurs $(4nj - 1 - 2j^2 + 2j - 2n)$ times; and the operator $\bar{\mathcal{H}}_i^{(j-1)}\bar{\mathcal{H}}_j^{(0)}\bar{\mathcal{H}}_k^{(0)}$ occurs $(\frac{3}{2}n^2 + \frac{1}{2}n + i^2 - i - 2ni)$ times. If all of these numbers are just added randomly, an overestimate is produced. For example, if i = j = 1, the nns part of the summation $\sum_{k>1} \bar{\mathcal{H}}_1^{(0)}\bar{\mathcal{H}}_1^{(0)}\bar{\mathcal{H}}_k^{(j-1)}$, which contains (n-1) terms, is the same size as a single term, since $((\bar{\mathcal{H}}_1^{(0)}\bar{\mathcal{H}}_1^{(0)})(\sum_k \bar{\mathcal{H}}_k^{(j-1)}))_{nns} = 0$.

In fact, all of the matrix elements have the general form $\sum_{m=0}^{n-1} a_m e^{im\theta}$, where θ is a multiple of $2\pi/n$. For the nns terms, it can be shown that

$$\langle (\sum_{m=0}^{n-1} a_m e^{im\theta})^2 \rangle = n(\langle a_n^2 \rangle - \langle a_n \rangle^2) \tag{D.8}$$

The summations yield:

$$\|(\bar{\mathcal{H}}^{(j+1)}t_c)\|^2_{nns} \sim F(n)^2 \langle \|(\bar{\mathcal{H}}_i^{(0)})^2\bar{\mathcal{H}}_j^{(j-1)}\|\rangle^2 t_c^6$$

$$F(n) = \left(\frac{8}{15} n^5 - \frac{2}{3} n^3 + \frac{2}{45} n\right)^{1/2}/8n^3 \sim .09\ n^{-1/2} \quad . \tag{D.9}$$

Assuming $\| (\bar{\mathcal{H}}^{(0)})^2 \bar{\mathcal{H}}^{(j-1)}_{nns} \| \sim \| (\bar{\mathcal{H}}^{(0)})^2 \| \| \mathcal{H}^{(j-1)}_{j,nns} \|$ implies:

$$\| \mathcal{H}^{(j+1)}_{nns} t_c \| \sim F(n) \| (\bar{\mathcal{H}}^{(0)} t_c)^2 \| \| \mathcal{H}^{(j-1)}_{j,nns} t_c \| \quad . \tag{D.10}$$

Since $\bar{\mathcal{H}}^{(j)}$ is proportional to $t_c^{\ j}$, one expects that if t_c is "small" $\| \bar{\mathcal{H}}^{(j+1)} \| >> \| \bar{\mathcal{H}}^{(j+3)} \|$ (assume the cycles are symmetrized, so that $\bar{\mathcal{H}}^{(j+2)}$ vanishes) and if t_c is "large", $\| \bar{\mathcal{H}}^{(j+1)} \| << \| \bar{\mathcal{H}}^{(j+3)} \|$. The interesting value of t_c is the one which makes $\| \bar{\mathcal{H}}^{(j+1)} \| \sim \| \bar{\mathcal{H}}^{(j+3)} \|$; if t_c is much smaller than this critical value, convergence is expected.

Assume that one has a (j-2)-order nk-quantum selective subcycle which is known to converge, so that $\| \bar{\mathcal{H}}^{(0)} \| >> \| \bar{\mathcal{H}}^{(2)} \|$ and $\| \bar{\mathcal{H}}^{(j-1)}_i \|_{nns} >> \| \bar{\mathcal{H}}^{(j+1)}_i \|_{nns}$. To create a j-order nk-quantum selective cycle requires increasing the cycle time by a factor of 2n. $\| \mathcal{H}^{(j+1)} \|_{nns}$ was calculated by examining the term in the propagator proportional to t_c^{j+2}. The largest nns terms proportional to t_c^{j+4}, under these assumptions, are:

$$\left(-i\bar{\mathcal{H}}^{(j+3)} t_c + \frac{1}{2} i t_c^{\ 3} \left((\bar{\mathcal{H}}^{(j+1)}) (\bar{\mathcal{H}}^{(0)})^2 + \bar{\mathcal{H}}^{(0)} \bar{\mathcal{H}}^{(j+1)} \bar{\mathcal{H}}^{(0)} + \bar{\mathcal{H}}^{(j+1)} (\bar{\mathcal{H}}^{(0)})^2 \right)\right)_{nns}$$

$$= \sum_{i>j>k>\ell>m} i(\bar{\mathcal{H}}^{(j-1)}_i \bar{\mathcal{H}}^{(0)}_j \bar{\mathcal{H}}^{(0)}_k \bar{\mathcal{H}}^{(0)}_\ell \bar{\mathcal{H}}^{(0)}_m + \text{permutations})_{nns}\ t^5_{ci} + \text{small terms.} \tag{D.11}$$

Again a substantial fraction of the r.h.s. cancels or is forced to be selective. Most of the remaining terms on the r.h.s. cancel with terms such as $\bar{\mathcal{H}}^{(j+1)} (\bar{\mathcal{H}}^{(0)})^2$ on the ℓ.h.s. The result is that, if

$\|(\bar{\mathcal{H}}^{(0)}t_c)^2\| \sim 1$, one expects that $\|\bar{\mathcal{H}}^{(j+3)}\|_{nns} \lesssim \|\bar{\mathcal{H}}^{(j+1)}\|_{nns}$. Thus, a converging (j-2)-order nk-quantum selective subcycle implies convergence for the j-order selective cycle if $\|\bar{\mathcal{H}}^{(0)}t_c\| << F(n)^{-1}$.

Equation (D.10) can be used iteratively, to calculate the first nns term as a function of successively lower-order terms. To begin the iteration, however, an expression for $\|\bar{\mathcal{H}}^{(2)}\|_{nns}$ for a first-order selective sequence (Figure 2(b) with $\mathcal{H}_\phi$ nonselective) is needed. It has been shown that (equation (III.16)):

$$(\bar{\mathcal{H}}^{(2)})_{nns} = (i/t_c)\left(\int_{t_3=0}^{t_c} dt_3 \int_{t_2=0}^{t_3} dt_2 \int_{t_1=0}^{t_2} dt_1\ \tilde{\mathcal{H}}_{int}(t_3)\tilde{\mathcal{H}}_{int}(t_2)\tilde{\mathcal{H}}_{int}(t_1)\right)_{nns}$$

$\tilde{\mathcal{H}}_{int}$ in this expression is $\mathcal{H}_\phi$, as discussed in relation to Figure III.3. This can be rewritten as

$$(\bar{\mathcal{H}}^{(2)})_{nns} = (-i/2n\Delta\tau_p)(\Delta\tau_p^3)\left(\sum_{i<j<k} + \frac{1}{2}\sum_{i=j<k} + \frac{1}{6}\sum_{i=j=k}\right)(\mathcal{H}_{\phi(i)}\mathcal{H}_{\phi(j)}\mathcal{H}_{\phi(k)})_{nns}$$

where $\phi(i)$ is the value of ϕ during i^{th} subcycle. Since the operators $\mathcal{H}_{\phi(i)}$ are nonselective, only a few terms in the summations are forced to be nk-quantum selective (note, however, the sum with i=j=k is nk-quantum selective, as are a few of the terms in the other sums). The possible values of i,j and k divide into two sets:

a) i and j are both in the first half of the cycle and k is in the second half, or i is in the first half and j and k are both in the second half. In this case the sum over the isolated index reduces to $n\,\bar{\mathcal{H}}^{(0)}$.

b) i, j and k are all in the same half of the cycle. In this case

no further reduction is possible. By construction of the sequence, $\|\mathcal{H}_{\phi(i)}\| = \|\mathcal{H}_{\phi(j)}\|$. If one assumes $<\|\bar{\mathcal{H}}^{(0)}\mathcal{H}_{\phi(i)}\mathcal{H}_{\phi(j)}\|> = <\|\mathcal{H}_{\phi(i)}\mathcal{H}_{\phi(j)}\bar{\mathcal{H}}^{(0)}\|>$, straightforward algebra then gives:

$$\|\bar{\mathcal{H}}^{(2)}\Delta\tau_p\|^2_{nns} \sim \frac{n}{12} <\|\mathcal{H}_{\phi(i)}\mathcal{H}_{\phi(j)}\mathcal{H}_{\phi(k)}\Delta\tau_p^3\|^2> + \frac{n^2}{8} <\|\bar{\mathcal{H}}^{(0)}\mathcal{H}_{\phi(j)}\mathcal{H}_{\phi(k)}\|^2> \quad . \tag{D.12}$$

$\|\bar{\mathcal{H}}^{(0)}\mathcal{H}_{\phi(i)}\mathcal{H}_{\phi(j)}\| \sim \|\bar{\mathcal{H}}^{(0)}\|\|\mathcal{H}_{\phi(i)}\mathcal{H}_{\phi(j)}\| \leq \|\bar{\mathcal{H}}^{(0)}\|\|(\mathcal{H}_{\phi(i)})^2\|$ is expected is $\|\mathcal{H}_{\phi(i)}\mathcal{H}_{\phi(j)}\mathcal{H}_{\phi(k)}\| \leq \|(\mathcal{H}_{\phi(i)})^3\|$.

Let $\|\mathcal{H}_{\phi(i)}\|^2 = \alpha K\|\bar{\mathcal{H}}^{(0)}\|^2$ (see Section 3.6.1). This implies

$$\|\bar{\mathcal{H}}^{(2)}\Delta\tau_p\|_{nns} \lesssim \left(\frac{n\alpha^3K^3}{12}\|(\bar{\mathcal{H}}^{(0)}\Delta\tau_p)\|^2 + \frac{n^2\alpha^2K^2}{8}\|(\bar{\mathcal{H}}^{(0)}\Delta\tau_p)^2\|^2\|\bar{\mathcal{H}}^{(0)}\Delta\tau_p\|^2\right)^{1/2} \quad . \tag{D.13}$$

The first-order sequence should converge if $\|(\mathcal{H}_\phi(2n\Delta\tau_p))^2\| \sim 1$, because equation (D.12) then gives $\|\bar{\mathcal{H}}^{(2)}\Delta\tau_p\|_{nns} << 1$. Combining this with earlier results, one expects a j-order nk-quantum selective sequence which is constructed from $\frac{1}{2}$ (j+1) phase cycles and $\frac{1}{2}$ (j+1) symmetrizations (and therefore has a cycle time $t_c = (2n)^{(j+1)/2}\Delta\tau_p$) to converge if

$$\|(\mathcal{H}_\phi(2n\Delta\tau_p))^2\| \lesssim 1 \text{ and } \|(\bar{\mathcal{H}}^{(0)}(2n)^{(j+1)/2}\Delta\tau_p)^2\| = \|(\bar{\mathcal{H}}^{(0)}t_c)^2\| << F(n)^{-1} \quad .$$

These constraints are intended to be conservative, and Chapter IV shows that this is indeed the case. The size of the first nonselective term, $\|\mathcal{H}^{(j+1)}\|_{nns}$, is

$$\|\bar{\mathcal{H}}^{(j+1)}\|_{nns}(2n)^{(j+1)/2}\Delta\tau_p \lesssim F(n)\|\bar{\mathcal{H}}_i^{(j-1)}\|_{nns}\|(\bar{\mathcal{H}}^{(0)})^2\|(\Delta\tau_p)^3(2n)^{3(j+1)/2}$$

$$\|\bar{\mathcal{H}}^{(j+1)}\|_{nns} \lesssim F(n)\|\bar{\mathcal{H}}_i^{(j-1)}\|_{nns}\|(\bar{\mathcal{H}}^{(0)}\Delta\tau_p)^2\|(2n)^{j+1}$$

$$= F(n)^2\,\|\bar{\mathcal{H}}_i^{(j-3)}\|_{nns}\|(\bar{\mathcal{H}}^{(0)}\Delta\tau_p)^2\|^2(2n)^{(j+1)+(j-1)}$$

$$= (F(n))^{(j-1)/2}\,\|\bar{\mathcal{H}}_i^{(2)}\|_{nns}\|(\bar{\mathcal{H}}^{(0)}\Delta\tau_p)^2\|^{(j-1)/2}(2n)^{j^2/4+j-5/4} \tag{D.14}$$

and $\|\mathcal{H}_i^{(2)}\|_{nns}$ is given in equation (D.13), so

$$\|\bar{\mathcal{H}}^{(j+1)}\|_{nns} \lesssim (F(n)^{(j-1)/2}\|(\bar{\mathcal{H}}^{(0)}\Delta\tau_p)^2\|^{(j-1)/2}(2n)^{j^2/4+j-5/4}(1/\Delta\tau_p)$$

$$\times\left(\frac{n^2\alpha^2K^2}{8}\|\bar{\mathcal{H}}^{(0)}\Delta\tau_p\|^2\|(\bar{\mathcal{H}}^{(0)}\Delta\tau_p)^2\|^2 + \frac{n\alpha^3K^3}{12}\|(\bar{\mathcal{H}}^{(0)}\Delta\tau_p)^3\|^2\right)^{1/2} . \tag{D.15}$$

We define the selectivity, S, to be $K^{1/2}\|\bar{\mathcal{H}}^{(0)}\|/\|\bar{\mathcal{H}}^{(j+1)}_{nns}\|$, which is the ratio of a typical nonzero matrix element of $\bar{\mathcal{H}}^{(0)}$ to a typical nonzero matrix element of $(\bar{\mathcal{H}}^{(j+1)})_{nns}$. We would like to calculate S as $\bar{\mathcal{H}}^{(0)}t_c$ approaches the limit of convergence, which is $\|(\bar{\mathcal{H}}^{(0)}t_c)^2\| \sim F(n)^{-1}$. Since $t_c = (2n)^{(j+1)/2}\Delta\tau_p$, $\|(\bar{\mathcal{H}}^{(0)}\Delta\tau_p)^2\| \sim (2n)^{-(j+1)}F(n)^{-1}$, and:

$$S = K^{1/2}\|\bar{\mathcal{H}}^{(0)}\|/\|\bar{\mathcal{H}}^{(j+1)}\|_{nns} = K^{-1}\,F(n)^{1/2}\,(2n)^{j^2/4+7/4}$$

$$\times\left(\frac{n^2\alpha^2}{8K} + \frac{n\alpha^3}{12}\,(F(n)\|(\bar{\mathcal{H}}^{(0)}t_c)^3\|/\|\bar{\mathcal{H}}^{(0)}t_c\|)^2\right)^{1/2} . \tag{D.16}$$

Equation (D.16) is the same as equation (III.39).

Appendix E. Some Matrix Relations

This Appendix will only treat properties of matricies that are not listed in standard linear algebra textbooks[101,102] and are required for the calculations of this work.

E.1 The Norm of a Matrix

The general definition of a norm of a n x n matrix A is a real-valued function $A \rightarrow \|A\|$ such that:[101]

$$\|A\| > 0 \text{ unless } A_{ij} = 0 \text{ for all } i, j \tag{E.1}$$

$$\|aA\| = |a| \, \|A\|, \text{ where A is any scalar} \tag{E.2}$$

$$\|A + B\| \leq \|A\| + \|B\| \tag{E.3}$$

Many choices for a norm are consistent with equations (E.1-3). The most useful choice for coherent averaging theory is:[9]

$$A = (\sum_{ij} |A_{ij}|^2/n)^{1/2} = (\mathrm{Tr}(A\,A^{\dagger})/n)^{1/2} \tag{E.4}$$

By inspection, $\|I\| = 1$, where I is the identity matrix. Several properties of this norm derive directly from the definition of the trace of a matrix; for example, $\|A\|$ is invariant under unitary transformation. Thus, if $A = U\,\Lambda\,U^{\dagger}$, $\|A\| = \langle \Lambda_{ij}^{2} \rangle^{1/2}$, the root-mean-squared eigenvalue of A, and $\|A^m\| = \langle \Lambda_{ij}^{2m} \rangle^{1/2}$, which is the square root of the (2m)th moment of the eigenvalues of A. This implies $\|A^m\| \geq \|A\|^m$.

Other useful properties are:

1. $\|U\| = (\mathrm{Tr}(U\,U^{\dagger})/n)^{1/2} = 1$, where U is any unitary matrix.
2. $\|A\| = (\mathrm{Tr}(A\,A^{\dagger})/n)^{1/2} = (\mathrm{Tr}(A^{\dagger}\,A)/n)^{1/2} = \|A^{\dagger}\|$.
3. $\|AB\| = \|B^{\dagger}A^{\dagger}\|$ (from property (2)) $= \|BA\|$ if A and B are Hermitian. Property (1) implies that this relation is also true if A and B are unitary; however, it does not hold for general A and B.

4. Again let $A = U \Lambda U^{\dagger}$, where Λ is diagonal (i.e. A is a normal[102] matrix). Then

$$\|A\Lambda\| = (\mathrm{Tr}(A\Lambda\Lambda A)/n)^{1/2} = (\mathrm{Tr}(A^2\Lambda^2)/n)^{1/2} = (\sum_i (A^2)_{ii}(\Lambda^2)_{ii}/n)^{1/2}$$

$$\leq (\sum_i (\Lambda^2)_{ii}(\Lambda^2)_{ii}/n)^{1/2} = \|\Lambda^2\| = \|A^2\| \ .$$

Since the norm is invariant under unitary transformation this implies that $\|AB\| \leq \|A^2\| = \|B^2\|$, where A and B are any two similar normal matricies.

5. $\|AB\| = (\mathrm{Tr}(ABB^{\dagger}A^{\dagger})/n)^{1/2} = (\mathrm{Tr}(A^{\dagger}ABB^{\dagger})/n)^{1/2} = (\sum_{ij}(A^{\dagger}A)_{ij}$ $(BB^{\dagger})_{ji}/n)^{1/2} \leq ((\sum_{ij}(A^{\dagger}A)_{ij})(\sum_{ij}(BB^{\dagger})_{ji})/n)^{1/2} = n^{1/2}\|A\| \ \|B\|$ so $\|AB\| \leq n^{1/2}\|A\| \ \|B\|$.

6. If A and B are two different matricies, but nothing else is known about them, then $(AB)_{ij}$ is the sum of n numbers which are expected to add randomly. This means that $|AB|^2_{ij} \sim n \langle |A_{ik}B_{kj}|^2 \rangle$ $\sim n \langle |A_{ik}|^2 \rangle \langle |B_{kj}|^2 \rangle$ so $\|AB\| \sim \|A\| \ \|B\|$.

E.2 Exponential Operators

The exponential of a matrix is defined by the Taylor series:[103]

$$\exp(A) = 1 + A + A^2/2 + \ . \ . \ . + A^n/n! + \ . \ . \ . \qquad \text{(E.5)}$$

Exponential operators arise naturally in the solution of the density matrix equation of motion, and frequently expressions such as exp(iAt) Bexp(-iAt) must be evaluated. Clearly the unitary transformation which diagonalizes A also diagonalizes exp(A), so if $A = U \Lambda U^{\dagger}$ then

$$\exp(A) = U \exp(\Lambda) \ U^{\dagger} \qquad \text{(E.6)}$$

$$(\exp(\Lambda))_{ij} = \delta_{ij} \exp(\Lambda)_{ii}$$

If A cannot be diagonalized (either because it is not normal or because the diagonalization would be too complicated), calculation of

exp(A) is difficult. The Taylor expansion (E.5) only converges rapidly if $\|A\| \leq 1$, since $\|A^n\| \gg \|A\|^n$ is possible as explained in the last section. Fortunately, angular momentum is the generator of rotations, and this fact often makes explicit calculation unnecessary. For example, $\exp(-iI_x\pi/2)\ I_z\ \exp(iI_x\pi/2)$ corresponds to a rotation of I_z by $\pi/2$ about the x-axis, and is therefore equal to $-I_y$.

Frequently an expression such as exp(A+B) must be simplified. If $[A,B] = 0$, then $\exp(A + B) = \exp(A)\exp(B)$; otherwise the expressions are complicated. Some useful expansions are:[103-105]

$$\exp(A+B) = \exp(A)\exp(B)\exp([B,A]/2)\exp(\tfrac{1}{6}([A,[A,B]] + 2[B,[A,B]])\ldots \tag{E.7}$$

$$\exp(A)\exp(B) = \exp(A+B+[A,B]/2 + [A,[A,B]]/12 + [[A,B],B]/12 + \ldots) \tag{E.8}$$

$$\exp(A)B\ \exp(-A) = B + [A,B] + [A,[A,B]]/2! \tag{E.9}$$

$$(\exp(A+B))_{ij} = (\exp(A))_{ii}\delta_{ij} + B_{ij}\left(\frac{\exp(A)_{ii} - \exp(A)_{jj}}{A_{ii} - A_{jj}}\right)$$

$$+ \sum_k \frac{B_{ik}B_{kj}}{A_{jj} - A_{kk}} \left\{\frac{\exp(A)_{ii} - \exp(A)_{jj}}{A_{ii} - A_{jj}} - \frac{\exp(A)_{kk} - \exp(A)_{jj}}{A_{kk} - A_{jj}}\right\}$$

$$+ \ldots \tag{E.10}$$

In equation (E.10) A is assumed to be diagonal, and B is assumed to be completely off-diagonal. Equation (E.7) is useful when the commutators can be readily calculated; for example, if $[A,[A,B]] = [B,[A,B]] = 0$ then $\exp(A + B) = \exp(A)\ \exp(B)\ \exp([B,A]/2)$. Equation (E.10) is useful if $\|A\| \gg \|B\|$, because the expansion is in powers of $\|B\|/\|A\|$.[106]

E.3 Tables of Commutators

$$[I_x, I_y] = iI_z \text{ (cyc)} \tag{E.11}$$

$$I^{\pm} = I_x \pm iI_y;\ [I^{\pm}, I_z] = \pm I^{\pm};\ [I^{+}, I^{-}] = 2I_z \tag{E.12}$$

$$\begin{aligned} &I^{o\pm} = 1/2 \pm I_z;\ [I^{+}, I^{o+}] = [I^{-}, I^{o-}] = [I^{o+}, I^{o-}] = 0; \\ &[I^{+}, I^{-}] = I^{o+} - I^{o-}; \\ &[I^{+}, I^{o-}] = -I^{+};\ [I^{-}, I^{o+}] = -I^{-} \end{aligned} \tag{E.13}$$

$$I_x = \begin{pmatrix} 0 & 1/2 \\ 1/2 & 0 \end{pmatrix} \qquad I_y = \begin{pmatrix} 0 & -i/2 \\ i/2 & 0 \end{pmatrix} \qquad I_z = \begin{pmatrix} 1/2 & 0 \\ 0 & -1/2 \end{pmatrix}$$

$$I^{+} = \begin{pmatrix} 0 & 1 \\ 0 & 0 \end{pmatrix} \qquad I^{-} = \begin{pmatrix} 0 & 0 \\ 1 & 0 \end{pmatrix} \qquad 1 = \begin{pmatrix} 1 & 0 \\ 0 & 1 \end{pmatrix}$$

$$I^{o+} = \begin{pmatrix} 1 & 0 \\ 0 & 0 \end{pmatrix} \qquad I^{o-} = \begin{pmatrix} 0 & 0 \\ 0 & 1 \end{pmatrix} \tag{E.14}$$

REFERENCES

1. O. Stern, Z. Physik. 7, 249 (1921); W. Gerlach and O. Stern, Ann. Physik. 74, 673 (1924).

2. F. Bloch, W. W. Hansen and M. Packard, Phys. Rev. 70, 474 (1946).

3. E. M. Purcell, H. C. Torrey, and R. Pound, Phys. Rev. 69, 37 (1946).

4. A. Abragam, The Principles of Nuclear Magnetism (Oxford, London, 1963).

5. C. Slichter, Principles of Magnetic Resonance (Harper & Row, New York, 1963; Springer-Verlag, Berlin, 1978).

6. T. C. Farrar and E. D. Becker, Pulse and Fourier Transform NMR (Academic, New York, 1971).

7. R. T. Schumacher, Magnetic Resonance (W. A. Benjamin, New York, 1970).

8. P. L. Corio, Structure of High-Resolution NMR Spectra (Academic, New York, 1966).

9. U. Haeberlen, "High Resolution NMR in Solids: Selective Averaging," Advances in Magnetic Resonance, Supplement 1 (Academic, New York, 1976).

10. I. I. Rabi, N. F. Ramsey and J. Schwinger, Rev. Mod. Phys. 26, 157 (1964).

11. B. L. Silver, Irreducible Tensor Methods (Academic, New York, 1976).

12. M. E. Rose, Elementary Theory of Angular Momentum (Wiley, New York, 1957).

13. J. W. Emsley and J. C. Lindon, NMR Spectroscopy Using Liquid Crystal Solvents (Pergamon, Oxford, 1975).

14. Haeberlen, Chapter 2.

15. Abragam, Chapter 3.

16. P. Diehl and C. L. Khetrapal, "NMR Studies of Molecules Oriented in the Nematic Phase of Liquid Crystals", NMR: Basic Principles and Progress, vol. 1.

17. A. Saupe, Z. Naturforsch. 19a, 161 (1964).

18. B. Bhagavantam and D. Suryanarayana, Acta. Cryst. 2, 21 (1949).

19. H. A. Jahn, Z. Kristall. 98, 191 (1933).

20. Corio, p. 160.

21. I. J. Lowe and R. E. Norberg, Phys. Rev. 94, 630 (1954).

22. Emsley and Lindon, Chapter 2.

23. P. Diehl, H. Kellerhals, and E. Lustig, "Computer Assistance in the Analysis of High-Resolution NMR Spectra", NMR: Basic Principles and Progress, volume 6 (Springer-Verlag, Berlin, 1972); Emsley and Lindon, p. 75.

24. Z. Luz and S. Meiboom, J. Chem. Phys. 59, 1077 (1973).

25. B. J. Gaffney and H. M. McConnell, J. Mag. Res. 16, 1 (1974).

26. J. Seelig and W. Niederberger, J. Am. Chem. Soc. 96, 2069 (1974); J. Seelig and W. Niederberger, Biochem. 13, 1585 (1974); A. Seelig and J. Seelig, Biochem. 13, 4839 (1974); J. Schindler and J. Seelig, Biochem. 14, 2283 (1975); J. Seelig and A. Seelig, Biochem. Biophys. Res. Commun. 57, 406 (1974).

27. P. Diehl and C. L. Khetrapal, Canad. J. Chem. 47, 1411 (1969).

28. S. Vega, T. W. Shattuck, and A. Pines, Phys. Rev. Lett. 37, 43 (1976); A. Pines, D. Wemmer, J. Tang and S. Sinton, Bull. Am. Phys. Soc. 21, 23 (1978).

29. G. Drobny, A. Pines, S. Sinton, D. Weitekamp, and D. Wemmer, Faraday Division of the Chemical Society Symposium 13, 49 (1979).

30. G. Bodenhausen, R. L. Vold, and R. R. Vold, J. Mag. Res. 37, 93 (1980).

31. M. E. Stoll, A. J. Vega, and R. W. Vaughan, J. Chem. Phys. 67, 2029 (1977).

32. W. P. Aue, E. Bartholdi, and R. R. Ernst, J. Chem. Phys. 64, 2229-2246 (1976); A. Wokaun and R. R. Ernst, Chem. Phys. Lett. 52, 407 (1977).

33. H. Hatanaka, T. Terao, and T. Hashi, J. Phys. Soc. Jpn. 39, 835-836 (1975); H. Hatanaka and T. Hashi, J. Phys. Soc. Jpn. 39, 1139 (1975).

34. A. Wokaun and R. R. Ernst, Molec. Phys. 36, 317 (1978).

35. This section is similar to W. S. Warren and A. Pines, "Analogy of Multiple-Quantum NMR to Isotopic Spin Labeling", J. Am. Chem. Soc. (in press).

36. E. L. Hahn, Phys. Rev. 80, 580 (1950).

37a. H. Y. Carr and E. M. Purcell, Phys. Rev. 94, 630 (1954).

37b. S. Meiboom and G. Gill, Rev. Sci. Instrum. 29, 688 (1958).

38. R. E. Smalley, B. L. Ramakrishna, D. H. Levy, and L. Wharton, J. Chem. Phys. 61, 4363 (1974).

39. M. Tinkham, Group Theory and Quantum Mechanics (McGraw-Hill: New York, 1964).

40. R. G. Jones, NMR: Basic Principles and Progress, vol. 1; (Springer-Verlag: Berlin, 1969), pp. 97-174.

41. H. C. Longuet-Higgins, Mol. Phys. 6, 445 (1963); J. T. Hougen, J. Chem. Phys. 39, 358 (1963).

42. J. Tang and A. Pines, J. Chem. Phys. 72, 3290 (1980).

43. A. Saupe, Z. Naturforsch. 20a, 572 (1965).

44. P. Diehl, H. Bosiger, and H. Zimmermann, J. Mag. Res. 33, 113 (1979).

45. J. Tang and A. Pines, J. Chem. Phys. 73, 2512 (1980).

46. C. Willegerodt and F. Durr, Chem. Ber. 20, 539 (1887); T. Koide, T. Oda and I. Nitta, Bull. Chem. Soc. Jap. 29, 738 (1956); T. Koide, Bull. Chem. Soc. Jap. 40, 2026 (1967).

47a. W. Niederberger, P. Diehl, and L. Lunazzi, Mol. Phys. 26, 571 (1973).

b. J. W. Emsley, J. C. Lindon, D. S. Stephenson, L. Lunazzi, and S. Pulga, J. Chem. Soc. Perkin II 1541 (1975).

48. S. Sinton and A. Pines, Chem. Phys. Lett. (in press); S. Sinton and J. B. Murdoch, private communications.

49. G. W. Gray and A. Mosley, Mol. Crys. Liq. Crys. 35, 71 (1976).

50. W. A. Anderson, Phys. Rev. 104, 850 (1956).

51. J. I. Kaplan and S. Meiboom, Phys. Rev. 106, 499 (1957).

52. S. Yatsiv, Phys. Rev. 113, 1522 (1959).

53. W. A. Anderson, R. Freeman and C. A. Reilly, J. Chem. Phys. 39, 1518 (1963).

54. J. I. Musher, J. Chem. Phys. 40, 983 (1964).

55. D. S. Saxon, Elementary Quantum Mechanics (Holden-Day, San Francisco, 1968).

56. L. D. Landau and E. M. Lifshitz, Statistical Physics (Pergamon, Oxford, 1958).

57. F. Bloch, Phys. Rev. 70, 460 (1946).

58. A. G. Redfield, Adv. Mag. Reson., volume 1 (Academic, New York, 1965).

59. L. I. Schiff, Quantum Mechanics (McGraw-Hill, New York, 1955).

60. C. N. Banwell and H. Primas, Mol. Phys. 6, 225 (1963).

61. S. Vega and A. Pines, J. Chem. Phys. 66, 5624 (1977).

62. A. Wokaun and R. R. Ernst, J. Chem. Phys. 67, 1752 (1977); S. Vega, J. Chem. Phys. 68, 5518 (1978).

63. D. Wemmer, Ph.D. Thesis, University of California, Berkeley (1979, published as Lawrence Berkeley Laboratory Report LBL-8042).

64. A. A. Maudsley, A. Wokaun and R. R. Ernst, Chem. Phys. Lett. 55, 9 (1978); A. Bax, P. G. DeJong, A. F. Mehlkopf and J. Smidt, Chem. Phys. Lett. 69, 567 (1980).

65. C. S. Yannoni, J. Am. Chem. Soc. 92, 5237 (1970).

66. J. B. Murdoch, private communication; J. B. Murdoch, W. S. Warren and A. Pines, to be published.

67. W. S. Warren, S. Sinton, D. P. Weitekamp and A. Pines, Phys. Rev. 43, 1791 (1979); W. S. Warren, D. P. Weitekamp and A. Pines, J. Mag. Reson. 40, 571 (1980).

68. W. S. Warren, D. P. Weitekamp and A. Pines, J. Chem. Phys. 73, 2084 (1980).

69. G. Drobny, A. Pines, S. Sinton, W. S. Warren and D. P. Weitekamp, Proc. Royal Soc. (in press).

70. W. S. Warren and A. Pines, J. Chem. Phys., submitted.

71. U. Haeberlen and J. S. Waugh, Phys. Rev. 175, 453 (1968).

72. M. Mehring, High Resolution NMR Spectroscopy in Solids (Springer-Verlag, Berlin, 1976).

73. W. Magnus, Commun. Pure Appl. Math. 1, 649 (1954).

74. J. S. Waugh, L. M. Huber, and U. Haeberlen, Phys. Rev. Lett. 20, 180 (1968).

75. D. P. Burum and W. K. Rhim, J. Chem. Phys. 71, 944 (1979).

76. Haeberlen, ref. 9, p. 178.

77. W. K. Rhim, A. Pines, and J. S. Waugh, Phys. Rev. B 3, 684 (1971).

78. F. A. Bovey, NMR Data Tables for Organic Compounds, volume 1 (Wiley, New York, 1967), p. 37.

79. G. Drobney, to be published.

80. D. Weitekamp, private communication.

81. G. Drobny, private communication; G. Drobny, D. P. Weitekamp, W. S. Warren and A. Pines, to be published.

82. J. E. Kilpatrick, K. S. Pitzer and R. Spitzer, J. Am. Chem. Soc. 69, 2483 (1947); B. R. Henry, I-F. Hung, R. A. MacPhail, and H. L. Strauss, J. Am. Chem. Soc. 102, 515 (1980).

83. J. Jeener, presented to Ampere Summer School, Basko Polje, Yugoslavia, 1971; A. Kumar, D. Welti and R. R. Ernst, J. Mag. Reson. 18, 69 (1975); L. Muller, A. Kumar and R. R. Ernst, J. Chem. Phys. 63, 5490 (1975);
G. Bodenhausen, R. Freeman, R. Niedermeyer and D. Turner, J. Mag. Reson. 26, 133 (1977).

84. Willy Chao-Wei Shih, Ph.D. Thesis, University of California, Berkeley (1979, published as Lawrence Berkeley Laboratory report LBL-10097).

85. Emsley and Lindon, section 4.2;
H. G. Hertz, Prog. Nucl. Mag. Res. Spectr. 3, 159 (1967);
L. C. Snyder and S. Meiboom, J. Chem. Phys. 44, 4057 (1966).

86. J. Kaplan, J. Chem. Phys. 28, 278 (1958); J. Kaplan, J. Chem. Phys. 29, 462 (1958); J. M. Anderson and A. C-F. Lee, J. Mag. Res. 3, 427 (1970).

87. S. Alexander, J. Chem. Phys. 37, 967 (1972); J. Chem. Phys. 37, 974 (1962).

88. P. D. Buckley, K. W. Jolley and D. N. Pinder, Prog. Nucl. Mag. Res. Spectr. 10, 1 (1975).

89. G. Binsch, Lecture notes from Bat-Sheva Workshop on Magnetic Resonance Spectroscopy, Rehovot, Israel, Sept. 1979; G. Binsch, "Band-Shape Analysis," Dynamic Nuclear Magnetic Resonance Spectroscopy (L. M. Jackson and F. A. Cotton, editors; Academic, N. Y., 1975), p. 45-82; R. A. Hoffman, Adv. Mag. Reson. 4, 88 (1970).

90. U. Fano, Rev. Mod. Phys. 29, 74 (1957)

91. C. E. Shannon, Bell Syst. Techn. J. (1948); N. Wiener, Cybernetics (MIT Press, Cambridge, 1948).

92. J. von Neumann, Mathematical Foundations of Quantum Mechanics (Princeton U. P., Princeton 1955), Chap. V.

93. For a recent set of reviews see The Maximum Entropy Formalism M. Tribus and R. D. Levine, eds (M.I.T. Press, Cambridge, 1978).

94. W. M. Elsasser, Phys. Rev. 52, 987 (1937).

95. R. L. Stratonovich, Sov. Phys. J.E.T.P. 1, 426 (1955).

96. E. T. Jaynes, Phys. Rev. 108, 171 (1957) and in ref. 93.

97. E. H. Wichmann, J. Math. Phys. 4, 888 (1963).

98. A. Katz, Principles of Statistical Mechanics (Freeman, San Francisco, 1967).

99. Y. Alhassid and R. D. Levine, J. Chem. Phys. 67, 4321 (1977), and in ref. 93.

100. See, for example, M. Brout, Phys. Rev. 115, 824 (1959); R. M. Mazo, J. Chem. Phys. 39, 1224 (1963); or for a different context K. F. Freed, J. Chem. Phys. 55, 5588 (1971).

101. C. H. Edwards, Advanced Calculus of Several Variables (Academic, New York, 1973).

102. F. Ayres, Jr., Theory and Problems of Matricies, Schaum's Outline Series in Mathematics (McGraw-Hill, New York, 1962).

103. W. Magnus, Comm. Pure Appl. Math, 7, 649 (1954).

104. R. M. Wilcox, J. Math. Phys. 8, 962 (1967).

105. J. E. Campbell, Proc. London Math. Soc. 29, 19 (1898).
H. F. Baker, Proc. London Math Soc. 34, 347 (1902).
F. Hausdorf, Ber. Verhandl. Saechs. Aka. Wiss. Leipzig, Math-Natur, Kl. 58, 19 (1906).

106. Corio, Appendix III.